

**POLY(LACTIC ACID)-POLY(ETHYLENE GLYCOL) COPOLYMERS FOR
USE AS DRUG DELIVERY SYSTEMS**

Susan Anne HAGAN
B. Sc. (Hons), MRPharmS

Thesis submitted to the
University of Nottingham
for the degree of
Doctor of Philosophy,
October 1998.

CONTENTS

Table of contents	
List of Figures	
List of Tables	
Abstract	
Acknowledgements	
Abbreviations	

TABLE OF CONTENTS

CHAPTER ONE	1
INTRODUCTION	1
1.1 THE CONCEPT OF DRUG TARGETING	1
1.2 THE IDEAL PARENTERAL DRUG DELIVERY SYSTEM	2
1.2.1 Requirements for a Drug Delivery System (DDS)	2
1.2.2 The Reticuloendothelial System (RES)	3
1.2.3 Colloidal Systems used in Drug Delivery	4
1.2.3.1 Non-Biodegradable Nanoparticles	4
1.2.3.2 Biodegradable Nanoparticles	5
1.3 FACTORS AFFECTING THE BIODISTRIBUTION OF COLLOIDAL CARRIERS	9
1.3.1 Particle Size	9
1.3.2 Surface Hydrophobicity/Hydrophilicity	10
1.3.3 Surface Charge	10
1.4 STERIC STABILISATION	11
1.5 SURFACE MODIFICATION BY PHYSICAL ADSORPTION	14
1.5.1 Physical Adsorption with Block Copolymers	14
1.5.2 Coated Model Polystyrene Particles	15
1.5.3 Coated Biodegradable Particles	20
1.6 NANOPARTICLES WITH COVALENTLY BONDED PEG/PEO IN DRUG TARGETING	23
1.7 PLA-PEG COPOLYMERS	25

1.8 PROTEIN ADSORPTION	31
1.9 MICELLES	36
1.9.1 Factors Affecting Micellar Properties	38
1.9.2 Drug Loading Into Micelles	39
1.9.2.1 Sites of Solubilisation	40
1.9.2.2 Factors Affecting Solubilisation	42
1.9.3 Micelles as a Drug Delivery System	45
1.10 AIMS OF THE PROJECT	50
CHAPTER TWO	52
MATERIALS AND METHODS	52
2.1 INTRODUCTION	52
2.2 PREPARATION AND CHARACTERISATION OF PLA-PEG COPOLYMERS	52
2.2.1 Materials	52
2.2.2 Size Exclusion Chromatography (SEC)	53
2.2.3 Determination of PEG/Lactide Ratio by NMR	53
2.3 PURIFICATION AND PREPARATION OF AQUEOUS DISPERSIONS OF PLA-PEG COPOLYMERS	55
2.3.1 Preparation of Unfractionated PLA-PEG Micelles (1.5:2 and 2:5 PLA-PEG)	55
2.3.2 Purification of PLA-PEG Aqueous Dispersions by Gel Permeation Chromatography (GPC)	55
2.3.3 Preparation of Fractionated PLA-PEG Micelles (1.5:2 PLA-PEG and 2:5 PLA-PEG)	55
2.3.4 Preparation of PLA-PEG Particles (4:2 and 6:2 PLA-PEG)	56
2.3.5 Preparation of 1.5:2 LPLA-PEG Particles	56
2.4 MICROSCOPY	56
2.4.1 Transmission Electron Microscopy (TEM) Method	56
2.4.2 Atomic Force Microscopy (AFM) Method	57
2.5 PARTICLE SIZING	57
2.5.1 Dynamic Light Scattering Method	57
2.6 DETERMINATION OF THE CRITICAL MICELLE CONCENTRATION (CMC) OF PLA-PEG MICELLES	58

2.6.1 Surface Tension Method for Determining CMC	58
2.7 ULTRACENTRIFUGATION ANALYSIS	59
2.7.1 Sedimentation Velocity Method	59
2.7.2 Sedimentation Equilibrium Method	60
2.7.3 Measurement of Partial Specific Volume	60
2.8 DETERMINATION OF PEG LAYER THICKNESS BY RHEOLOGICAL MEASUREMENTS	61
2.8.1 Preparation and Sizing of PLA-PEG Aggregates for Rheological Measurements	61
2.8.2 Rheological Measurements	61
2.9 ANALYSIS OF SURFACE CHEMISTRY AND STRUCTURE	62
2.9.1 Static Secondary Ion Mass Spectrometry (SSIMS) Method	62
2.9.2 X-Ray Photoelectron Spectroscopy (XPS) Method	62
2.10 THE STABILITY OF PLA-PEG AQUEOUS DISPERSIONS TO ADDED SALT	63
2.10.1 Method	63
CHAPTER THREE	66
PHYSICOCHEMICAL CHARACTERISATION AND SIZE ANALYSIS OF PLA-PEG SYSTEMS	66
3.1 INTRODUCTION	66
3.2 COMPOSITION OF PLA-PEG COPOLYMERS	66
3.2.1 Size Exclusion Chromatography	66
3.3 PURIFICATION OF AQUEOUS DISPERSIONS OF PLA-PEG COPOLYMERS	67
3.3.1 Gel Permeation Chromatography (GPC)	67
3.3.2 The Gel Permeation Chromatography of PLA-PEG Copolymers	68
3.3.3 Nuclear Magnetic Resonance (NMR) of PLA-PEG Copolymers	72
3.3.4 Calibration of the GPC Sepharose CL-4B Column	73
3.3.5 Assessment of Stability using GPC	76
3.3.6 Discussion	77
3.4 MICROSCOPY	81
3.4.1 Analysis of Micelles/Particles by Microscopy	81

3.4.2.1 Transmission Electron Microscopy (TEM)	81
3.4.2.2 Calibration of TEM	82
3.4.2.3 TEM of PLA-PEG Micelles	82
3.4.2.4 TEM of PLA-PEG Particles	86
3.4.2.5 TEM of 1.5:2 LPLA-PEG Particles	86
3.4.3.1 Atomic Force Microscopy (AFM)	90
3.4.3.2 Atomic Force Microscopy (AFM) of PLA-PEG Particles	92
3.5 PARTICLE SIZING	96
3.5.1 Dynamic Light Scattering (DLS)	96
3.5.2 Determination of the Hydrodynamic Radius of PLA-PEG Micelles and Particles	97
3.5.3 Determination of the Hydrodynamic Radius of 1.5:2 LPLA-PEG Particles	98
3.5.4 Discussion	98
3.6 DETERMINATION OF CMC OF PLA-PEG SYSTEMS	101
3.6.1 Methods for Determining Critical Micelle Concentration (CMC)	101
3.6.2 CMC of Polysorbate (Tween) 80 Micelles	104
3.6.3 CMC of PLA-PEG Micelles	106
3.7 ULTRACENTRIFUGATION ANALYSIS	113
3.7.1 Sedimentation Velocity	113
3.7.2 Sedimentation Velocity Experiments	114
3.7.3 Sedimentation Equilibrium	114
3.7.4 Sedimentation Equilibrium Analysis	119
3.7.5 Discussion	120
3.8 SUMMARY	122
CHAPTER FOUR	125
SURFACE CHARACTERISATION OF PLA-PEG COPOLYMERS	125
4.1 INTRODUCTION	125
4.2 DETERMINATION OF PEG LAYER THICKNESS BY RHEOLOGICAL MEASUREMENTS	126
4.2.1 The Significance of the PEG Layer Thickness	126
4.2.2 Measurement of PEG Layer Thickness	127
4.2.3 Rheological Data for PLA-PEG Copolymers	128

4.2.4 Dynamic Light Scattering Results for Concentrated PLA-PEG Dispersions	132
4.2.5 Calculation of PEG Layer Thickness	138
4.2.6 Discussion	139
4.3 ANALYSIS OF SURFACE CHEMISTRY AND STRUCTURE	148
4.3.1 Static Secondary Ion Mass Spectrometry (SSIMS)	148
4.3.2 Static Secondary Ion Mass Spectrometry (SSIMS) of PLA-PEG Particles	148
4.3.3 X-Ray Photoelectron Spectroscopy (XPS)	153
4.3.4 X-ray Photoelectron Spectroscopy of PLA-PEG Particles	154
4.4 THE STABILITY OF PLA-PEG AQUEOUS DISPERSIONS TO ADDED SALT	162
4.4.1 Theory of Cloud Point Testing	162
4.4.2 Mechanism of Clouding of PEG-Stabilised Aggregates	162
4.4.3 Cloud Point Temperatures of PLA-PEG Micelles/Particles	164
4.4.4 Implications of Cloud Point Temperatures	171
4.5 SUMMARY	172
CHAPTER FIVE	173
DRUG LOADING POTENTIAL OF PLA-PEG MICELLES AND PARTICLES	173
5.1 INTRODUCTION	173
5.2 “MODEL” DRUGS	173
5.2.1 Sudan Black B	173
5.2.2 Testosterone	175
5.3 DRUG LOADING OF TESTOSTERONE AND SUDAN BLACK B INTO PLA-PEG MICELLES AND PARTICLES	175
5.3.1 Method of Drug Incorporation	175
5.3.2 Verification of Drug Loading by Sedimentation Velocity Experiments	176
5.3.2.1 Method	176
5.3.2.2 Calculation and Implications of Sedimentation Coefficients	177
5.3.3 Quantitation of Drug Loading	183
5.3.4 Discussion	186
5.4 INFLUENCE OF HYDROPHOBICITY ON DRUG LOADING	191
5.4.1 Testosterone Esters	191
5.4.2 Quantitation of Drug Loading of Testosterone Esters	192

5.4.3 Discussion	192
5.5 COMPARISON OF DRUG LOADING BETWEEN PLA-PEG AND SIMILAR SYSTEMS	196
5.6 <i>IN-VITRO</i> RELEASE OF SUDAN BLACK B FROM 4:2 PLA-PEG PARTICLES	197
5.6.1 Introduction	197
5.6.2 Method of <i>In-Vitro</i> Release	197
5.6.3 Results and Discussion of <i>In-Vitro</i> Release Study	202
5.7 SUMMARY	207
CHAPTER SIX	209
<i>IN VITRO</i> AND <i>IN VIVO</i> STUDIES OF PLA-PEG COPOLYMERS	209
6.1 INTRODUCTION	209
6.2 RADIOLABELLING OF PLA-PEG COPOLYMERS	209
6.2.1 Radiolabelling of Colloidal Systems	209
6.3 STABILITY OF RADIOLABEL IN PLA-PEG COPOLYMERS	212
6.3.1 Method for In-Vitro Study of Indium-111-Oxine and PLA-PEG Copolymers	212
6.3.2 Results and Discussion	213
6.3.3 Implications for In vivo Experiments	220
6.4 BIODISTRIBUTION OF PLA-PEG MICELLES AND PARTICLES	222
6.4.1 Introduction	222
6.4.2 Preparation of Radiolabelled PLA-PEG Micelles and Particles for Biodistribution Studies	222
6.4.3 Rat Biodistribution Studies	223
6.4.4 Results of Biodistribution Studies on PLA-PEG Micelles	224
6.4.5 Biodistribution Studies on PLA-PEG Particles	228
6.4.6 Discussion	228
6.5 LIVER DISTRIBUTION STUDY OF 4:2 PLA-PEG PARTICLES	233
6.5.1 Method	233
6.5.2 Results	234
6.6 GENERAL DISCUSSION OF <i>IN VIVO</i> STUDIES	234
6.7 SUMMARY	239

CHAPTER SEVEN	240
OVERVIEW AND FUTURE WORK	240
7.1 SUMMARY	240
7.2 FUTURE WORK	243
APPENDIX	246
REFERENCES	249

LIST OF FIGURES

Chapter One

- Figure 1.1 Structures of Polylactic Acid (PLA) and Polyglycolic Acid (PGA)
Figure 1.2a Structure of Poloxamers
Figure 1.2b Structure of Poloxamines
Figure 1.3 Structure of PLA-PEG Copolymer

Chapter Two

- Figure 2.1 Turbidimeter for cloud point measurement

Chapter Three

- Figure 3.1a Gel Permeation Chromatograph of 1.5:2 PLA-PEG
Figure 3.1b Gel Permeation Chromatograph of 2:5 PLA-PEG
Figure 3.2a Gel Permeation Chromatograph of 4:2 PLA-PEG
Figure 3.2b Gel Permeation Chromatograph of 6:2 PLA-PEG
Figure 3.3 Transmission Electron Micrograph of Fractionated 1.5:2 PLA-PEG Micelles (Magnification = 100K)
Figure 3.4 Transmission Electron Micrograph of Fractionated 2:5 PLA-PEG Micelles (Magnification = 100K)
Figure 3.5 Transmission Electron Micrograph of Peak Two Material from 1.5:2 PLA-PEG Copolymer (Magnification = 100K)
Figure 3.6 Transmission Electron Micrograph of Fractionated 4:2 PLA-PEG Particles (Magnification = 100K)
Figure 3.7 Transmission Electron Micrograph of Fractionated 6:2 PLA-PEG Particles (Magnification = 100K)
Figure 3.8 Transmission Electron Micrograph of Fractionated 1.5:2 LPLA-PEG Particles Before Sonication (Magnification = 100K)
Figure 3.9 Transmission Electron Micrograph of Fractionated 1.5:2 LPLA-PEG After Sonication (Energy Level = 8; 10 minutes) (Magnification = 200K)
Figure 3.10 Sweeping of 4:2 PLA-PEG Particles Using an Atomic Force Microscope

- Figure 3.11 4:2 PLA-PEG Particles as Imaged Using Atomic Force Microscopy (AFM)
- Figure 3.12 6:2 PLA-PEG Particles as Imaged Using Atomic Force Microscopy (AFM)
- Figure 3.13 Plot of Log Concentration of Tween 80 against Surface Tension for the Determination of the CMC
- Figure 3.14 Determination of the CMC of 1.5:2 PLA-PEG Copolymer using Surface Tension Measurements
- Figure 3.15 Determination of the CMC of 2:5 PLA-PEG Micelles using Surface Tension Measurements
- Figure 3.16 Sedimentation Velocity Profiles of 1.5:2 PLA-PEG Micelles at an Absorbance of 231 nm
- Figure 3.17 Sedimentation Velocity Profiles for 2:5 PLA-PEG Micelles at an Absorbance of 225 nm
- Figure 3.18 Sedimentation Velocity Profiles of 4:2 PLA-PEG Particles at an Absorbance of 226 nm
- Figure 3.19 Sedimentation Velocity Profiles of 6:2 PLA-PEG Particles at an Absorbance of 226 nm

Chapter Four

- Figure 4.1 Strain Sweep at a Frequency of 1 Hz for 1.5:2 LPLA-PEG with a Volume Fraction of 0.148
- Figure 4.2 Frequency Sweep for 1.5:2 LPLA-PEG with a Volume Fraction of 0.148
- Figure 4.3 Frequency Sweep for 1.5:2 LPLA-PEG with a Volume Fraction of 0.26
- Figure 4.4 Plot of G^* , G' and G'' vs Volume Fraction at a Frequency of 0.1 Hz for 1.5:2 LPLA-PEG
- Figure 4.5 Plot of G^* , G' and G'' vs Volume Fraction at a Frequency of 0.1 Hz for 1.5:2 PLA-PEG
- Figure 4.6 Plot of G^* , G' and G'' vs Volume Fraction at a Frequency of 0.1 Hz for 4:2 PLA-PEG
- Figure 4.7 Plot of G^* , G' and G'' vs Volume Fraction at a Frequency of 0.1 Hz for 6:2 PLA-PEG

- Figure 4.8 Plot of G^* , G' and G'' vs Volume Fraction at a Frequency of 0.1 Hz for 2:5 PLA-PEG
- Figures 4.9 Positive Ion SIMS Spectrum for 4:2 PLA-PEG Nanoparticles
- Figures 4.10 Negative Ion SIMS Spectrum for 4:2 PLA-PEG Nanoparticles
- Figure 4.11 Structures of the PLA and PEG Monomers (carbon and oxygen atoms numbered to aid interpretation)
- Figure 4.12 Carbon C1s Envelopes for XPS Analysis of 4:2 PLA-PEG Nanoparticles
- Figure 4.13a Cloud Point Curve of PEG 8000 Solution
- Figure 4.13b Cloud Point Curve of Poloxamer 407 Dispersion
- Figure 4.13c Cloud Point Curve of Unfractionated 1.5:2 PLA-PEG Dispersion
- Figure 4.14 Comparison of Cloud Point Temperatures for 1.5:2 and 2:5 PLA-PEG Dispersions with 4:2 and 6:2 PLA-PEG Dispersions

Chapter Five

- Figure 5.1a Structure of Sudan Black B
- Figure 5.1b Structure of Testosterone
- Figure 5.2a Sedimentation Velocity Profiles for 2:5 PLA-PEG Micelles
- Figure 5.2b Sedimentation Velocity Profiles for 2:5 PLA-PEG Micelles with Sudan Black B Incorporated
- Figure 5.3a Sedimentation Velocity Profiles for 6:2 PLA-PEG Particles
- Figure 5.3b Sedimentation Velocity Profiles for 6:2 PLA-PEG Particles with Sudan Black B Incorporated
- Figure 5.4 TEM picture of 4:2 PLA-PEG Particles with SBB Incorporated (Magnification = 200K)
- Figure 5.5a Structure of Testosterone Propionate
- Figure 5.5b Structure of Testosterone Isocaproate
- Figure 5.5c Structure of Testosterone Enanthate
- Figure 5.6 In vitro release of SBB from 4:2 PLA-PEG particles

Chapter Six

- Figure 6.1 Structure of Indium-111-Oxine Radiolabel
- Figure 6.2 Serum stability control experiment: 6:2 PLA-PEG 1% w/v Particles and 50% v/v Serum Run on a PD10 Column (Sepharose CL-4B)

- Figure 6.3 Activity of 1% w/v 6:2 PLA-PEG Particles Radiolabelled with Indium (111) Oxine
- Figure 6.4 Serum Stability Data for 6:2 PLA-PEG Particles Incubated in 50% v/v Serum
- Figure 6.5 Activity of Indium (111) Oxine After Incubating for Three Hours in 50% v/v Serum
- Figure 6.6 Data from Biodistribution Studies of Purified 1.5:2 and 2:5 PLA-PEG Micelles
- Figure 6.7 Blood elimination curves for 1.5:2 PLA-PEG, 2:5 PLA-PEG and Indium-111-Oxine in the rat model
- Figure 6.8 Data from Biodistribution Studies of Purified 4:2 and 6:2 PLA-PEG Particles

LIST OF TABLES

Chapter Two

Table 2.1	Characterisation of PLA-PEG Copolymers by Size Exclusion Chromatography (SEC)
-----------	---

Chapter Three

Table 3.1	Polydispersity of PLA-PEG and Related Copolymers After Synthesis
Table 3.2	Relative Proportions of the Two Peaks Produced by Aqueous GPC
Table 3.3	Characterisation of PLA-PEG Copolymers by Size Exclusion Chromatography (SEC) Before and After Aqueous Gel Permeation Chromatography (GPC)
Table 3.4	Comparison of NMR Peak Integration for Fractionated PLA-PEG Copolymers
Table 3.5	Results of Calibration of Sepharose CL-4B Column (2.6 x 40 cm)
Table 3.6	Dynamic light scattering results for 1.5:2 and 2:5 PLA-PEG Micelles
Table 3.7	Dynamic light scattering results from 4:2 and 6:2 PLA-PEG Particles
Table 3.8	Summary of Particle Size Analysis by Dynamic Light Scattering and Microscopy
Table 3.9	Micellar Sizes of Similar Copolymers as Measured by DLS
Table 3.10	CMC Values of Related Copolymers
Table 3.11	Molecular Weight Data for Copolymer Micelles/Particles obtained from Sedimentation Equilibrium Experiments
Table 3.12	Summary of DLS and Sedimentation Equilibrium Data

Chapter Four

Table 4.1	DLS Analysis of 10% w/v PLA-PEG Dispersions
Table 4.2	PEG layer Thickness Measurements Estimated from Rheological Measurements
Table 4.3	Comparison of PEG layer Thicknesses of PLA-PEGs with Similar Copolymer Systems
Table 4.4	Molecular Dimensions of PLA-PEG Micelles/Particles
Table 4.5	Binding Energy Values for PLA and PLA-PEG Copolymers

- Table 4.6 XPS Analysis of 4:2 and 6:2 PLA-PEG Copolymers
- Table 4.7 Stoichiometry of 4:2 and 6:2 PLA-PEG for Carbon from XPS Carbon 1s Spectra
- Table 4.8 Stoichiometry of 4:2 and 6:2 PLA-PEG for Oxygen from XPS Oxygen 1s Spectra
- Table 4.9 Comparison of PLA-PEG Nanoparticles with Coated PLGA Nanoparticles and Polystyrene Particles with Grafted PEG 2000 of Differing Surface Densities
- Table 4.10 Cloud point temperatures (T_c) for 1% w/v PLA-PEG copolymers in the presence of Na_2SO_4
- Table 4.11 Comparison of Cloud Point Temperatures for Fractionated and Unfractionated PLA-PEG

Chapter Five

- Table 5.1 Sedimentation Coefficients of PLA-PEG Copolymers
- Table 5.2 Sedimentation Velocity Analysis of Fractionated PLA-PEG Micelles
- Table 5.3 Sedimentation Velocity Analysis of Fractionated PLA-PEG Particles
- Table 5.4 Drug Incorporation Studies of Testosterone and Sudan Black B into Fractionated PLA-PEG Micelles and Particles
- Table 5.5 Drug Incorporation Studies of Testosterone Esters into Fractionated 4:2 PLA-PEG Particles
- Table 5.6 Review of Drug Loading into PLA and PLGA Particles

Chapter Six

- Table 6.1 Stability of Indium-111-Oxine Radiolabel in 4:2 and 6:2 PLA-PEG Particles (mean \pm s.d.)
- Table 6.2 Blood Clearance Values for High and Low Concentration PLA-PEG Micelle In vivo Studies
- Table 6.3 Blood Clearance Values for PLA-PEG Particle In vivo Studies
- Table 6.4 Location of 4:2 PLA-PEG Particles in the Rat Liver After Differential Centrifugation

ABSTRACT

Block copolymers of polylactide and poly(ethylene glycol) (PLA-PEG) were investigated as biodegradable drug delivery systems. They are defined by the differing molecular weight ratios of polylactide to poly(ethylene glycol). Copolymers containing more hydrophilic PEG than hydrophobic PLA per molecule self-dispersed in water giving spherical nonionic micelles. Purification by gel permeation chromatography gave two peaks. The first peak only formed micelles (the second was PLA-depleted). Analysis by dynamic light scattering (DLS) and transmission electron microscopy (TEM) gave diameters of 15.6nm and 18.9nm for 1.5:2 and 2:5 PLA-PEG micelles respectively.

PLA-PEG copolymers with more PLA than PEG per molecule (4:2 and 6:2 PLA-PEG) formed "solid particles" by the solvent-precipitation method. GPC purification again gave two peaks, but smaller second peaks. DLS analysis gave diameters of 15.1nm and 20.8nm for 4:2 and 6:2 PLA-PEG particles respectively (confirmed by TEM and atomic force microscopy (AFM)).

Static secondary ion mass spectrometry and X-ray photoelectron spectroscopy showed PEG at the surface of 4:2 and 6:2 PLA-PEG in water and acetone. Stability testing to salt suggested sterically stability. Rheological measurements determined PEG chain layer thicknesses, with the thickest chain for 2:5 PLA-PEG (where PEG chain length is 5000gmol^{-1} compared with 2000gmol^{-1}).

Testosterone and sudan black B (SBB), were used as "model" drugs with different hydrophobicities. Ultracentrifugation sedimentation velocity studies confirmed drug incorporation. Aromatic SBB loaded readily ($\geq 59.0\%w/w$) compared with steroidal testosterone ($< 2\%w/w$). Loading of testosterone esters of varying hydrophobicity into PLA-PEG particles showed little difference compared to between testosterone and SBB, suggesting that aromaticity is more significant. *In vitro* release studies (4:2 PLA-PEG particles/SBB) showed a small burst release, then linear release to twenty-eight days.

In vivo studies in the rat, using a radioactive marker, demonstrated extended blood circulation times for PLA-PEG micelles during the three-hour study, with increased blood levels and lower liver uptake for 1.5:2 over 2:5 PLA-PEG micelles. PLA-PEG particles were directed to the liver.

ACKNOWLEDGEMENTS

I would like to thank my supervisors Professor L. Illum, Dr M.C. Garnett, Professor M.C. Davies and Professor S.S. Davis for their guidance, help and encouragement during the course of this thesis. I also wish to thank Professor Davis for the provision of the excellent research facilities within the department.

In addition, I wish to thank all the technical staff of the Department of Pharmaceutical Sciences for their help and patience.

Many thanks also go to Dr. Steve Harding, Immo Fiebrig and Helmut of the Department of Food Science for their help with the ultracentrifugation work. Thanks also to Dr Th. Tadros, Dr Philip Taylor and Gallia of Zeneca Agrochemicals for their help with the rheology work. Thanks are due to Wu Lin for his help with the early TEM work and Trevor Gray of Queens Medical Centre for his time and help with all the TEM work and Kevin Shakesheff for helping with the AFM work. Thanks also to Alex for his help and advice on the XPS and SSIMS work. Thanks are also extended to Helen Redhead, Jonathan Neal and Susan Dunn for performing the animal work.

Further thanks goes to Stuart Purkiss at Zeneca Pharmaceuticals for preparing the PLA-PEG copolymers and performing the NMR and SEC work and for his input at various stages. Thanks to everyone else in the project team at Zeneca who contributed.

On a more personal note, I wish to thank Dr. Allan Coombes for his continuing help and advice and Dr. Colin Melia for his encouragement and support. Thanks also to Prof. S. Bear for his advice on so many matters. Also thanks to everyone in Lab 427 and the particle group who made working there such fun, especially Ian (I remember that Friday afternoon!) and Gazala.

Otherwise, I wish to thank Vanessa for her help with the statistics (who'd have thought A-level maths had a use!) and Dr. Norman Rogers for his help with the statistics and structures and generally for his support. Big thanks also to my friends Caroline, Helen, Vanessa and Clare and everyone else who have encouraged and supported me and kept me smiling. Similarly I wish to thank my mum and dad and sister, Julia, and Angela and David for always being there.

Last but not least, I must thank my husband Steve for believing in me even when I did not believe in myself. Thanks Steve.

ABBREVIATIONS

ADR	Adriamycin
AFM	Atomic Force Microscopy
ANOVA	Analysis of variance
BBB	Blood Brain Barrier
BPEA	Butylpoly(oxypropylene)-Poly(oxyethylene) Ether of 2-Hydroxyacetaldehyde
CMC	Critical Micelle Concentration
CMT	Critical Micelle Temperature
Da	Dalton
DLPLA	Poly(D,L-lactic acid)
DLS	Dynamic Light Scattering
DPPC	Dipalmitoyl Phosphatidylcholine
DSC	Differential Scanning Calorimetry
DSPC	Distearoyl Phosphatidylcholine
DTPA-SA	Diethylenetriamine Pentaacetic Acid Stearyl Amide
FITC	Fluorescein Isothiocyanate
FPEG	Ferrocenyl Moiety of PEG
g	Gram
G*	Complex modulus
G'	Storage modulus
G''	Loss modulus
GFA	Glia Fibrillar Acid
GPC	Gel Permeation Chromatography
HDL	High-density Lipoproteins
HBSS	Hank's balanced salt solution
HSA	Human Serum Albumin
LPLA	Poly(L-lactic acid)
LPLA-PEG	Poly(L-lactic acid)-Polyethylene glycol
LUV	Large Unilamellar Vesicles
MBq	Mega Becquerel
µg	Microgram
ml	Millilitre
mol	Moles
MUV	Multilamellar Vesicles
Mw	Molecular weight
NMR	Nuclear Magnetic Resonance
Pa	Pascal
PAGE	Polyacrylamide Gel Electrophoresis
P(Asp)	Polyaspartic acid
PBLA	Polyethylene Oxide-co-β-Benzyl L-Aspartate
PCL	Polycaprolactone
PEG	Polyethylene glycol
PEG-PE	dioleoyl-N(monomethoxypoly(ethylene glycol)succinyl)phosphatidylethanolamine
PEO	Polyethylene oxide

PLA	Poly(D,L-lactic acid)
PLA-PEG	Poly(D,L-lactic acid)-Polyethylene glycol
PLGA	Poly(lactide-co-glycolide)
PPO	Poly(propylene oxide)
RES	Reticuloendothelial System
SBB	Sudan Black B
SDS-PAGE	Sodium Dodecyl Sulphate-Polyacrylamide Gel Electrophoresis
SEC	Size Exclusion Chromatography
SEM	Scanning Electron Microscopy
SIMS	Secondary Ion Mass Spectrometry
SSIMS	Static Secondary Ion Mass Spectrometry
STM	Scanning Tunnel Microscopy
SUV	Small Unilamellar Vesicles
TEM	Transmission Electron Microscopy
UV	Ultra-Violet
XPS	X-ray Photoelectron Spectroscopy

“If you think you can, you can. If you think you can’t, you’re right.”

Mary Kay Ash

CHAPTER ONE

INTRODUCTION

1.1 THE CONCEPT OF DRUG TARGETING

Despite the many advances in drug delivery in recent years, the achievement of improved selective action of drugs in the body remains a major goal. A great deal of current research is therefore being performed on the development of systems for the “targeting” of drugs to specific sites within the body. This approach was initiated by Ehrlich (1906), who hoped for a “magic bullet” which would be both potent and selective for a particular receptor. Continuing this theme, the idea of a “magic gun” was formed (Tomlinson, 1983), which would act as a carrier, taking drug molecules to the site of action and then releasing them. This would be particularly advantageous with anticancer therapy, where compounds often have a low therapeutic index and are non-specific, giving rise to unpleasant side effects. Frequently, only a fraction of the drug injected reaches its site of action, and the rest is distributed throughout the body depending on the drug characteristics. Also, drugs are commonly lipophilic and may be insoluble or unstable in aqueous media and therefore unsuitable for parenteral injection.

Although more soluble derivatives can be synthesised, this has often led to a decrease in therapeutic effect (Leyland-Jones, 1993). Drugs have been formulated into organic surfactants, such as Tween 80 solutions, but this has been associated with anaphylactic reactions (O'Dwyer *et al*, 1986), whereas changing the pH of the media to effect solubilisation can cause vasculitis or venous inflammation at the injection site (Leyland-Jones, 1993). Therefore, there is still a continuing need for new drug delivery systems to attempt to solve the problems posed in the administration of both new and existing drugs.

Several methods of targeting drug to a specific site via a carrier system have been explored. One such is the modification of the drug substance to give a prodrug (Bodor *et al*, 1975). Another is the use of either monoclonal antibodies, their immunologically active fragments (F(ab)) or target-recognising proteins, which can be conjugated with colloidal particles or drugs and act as “homing” devices for specific antigens or target

sites within the body (Illum *et al*, 1984; Blume *et al*, 1993). However, no practical applications for drug therapy have yet been obtained. Several problems have been identified in the use of monoclonal antibodies for drug targeting. These include uptake of the antibodies by the reticuloendothelial system (RES), otherwise known as the mononuclear phagocytic system (MPS), which clears most of the antibodies from the circulation, leaving only a few to carry out the selective action on tumours. Antibodies with anticancer drugs can also be taken up by normal cells, causing toxic side effects. Monoclonal antibodies may also have low permeability from blood vessels into cancerous tissues (Yokoyama, 1992). This may be a consequence of the decreased blood flow in cancerous tissues, added to the low convectional transport across the vascular walls of such tissues due to their higher interstitial pressure over normal cells. A further approach is to alter the properties of the drug delivery system used to carry the drug to its site of action. Various colloidal drug delivery systems have been considered, including emulsions, liposomes, natural carriers (such as cells) and both synthetic and natural polymeric microparticles and nanoparticles. The use of polymeric particles in drug delivery will now be considered further.

1.2 THE IDEAL PARENTERAL DRUG DELIVERY SYSTEM

1.2.1 Requirements for a Drug Delivery System (DDS)

When injecting a drug delivery system into the body, the effect of this system on the host must be considered and vice versa. The necessary attributes for the ideal parenteral DDS with a view to drug targeting are as listed below (Tomlinson, 1983; Davis and Illum, 1986). The preparation should:

- Show selectivity for the target site.
- Be able to load and protect drug.
- Have controllable release of the drug at the site of action.
- Be stable *in vitro* and *in vivo* until site of action is reached (i.e. minimal drug leakage).
- Show no toxic or immunogenic effect on the host.
- Be biodegradable and biocompatible.
- Be inexpensive and able to be sterilised.
- Be easily prepared on an industrial scale.

The above list can be quite formidable to achieve and much research is still needed. Various research groups have explored the use of colloidal systems in drug delivery over several years. A drug could be incorporated into the hydrophobic core of such a system and thereby be protected from inactivation by contact with the blood, proteins and enzymes. The hydrophobic core can also affect the release rate of the drug into the surrounding media, usually decreasing the release (Yokoyama *et al*, 1994a). Drug delivery systems may also increase the drug circulation and enhance the bioavailability of water-insoluble drugs.

1.2.2 The Reticuloendothelial System (RES)

The major challenge for an intravenously injected colloidal drug delivery system is to avoid the response to foreign particles mediated by the reticuloendothelial system (RES).

This is the collective name for a group of highly phagocytic mononuclear cells that are distributed throughout the body, either at fixed sites or free in the circulation. Highest concentrations of these cells are found in the liver (as fixed macrophages known as Kupffer cells), the spleen and the bone marrow (Douglas *et al*, 1987). Thus, when colloidal particles are injected into the bloodstream, the liver may take them up very efficiently. This uptake can lead to over 90% of particles being phagocytosed by the liver, with a half-time of less than one minute (Illum *et al*, 1982). Uptake is facilitated by the substantial blood flow through the liver, with 25% of the cardiac output passing through, and also by the structure of the liver. The capillaries found in other tissues have been replaced in the liver by large blood vessels known as sinusoids, which have a more open structure and act as a filter. The macrophages are located in these sinusoids and are therefore able to ingest any passing colloidal particles. These particles are then exposed to oxidising agents and degradation by the enzymes of the lysosomes. Similarly, the structure of the spleen also consists of open sinusoids, which are designed to remove larger colloidal particles.

The ability of the reticuloendothelial system to react to a colloidal particle is determined by which blood components interact with the particle on injection into the blood. These blood components are known as opsonins and dysopsonins. Opsonins are plasma components that promote particle uptake by the RES, and dysopsonins are plasma components that reduce or inhibit the uptake of particles. The interplay between

opsonins and dysopsonins may determine whether the mononuclear cells of the RES take up a particle, and the rate of particle uptake.

1.2.3 Colloidal Systems used in Drug Delivery

Colloidal drug delivery systems discussed here are particulate systems, known as microparticles and nanoparticles. Nanoparticles is the collective name for nanospheres and nanocapsules in the diameter size range of about 1 to 1000 nm. Nanospheres have a matrix type structure, whereas nanocapsules have a polymeric shell and inner core. Drug is either adsorbed at the surface or more usually, entrapped/dissolved in the particle core. Similarly, microparticles are in the size range 1 to 1000 μm , and are split into microspheres and microcapsules. The systems discussed here will be nanospheres and microspheres, but the less specific terms, microparticles and nanoparticles, are often used.

Other colloidal systems used in drug delivery are liposomes and micelles. Liposomes usually consist of one or more concentric phospholipid bilayers, separated by aqueous sections formed spontaneously when phospholipids come into contact with water. Within each bilayer, the hydrophobic acyl ends of the phospholipids are opposite each other, with the hydrophilic polar ends placed along the outer rim. Liposomes can be prepared in different sizes, namely small unilamellar (SUV), large unilamellar (LUV) and multilamellar (MLV). Micelles will be discussed later in this chapter.

1.2.3.1 Non-Biodegradable Nanoparticles

In recent years, much work has been performed on non-biodegradable polystyrene latex particles. These have acted as a model system that can be easily characterised and reproduced with little variation in the characteristics of the particles. Polystyrene particles are available in many different sizes with narrow size distributions, allowing the effect of particle size on drug delivery to be studied. These nanoparticles of various sizes are all directed to the liver after intravenous injection into both rats and rabbits (Illum *et al*, 1986b).

Non-biodegradable polyacrylamide nanoparticles have also been synthesised and loaded with drug, but manufacture of these nanoparticles is difficult, involving large amounts of organic solvents and chemical initiators (Allémann *et al*, 1993). Early work on

poly(alkyl methacrylate) nanoparticles was performed on poly(methyl methacrylate) (PMMA) nanoparticles, and drugs were added either by incorporation during the polymerisation process or by adsorbing the drug to previously polymerised nanoparticles. High incorporation efficiencies were achieved with both methods, but due to the lack of biodegradability and the need for a chemical or physical polymerisation initiator, these nanoparticles have not been used commercially. Similarly, acrylic acid and acrylamide have been studied as nanoparticle systems (Lukowski *et al*, 1992), but only as model polymeric systems and not for commercial use. These particles were also located in the RES after intravenous injection (Lukowski *et al*, 1992).

Although the use of these nanoparticles has allowed much information to be collected on the factors that affect the biodistribution of such particles (discussed below), no commercial applications are likely to result as no degradation of the particles would occur *in vivo*.

1.2.3.2 Biodegradable Nanoparticles

Research has now moved towards the use of biodegradable nanoparticles, which have the potential to be exploited for therapeutic use in humans. Poly(alkyl cyanoacrylate) (PACA) nanoparticles have been studied extensively (Douglas *et al*, 1987; Allémann *et al*, 1993) and are prepared by the emulsion-polymerisation technique. This produces particles within the size range 30 nm to 200 nm. Drug has been incorporated into these nanoparticles during polymerisation, but this can lead to a reduction in drug activity if the drug binds covalently to the polymer. Both hydrophilic and hydrophobic drugs have been loaded successfully (Allémann *et al*, 1993), but further research is needed to assess the toxicity and biodegradability of these systems before they can be applied in drug delivery. After intravenous injection, these nanoparticles localise in the liver due to uptake by the Kupffer cells of the RES (Douglas *et al*, 1987). This uptake can be minimised and methods of achieving this will be discussed later in this introduction. Nanoparticles prepared by polymerisation may, however, contain unreacted toxic monomers, and have a risk of reaction between any loaded drug and the monomer. Therefore, other means of nanoparticle preparation have been explored. One method that has been researched is the use of natural macromolecules such as human serum

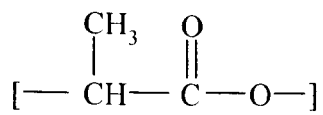
albumin (HSA). Nanoparticles of this protein have been prepared by several methods, including heat denaturation (Chen *et al.*, 1994) or cross-linking of a water-in-oil emulsion of albumin (Lin *et al.*, 1994). Most drugs incorporated have been water soluble (Chen *et al.*, 1994) and high entrapment efficiencies have been achieved (Allémann *et al.*, 1993).

Other possibilities for material for nanoparticle preparation are synthetic polymers. The most research has been performed on the poly(α -esters), (that is, ester polymers prepared from α -hydroxy acids), particularly poly(lactic acid), otherwise known as polylactide (PLA), and poly(glycolic acid) (PGA) (Figure 1.1). These are usually prepared by ring-opening polymerisation of the lactide or glycolide. Polylactide comes in two forms: poly(L-lactide) (LPLA) and poly(DL-lactide) (DLPLA), where LPLA is more crystalline. Poly(DL-lactide) is referred to as simply PLA in this thesis. Poly(glycolic acid) is the more hydrophilic of the two polymers and will therefore degrade faster than PLA, as the degradation is mostly hydrolytically controlled with the eventual degradation products being water and carbon dioxide (Langer, 1993). Copolymers of PLA and PGA have also been widely studied, with differing release rates and degradation achieved by varying the ratio and molecular weight of PLA:PGA. These copolymers are known as poly(lactide-co-glycolide) (PLG), or poly(lactic-co-glycolic acid) (PLGA).

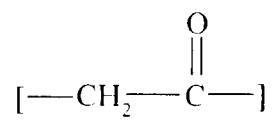
PLA and PGA have been widely researched for therapeutic applications due to their biodegradability *in vivo* and toxicological acceptability. PLA is degraded by hydrolytic deesterification *in vivo* to lactic acid, a normal metabolite in the glycolytic cycle of carbohydrate metabolism (Kulkarni *et al.*, 1971). Devices made from PLA for bone fracture internal fixation (Biofix and Phusilines) and from PLGA for anticancer drug delivery systems (Zoladex) are now commercially available (Vert *et al.*, 1995). PLGA microspheres have been explored for use as an implant in the brain and found to be biocompatible (Menei *et al.*, 1993). The large range of properties of these polymers (they can be made into films, fibres, rods or nanoparticles) should allow their therapeutic uses to increase further.

Nanoparticles of PLA and PLGA can be prepared by an emulsion-evaporation process. Here, the polymer is dissolved in a chlorinated solvent and emulsified in an aqueous phase containing a surfactant. The organic solvent is then evaporated. Another method

Figure 1.1 – Structures of Polylactic Acid (PLA) and Polyglycolic Acid (PGA)



PLA



PGA

of preparation is the “salting-out procedure”, where an emulsion technique is used which eliminates the need for the chlorinated solvents and surfactants used with the emulsion-evaporation process (Allémann *et al*, 1993). In this technique, a saturated electrolyte or nonelectrolyte solution is added to a solution containing poly(vinyl alcohol) and an acetonic solution of the polymer. An oil-in-water emulsion is produced and water added to allow complete diffusion of the acetone into the aqueous phase, inducing nanoparticle formation. A further method of preparation is the solvent-precipitation method proposed by Fessi *et al* (1988). This involves dissolving the polymer in a water-miscible solvent, and adding this solution to a non-solvent for the polymer (usually water), which causes it to precipitate out as nanoparticles. The solvent is then evaporated, leaving a dispersion of nanoparticles.

Various drugs have been incorporated into nanoparticles and microparticles prepared from PLA and PLGA polymers, and an overview of this drug loading is given in Chapter Five of this thesis. Proteins, peptides and hormones have also been successfully incorporated into PLGA copolymers (Couvreur and Puisieux, 1993; Heya *et al*, 1994; Niwa *et al*, 1994; Okada *et al*, 1994; Lu and Park, 1995), and they have the potential for use in vaccine delivery (Alonso *et al*, 1994; Coombes *et al*, 1995; Yan *et al*, 1995).

In vivo work with PLA and PLGA has shown that nanoparticles prepared from these polymers are predominantly localised in the liver. Krause *et al* (1985) showed that PLA nanoparticles (< 1000 nm) injected intravenously into rats were mainly found in the liver (42.9% of injected dose), kidney (5.42%) and bone marrow (1.96%) at two hours after injection. Similarly, Allémann *et al* (1994) noted that PLA nanoparticles (736 nm) were mainly concentrated in the liver (55.22% of the injected dose) and spleen (8.41%), twenty-four hours after intravenous injection into rats. PLGA nanoparticles (approximately 100 nm diameter) were also predominantly taken up by the liver (89.8% of the injected dose) three hours after intravenous injection into rats (Dunn *et al*, 1997), with the spleen accounting for a smaller percentage than the PLA nanoparticles (3.1%). Less than 10% of the injected dose remained in the circulation, fifteen minutes after injection of the nanoparticles.

Other candidates for use as biodegradable nanoparticles are derivatives of the poly(organo phosphazene) polymers. These polymers have an inorganic backbone consisting of alternating nitrogen and phosphorus atoms linked by alternating single and

double bonds. Particles have been produced, by the precipitation solvent evaporation method, from a poly(organo phosphazene) derivative cosubstituted with phenylalanine and glycine ethyl ester side groups (Vandorpe *et al.*, 1996). This method formed nanoparticles of about 200 nm diameter, with the formation and colloidal stability controlled by attractive hydrophobic forces between the phenylalanine ester groups and electrostatic repulsions between the carboxyl groups formed from partial hydrolysis of the ester bonds.

1.3 FACTORS AFFECTING THE BIODISTRIBUTION OF COLLOIDAL CARRIERS

1.3.1 Particle Size

As described above, most colloidal particles are directed to the cells of the reticuloendothelial system, particularly the liver, on injection into the bloodstream. The physicochemical characteristics of the particles and their effect on this RES uptake will now be considered in more detail.

The size of particles is important in determining their *in vivo* biodistribution. This parameter can be manipulated to achieve “passive” targeting, where targeting is achieved by using a natural physiological process of the body. Particles of greater than 7 to 12 μm in size are mechanically trapped in the capillary beds of the lungs, whereas smaller fibre-shaped particles of less than 5 μm can be trapped in the lungs in a “log-jam” effect (Illum *et al.*, 1982). Colloidal particles of 0.1 to 2 μm are mostly taken up by the cells of the reticuloendothelial system of the liver and spleen, such as the liver Kupffer cells. This could also be exploited for passive targeting, for delivering anti-infectives in diseases such as candidiasis or leishmaniasis, or cytotoxics in some forms of leukaemia (Davis and Illum, 1986).

Particles of less than 100 nm offer the possibility of vascular escape through the fenestrations (i.e. openings) in the liver endothelium (Douglas *et al.*, 1987), if they can evade capture by the RES. The sinusoids of the liver, unlike the capillaries in other tissues, have no basement membrane and are discontinuous. As the capillaries are fenestrated, with fenestrae of around 100 nm, theoretically the nanoparticles could extravasate. Once through these gaps, they would reach the space of Disse and the

possibility of uptake by the liver parenchymal cells (hepatocytes) is presented (Davis and Illum, 1986). This possibility is illustrated by viruses, which can be considered to be a naturally occurring model of a drug carrier, penetrating specific cells, and avoiding RES recognition. They may also penetrate through the sinusoidal and fenestrated capillaries, which have pores of 100 nm in diameter (Yokoyama *et al*, 1990).

1.3.2 Surface Hydrophobicity/Hydrophilicity

When a colloidal particle is injected into the blood, it comes into contact with the various blood components, which can coat the particle surface. This process is known as opsonization if the blood components are opsonins, and leads to RES uptake. The likelihood of opsonization is related to the hydrophobicity of the particle surface. Van Oss (1987) studied the uptake of blood components onto the surface of bacteria and the effect of this on RES uptake, and concluded that surface hydrophobicity was an important factor. Thus, hydrophilic particles were made more hydrophobic by the adsorption of immunoglobulin G (IgG) to their surface, which then allowed uptake of the particles by the RES. Conversely, hydrophobic particles are taken up by macrophages without the need for opsonization (Douglas *et al*, 1987). This is explained by van der Waals (hydrophobic) interactions between the macrophages and the hydrophobic particles, such that the more hydrophobic the particle, the greater the van der Waals attractive forces between the particle and the macrophage, and the greater the chance of particle uptake. However, increasing hydrophilicity alone is not enough to prevent RES uptake. For example, Allémann *et al* (1994) compared the biodistribution in rats of uncoated poly(D,L-lactic acid) nanoparticles with similar nanoparticles coated with hydrophilic poly(vinyl alcohol) after intravenous injection. They found that the presence of the poly(vinyl alcohol) at the nanoparticle surface did not prevent the intense phagocytosis by the RES. They concluded that hydrophilicity alone could not prevent RES uptake if opsonin-activating groups were present at the nanoparticle surface (e.g. the hydroxyl groups).

1.3.3 Surface Charge

Particles with different surface charges have been shown to have a similar surface charge after incubation in serum. This is due to the adsorption of serum components, which

shield the charge of the particle, creating a new charge. However, the initial surface charge contributes to the general surface characteristics of the particle and can determine which serum components adsorb to the particle surface. The size and magnitude of this charge can either attract or repel serum components; i.e. serum components with the same sign of charge will be adsorbed less, and those with opposite charge will be adsorbed more. However, this parameter is not as influential as surface hydrophobicity. Research has shown that particle surface charge can affect the biodistribution of colloidal particles. Increasing the negative surface potential of liposomes by altering phosphatide content showed a decrease in liposome uptake by mouse macrophages, when the liposomes were opsonized by complement (Roerdink *et al*, 1983). Similarly, other authors have observed faster clearance from the circulation with negative liposomes compared with positive or neutral liposomes (Juliano *et al*, 1975; Richardson *et al*, 1978). Other studies on liposomes have shown that RES uptake can be reduced, and prolonged circulation times achieved with liposomes with a terminal negative charge, but that even better results are found with uncharged terminal groups (Allen, 1994). Therefore, although particle charge affects the biodistribution and uptake by the RES of some colloidal systems, the effect is not as pronounced as for particle size or hydrophobicity.

1.4 STERIC STABILISATION

Passive targeting of colloidal systems to the RES and lungs can be achieved as described above, by manipulating their natural path within the body. Active targeting to a desired site of action has proved more difficult, but it is recognised now that by altering the surface characteristics, the path of a colloidal drug delivery system *in vivo* can be altered. The particle surface characteristics determine whether a particle will attract opsonins or dysopsonins, and the most important factors in determining RES uptake are the coating of the particles with opsonins from the blood, and the adhesion of the coated particles to macrophages (usually the Kupffer cells of the liver). Therefore, a method of preventing opsonisation and/or promoting dysopsonisation should lead to decreased uptake by the RES and allow the potential for active targeting.

One method of reducing RES uptake is to preblock the Kupffer cells by injecting a RES depressant such as dextran sulphate or latex particles. Illum *et al* (1986a) showed that,

after such treatment, only 30% of subsequently injected polystyrene particles were found in the liver and spleen of rabbits, compared with 90% for untreated animals. However, this strategy for reducing RES uptake is far from ideal as impairment of the RES can have serious consequences. Another method of avoiding uptake is thus required.

It is reasonable that a drug carrier that prolongs the circulation of a drug in the blood may also prolong its efficacy by allowing longer access to the site of action. Much research in the drug targeting field has therefore concentrated on prolonging the circulation time of potential drug delivery systems in the blood. Originally, it was noted that most cells *in vivo* have a surface glycocalyx of glycoproteins and glycolipids, making the cell surfaces hydrophilic and negatively charged (Allen, 1994a).

Conclusions were drawn that these surface groups and the properties of the surface were therefore responsible for the non-recognition of circulating cells such as red blood cells.

Research was then concentrated on emulating these surface properties, to see if similar results could be achieved with drug carriers. A certain degree of success has been achieved with the glycolipid, monosialoganglioside GM₁, with a reduction in the uptake by the RES of the liver and concomitant increase in blood circulation of liposomes noted (Allen, 1994a and b). However, potential problems with commercial acceptability of liposomes containing GM₁ led to research for a substitute that would give comparable results *in vivo*.

Research has now shown that the hydrophilic polymer, polyethylene glycol (PEG), also known as polyethylene oxide (PEO) or polyoxyethylene (POE), can be applied to the surfaces of colloidal particles (Illum and Davis, 1983) and liposomes (by linking to phospholipids) (Allen 1994a and b) and gives a similar effect to GM₁. Generally, low molecular weight polymers (usually those of less than 10,000 g mol⁻¹) with hydroxyl end groups are referred to as polyethylene glycol, whereas higher molecular weight polymers are known as polyoxyethylene or polyethylene oxide. It is prepared by polymerisation using a catalyst which can be cationic, anionic or co-ordinated anionic. Polyethylene glycol contains ether oxygen groups as part of its structure (CH₂-CH₂-O)_n, and this allows the formation of hydrogen bonds with water, when PEG is in aqueous solution.

PEG is therefore highly water soluble at ambient temperatures due to its ability to tetrahedrally co-ordinate water molecules about its ether group through hydrogen bonding, occupying the spaces in the water structure with minimum disruption to that

structure (Llanos and Sefton, 1993). The hydrophilic, hydrated PEG chains can form a “polymer brush” when applied to the surface of a hydrophobic colloidal entity (Allen, 1994b), and have been shown to be effective in preventing protein adsorption, platelet adhesion and bacterial adhesion (Amiji and Park, 1994). These properties of PEG are thought to be due to its lack of reactivity towards proteins and cells. PEG is therefore biocompatible and has been shown to give no adverse physiological response after repeated intravenous dosing of PEG 4000 into beagles over a twelve month period (Carpenter *et al*, 1971). PEG is therefore a suitable polymer for *in vivo* use and for incorporation into drug delivery systems.

The amphipathic polymers poly(2-methyl-2-oxazoline) (PMOZ) and poly(2-ethyl-2-oxazoline) (PEOZ), have also been shown to provide similar protection to GM₁ with liposomes, providing similar resistance to RES uptake to PEG-modified liposomes (Woodle *et al*, 1994). This effect of creating a hydrophilic barrier to reduce uptake by the RES of the body and allow the drug carrier system to remain in circulation has been termed “steric stabilisation”. In this context, it has been defined as “repulsion between particles which is generated by oligomers or polymers attached to, or adsorbed to, the particle surface” (Harper *et al*, 1991). This has been accomplished by physically adsorbing or grafting hydrophilic polymer chains onto the surface of the particle. The dimensions of the stabilising chains need to be greater than the range of the attractive van der Waals forces (Illum, 1987; Illum *et al*, 1987a; Napper, 1989) to provide a net repulsive force between the particles and the cells. This steric barrier is therefore able to prevent or alter the opsonisation and the close approach of macrophages necessary for the adhesion to the cell surface and hence, the engulfment. The best steric barriers have been produced with hydrophilic, uncharged surfaces.

The theory behind this phenomena can be described in terms of the DLVO theory of colloid stability (Rutter and Vincent, 1980). If the particles are charged, both attractive (van der Waals) and repulsive (Coulombic) forces may exist and will vary with the distance between the particle and the cell. A net attractive force can be present when a negatively charged particle and a cell are a certain distance apart, which will become a repulsive force as the two approach each other and will appear as a potential energy barrier (Illum, 1987). This barrier may be overcome if it is small or the particle possesses additional kinetic energy, and adhesion can occur. However, in the case of

sterically stabilised particles, the potential energy barrier is high and therefore more difficult to overcome, so as to minimise the possibility of adhesion to the cell.

1.5 SURFACE MODIFICATION BY PHYSICAL ADSORPTION

1.5.1 Physical Adsorption with Block Copolymers

Research has been aimed at positioning PEG at the surface of colloidal systems to provide a steric barrier. One method of achieving this is by physically adsorbing block copolymers to the surface of nanoparticles. Copolymers are defined as polymers consisting of several different monomer units. There are four main types of copolymer: random, alternate, graft and block copolymers. The two types that will be discussed here are graft and block copolymers. Graft copolymers have chemically linked pairs of homopolymers and may resemble a comb, with one homopolymer forming the backbone and the other covalently attached at various positions along this backbone. Conversely, block copolymers have terminally connected homopolymers, such that a monomer consists of just one connection between the different homopolymers, as opposed to many for the graft copolymers. Block copolymers can be classified as diblock or triblock, according to the number of blocks present in each copolymer. The simplest type, is known as a diblock or AB block copolymer, and consists of two blocks, one of A units and one of B units. Triblock copolymers are known for example as ABA block copolymers, and consist of three blocks, where an A block is connected to both terminals of the B block. The other type of block copolymer, known as a multiblock copolymer or (AB)_n block copolymer alternately repeats A and B blocks in one polymer chain, and is not usually used in pharmaceutical work.

In order to provide steric stabilisation for nanoparticles, block copolymers need to be composed of a hydrophobic block and a hydrophilic block (commonly PEG). The hydrophobic block is required to anchor the block copolymer to the particle surface, so it must have a high affinity for the particle surface and not be easily displaced by the plasma proteins. On the other hand, the hydrophilic block is needed to extend into the aqueous environment to prevent opsonization and therefore the uptake of particles by the RES. The length of the hydrophilic segment and its flexibility determines how successful the steric repulsion is at overcoming the van der Waals forces (Amiji and

Park, 1994). Thus, block copolymers are more effective at stabilising nanoparticles than homopolymers when physical adsorption is used, due to the different but complementary roles of the two segments. Most research to date has centred on the ABA block copolymers, poloxamers and poloxamines.

Poloxamers and poloxamines (commercially known as Pluronics (BASF) or Synperonics (ICI Surfactants) and Tetronics respectively) are ABA block copolymers. For poloxamers, the A blocks are composed of hydrophilic PEO and the B block is the lipophilic polypropylene oxide (PPO) block (PEO-PPO-PEO), whereas poloxamines are tetrafunctional with four PEO-PPO blocks joined by a central ethylenediamine bridge ((PEO-PPO)_{2-x}-(PPO-PEO)₂). The general structures are illustrated in Figure 1.2. The Pluronic/Synperonic copolymers each have a number that gives an indication of the molecular weight, such that the first one or two numbers indicates the molecular weight of the PPO block and the last number signifies the weight fraction of the PEO block.

The notation also begins with L for liquid, P for paste or F for flakes. These polymers have been adsorbed onto hydrophobic particles to give a sterically stabilised coating layer, with the hydrophobic PPO part adsorbed to the particle surface and the hydrophilic PEO chains providing the steric stabilisation by forming an outer layer towards the aqueous medium. They are able to adsorb strongly to hydrophobic surfaces and are not displaced by dilution in aqueous buffer. The following sections will discuss the progress of these systems as coating layers on nanoparticles.

1.5.2 Coated Model Polystyrene Particles

Polystyrene particles have been used as a model system due to their ease of use, narrow size distribution and commercial availability in a wide range of particle sizes. They can be easily radiolabelled with iodine-131 to allow their path *in vivo* to be followed either by gamma scintigraphy or by sacrifice and organ removal. The *in vivo* and *in vitro* experiments discussed here all involve radiolabelled polystyrene particles and detection of the biodistribution by one of those techniques.

Early work by Illum and Davis (1983) showed the effect on the *in vivo* distribution of radiolabelled polystyrene microspheres after coating with nonionic surfactant. This work illustrated the difference between uncoated polystyrene microspheres (1.27 μm

diameter) and microspheres coated with Poloxamer 338 when injected intravenously into rabbits. While the uncoated microspheres were cleared rapidly from the blood by the reticuloendothelial system, the coated microspheres showed a reduced RES uptake and a corresponding increase in the blood activity. When the Poloxamer 338 coating was compared with another surfactant (Illum and Davis, 1984), Poloxamer 188, using smaller polystyrene microspheres of 50-60 nm, the Poloxamer 338 microspheres showed a much reduced RES uptake over both 188 coated microspheres and uncoated microspheres after intravenous injection into rabbits. The uncoated microspheres were again cleared at a rate of about 90% of the injected dose to the RES, with a half time for clearance of 50 seconds. This difference between the poloxamers was attributed to differences in their composition, especially of the PEO chain. Poloxamer 188 has an average ethylene oxide block of 75 (in mol) compared with 128 for Poloxamer 338, which corresponds to estimated adsorbed layer thicknesses of 14 nm and 26 nm respectively. The effect of the copolymer composition was studied further for a range of poloxamers and poloxamines, using mouse peritoneal macrophages as a model for RES uptake (Illum *et al*, 1987a). The physicochemical characteristics of the coated particles were also studied, with regard to the adsorbed layer thickness, the surface charge (as measured by zeta potential) and the critical flocculation temperature. This paper showed that the adsorbed layer thickness of the coating on the polystyrene particles (60 nm) was directly dependent on the ethylene oxide content and independent of the propylene oxide content. From measurements of the adsorbed layer thickness compared with the estimated sizes for the poloxamers 188 and 338, it was concluded that the PEO chains are usually in the loop conformation on the surface of the particles (Illum *et al*, 1987a). Adsorption of the copolymers to the particle surface also led to a decrease in the negative surface charge (zeta potential), making the particles more neutral and less susceptible to RES uptake. The critical flocculation temperature gives a measure of the ability of a polymer to stabilise particles by steric stabilisation and became constant once the adsorbed layer thickness was over about 50 Å. When these physicochemical data were correlated with the results of the mouse peritoneal macrophage uptake experiments, it was clear that the greater the adsorbed layer thickness, the lower the relative phagocytic uptake. Greater adsorbed layer thicknesses also corresponded to a greater decrease in surface charge. The molecular weight of the

PPO was found to be important in anchoring the copolymer to the particle surface, preventing desorption and displacement of the copolymer *in vivo*, with higher PPO molecular weights giving better anchoring (Illum *et al*, 1986b).

Thus, the magnitude of the adsorbed layer thickness and its ability to sterically stabilise the particle surface and suppress surface charge are important for decreasing the uptake of colloidal particles by the reticuloendothelial system. Hydrophilicity of the surface alone is not enough. This was illustrated in a paper by Illum *et al* (1986b), where the efficiency of coating polystyrene particles with hydrophilic materials (secretory immunoglobulin A (SIgA), egg lecithin and the poloxamers 188 and 388) was compared with respect to reducing liver uptake in *in vivo* experiments in rabbits and mouse peritoneal macrophage uptake experiments. The *in vivo* experiments showed that the SIgA and lecithin only reduced the liver/spleen uptake by 2% and 14% respectively, compared with a reduction in liver/spleen uptake by 20% for poloxamer 188 and 44% for poloxamer 388. Mouse peritoneal macrophage experiments also confirmed this order of uptake. In the case of the poloxamer 388, the particles were redistributed to some extent to the bone marrow instead. Redirection to the bone marrow after intravenous injection into rabbits has also been noted with Poloxamer 407 (Illum and Davis, 1987). Here, the liver/spleen uptake was reduced further than for Poloxamer 338, down to 17% of the activity, of which 10% could be attributed to the activity in the circulation (blood pool), i.e. not due to particle uptake. Targeting of the bone marrow would be useful both for treating diseases of the bone marrow, such as bone marrow cancer and for radiodiagnostics.

The promising results seen with regard to bone marrow targeting for particles coated with poloxamer 407 were investigated further. Polystyrene particles (70 nm) coated with poloxamer 407 were compared with “solid” unilamellar liposomes (DSPC/Chol/DCP), which had been incubated with poloxamer 407 (Moghimi *et al*, 1991a). However, no poloxamer coating could be found at the liposome surface in physicochemical analysis and no significant difference in biodistribution was observed after intravenous injection into rats. Research was therefore concentrated on colloidal particles, and further studies on coated polystyrene particles (less than 150 nm) showed that the particles were sequestered in the sinusoidal endothelial cells of the bone marrow after intravenous injection into rabbits, suggesting that the steric barrier was being

overcome and a specific interaction with the cell surface was occurring (Porter *et al*, 1992). This specificity of interaction was further implied by the lack of bone marrow uptake seen with other poloxamer and poloxamine coatings. The conclusions were complicated further by the discovery that only Poloxamer 407 from one supplier gave the pronounced bone marrow uptake (Porter *et al*, 1992). This was attributed to differences in the molecular weight distribution of the polymer.

Targeting of the vascular circulation has also been achieved by coating polystyrene particles (50-60 nm) with poloxamine 908 (Illum *et al*, 1987b). These particles showed little uptake by the liver/spleen, but remained in the circulation, with 60% of particles detected in the circulation after one hour compared with 3% of the uncoated polystyrene particles. In this case, non-recognition by the reticuloendothelial system has been achieved, with a significantly prolonged circulation time.

Spleen targeting has been achieved by using larger polystyrene microspheres (220-300 nm) coated with poloxamine 908. Following intravenous injection into rats, these microspheres were accumulated in the spleen by a filtration mechanism (Moghimi *et al*, 1991b). These microspheres could then be phagocytosed by the macrophages of the red pulp 24 hours after administration (Moghimi *et al*, 1993a). This was postulated as being due to either loss of the surface adsorbed poloxamine 908 or “neutralisation” of the anti-phagocytic effect of the poloxamine 908 within the spleen.

Lymphatic targeting has been attempted also using polystyrene microspheres as model colloidal particles. A wide range of poloxamers and poloxamines were used to coat the polystyrene particles (60 nm) and then the particles were injected sub-cutaneously into the rat footpads (Moghimi *et al*, 1994). A correlation was found between the length of the stabilising PEO chains of the poloxamers and poloxamines, the drainage of nanoparticles from the injection site and their passage across the tissue lymph interface in the dermal lymphatic capillaries of the rat footpad. This correlation was that the longer the PEO chains, the faster the drainage. Therefore, whereas nanoparticles with PEO chains of 5-15 ethylene oxide units were effectively opsonized in the lymphatics, nanoparticles with longer PEO chains were rapidly drained and reached the systemic circulation. With the shorter chains, lymphatic targeting could be successfully achieved, with up to 40% of the administered dose sequestered by the macrophages of the regional lymph nodes.

1.5.3 Coated Biodegradable Particles

While the above results were very promising and yielded much data on the principles involved in avoiding the reticuloendothelial system and targeting specific areas of the body, the systems involved can have no clinical application as they are non-biodegradable. More recent research has therefore concentrated on producing similar systems to those described above, but replacing the non-degradable polystyrene particles with biodegradable particles.

As mentioned above, the diameter of the nanoparticles is important, with some larger coated nanoparticles (over 200 nm) being directed to the spleen, and smaller coated nanoparticles (60-200 nm) able to remain in the vascular compartment or target the bone marrow or lymph nodes. Liu *et al* (1992) and Litzinger *et al* (1994) have carried out studies on the effect of liposome diameter on the circulation time and organ distribution after intravenous injection into mice. These groups studied liposomes stabilised with ganglioside GM₁ and PEG respectively, to provide the hydrophilic coating necessary for RES avoidance. Liu *et al* (1992) noted that with their system (liposomes of phosphatidylcholine, cholesterol and GM₁), optimal circulation was achieved when the liposome size was in the diameter range 70 to 200 nm. Increasing the diameter further resulted in increased spleen uptake with a corresponding decrease in the circulating blood level. Spleen uptake became predominant when the liposome size was increased above 300 nm. Similarly, Litzinger *et al* (1994) noted that their liposomes (containing dioleoyl-N-(monomethoxypoly(ethylene glycol)succinyl)-phosphatidylethanolamine (PEG-PE)) also showed long circulation times for liposomes of 150-200 nm, whereas liposomes over 300 nm were directed to the spleen.

It was therefore important to produce PEG-coated particles of less than 200 nm diameter if long blood circulation times were to be achieved. Scholes *et al* (1993) succeeded in producing biodegradable PLGA nanoparticles in this size range by varying the parameters of the solvent evaporation technique. Small particle sizes (down to 90 nm) could be reproducibly formed by the use of low PLGA concentration, increased surfactant concentration and a two stage emulsification process. Particles below 200 nm diameter were also produced from poly(beta-malic acid-co-benzyl malate) (PMLABeH) copolymers using the precipitation-solvent evaporation method (Stolnik *et al*, 1994), which was subsequently also used to produce PLGA particles (Scholes, 1994).

These particles were coated with poloxamers and poloxamines as the polystyrene particles had been previously. PLGA nanoparticles were surface modified with poloxamers and poloxamines either by adsorption of the copolymers to previously prepared nanoparticles or by incorporation into the nanoparticles during production (Dunn *et al*, 1997). Radiolabelling of the nanoparticles for *in vitro* and *in vivo* analysis was achieved by incorporating indium-111-oxine into the nanoparticles during production. Nanoparticles coated with Poloxamer 407 or Poloxamine 908 showed prolonged blood circulation times and a combined reduction in liver and spleen accumulation after intravenous injection into rats. Three hours after injection, 39% of the dose for Poloxamer 407 and 28% of the Poloxamine 908 dose remained in the blood circulation. On comparison with polystyrene-coated nanoparticles, the blood elimination profiles and biodistribution were similar. *In vivo* studies in the rabbit model also gave similar results, with long blood circulation times and reduced RES uptake again observed (Dunn *et al*, 1997).

Similarly, PLGA nanospheres have been coated with biodegradable polylactic acid-polyethylene glycol (PLA-PEG) copolymers (Stolnik *et al*, 1994). This coating was shown to decrease the negative surface charge, increase hydrophilicity and provide steric stabilisation when adsorbed to PLGA or polystyrene nanospheres, in comparison with uncoated nanospheres. When injected intravenously into rats, the biodistribution was greatly changed for the coated PLGA nanospheres in comparison with the uncoated PLGA nanospheres. Extended blood circulation levels were noted with the two PLA-PEG copolymers used (3:4 and 2:5 PLA-PEG), with similar levels to Poloxamine 908 coated systems being achieved. The blood clearance profiles and deposition of nanospheres in the liver and spleen were also similar to Poloxamine 908 coated systems. However, with the polystyrene coated systems, the PLA-PEG coated nanospheres showed an initial high blood circulation level similar to Poloxamine 908 coated nanospheres, which then fell dramatically between one and two hours post-administration (Stolnik *et al*, 1994). Thus at three hours post-injection, the liver uptake of the coated nanospheres was similar to that of the uncoated polystyrene particles. The authors suggested that the reason for this might be a difference in the adsorption stability of the PLA-PEG coatings on the polystyrene and PLGA nanospheres. Adsorption of protein onto the surface of coated nanospheres is thought to occur gradually, in

comparison with polystyrene latex particles where the whole surface is thought to be coated instantaneously (Senior *et al*, 1991). The PLA group of the PLA-PEG copolymers is the more hydrophobic group, which would be expected to anchor the PLA-PEG copolymers to the hydrophobic particle surface. This appears to anchor better to a surface of similar structure, i.e. PLGA nanospheres, compared with the polystyrene nanospheres, and therefore be more stable to the desorption and displacement that allows the gradual adsorption of plasma proteins. The mechanism for this difference is unclear. Lymph node targeting has also been explored with biodegradable nanospheres. Here, the nanospheres were injected subcutaneously, which is considered to be the most appropriate route for reaching the regional lymph nodes (Hawley *et al*, 1995). Sub-100 nm PLGA nanospheres were coated with poloxamers and poloxamines and radiolabelled with indium-111-oxine. The lymphatic distribution was then determined after subcutaneous injection into the rat. Coated nanospheres showed an increased lymphatic uptake by the regional lymph nodes over uncoated nanospheres, with a maximum lymph node uptake of 17% achieved, showing great promise for lymphatic targeting.

More recent studies have investigated coating the surface of polystyrene and PLGA nanoparticles with PLA-PEG copolymers (1.5:0.75, 1.5:2 and 2:5 PLA-PEG) (Hawley *et al*, 1997). Here, PLA-PEG copolymers were either physically adsorbed to the nanoparticle surface or used as a co-precipitate to form PLGA-PLA-PEG nanoparticles.

In vivo studies in rats injected subcutaneously showed that, depending on the PLA-PEG copolymer used, lymph node localisation could be dramatically enhanced. Of the three PLA-PEG copolymers studied, the 1.5:2 and 2:5 PLA-PEG copolymers were too hydrophilic to be taken up by the lymph node macrophages when coated onto polystyrene particles, so that the lymph node localisation of nanoparticles coated with these copolymers was reduced in comparison with the uncoated control. However, with PLGA particles, all coated systems showed enhanced lymph node localisation over the uncoated control nanoparticles. The 1.5:0.75 PLA-PEG copolymer coating gave the best results, with 15% lymph node uptake after 24 hours for both polystyrene and PLGA coated nanoparticles. Coating of the nanoparticles with PLA-PEG copolymers also increased the drainage of the nanoparticles from the injection site, compared with uncoated nanoparticles, with the rate of drainage increasing with increasing PEG chain length.

For nanoparticles prepared by co-precipitation of PLGA and 1.5:0.75 PLA-PEG copolymer, the lymph node uptake was highest with a 75% and 65% PLGA content (16% and 17% of lymph node uptake respectively) (Hawley *et al.* 1997). The drainage of nanoparticles from the injection site also increased with increasing percentage of PLA-PEG in the nanoparticles, in line with the coated nanoparticle results.

Other biodegradable nanospheres that are being considered for drug targeting are sterically stabilised human serum albumin (HSA) nanospheres. These have been prepared with a size of less than 200 nm using a modified coacervation method and crosslinking with methyl polyethylene glycol modified oxidised dextran (Dextranox-MPEG) (HSA-mPEG), to give the sterically stabilised surface layer (Lin *et al.* 1994).

When injected intravenously, both HSA and HSA-mPEG nanospheres gave a similar biodistribution profile, with 27.4% and 32.3% of the injected dose being associated with the carcass and 19.4% and 21.1% of the dose associated with the gut tissue, for HSA and HSA-mPEG respectively (Dunn, 1995). The activity in the gut was unexpected, so a time course experiment was carried out. Again, HSA and HSA-mPEG gave similar biodistribution patterns. For both HSA and HSA-mPEG nanospheres, at five minutes post-injection, most of the injected dose was in the liver, but this activity decreased with time and relocated in the carcass, thyroid and gut. Over 20% of the injected dose was found in the gut at three hours post-injection for both systems. This was suggested as being due to degradation of the HSA in the lysosomal compartment of the liver, allowing iodinated metabolites to be selectively directed to the gut tissue.

1.6 NANOPARTICLES WITH COVALENTLY BONDED PEG/PEO IN DRUG TARGETING

Steric repulsion with homopolymers is not usually effective when physically adsorbed. Only high molecular weight PEO homopolymers ($MW > 100,000 \text{ g mol}^{-1}$) are effectively adsorbed onto hydrophobic surfaces, and other molecules, such as proteins and cells, which have a higher affinity for the surface, can still easily remove these. Indeed, even the block copolymers described above carry the risk of being desorbed from a particle surface after injection into the body, as illustrated by the PLA-PEG copolymers when used as coatings for polystyrene nanospheres (Stolnik *et al.* 1994).

Homopolymers need to be covalently grafted to provide a stable hydrophilic layer. This is only possible if the surface has functional groups that can react with PEO derivatives, is pre-modified with reactive functional groups or if grafting is performed by using UV or gamma radiation.

There are drawbacks to grafting, including the requirement for multiple steps due to the lack of functional groups available for modification on many polymers, but grafting of PEG to polystyrene nanospheres has produced further information on the surface characteristics required for steric stabilisation with PEG. Dunn *et al* (1994) described an experiment where the effect of altering the PEG chain density of polystyrene-PEG particles was studied. Particles were prepared by varying the copolymerising reaction of styrene with a PEG macromonomer. The surface density of the particles was then determined by X-ray photoelectron spectroscopy (XPS). When injected intravenously into rats, the biodistribution was shown to be related to the density of PEG at the surface of the nanoparticles (after three hours). Liver uptake was related to the surface density, with the lowest surface density of PEG giving the highest uptake. As the PEG surface density increased, the liver uptake was reduced, with a corresponding increase in circulating blood levels.

Another approach to covalently bonding the PEG groups is to produce “self-forming” systems. These can take the form of particles, micelles or liposomes (micelles are described further below). Self-forming nanospheres have been produced by Gref *et al* (1994) using diblock copolymers of PLGA, polycaprolactone (PCL) and their copolymers covalently bonded to PEG of different molecular weights. These nanospheres were prepared by dissolving the copolymer in an organic solvent and then forming an emulsion (oil in water) in an aqueous phase by vortexing and sonicating. The solvent was then evaporated to leave nanospheres. PEG was confirmed at the surface of these nanospheres using XPS and the nanospheres were radiolabelled with indium-111-DTPA-SA (diethylenetriamine pentaacetic acid stearyl amide). Intravenous injection into mice showed that blood circulation times increased with increasing PEG molecular weight. This was explained by an increased thickness of the PEG layer with the increased molecular weight, preventing opsonization of the nanospheres. Five minutes post-injection, 66% of uncoated PLGA nanospheres had been removed by the liver, compared with about 30% of PEG-PLGA (PEG=20000 gmol⁻¹) nanospheres in the

liver at five hours. These nanospheres appeared to possess the steric stability required for drug targeting and the physical stability offered by covalently attached PEG as opposed to physically adsorbed PEG as part of a block copolymer.

Further work by the same group has involved the study of a wider range of diblock copolymers of the type PEG-R (where R is polyester or polyanhydride). To increase the surface density of PEG on the nanoparticles, multiblock (brush) $(\text{PEG})_n\text{-R}$ copolymers were synthesised, where the R polymer block is covalently attached to more than one PEG block (Peracchia *et al*, 1997). The increased PEG surface density was confirmed by ESCA studies, with even higher PEG surface densities being obtained with high molecular weight PEG polymers (PEG = 20000 Da). The morphological structure and encapsulation properties of the nanoparticles were studied. These revealed that with PEG-PCL particles, the drug and polyester did not interact, but were segregated in separate domains. Conversely, with PEG-PLGA nanospheres there was interaction between the polymer and drug. It was also noted that, unlike the diblock copolymers, the PEG drastically increased the size of the particles made from the multiblock copolymers (from 100-120 nm for uncoated particles to 180-240 nm for PEG-coated nanoparticles), with the size increasing with increasing PEG chain length. The encapsulation efficiency of the four-block copolymers also dropped to around 70%, compared with 75-95% for the corresponding diblock copolymers, and non-coated particles. In vitro release studies on diblock copolymers showed a biphasic release, with continuous release over several hours, and different kinetics for the different polymers. The presence of the PEG did not affect the overall amount of drug released. However, with the multiblock copolymers, the burst effect was reduced and the drug release slowed down. The authors concluded that although the drug is in the particle core, the characteristics of the PEG coat affected the time course of the drug release.

1.7 PLA-PEG COPOLYMERS

Biodegradable block copolymers produced from polylactic acid (PLA) and poly(ethylene glycol) (PEG) exhibit good potential for formulating drug delivery systems. The use of the individual polylactic acid and polyethylene glycol components in drug delivery have already been discussed, and the biocompatibility of these two polymers makes them

suitable candidates for further investigation. PLA-PEG copolymers with various PLA:PEG ratios, molecular weights, structure and solubility can be synthesised, using either the racemic poly(D,L-lactic acid) or isomeric poly(L-lactic acid). Poly(D,L-lactic acid) is entirely non-crystalline, whereas poly(L-lactic acid) can form a crystalline phase (it is a semi-crystalline polymer). This crystallinity of the LPLA makes it less soluble in organic solvents than the DLPLA, and reduces the rate of water uptake of the polymer and hence the biodegradation rate compared with DLPLA. There has been considerable interest in the synthesis and characterisation of these copolymers. PLA-PEG copolymers are AB linear block copolymers, with the general structure shown in Figure 1.3. These copolymers have been synthesised by different groups, using different catalysts, creating copolymers with differing molecular weight distributions. Zhu *et al* (1986) synthesised PLA-PEG copolymers containing poly(D,L-lactic acid), using aluminium and stannous-based catalysts. Cohn and Younes (1988a) synthesised a range of PLA-PEG copolymers using poly(L-lactic acid) and PEG, in the presence an antimony trioxide (Sb_2O_3) catalyst by a polyesterification reaction of the lactic acid in the presence of PEG. Another group working with poly(D,L-lactic acid) and PEG used ring-opening polymerisation in the presence of various catalysts to synthesis PLA-PEG copolymers (Deng *et al*, 1990). They found that stannous octoate was the best catalyst for copolymerisation of D,L-lactide with PEG, giving a high yield and molecular weight, whereas antimony trioxide was a poor one. The same group later used a complex aluminium catalyst, triisobutylaluminium with phosphoric acid and water ($\text{Al}(\text{i-Bu})_3\text{-H}_3\text{PO}_4\text{-H}_2\text{O}$), as the initiator (Deng *et al*, 1995). Hu and Liu (1994a and b) also synthesised PLA-PEG copolymers of poly(L-lactic acid) and PEG, using a stannous octoate catalyst.

Research has not been confined to AB block copolymers. ABA block copolymers have also been synthesised where A is poly(L-lactic acid) and B is polyoxyethylene (Youxin and Kissel, 1993), using aluminium isopropoxide as catalyst. Similarly, ABA PLA-PEO-PLA block copolymers have been synthesised and studied by Shah *et al* (1994) (using a stannous 2-ethylhexanoate catalyst), Rashkov *et al* (1996) (using a CaH_2 catalyst) and Li *et al* (1996) (using a CaH_2 or zinc powder catalyst). Blends of PLA-PEG copolymers with other biodegradable polymers have also been studied (Zhang *et al*, 1995) for potential biomedical applications.

The research described above has centred on the chemical and physical characterisation

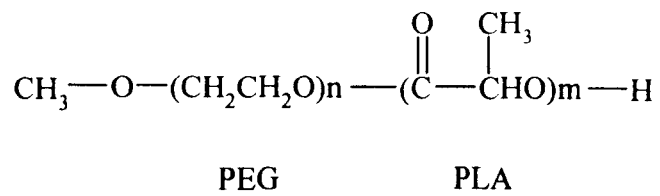


Figure 1.3 – Structure of PLA-PEG Copolymer

of the PLA-PEG copolymers. This has involved various chemical techniques including nuclear magnetic resonance (NMR), size exclusion chromatography (SEC) and differential scanning calorimetry (DSC). The hydrolytic degradation of the PLA-PEG copolymers has also been widely studied (Zhu *et al.*, 1986; Cohn and Younes, 1988b; Hu and Liu, 1994a and b; Liu *et al.*, 1994; Shah *et al.*, 1994; Youxin *et al.*, 1994), with variation of the amount of PEG in the copolymer enabling the degradation rate of the copolymer to be controlled.

The main focus of the interest in PLA-PEG copolymers is their potential for use in biomedical applications. PLA-PEG copolymers of low molecular weights have been successfully explored as a carrier for bone morphogenetic protein (BMP) as implants into bones (Miyamoto *et al.*, 1993). Zhu *et al.* (1986; 1990) studied AB PLA-PEG copolymer matrixes as potential drug delivery systems, observing that drug release increased with increasing PEG content. Cohn and Younes (1988b) synthesised a family of poly(lactic acid)/poly(ethylene oxide) block copolymers in an attempt to provide biodegradable elastomers for cardiovascular implants. With these copolymers, the lactic acid sequences form degradable 'hard' blocks of the copolymer, whilst flexibility and elastic recovery properties were associated with the PEG 'soft' segments. Youxin *et al.* (1994) studied the potential of LPLA-PEG-LPLA block copolymers as potential parenteral drug delivery systems, using bovine serum albumin as a model drug, and noted a pulsatile release of drug controlled by the structure and properties of the copolymer.

The ability of PLA-PEG copolymers to form nanoparticles has also been studied. Zhu *et al.* (1989) prepared 'super microcapsules' of 40-100 nm diameter for drug delivery, by phase separation of poly(ethylene oxide)-polylactide star-type copolymers. Similar higher molecular weight copolymers have been synthesised by Gref *et al.* (1994) for drug targeting applications, using poly(lactide-co-glycolic acid) (PLGA) or polycaprolactone (PCL), attached to PEG. These copolymers formed nanoparticles of mean diameter of 140 nm, that were able to incorporate drug and avoid uptake by the RES after intravenous injection into mice. Later work by the same group also looked at PLA attached to multiple blocks of PEG (see above section 1.6), to increase the surface density of PEG at the nanoparticle surface (Peracchia *et al.*, 1997). PLA-PEG nanoparticles have been prepared by Bazile *et al.* (1995) by the precipitation-solvent

diffusion method. In this case, nanoparticles were prepared either from the PLA-PEG copolymers as synthesised or with PLA blended into the preparation process. This gave nanoparticle sizes ranging from 56 nm to 112 nm for the PLA-PEG copolymers alone, or up to over 200 nm when PLA was blended with the PLA-PEG. After intravenous injection into rats of ^{14}C -labelled nanoparticles, the circulating half-life of PLA-PEG nanoparticles (PEG Mw=5000, PLA theoretical Mw=30000) improved by a factor of 180 over uncoated PLA nanoparticles. They also found that in ex-vivo experiments with cultured THP-1 monocytes, the uptake by the monocytes was dependent on the PEG chain length, but once the surface density of PEG had plateaued, the chain length ceased to be important.

Another group (Allémann *et al*, 1996) has studied the effect of coating PLA nanoparticles (988 nm) with PEG (Mw=20000) and using the nanoparticles as a carrier for hexadecafluoro zinc phthalocyanine (ZnPcF_{16}). This compound is a second-generation sensitiser for the photodynamic therapy of cancer, and the tumour response of the nanoparticle formulation was compared with the response from a Cremophor EL emulsion. The authors demonstrated extended circulation of the PEG-coated nanoparticles after intravenous injection into mice thereby allowing prolonged tumour sensitivity towards the photodynamic therapy, and also an improved response of the tumour to the photodynamic therapy over the emulsion formulation.

Micelles prepared from PLA-PEG copolymers have also been studied in recent research. Zareie *et al* (1996) studied micelles prepared from PLA-PEG copolymers produced by transesterification of poly(D,L-lactic acid) (Mn=1866) with PEG (Mn=3300-4000). These micelles were studied using dynamic light scattering (DLS), scanning electron microscopy (SEM) and scanning tunnel microscopy (STM). Micelle sizes were found to be around 80 nm and 112 nm from DLS for micelles containing 35% (of their monomer molecular weight) of PEG and micelles containing 60% of PEG respectively. The microscopy techniques showed micelles of larger sizes (up to 135 nm for 35% PEG micelles and 172 nm for 60% PEG micelles using STM). The authors attributed this increase in size to the interaction of the micelles with the substrate surface and dislocation of the micelles by the STM scanning tip.

PLA-PEG micelles have been studied as potential carriers of the drug taxol (Zhang *et al*, 1996). The PLA-PEG copolymers were prepared by ring-opening polymerisation in

the presence of stannous octoate, producing copolymers with a PEG chain length of 2000 and PLA to PEG ratios of 40:60 and 50:50. Up to 25% w/w taxol was loaded into PLA-PEG copolymer matrices and on dissolution, this was completely solubilised within the micelles. The taxol was strongly bound or associated with the PLA-PEG copolymers even below the critical micelle concentration (cmc).

The two different blocks of PLA-PEG copolymers can share the functions required by drug carriers: the outer shell is responsible for interactions with biocomponents (proteins and cells) which affect biodistribution and the core is responsible for carrying the drug.

PLA-PEG copolymers form micelles or nanoparticles with the polylactic acid (PLA) providing a hydrophobic core and the polyethylene glycol (PEG) forming a hydrophilic shell around the core, with the PEG chains extending into the aqueous media. This hydrophobic core can potentially act as a microreservoir for hydrophobic drugs allowing PLA-PEG copolymer to be used as a drug delivery system. Incorporation of a drug into the core of a delivery system can also protect and stabilise the drug. Utilisation of PLA-PEG copolymers as drug delivery systems would be advantageous due to the small sizes of the micelles and particles formed, which have the potential to circulate for extended periods in the bloodstream as discussed previously (section 1.3.1). PLA-PEG copolymer systems would be easy to administer and sterilise as parenteral drug delivery systems, as their small size would allow them to pass through filters with sub-micron pores, allowing sterilisation by filtration. Their biodegradability and biocompatibility also means that there would be no long-term accumulation after injection into the body.

PLA-PEG copolymers therefore offer control of particle size, good structural stability, water solubility for micelle-forming systems, and potential for control of size through changing the chain length. Their stability should be higher than liposomes as the hydrophobic segments intertwine with each other through inter- and intramolecular interactions, whereas in liposomes hydrophobic interaction is limited to between adjacent lipids (Yokoyama *et al*, 1990). The subject of this thesis is therefore to investigate further the potential of PLA-PEG copolymers for use as drug delivery systems.

Amphiphatic, linear AB block copolymers composed of hydrophobic polylactide (PLA) blocks and hydrophilic polyethylene glycol (PEG) blocks, with PEG content ranging from 25% to over 70% are the subject of the investigations in this thesis. The triblock

copolymer Poloxamer 407 has been included in some of these studies for comparison with PLA-PEG dispersions, as an example of a copolymer that has produced encouraging results in drug delivery. Similarly, PLGA particles are also included for comparison in some studies as an example of biodegradable nanoparticles, with high molecular weight and a hydrophobic surface. The PLA-PEG copolymers discussed here are either directly dispersible in aqueous media, self-associating to form micellar complexes less than 50 nm in diameter or are formed by a precipitation-solvent evaporation method, producing a dispersion of more “solid” nanoparticles of less than 50 nm in the aqueous media. Control over the chain length, ratio of the hydrophilic and hydrophobic components and the copolymer structure (branched or comb-type) is possible, and offers the potential for modifying the size and surface characteristics of the association complexes formed in water. PLA-PEG copolymers with PEG content in excess of 50% form micellar systems, whilst PLA-PEG copolymers with PEG content less than 50% (higher PLA content) are insoluble in water and form more solid nanoparticle structures. Micelles differ from nanoparticles in that they are dynamic systems; that is, they can break down and reform. Micelles also have a minimum concentration required for their formation, the critical micelle concentration (CMC). Nanoparticles do not have this restriction and are therefore less sensitive to dilution. The concept of micelles as a drug delivery system is discussed further below.

1.8 PROTEIN ADSORPTION

All colloidal systems will encounter plasma proteins on injection into the body, modifying the surface and therefore the properties of the system. These proteins can cause opsonization, whereby the adsorption of plasma proteins allows interaction with macrophages and subsequent uptake by these cells. There are several proteins in the blood that can interact with colloidal systems. Albumin is the most abundant blood protein, but does not act as an opsonin. Conversely, the immunoglobulins are likely to affect the fate of a colloidal system as the immunoglobulin IgG is a strong opsonin. Immunoglobulins can bind to particles either by simple adsorption or by a specific reaction with an antigen at the particle surface (Juliano, 1988). An example of the latter is the binding of IgG to liposomes composed of glycolipids, which can trigger specific

IgG binding, leading to direct opsonization or activation of complement. The complement system is composed of twenty different blood proteins that can interact in a complex cascade involving specific binding and proteolytic activation steps. The aim of this complement activation is to produce the “membrane attack complex”, which causes lysis of cells and proteins. The binding of fragments to complement component C3 then opsonises these. Complement is activated by either the formation of an antibody/antigen complex or by accelerating the spontaneous conversion of C3 to its active form, C3b, a known opsonin.

Another protein that plays a role in opsonization is fibronectin. This is a large complex glycoprotein, responsible for helping cell attachment to the extracellular matrix. However, mononuclear phagocytes have cell surface receptors for fibronectin, and it can be a strong opsonin, as illustrated by Pişkin *et al* (1994), who showed that preadsorbing polystyrene particles (2.5 µm) with fibronectin significantly enhanced phagocytosis.

The type of opsonization that occurs will influence the fate of particles. Opsonization by IgG leads to interaction with the Fc receptors on RES phagocytes, causing clearance by first-order kinetics by the spleen. Opsonization with complement-fixing IgM, which allows interaction with receptors for C3 fragments, leads to accumulation in the liver (Juliano, 1988). Determining which proteins adsorb to the particle surface can therefore aid the understanding of the processes that are involved in the biodistribution of colloidal systems.

Protein adsorption to colloidal systems can be detected by polyacrylamide gel electrophoresis (PAGE). In this technique, the particles can be incubated with plasma, then washed and the bound proteins compared with protein standards. This technique, while providing valuable information, has the drawback in that loosely bound proteins will probably be removed by washing. SDS-PAGE (sodium dodecyl sulphate-PAGE) was used to study the adsorption of plasma and serum proteins to polystyrene microspheres coated with the block copolymers, poloxamers and poloxamines (Norman *et al*, 1993). These studies showed that the amount of protein adsorbed to the block copolymer coated system was less than that for the polystyrene system. Also, with increasing PEO chain length, the total amount of protein adsorbed was reduced. However, protein adsorption was not just dependent on hydrophilicity, but on other

factors such as surface conformation, density and steric stabilisation effects. The reduction in the adsorption of larger molecular weight proteins to coated systems over polystyrene was attributed to difficulties in penetrating the PEO layer to reach the polystyrene surface. Regarding the total amount of protein adsorbed, the hydrophilic/hydrophobic balance between the PEO and PPO appears to be the critical parameter. This was illustrated with poloxamers, where those having the same PPO chain length adsorbed similar amounts of protein, whereas poloxamers with similar PEO chain lengths but longer PPO chain lengths reduced protein adsorption further. This is due to the anchoring effect of the PPO chains. Poloxamer 407 and Poloxamine 908 showed the least protein adsorption, as would be expected from their biodistribution patterns, with no apparent differences between the proteins adsorbed to particles coated with these systems. Tan *et al* (1993) also found the poloxamers and poloxamines with higher HLB values more effective at reducing adsorption of plasma proteins to particles. They found that Pluronic F108 and Tetronic T908 were equally effective in preventing fibrinogen adsorption, while being more effective at preventing adsorption than similar copolymers with lower HLB values. Further, they again illustrated the importance of the anchoring PPO block by considering PEG homopolymer (Mw 22000). This was the least effective at preventing protein adsorption, when compared with F108, T908 and sodium dodecyl sulphate, despite the greater molecular weight of the PEG compared with the PEO chains of the F108 and T908.

Similarly, Blunk *et al* (1993) analysed polystyrene particles (60 nm) coated with poloxamers 184, 188 and 407 with two-dimensional PAGE, and found that the more hydrophobic the particles, the greater the total protein adsorbed. The authors found differences in both the qualitative and quantitative protein adsorption patterns, with the more hydrophobic poloxamer 184 adsorbing more protein than the other poloxamers studied, with IgG and transferrin being the major proteins detected.

More recent research has shown that for polystyrene and PLGA particles coated with either Poloxamer 407, Poloxamine 904 or Poloxamine 908, increasing the length of the PEO chain decreased protein adsorption to the surface (Armstrong *et al.* 1997). Comparing the polystyrene and PLGA particles, the naked polystyrene particles bound 25% more human serum albumin (HSA) than the naked PLGA particles, whereas polystyrene particles coated with Poloxamer 407 or Poloxamine 908 were equally

effective in reducing protein adsorption, but when coated onto PLGA particles, Poloxamer 407 had a clear advantage. Coating of polystyrene particles with the PLA-PEG copolymers (1.5:2 and 2:5) gave a similar reduction in protein adsorption to that observed with Poloxamine 908, with no protein layer being detected by photon correlation spectroscopy (PCS) on the coated particles after incubation with HSA (Stolnik *et al*, 1994b).

Polyethylene oxide (PEO) has been much studied as a means of preventing protein adsorption. Much work has centred on the block copolymers, poloxamers and poloxamines, as discussed above. Amiji and Park (1992) showed that poloxamers having 56 or more PO residues were better at preventing plasma protein adsorption and platelet adhesion than poloxamers with 30 PO residues. This research is not restricted to colloidal systems. Protein adsorption has been studied with regard to many biological surfaces, including fused-silica capillaries in capillary electrophoresis, where protein adsorption can also be reduced by coating with poloxamers (Ng *et al*, 1994).

With liposomes, PEG-DSPE has been shown to produce a non-specific reduction in protein binding to liposomes over conventional liposomes (Allen, 1994b). Conventional liposomes have been shown to adsorb proteins at their surface within one minute of incubating in plasma, whereas it took several hours for PEG-containing liposomes to adsorb significant amounts. The proteins that were adsorbed could be removed by gel permeation chromatography (GPC), suggesting weak binding. Similarly, the uptake of poly(D,L-lactic acid) nanoparticles by lymphocytes and monocytes has been studied, with and without a PEG (Mw 20000) coating, in the presence and absence of plasma (Leroux *et al*, 1994). The PEG coating significantly decreased the nanoparticle uptake by both the monocytes and lymphocytes, in both saline and plasma, giving evidence of the protein resistance of PEG.

The mechanism whereby PEG/PEO induces protein resistance is thought to be due to a steric repulsion effect. As the protein approaches the PEO surface by diffusion, there is a van der Waals attraction between the protein and the PEO surface through the water. Closer approach of the protein results in compression of the PEO chains, causing a steric repulsion effect (Jeon *et al*, 1991). There is a further van der Waals attraction between the substrate (i.e. the hydrophobic surface) and the protein. This attraction decreases with increasing PEO chain length and surface density. Therefore, a long PEO

chain length and high surface density should lead to the most protein resistance, with surface density being more important than chain length (Jeon *et al*, 1991). One of the reasons for the success of PEO in protein resistance among the water soluble synthetic polymers is that it shows the weakest van der Waals attraction. The magnitude of the van der Waals attraction becomes negligible compared to the steric repulsion caused by compression of the PEO chains (Jeon *et al*, 1991). Studies have also shown that linear PEO is more effective than branched PEO at preventing protein adsorption (Bergström *et al*, 1994). This is believed to be due to a restriction in the conformational freedom of the branched PEO chains compared with the linear chains. Other factors that are thought to be important in the ability of PEO to resist protein uptake are the hydrophilicity, the terminal group chemistry, the chain mobility and steric exclusion effects (Llanos and Sefton, 1993). The unique solution properties and molecular conformation of PEO in aqueous solution are also important. PEO is thought to fill the voids in the water structure while minimally disturbing the water structure, leading to a decreased tendency for hydrophobic interactions (Stolnik *et al*, 1995). Water molecules are hydrogen bonded to the ether oxygens of PEO, forming “structured” water. The dependence of protein resistance on PEO chain length has been suggested as due to low molecular weight PEO only being associated with tightly-bound water. Conversely, at higher PEO chain lengths, the chain begins to fold in on itself, trapping more loosely-bound water between the segments to form a repulsive hydrated layer. This folding is only possible at longer PEO chain lengths, with at least 1500 gmol⁻¹ being required (Stolnik *et al*, 1995). The high mobility of the chains also prevents protein adsorption by decreasing the contact time between the surface and the proteins.

As well as opsonins, there are plasma proteins that can retard or inhibit uptake of particles by the RES, and these are known as dysopsonins. Moghimi and Patel (1989) found that saturated ammonium sulphate fractions in the ranges 0-35% (γ -globulins) and 50-65% (small molecular proteins) suppressed liposome uptake by Kupffer cells. Later research studied uncoated polystyrene and colloidal gold particles, both uncoated and coated with poloxamine 908 (Moghimi *et al*, 1993b). The interaction of these particles with freshly isolated rat liver sinusoidal cells was examined by electron microscopy.

Both of the uncoated systems were found in the Kupffer cells, with the opsonization of the gold particles being identified as due to fibronectin. In contrast, there was little uptake of the Poloxamine 908 coated particles by the Kupffer cells, indicating that the Poloxamine 908 was preventing the adsorption of fibronectin to the surface of the gold particles. The Kupffer cells were unable to recognise the Poloxamine 908 particles before and after opsonization, whereas liver endothelial cells endocytosed the particles before opsonization but did not recognise the particles after the opsonization process.

This was thought to be a result of dysopsonic activity in the plasma. Further studies using polystyrene particles (whose uptake by phagocytes is known to be independent of opsonization) showed that although coating of the particles with Poloxamine 908 dramatically reduced their uptake by liver sinusoidal cells, the interaction was further reduced in the presence of plasma or serum. A heat stable serum component ($M_w > 100$ kDa) was found to regulate this effect. The authors therefore concluded that although Poloxamine 908 effectively blocked opsonization, it still allowed dysopsonisation to take place. Dysopsonic activity is also apparent with naked polystyrene particles, where a reduction in the uptake by Kupffer cells is noted after incubation in the presence of serum compared with particles incubated with no serum present (Dunn *et al*, 1995).

Recognition and uptake of colloidal systems by the reticuloendothelial system is therefore due to a combination of the hydrophobicity of the surface, the opsonization of the surface by plasma proteins of the blood, and dysopsonisation by plasma (or serum components). Biodistribution is controlled by a balance of opsonins and dysopsonins that adsorb to the particle surface depending on its characteristics.

1.9 MICELLES

When the concentration of aqueous solutions of many amphipathic substances is increased, a distinct deviation from solution ideality occurs as self-association results and micelles are formed. This change can be detected experimentally by measuring, for example, surface tension, the molar conductivity of the solution (for ionic micelles), or light scattering, and plotting these parameters as a function of concentration. The change in the slope indicates the onset of non-ideality where micelles are formed and is referred to as the critical micelle concentration (cmc). The micelles are in dynamic

equilibrium with free molecules (known as monomers or unimers) and are therefore continually breaking down and reforming.

Micelle formation is brought about by the amphiphiles reaching a state of minimum free energy. Water-hydrocarbon contacts are entropically unfavourable, whereas micelle formation leads to the more favourable hydrophobic interactions between the non-polar groups of the amphiphiles by removing the hydrophobes from the aqueous solution. The hydrophobic groups are therefore in the core of the micelles and the hydrophilic groups are in contact with the aqueous medium, forming a shell around the micelle core, otherwise known as the palisade layer or mantle.

Micelles are considered to be in an association-dissociation equilibrium with their monomers. The cmc tends to be a range of concentrations, where the solution shows a gradual change in properties rather than a precise concentration, as micelle formation is not a distinct phase but remains in equilibrium with monomers. It is therefore difficult to determine the cmc exactly, and there can be wide variability of values between methods (Kabanov *et al*, 1992; Yu *et al*, 1992). The monomer concentration remains fairly constant above the cmc, in equilibrium with the micelles.

Block copolymers have potential in drug delivery systems as each block can have different characteristics, allowing it to perform a specific function. A block copolymer consisting of two blocks, of which one is soluble and one insoluble in the surrounding media can form intermolecular micelles. Thus, in aqueous media, a block copolymer with hydrophobic and hydrophilic blocks could form micelles with the hydrophobic block as the micelle core and the hydrophilic block surrounding the core and in contact with the aqueous media. AB block copolymers are most suitable for micelle formation due to their size, association number and micelle stability due to the simple architecture of their molecules (Yokoyama, 1992). The rate of dissociation of the block copolymer micelles into free polymer chains is likely to be slow, as the inner core is stabilised by hydrophobic interactions. These hydrophobic interactions may be strong, giving the cores a low mobility and solid-like character, as opposed to the liquid-like cores of lower molecular weight micelles (Kwon *et al*, 1993a).

1.9.1 Factors Affecting Micellar Properties

Block copolymers form micelles with much lower cmc values than those for low molecular weight surfactants (Yokoyama *et al*, 1994a). This is because a block copolymer molecule has more interaction sites for other copolymer molecules than low molecular weight surfactants. A consequence of this lower cmc is that stable micelles will exist in an *in vivo* situation for longer periods of time than for a low molecular weight surfactant, and drug delivery can be controlled by the micelle properties rather than the properties of the single copolymer chains.

The micellar behaviour of block copolymers mostly depends on their molecular characteristics, which are the type, molecular weight and block composition of the copolymer, and also, the selectivity and solubility parameters of the solvent (i.e. whether polar or non-polar), the temperature and the concentration ranges studied.

An increase in molecular weight usually results in an increase in micellar diameter and aggregation number (Bahadur *et al*, 1985). A similar trend is seen with an increase of the water insoluble block of the copolymer, in this case the hydrophobic chain length.

Generally, cmc is also seen to decrease with increasing hydrophobe (Oranli *et al*, 1985).

Block copolymers with PEO (PEG) as their hydrophile show an increase in cmc and decrease in aggregation number with increasing PEO chain length, and therefore increasing hydrophilicity.

For most non-ionic surfactants, an increase in micellar hydrodynamic radius and decrease in cmc are observed with increasing temperature (Al-Saden *et al*, 1982). This increase is seen up to the cloud point, where the solution becomes turbid and there is separation into two phases (section 4.4). An increase in aggregation number may also be noted (Luo *et al*, 1993). However, there are exceptions, such as with micelles formed using styrene-butadiene and styrene isoprene block copolymers in n-heptane, where an increase in temperature leads to a decrease in the hydrodynamic radius. This decrease is thought to be accounted for by a decrease in micellar weight or aggregation number (Bahadur *et al*, 1985; Oranli *et al*, 1985). For the poloxamers, it has been noted that not all of these copolymers form micelles, and in some cases micellisation only occurs when the temperature is increased to the critical micelle temperature (CMT). The CMT is mainly dependent on the length of the hydrophobic block, although the length of the hydrophilic block does have some influence (Almgren *et al*, 1992).

Micelles are assumed to be dense spherical formulations and as such will undergo little deformation in moderate concentrations as they approach each other. However, as the concentration is increased, the interaction becomes more important, determining the properties of the solution. Here, the micelle experiences Van der Waals forces of attraction between the amphiphiles and the solvent, as well as the local interactions between micelles (Lobaskin and Pershin, 1993). An increase in temperature will also increase intermicellar interactions (Lobaskin and Pershin, 1993) and a decrease in micelle-solvent interactions will occur (Al-Saden *et al*, 1982). Interaction of the micelles will cause contraction of the polymer chains, squeezing out the solvent, even if not much solvent is present.

As the concentration is increased, starting from a dilute solution of the block copolymer, where the copolymer exists as monomers, the hydrodynamic radius increases (Al-Saden *et al*, 1982; Lobaskin and Pershin, 1993). When the cmc is reached, the hydrodynamic radius of the micelles is constant (Al-Saden *et al*, 1985; Lobaskin and Pershin, 1993).

At concentrations far from the cmc, micelle properties such as aggregation number are only weakly dependent on concentration (Leibler *et al*, 1983). The equilibrium between monomers and micelles will shift towards the micelles as the concentration is increased (Oranli *et al*, 1985), and with further increases gelation may occur (Almgren *et al*, 1992; Luo *et al*, 1993). This may also occur with an increase in temperature, when the micelles pack close enough to prevent micelle translational motion. The amount of water associated with the PEO becomes much less as the temperature increases, allowing the micelles to pack closer together. Gelation results when the micellar solution reaches a concentration where the micelles can pack closely enough to undergo a transition from mobile fluid to immobile gel.

1.9.2 Drug Loading Into Micelles

Solubilisation has been defined as the preparation of a thermodynamically stable isotropic solution of a substance normally insoluble or very slightly soluble in a given solvent by the introduction of an additional amphiphilic component or components (Attwood and Florence, 1983). Therefore, as surfactants are amphiphiles, which form micelles at concentrations above the cmc, solubilisation of drugs by micelles can occur.

Drug loading into micelles is usually referred to as solubilisation, but other terms may also be used, including incorporation. Similarly, the compound or drug that is incorporated/solubilised by the micelles is often referred to as the solubilisate.

1.9.2.1 Sites of Solubilisation

The site of solubilisation within the micelle is important for the successful retention of the solubilised agent and control of the release into the environment (Goldenberg *et al.*, 1993). Solubilisation deep within the micellar core would be expected to be the least easily displaced and require a more specific interaction of the micelle with the drug target to allow release of the drug at the appropriate site. Micelles from conventional surfactants and block copolymer micelles have solubilised a wide range of drug compounds, and block copolymer micelles can also solubilise homopolymer. In this case, true solubilisation can only occur when the molecular weight of the homopolymer is less than that of the miscible block of the copolymer (Quintana *et al.*, 1995).

There are two possible sites of solubilisation in PEG-containing micelles. The chemical nature of the solubilisate determines in which of these sites solubilisation will occur. The first site, that of the non-polar core will solubilise hydrophobic compounds, whereas the second site, that of the polyethylene oxide shell surrounding the core (the palisade layer), will solubilise more polar compounds. As most drugs are hydrophobic, they can be incorporated into the micelle core either by covalently conjugating the drug to the monomer molecule or by noncovalent bonding, such as hydrophobic or ionic interactions (Yokoyama, 1992). However, there are examples in the literature of substances solubilised in the hydrophilic shell of micelles. Elworthy and Lipscomb (1968) concluded that the most likely site of solubilisation of griseofulvin in surfactants based on hexadecanol and PEG was the polyoxyethylene part of the micelles. They based this conclusion on results that PEG solutions increased the solubility of griseofulvin, and that increasing the length of PEG chains in the micelles also increased solubility. Mukerjee (1971) observed that polyoxyethylated nonionic micelles could, in theory, solubilise organic substances or electrolytes in their mantles, as these areas can behave as concentrated solutions of oxyethylene groups. The oxyethylene groups at the surface of a micelle are likely to be in closer proximity due to the geometry of micelles, than solutions of PEG, where the polymer exists as random coils. Mukerjee also noted

that *p*-hydroxybenzoic and *p*-aminobenzoic acids were predominantly solubilised in the polyoxyethylene mantle of surfactants composed of alkyl chains and polyoxyethylene. This may be due to hydrogen bonding between the hydroxyl groups of the drugs and the polyoxyethylene chains. Indeed, when these drugs were esterified, more hydrophobic compounds were produced from the loss of their hydroxyl groups, decreasing the ability to hydrogen bond. The solubility of the drugs in the core increased, with a corresponding decrease in solubility in the polyoxyethylene mantle (Mukerjee, 1971).

Differentiation between the two sites of solubilisation can be determined by techniques such as NMR, UV Spectroscopy, X-ray diffraction, ESR and other indirect techniques including solubility in model solvent systems (Goldenberg *et al*, 1993). It is however difficult to model micellar domains using model solvents that are not amphiphilic and form isotropic structures. Added discrepancies would occur if the solubilisation were at the hydrophobic/hydrophilic interface. The differences between solubility in the micelle core and that in bulk liquid are partly due to the Laplace pressure inside a micelle, which results from the curved interfacial region of the micelle, and opposes the entry of molecules into the micelle. This excess pressure inside spherical droplets, ΔP , is defined by the Laplace equation:

$$\Delta P = \frac{2\gamma}{r}$$

where γ is the interfacial tension and r is the radius. Micelle interiors may also be more solid-like than bulk hydrocarbons. Mukerjee's theoretical model for the prediction of location of solubilisate could also be used (Mukerjee, 1971). This is based on the assumption that the amount of the agent solubilised in the core and in the palisade layer is proportional to the number of equivalents of surfactant hydrophobe chain moiety and the number of equivalents of surfactant ethylene oxide groups, respectively. However, it has been shown that the predictions from this model do not match experimental results, which suggests that the model may be an over-simplification. This casts doubt on the usefulness of a theoretical model which does not account for factors such as micelle size, solubilising capacity and agent-agent-interaction (Goldenberg *et al*, 1993).

There was also a lack of agreement between the experimental results from different methods presented in the paper by Goldenberg *et al* (1993), which meant that no firm conclusions were possible from their results about the location of the solubilisate in the micelle.

1.9.2.2 Factors Affecting Solubilisation

Solubilisation of agents in the micellar core increases the size of the micelles in two ways (Mukerjee, 1980; Al-Saden *et al*, 1982). The core or palisade layer of the micelle is enlarged by the solubilisate, and the association number also increases due to a need for additional surfactant molecules to maintain the integrity of the micelle and increase its volume, although this generally only results when solubilisation is in the core (Attwood *et al*, 1971). This has been noted with both conventional surfactant micelles (Attwood *et al*, 1971) and block copolymer micelles (Quintana *et al*, 1995), and the larger the drug, the greater the effect on the association number. Generally, solubilisation capacity increases with an increase in hydrophobe chain length (hydrophobicity) when solubilisation takes place within the micellar core (Jacobs *et al*, 1972; Al-Saden *et al*, 1982). This dependence may be linear or may increase faster than the hydrophobe content. There may also be a limit in the increased solubilisation capacity seen by increasing chain length. Arnarson and Elworthy (1981) noted that for a series of nonionic polyoxyethylene mono-ethers (C_xE_y , where x is the number of carbons in the hydrocarbon chain and y the number of polyoxyethylene groups), the solubilising ability of the micelles increased up to C_{16} , but further increases in hydrocarbon chain length led to a decrease in solubilisation. They speculated that this unexpected decrease was due to intrusion of part of the polyoxyethylene chain into the hydrocarbon core of the micelles. This effect may be due to an attempt to maintain the longer hydrocarbon chains of the core in a liquid state.

When the solubilisation takes place in the palisade layer (the PEG shell), increasing the ethylene oxide chain length usually gives an overall increase in solubilisation capacity as although the aggregation number decreases, the number of micelles formed increases thus giving an increased total amount solubilised (Al-Saden *et al*, 1982; Goldenberg *et al*, 1993). Conversely, decreasing the ethylene oxide chain length in a series of nonionic surfactants will give an increase in hydrophobicity and corresponding increase in

solubilisation efficiency as defined by the moles of drug solubilised per mole of ethylene oxide (Goodhart and Martin, 1962; Gouda *et al.*, 1970).

Hurter and Hatton (1992) have studied in some detail the solubilisation of polycyclic aromatic hydrocarbons into poly(ethylene oxide-propylene oxide) micelles. They found that the micelle-water partition coefficient, K_{mw} , of the compounds increased with increasing polypropylene oxide content (i.e. increasing hydrophobe content) for a given total polymer concentration. However, when K_{mw} was normalised with PPO content, an increase in the partition coefficient was still observed; the normalised partition coefficient, K'_{mw} , should be constant as the mass fraction of PPO increases if the solubilisation behaviour was solely dependent on the composition of the polymer in solution (Hurter *et al.*, 1993). As a small increase in K'_{mw} was seen instead, this suggested structural changes within the micelle due to changes in polymer composition. These authors also studied the effect of concentration on solubilisation, and found that the partition coefficient, K_{mw} , remained constant over the concentration range studied. This indicated that the micelle structure was unchanged and the increase in solubilisation with concentration was due to an increase in the number of micelles rather than an increase in micelle size. It is usual for an increase in concentration and/or temperature to give an increase in the amount solubilised. The temperature effect is particularly noticeable in systems where the micelle size increases with temperature. An example of this was given by Saito *et al.* (1994), who showed that the solubilisation of estriol in Pluronic L-64 micelles increased with increases in both temperature and concentration. They attributed this increase in solubilisation with temperature as due to an increase in micelle size and increased wetting of the drug. It is important to remember that the aqueous solubility of the agent may also increase, as the results may be misleading if this is not taken into account. Another example with Pluronic L-64 micelles was provided by Pandya *et al.* (1993), who showed an increase in solubilisation of diazepam with increasing temperature and concentration. The increased solubilisation with temperature was again attributed to an increase in association number and size of the micelles, and also to a decrease in cmc, which is affected by temperature. A decreased cmc leads to an increase in the micelle concentration, thus improving solubilisation.

Hurter *et al.* (1993) considered a theoretical model for solubilisation based on the mean-

field lattice theory. This supported the conclusions of the previous experimental work of this group (Hurter and Hatton, 1992) regarding the increase in micelle-water partition coefficient with increased polypropylene oxide content of the copolymer. The model also showed that for naphthalene being solubilised by Pluronic micelles, the amount solubilised in the core fell off sharply as the radius of the core (i.e. the outer edge of the homogenous PPO core) was approached, and thus at the beginning of the polyethylene oxide corona region. They attributed this to a greater restriction on the possible orientations of the solute molecules in the interfacial region (between the PPO and PEO regions), as some conformations would result in unfavourable solute/EO segment and solute/water contacts. From this, it is apparent that smaller micelles will solubilise less if there is a significant energetic disadvantage to the solute in penetrating the corona of the micelle. This is because there will effectively be a “dead volume” in the core which will be less attractive to the solute molecule than the more hydrophobic inner core (Hurter and Hatton, 1992). Therefore, as this dead volume is of constant thickness, the fraction of the core volume affected will decrease as core size increases.

Hurter and Hatton (1992) also compared solubilisation by micelles prepared from the branched Tetronic copolymers with the Pluronic micelles. They concluded that the structure of the polymer was important, with linear copolymers (Pluronics) solubilising more drug than branched copolymers (Tetronics). This was thought to be due to the ability of the linear copolymers to form tighter micelles, due to configurational restraints on the branched polymers, leading to a more hydrophobic environment in the micelle core of the linear copolymers.

Although in general, micelles formed from block copolymers and conventional surfactants behave in a similar manner, there are important differences between them. Block copolymer micelles consist of blocks of several monomer units that can have many different configurations. The area occupied by each polymer at the interface between the core and the aqueous media is relatively large in order to gain greater entropic freedom, and is partly protected by the chains of the block copolymer that are compatible with the media (Nagarajan *et al.*, 1986). The entropy due to the numerous configurations of the polymer chains compensates for the increased interfacial free energy, but with conventional surfactants, fewer configurations are possible due to their shorter chains. Consequently, the area occupied by each surfactant molecule is smaller

to ensure that the free energy of the interface is small. Therefore, micelles formed from conventional surfactants depend on interfacial interactions and give relatively rigid structures compared with block copolymer micelles. These interfacial interactions are expected to affect the solubilisation in surfactant micelles, whereas interactions between the solubilisate and polymer block will affect the solubilisation in block copolymer micelles (Nagarajan *et al*, 1986).

1.9.3 Micelles as a Drug Delivery System

The structural properties of micelles, with their hydrophobic core and hydrophilic outer shell, make them potential candidates for drug delivery, particularly for drug targeting applications. As low water solubility of drug-polymer conjugates can lead to synthesis and injection problems, due to precipitation caused by high localised concentrations (Yokoyama *et al*, 1994a), the water solubility of micelle systems is also an advantage.

As micelles are formed by intermolecular noncovalent interactions between polymer chains, and are in equilibrium, they can eventually break down into free polymer chains and complete excretion is possible via renal filtration (due to their low molecular weight). Therefore, long-term accumulation of micelles in the body is unlikely to be a problem. Several groups have studied the ability of micelles to carry drug in an *in vivo* situation. One of the most interesting and successful applications of micelles for drug delivery is the work by Yokoyama *et al* (1990, 1991, 1993, 1994a, 1994b, 1994c, 1994d), and Kwon *et al* (1993a, 1993b, 1994a, 1994b, 1995), which has been described over the past few years.

These groups have synthesised block copolymers composed of poly(aspartic acid) (P(Asp)) and PEG. Aspartic acid is a naturally occurring amino acid, and in polymeric form, may be biodegradable. The anticancer drug, adriamycin (ADR), was conjugated to the copolymer, so that the drug would remain with the carrier until released in a manner controlled by the carrier, and to allow very high quantities of adriamycin to be loaded (Kwon *et al*, 1994b). Adriamycin is a very effective anticancer drug, but has many toxic side effects, including cardiotoxicity, that are dose-dependent (Yokoyama, 1992). As P(Asp) is a polyamino acid, it is possible that ADR may be released from the copolymer by hydrolysis, after uptake by the target cells (Yokoyama, 1992). These block copolymer conjugates were water soluble and shown by gel permeation

chromatography (GPC) to form micelles in aqueous solution (Yokoyama *et al.*, 1993). Micelle formation has also been confirmed *in vitro* (Yokoyama *et al.*, 1990) and *in vivo* (Yokoyama *et al.*, 1991), using gel permeation chromatography. For the *in vivo* experiments, plasma samples were taken at one hour post-injection and when analysed by GPC, the elution volume of the samples corresponded to that for micelles. The micelles were reported to be between 20 nm to 40 nm in size (Kwon *et al.*, 1994a). *In vivo* studies of the PEG-P(Asp(ADR)) micelles have been very promising. High anticancer activity was found against murine leukemia P388 and several solid tumours. When used against P388 leukemia (intraperitoneal injection in 0.9% NaCl solution), this system prolonged the survival time of mice (Yokoyama *et al.*, 1990). Free adriamycin will also prolong the survival time of mice inoculated with these tumour cells, but with serious side effects, including a pronounced decrease in body weight (15%). The PEG-P(Asp(ADR)) micelles were able to achieve comparable survival times with only a temporary weight loss, and possessed a wider therapeutic range than free adriamycin. Similarly, increased or comparable anticancer activity was achieved with solid tumours after intravenous injection of PEG-P(Asp(ADR)) micelles (Yokoyama *et al.*, 1991). Significantly higher antitumour activity was observed for murine colon adenocarcinoma 26 (C26) with the PEG-P(Asp(ADR)) micelles over adriamycin, which gave only moderate tumour inhibition at the maximum tolerated dose (10 mg/kg) (Yokoyama *et al.*, 1994a). The antitumour activity was highly dependent on the composition of the block-copolymer conjugate (Yokoyama *et al.*, 1994b). The compositions of the conjugates are described by three numbers, e.g. 120-81(84), where the first number refers to the molecular weight of the PEG chain, which would be 12000 in this case, the second refers to the molecular weight of the P(Asp) chain (8100) and the number in brackets represents the adriamycin substitution percentage with respect to the Asp residue. Thus, the authors found that whereas a PEG-P(Asp(ADR)) copolymer-conjugate with a composition of 10-48(12) did not show any tumour inhibition against the control over 35 days, for the compositions 20-10(44), 50-09(73), 120-21(104), 120-41(78) and 120-81(84), the tumour completely disappeared. Conversely, the *in vitro* cytotoxic activity of the conjugates against C26 tumour cells was independent of composition. The authors concluded that this difference between *in vitro* and *in vivo*

reflected the effective selective delivery of the conjugates to the tumour.

Poly(aspartic acid)-poly(ethylene glycol) micelles conjugated with adriamycin have shown selective delivery to tumours within mice (Yokoyama *et al.* 1994a). The authors postulated that this was due to the hydrated outer PEG shell of the micelles, which allowed them to be preferentially taken up and retained by the tumour, in a way similar to the enhanced permeation and retention of macromolecules described by Matsushima and Maeda (1986).

These micelles have also shown long circulation times in blood, and a corresponding low uptake by the reticuloendothelial system (Kwon *et al.*, 1993a, 1994a, 1994b). Free adriamycin binds rapidly to tissues after iv. injection, and the levels circulating in the blood drop quickly. The PEG-P(Asp(ADR)) conjugates showed a greater accumulation in tumours after 24 hours (10 % dose per g tumour) over free adriamycin (0.90 % dose per g tumour), indicating that the previous conclusion of selective delivery to tumours was correct.

More recent research has shown the presence of physically entrapped adriamycin in the micelles, in addition to the chemically conjugated adriamycin (Yokoyama *et al.*, 1994c, 1994d, 1995). The effect of this physically entrapped adriamycin was subsequently investigated to study its contribution to the anti-tumour activity of the PEG-P(Asp(ADR)) micelles, and it was concluded that this adriamycin was likely to contribute to the anti-tumour effects (Yokoyama *et al.*, 1994c). Physically entrapped adriamycin could be removed by dialysis in organic solvents. *In vitro* serum stability experiments indicated that the presence of physically entrapped adriamycin decreased the stability of the PEG-P(Asp(ADR)) micelles in rabbit serum (Yokoyama *et al.*, 1994d). The presence of this physically entrapped adriamycin in the PEG-P(Asp(ADR)) micelles suggests that PEG-P(Asp(ADR)) micelles could be used to carry other hydrophobic anti-tumour drugs, to increase the tumoricidal activity of the conjugated adriamycin.

The same research group has also studied the physical entrapment of adriamycin into AB block copolymer micelles consisting of poly(ethylene oxide-co- β -benzyl L-aspartate) (PEO-PBLA) (Kwon *et al.*, 1995). *In vitro* experiments using GPC and serum albumin showed the adriamycin to be stably incorporated into the micelles.

Another group has also explored micelles as a potential drug delivery system. Kabanov

et al (1989) considered the use of Pluronic P85 micelles for targeting neuroleptic drugs to the brain. They injected a micellar solution loaded with the drug haloperidol intraperitoneally into mice, and compared the biological action of the drug in micelles with that of free drug by considering the development of a specific neurolepsy and its lethal dose (LD₉₅). The authors observed a five-fold increase in the toxicity of the haloperidol in micelles compared with free drug (shown by a decrease in LD₉₅). Insulin was then conjugated to an “anchor” moiety, which was a Pluronic analog, BPEA (butylpoly(oxypropylene)-poly(oxyethylene) ether of 2-hydroxyacetaldehyde), to give Ins-BPEA. This allowed incorporation of the target-recognising molecule (i.e. insulin) into the Pluronic P85 micelles. When this was compared with free drug, the toxicity increased by twenty-five-fold. This was concluded to be a result of the insulin moiety on the surface of the micelles interacting with the insulin receptors on the surface of cells, leading to increased interactions between the micelles and membranes. A brain-specific antibody, glia fibrillar acid antigen of brain glial cells (anti-GFA) was then conjugated to the BPEA molecules. This drastically increased the toxicity of haloperidol, giving an increase of nearly 500-fold over the free drug. Although there was an increased toxicity when the anti-GFA was incorporated into the Pluronic P85 micelles without the BPEA, it was lower than with the BPEA bound antibodies and the BPEA method was successful in binding all the antibodies tested. However, these authors did not clarify whether the increase in *in vivo* activity was due to micelle formation or due to an increase in the permeability of biological membranes owing to the polymeric amphiphile (Yokoyama *et al*, 1994a). There was also no evidence for micelle formation under physiological conditions. Micelle formation was assumed, but due to the high stated cmc value of Pluronic P85 micelles (4.5% w/v), this was not necessarily true.

However, a later paper (Kabanov *et al*, 1992) states that after measurement of the cmc of Pluronic P85 micelles using the dye solubilisation technique, the cmc was found to be 0.01% w/v. No comment is given about the discrepancy in values between the two papers. If the latter value were correct, it would be more reasonable to expect micelles to be present in circulation. However, the concentrations of Pluronic P85 injected were high at 10% w/v, which could cause cell membrane damage.

This later paper by Kabanov *et al* (1992) again studied Pluronic P85 as a means of drug

targeting from blood into the brain, and also to the lungs. The diameters of the micelles in this case were in the range of 11 - 17 nm. The model drug, fluorescein isothiocyanate (FITC) was incorporated into the micelles, which could then be studied using fluorescence. When injected intravenously into mice, a marked increase in the amount of FITC delivered to the lungs was noted when solubilised in Pluronic P85 when compared with free FITC. It has been suggested that this may be due to the membranotropic properties and small size of the micelles. The conjugation of Pluronic P85 molecules with either protein ligands to selectively interact with specific cell types, or antibodies against a target-specific antigen was again discussed. Firstly, conjugation with insulin "vector" which, as it is capable of specific binding with various cell types, showed an increase in the FITC fluorescence in all tissues including the brain. Secondly, conjugation of the pluronic with the antibodies to the antigen of brain glial cells (α_2 -glycoprotein) was described, where a considerable increase of fluorescence due to FITC was seen in the brain and a decrease seen in the lungs. It is possible that the micelles themselves penetrate the blood brain barrier (BBB) by, for example, transcytosis, but it must be considered that the antibody can also interact on the external side of the BBB.

Control of drug release from micelles can also be initiated from an external source. Takeoka *et al* (1995) showed that electrochemical drug release was possible from micelles, by producing redox-active micelles of non-ionic surfactants with a ferrocenyl moiety (FPEG). This system forms micelles in the reduced form (FPEG), but exists as monomers in the oxidised form (FPEG⁺). This reversible change could be electrochemically controlled, to effect drug release. The hydrophobic model drug, perylene, was incorporated into the micelles, and could be released by using controlled potential bulk electrolysis.

Another example of micelle use in drug delivery is given by Alkan-Onyuksel *et al* (1994). They prepared mixed micelles from bile salt and phospholipid, and loaded them with the poorly water soluble anticancer drug, taxol. On dilution, the micelles spontaneously formed drug-loaded liposomes, but were stored as freeze-dried mixed micelles due to their greater stability. The mixed micelle formulation retained the anticancer activity when tested in cultured cell lines and seemed less toxic than the standard nonaqueous vehicle of taxol containing Cremaphor EL in survival (LD₅₀) tests

in mice.

Micelle-containing products have reached the market place. One, known as “Amphocil”, is composed of disk-like mixed micelles of cholesteryl sulphate and the drug, amphotericin, and this product shows an improved therapeutic index over both the free drug and another marketed micellar formulation, “Fungizone”, which consists of amphotericin in deoxycholate micelles (Lasic, 1992).

1.10 AIMS OF THE PROJECT

This introduction has discussed using colloidal systems as a means of delivering drug within the body. Previous work involving coating of hydrophobic nanoparticles with block copolymers containing the hydrophilic polymer, polyethylene oxide (PEO), otherwise known as polyethylene glycol, has been discussed. The characteristics of these nanoparticles and their effect on the eventual fate of the nanoparticles within the body have been described, as have the successes achieved so far. This project aims to continue this work by studying a novel range of block copolymers, composed of the hydrophobic biodegradable polylactide (PLA) with the hydrophilic biocompatible polyethylene glycol (PEG). These copolymers have the necessary hydrophilic PEG to provide a hydrophilic shell, with the hydrophobic core to allow the uptake of hydrophobic drugs.

The aim of this project is therefore to explore the PLA-PEG copolymers as potential drug delivery systems for use in drug targeting applications. Studying this will involve a wide range of experiments to investigate the different attributes of the nanoparticles, from the physicochemical properties to the drug loading and biodistribution. The surface chemistry, which is important in determining the extent and type of protein adsorption after intravenous injection into the blood, can be determined by the highly sensitive surface analytical techniques static secondary ion mass spectrometry (SSIMS) and X-ray photoelectron spectroscopy. Rheological analysis and determination of the cloud point temperatures can give further information on the surface PEG. This information can be used to predict and explain the *in vivo* behaviour of the systems. As potential drug delivery systems, the ability of the PLA-PEG systems to load drug is very important, and will be studied with the model hydrophobic drugs, sudan black B

(SBB) and testosterone. Release of drug is also crucial and can be investigated with sudan black B.

Finally, to allow the complete picture, the systems must be able to incorporate a radiolabel, allowing the fate of the systems to be followed in an *in vivo* situation. Radiolabelling of the PLA-PEG systems and biodistribution in the rat will therefore also be considered.

CHAPTER TWO

MATERIALS AND METHODS

2.1 INTRODUCTION

This chapter introduces most of the methods used for preparing and characterising PLA-PEG nanoparticles and micelles. From chapter one, it is apparent that the properties of the PLA-PEG systems will affect both their drug loading capacity and their biodistribution performance *in vivo*, which are crucial qualities for potential drug delivery systems. To be able to predict these attributes, the size, composition and surface characteristics of the dispersions are important, as well as the performance of the systems *in vitro*.

2.2 PREPARATION AND CHARACTERISATION OF PLA-PEG COPOLYMERS

2.2.1 Materials

The linear (AB) block copolymers described in this thesis were derived from poly(DL-lactic acid) or poly(L-lactic acid) and methoxy polyethylene glycol [PEG 2000 gmol^{-1} and PEG 5000 gmol^{-1}] and were supplied by Zeneca Pharmaceuticals (Alderley Park, Macclesfield, U.K.). The copolymers were synthesised by ring opening polymerisation of lactide, using a stannous octoate catalyst, at 160 °C. This involved stirring together under nitrogen, purified methoxy polyethylene glycol, (after rigorous drying for one hour at 0.1 mmHg (13.3 Pa)) and freshly prepared rigorously dried D,L-lactide or L-lactide. Stannous octoate (stannous 2-ethylhexanoate) was then added as a catalyst and the mixture refluxed for three hours. This produced straw-coloured, slightly viscous liquids that solidified on cooling (Churchill and Hutchinson, 1986). The lengths of the PLA and PEG blocks were controlled by the starting materials, with the length of the PLA block controlled by the initial input of lactide, and the PEG blocks being of a fixed length of either 2000 gmol^{-1} or 5000 gmol^{-1} . The 1.5:2, 2:5, 4:2 and 6:2 PLA-PEG copolymers appeared clear after solidification whereas the 1.5:2 LPLA-PEG appeared white. The

copolymers were then used as received from Zeneca Pharmaceuticals.

The copolymers have been designated 1.5:2 PLA-PEG, 2:5 PLA-PEG, 4:2 PLA-PEG, 6:2 PLA-PEG and 1.5:2 LPLA-PEG respectively. The numeric values signify the molecular weights of the PLA and PEG blocks; for example, 4:2 PLA-PEG indicates approximate molecular weights of 4000 for the PLA block and 2000 for the PEG block, whereas 2:5 PLA-PEG indicates a PLA block of approximately 2000 and a PEG block of 5000. All the copolymers are produced using D,L-lactide with the exception of 1.5:2 LPLA-PEG, which was synthesised from the more crystalline L-lactide, and thus carries the prefix “L-” before PLA-PEG, as opposed to 1.5:2 PLA-PEG, which was synthesised from D,L-lactide and therefore carries no prefix.

2.2.2 Size Exclusion Chromatography (SEC)

Molecular weights of the copolymers and their polydispersities were determined by size exclusion chromatography (SEC) on three PL Gel 10E3 Å columns (30 cm x 7.5 mm). Dimethyl formamide was used as the mobile phase, at a flow rate of 1 ml/minute, and the columns (calibrated using polystyrene standards) were thermostatted at 70°C. The peaks were detected by refractive index, with the signal captured by HP Chem Station software and analysed using Polymer Laboratories GPC/SEC software. This work was performed by Zeneca Pharmaceuticals (Alderley Park, Macclesfield, UK) and the resulting molecular weights and polydispersities (Mw/Mn) are shown in Table 2.1.

2.2.3 Determination of PEG/Lactide Ratio by NMR

The PLA-PEG copolymers were examined by NMR in CDCl₃ solution, using a Bruker AC250 250 MHz Fourier Transform NMR Spectrometer. The areas at the resonance peaks were integrated and the integrals from the multiplets at 1.55 ppm δ shift (PLA methyl group) and 3.65 ppm δ shift (PEG methylene groups) were converted to a weight ratio assuming the MeOPEGs have weight average molecular weights of 2000 Da and 5000 Da. This work was performed by Zeneca Pharmaceuticals (Alderley Park, Macclesfield, UK) on 1.5:2 and 2:5 PLA-PEG.

Table 2.1

Characterisation of PLA-PEG Copolymers by Size Exclusion Chromatography (SEC)

Sample	Lactide	PEG Chain (Mw)	Mw	Mn	Polydispersity
1.5:2 LPLA-PEG	L	2000	3446	3193	1.08
1.5:2 PLA-PEG	D,L	2000	3518	3233	1.09
4:2 PLA-PEG	D,L	2000	6433	5179	1.24
6:2 PLA-PEG	D,L	2000	7798	6498	1.20
2:5 PLA-PEG	D,L	5000	6307	5803	1.09

2.3 PURIFICATION AND PREPARATION OF AQUEOUS DISPERSIONS OF PLA-PEG COPOLYMERS

2.3.1 Preparation of Unfractionated PLA-PEG Micelles (1.5:2 and 2:5 PLA-PEG)

Aqueous dispersions of the 1.5:2 and 2:5 PLA-PEG copolymers were prepared by dissolving the copolymer in water purified by ion exchange and charcoal absorption (Elga Stat, Elga Ltd., High Wycombe, Bucks. U.K.) to give final concentrations in the range 0.1 - 10% w/v. The copolymer/water system was generally retained at room temperature for several hours with occasional shaking, until clear dispersions were obtained.

2.3.2 Purification of PLA-PEG Aqueous Dispersions by Gel Permeation Chromatography (GPC)

Purification of the PLA-PEG copolymer dispersions was achieved by aqueous gel permeation chromatography (GPC). Initially, a C26/40 column containing sepharose CL-4B (2.6 x 30 cm) was employed for preliminary work on the analysis of the copolymers. Samples (10ml) were loaded at concentrations ranging from 1 to 5% w/v, using a peristaltic pump (12000 Varioperpex, LKB Bromma, Sweden) and eluted at 80 ml/h with deionised water. Peaks were detected using a refractive index detector (Gilson model 131, Villiers, France) with deionised water as the reference and the signal was interpreted using a potentiometer chart recorder (Auto-graph S, Shandon Southern Instruments Ltd., Surrey, UK).

2.3.3 Preparation of Fractionated PLA-PEG Micelles (1.5:2 PLA-PEG and 2:5 PLA-PEG)

PLA-PEG micelles were also produced after fractionation by gel permeation chromatography (GPC) (Sephacrose CL-4B). Preparatory runs were performed using a larger XK50/30 column, packed with sepharose CL-4B (5 x 30 cm) with the aid of a RK50 reservoir. Samples (5% w/v, 20 ml) were eluted through this column at a flow rate of 180ml/h. Peaks were detected and interpreted as before (section 2.3.2). The eluent from the GPC columns was collected using a fraction collector (2112 Redirac, LKB Bromma, Sweden) and the fractions corresponding to the peaks were freeze-dried

(Edwards, Sussex, England), and the copolymers redispersed as above (section 2.3.1).

2.3.4 Preparation of PLA-PEG Particles (4:2 and 6:2 PLA-PEG)

Particulate dispersions of 4:2 and 6:2 PLA-PEG were prepared using the precipitation/solvent evaporation method described previously (Fessi *et al.*, 1988). This involved dissolving the copolymer (0.025g to 2g) in 10 ml of acetone (HPLC grade, Fisons Chemicals, Loughborough, U.K.) and then adding this solution dropwise to 20 ml of deionised water, whilst stirring using a magnetic stirrer. The stirred solution was left overnight to allow the acetone to evaporate, leaving a dispersion of PLA-PEG particles (0.25% to 10% w/v) in water.

PLA-PEG particles were also produced after fractionation by gel permeation chromatography (GPC) (Sephacel CL-4B) as described above (section 2.3.3). After separation of a dispersion (5% w/v) by GPC, samples were freeze dried and the copolymers reprepared as above.

2.3.5 Preparation of 1.5:2 LPLA-PEG Particles

These particles were prepared as described above for 4:2 and 6:2 PLA-PEG.

2.4 MICROSCOPY

2.4.1 Transmission Electron Microscopy (TEM) Method

Aqueous dispersions of the fractionated and unfractionated 1.5:2 LPLA-PEG, 1.5:2 PLA-PEG and 2:5 PLA-PEG copolymers, fractionated 4:2 and 6:2 PLA-PEG, and Poloxamer 407 were examined at a concentration of 1% w/v, in an air dried condition using transmission electron microscopy (TEM). Samples were negatively stained by mixing three drops of the copolymer system with three drops of phosphotungstic acid (adjusted to pH 4 using potassium hydroxide). Specimens were then prepared by applying one drop of the dispersion onto a carbon coated EM grid. The grid was held horizontal for 20 seconds to allow the molecular aggregates to settle. The excess fluid was then drained using absorbent paper and the grid air dried. Specimens were examined using a Jeol 1200 EX12 transmission electron microscope (Jeol, Tokyo, Japan).

2.4.2 Atomic Force Microscopy (AFM) Method

This analysis was performed on fractionated 4:2 and 6:2 PLA-PEG particles, at a concentration of approximately 0.001% w/v. The sample (5 μ l) was applied by drop-casting onto a freshly cleaved square of mica (1 cm²), which was then analysed.

Atomic force images were obtained by using a Polaron SP300 (VG Microtech, Uckfield, UK). Silicon nitride probes were mounted on cantilevers with spring constants of 0.064 and 0.032 N/m (Park Scientific, California, USA) and were used at imaging forces between 1.0 and 0.1 nN, with a scan frequency of 10 Hz.

2.5 PARTICLE SIZING

2.5.1 Dynamic Light Scattering Method

Dispersions of the fractionated 1.5:2 PLA-PEG and 2:5 PLA-PEG copolymers of concentration 1% w/v, were produced as described above. A comparison was also made with 1% w/v aqueous dispersions prepared from freeze dried unfractionated material and with 1% w/v Poloxamer 407. Also analysed were 1% w/v dispersions of the 4:2 and 6:2 PLA-PEG copolymers, and a 0.5% w/v dispersion of LPLA-PEG copolymer. The dispersions were prepared as described above in section 2.3.2.

Samples were analysed by dynamic light scattering, using a Malvern System 4700 dynamic light scattering photometer, with a Siemens Helium/Neon laser light source operating at a wavelength of 632.18 nm at 40 mW, with an assumed refractive index of 1.60 and viscosity of 8.9×10^{-3} Pas. The sample cell was cleaned before each measuring run by flushing for at least 5 minutes with deionised water, using a filling apparatus similar to that described by Sanders and Cannell (1980), and dried with ultrafiltered air.

Traces of deionised water were removed from the cell by vacuum prior to injection of samples. Polymer dispersions prepared as outlined above were injected into the sample cell from a 1 ml disposable syringe through a 0.2 μ m Millipore filter (type HA) and hypodermic needle.

Ten measuring runs were performed on samples of each copolymer in triplicate to provide data for the effective hydrodynamic radius and polydispersity of each sample.

The sample time for PLA-PEG micelles was 5 μ s and the experimental duration 90

seconds, whereas with PLA-PEG and LPLA-PEG particles, the sample time was determined by the Malvern system and the experimental duration was 30 seconds. All measurements were performed at 25°C at a measurement angle of 90°. The polydispersity, which is an indication of the narrowness of the particle size distribution, with increased values showing a greater spread of particle sizes, was also measured, being calculated by the Malvern 4700 software. This measures the variance of the distribution in decay times, and hence the particle size, and gives a log normal intensity distribution for the measured data from which a polydispersity value is calculated.

2.6 DETERMINATION OF THE CRITICAL MICELLE CONCENTRATION (CMC) OF PLA-PEG MICELLES

2.6.1 Surface Tension Method for Determining CMC

Surface tension measurements (γ) of dilute aqueous solutions of fractionated PLA-PEG copolymer were measured using the Wilhelmy plate method by a Dynamic Contact Angle (DCA) analyser (DCA-322, Cahn Instruments, CA, USA). All glassware was cleaned using chromic acid and a glass cover slip employed as the glass plate. The plate was suspended from a microbalance (calibrated with standard weights) and the surface tension of each copolymer solution measured at 20 °C \pm 0.5 °C. The required concentrations were obtained by diluting a stock solution of copolymer with distilled water (HPLC grade, Fisons Chemicals, Loughborough, U.K.) and allowing to equilibrate overnight. Each concentration was performed in triplicate, with frequent distilled water readings performed as a control. A control experiment on Polysorbate 80 (Tween 80, Sigma Chemical Company, St. Louis, USA) was also performed at 25 °C \pm 0.5 °C. Measurement of the receding force was taken after 300 seconds and the surface tension measurements plotted against the logarithm of the concentration of the copolymer. The surface tension values were calculated using the equation,

$$F = mg + \gamma p \cos\theta,$$

where F is the total force recorded by the balance of the DCA analyser.

m is the mass of the plate,

g is the acceleration due to gravity,

γ is the surface tension of the liquid,

p is the perimeter of the plate,

and θ is the contact angle (Andrade *et al.*, 1985).

The perimeter value was measured for each batch of glass slides used ($n=30$) and input into the DCA program before the experiment was commenced.

The effect of ageing on the HPLC water was also examined. This experiment was performed in duplicate, by performing a surface tension measurement with the glass slide at zero immersion for a period of one hour.

2.7 ULTRACENTRIFUGATION ANALYSIS

2.7.1 Sedimentation Velocity Method

A Beckman Optima XL-A analytical ultracentrifuge equipped with scanning absorption optics and a monochromator was used in sedimentation velocity experiments, in order to assay the homogeneity and determine the sedimentation coefficients of the samples (Harding, 1984).

Solutions were prepared of fractionated material from the first elution peak (250 μ l, 0.2% w/v) and scanned against deionised water (250 μ l) loaded into a 10 mm pathlength cell. Sedimentation runs were then performed at 40,000 revs/minute and 20 °C, with UV scanning every ten minutes at 231 nm for 1.5:2 PLA-PEG and 225 nm for 2:5 PLA-PEG. Absorption profiles were subsequently obtained and overlaid to determine an “apparent” sedimentation coefficient, s_{20} , (i.e. not extrapolated to zero concentration) (Harding, 1984).

The same experiment was then performed on 4:2 and 6:2 PLA-PEG particles. 0.2% w/v PLA-PEG dispersions (350 μ l) were scanned against 400 μ l of deionised water loaded into a 10 mm pathlength cell. The run was then performed at 25,000 revs/min and 20 °C, with UV scanning every ten minutes at 226 nm.

2.7.2 Sedimentation Equilibrium Method

A Beckman Optima XLA analytical ultracentrifuge was used to determine the weight average molecular weight of solutions of the fractionated 1.5:2 and 2:5 PLA-PEG copolymers and Poloxamer 407 respectively, as described by Morgan *et al* (1990), under micelle forming (aqueous) conditions. These data were subsequently used to provide an estimate of the association number of copolymer molecules per micelle. The ultracentrifuge employed Rayleigh interference optics, a 5 mW He-Ne laser light source (632.18 nm) and an RTIC temperature control system. A low speed was used (5000 rpm) to avoid meniscus depletion conditions. The meniscus concentration therefore remained measurable and was obtained by mathematical manipulation of the fringe data (Creeth and Harding, 1982). The solution was loaded into a 30 mm pathlength double sector cell (200 μ l, 0.2% w/v) and the temperature was maintained at 20°C. Thermodynamic non-ideality was assumed to be negligible at the copolymer concentration used.

Whole cell apparent weight average molecular weights (M_w^0 , app.) were obtained from the limiting value of the M^* function at the cell base (Harding *et al*, 1992). The aggregation number of copolymer molecules in a micelle/particle was then calculated by dividing by the copolymer molecular weight. The aggregation number is the average number of copolymer molecules per aggregate.

2.7.3 Measurement of Partial Specific Volume

When a solute is added to a solvent, the total volume of the solution is not the sum of the volumes, but is related to the nature of both. The change in volume caused by the addition of a solute to a particular solvent is known as the partial specific volume, v , and is defined as the volume change upon addition of 1 g of solute to a large volume of solution whilst keeping all other parameters constant.

The partial specific volume was measured using a densitometer with deionised water as reference. Ten density readings were taken at concentrations of 0.25% w/v, 0.5% w/v and 1.0% w/v for each PLA-PEG copolymer sample. The mean density was then plotted against the concentration of the copolymer giving a linear dependency and the partial specific volume was then estimated from the slope of this line.

2.8 DETERMINATION OF PEG LAYER THICKNESS BY RHEOLOGICAL MEASUREMENTS

2.8.1 Preparation and Sizing of PLA-PEG Aggregates for Rheological Measurements

Dispersions of PLA-PEG micelles and particles (10% w/v) were prepared using the precipitation/solvent evaporation method as described above in section 2.3. All samples were prepared with fractionated PLA-PEG copolymers with the exception of LPLA-PEG copolymer, where unfractionated copolymer was also used. More concentrated dispersions were produced by evaporation of the 10% w/v dispersion, using an oven adjusted at 50 °C, and lower concentrations were prepared by diluting the 10 %w/v dispersion with deionised water. This gave dispersions with concentrations ranging from ~ 6% w/w to ~ 27% w/w. The hydrodynamic radius, R_h , of the particles was determined by dynamic light scattering (DLS), using a dilute dispersion of aggregates prepared and analysed as described in section 2.5.1.

2.8.2 Rheological Measurements

Dynamic (oscillatory) measurements were carried out using a Bohlin VOR (Bohlin Reologie, Lund, Sweden) interfaced with an IBM computer, as described previously (Prestidge and Tadros, 1988; Liang *et al*, 1992). This instrument operates in the frequency range 10^{-3} - 20 Hz and it has interchangeable torsion bars covering a wide range of sensitivities. Measurements were carried out in the frequency range 10^{-2} - 5 Hz at 25 ± 0.1 °C. A coaxial cylinder (C25) with a moving cup of radius 27.5 mm and a fixed bob of radius 25.0 mm was used. Initially, the frequency was kept constant at 1 Hz and the strain amplitude was gradually increased, up to approximately 0.2, whilst measuring the rheological parameters. This allows the linear viscoelastic region to be defined, where the rheological parameters are independent of strain amplitude. Measurements were then carried out in the linear viscoelastic region as a function of frequency. The experiments were performed at several different concentrations of the respective PLA-PEG aggregates.

From the stress and strain amplitudes (τ_0 and γ_0 respectively) and the phase angle shift, δ it is possible to obtain the following rheological parameters,

$$G^* = \frac{\tau_0}{\gamma_0}$$

$$G'' = |G^*| \sin \delta$$

$$G' = |G^*| \cos \delta$$

where G^* is the complex modulus,

G' is the storage modulus (the elastic component)

and G'' is the loss modulus (the viscous component).

Together with the particle diameter, these parameters can be employed to calculate the PEG layer thickness, as described in section 4.2.5, and also the radius of the core.

2.9 ANALYSIS OF SURFACE CHEMISTRY AND STRUCTURE

2.9.1 Static Secondary Ion Mass Spectrometry (SSIMS) Method

Dispersions (1% w/v, 200 μ l) of 4:2 and 6:2 PLA-PEG copolymers, in both chloroform (Fisons Scientific Equipment, Loughborough, U.K.) and as nanoparticles in aqueous media, were dropped onto aluminium foil and allowed to dry by evaporation. The samples were then analysed by static SIMS using a VG Ionex SIMSLAB 3B instrument (VG Scientific Ltd., Sussex, U.K.), employing a differentially pumped EX05 ion gun and a 12-12M quadrupole mass spectrometer. Argon atoms at 2 keV were used as the primary source with an equivalent current of 0.8 nA. The total dose per sample was approximately 5×10^{12} atoms/cm², which is within the regime of the static SIMS experiment (Briggs and Hearn, 1986). Emitted secondary ions were analysed in terms of their mass/charge ratio (m/z), to give positive and negative spectra which were interpreted by conventional mass spectrometry rules (McLafferty, 1980).

2.9.2 X-Ray Photoelectron Spectroscopy (XPS) Method

1% w/v dispersions (25 μ l) of 4:2 and 6:2 PLA-PEG copolymer, both in chloroform and as nanoparticles in aqueous media, were dropped onto aluminium foil and allowed to

dry. Analysis of the samples was then performed using a VG Scientific ESCALAB Mk II electron spectrometer (VG Scientific Ltd., Sussex, U.K.) employing Mg K α X-rays ($h\nu = 1253.6$ eV) with electron take off angle of 45°. The X-ray gun was operated at 10 kV and 34 mA, and survey spectra (0 - 1000 eV binding energy) were run, followed by high resolution spectra of the C 1s and O 1s regions. The data was collected and analysed using a VGS 5000S data system based on a DEC PDP 11/73 computer. Peak fitting was carried out with a linearly subtracted background and Gaussian peaks with 30% Lorentzian character. Spectra were corrected for sample charging by referencing photoelectron peaks to C-C/C-H at 285 eV. The atomic composition for each sample was calculated from the C1s and O1s envelope intensities using an O1s sensitivity factor of 2.85 relative to C1s.

2.10 THE STABILITY OF PLA-PEG AQUEOUS DISPERSIONS TO ADDED SALT

2.10.1 Method

The stability of dispersions to electrolyte addition was measured by determining the temperature of turbidity increase (the cloud point temperature (T_c)), for 1% w/v aqueous solutions of poly(ethylene glycol) molecular weight 8000 (PEG 8000), Poloxamer 407, 1.5:2 PLA-PEG copolymer and 2:5 PLA-PEG copolymer, as a function of molar concentration of added Na₂SO₄ (Sigma Chemical Company, St. Louis, USA), using a turbidimeter. Salt concentration was varied between 0 and 0.5 M. In addition, the unfractionated PLA-PEG was compared with the fractionated copolymer. Also, for Poloxamer 407, and 1.5:2 and 2:5 PLA-PEG (both fractionated and unfractionated), a solid phase separation temperature (T_s) was measured, which was taken as the point of decrease in turbidity after a plateau region was observed.

The test method was similar to that described by Cornet and Ballegooijen (1966) for measurement of theta temperatures of polymer solutions, in that the sample was illuminated using a light source and changes of turbidity with temperature were recorded by a change in light transmission detected by a photo cell (Figure 2.1). The glass cuvette containing the solution was inserted into a thermostatically controlled water jacket. The sample temperature was recorded using a temperature probe inserted into the sample cell

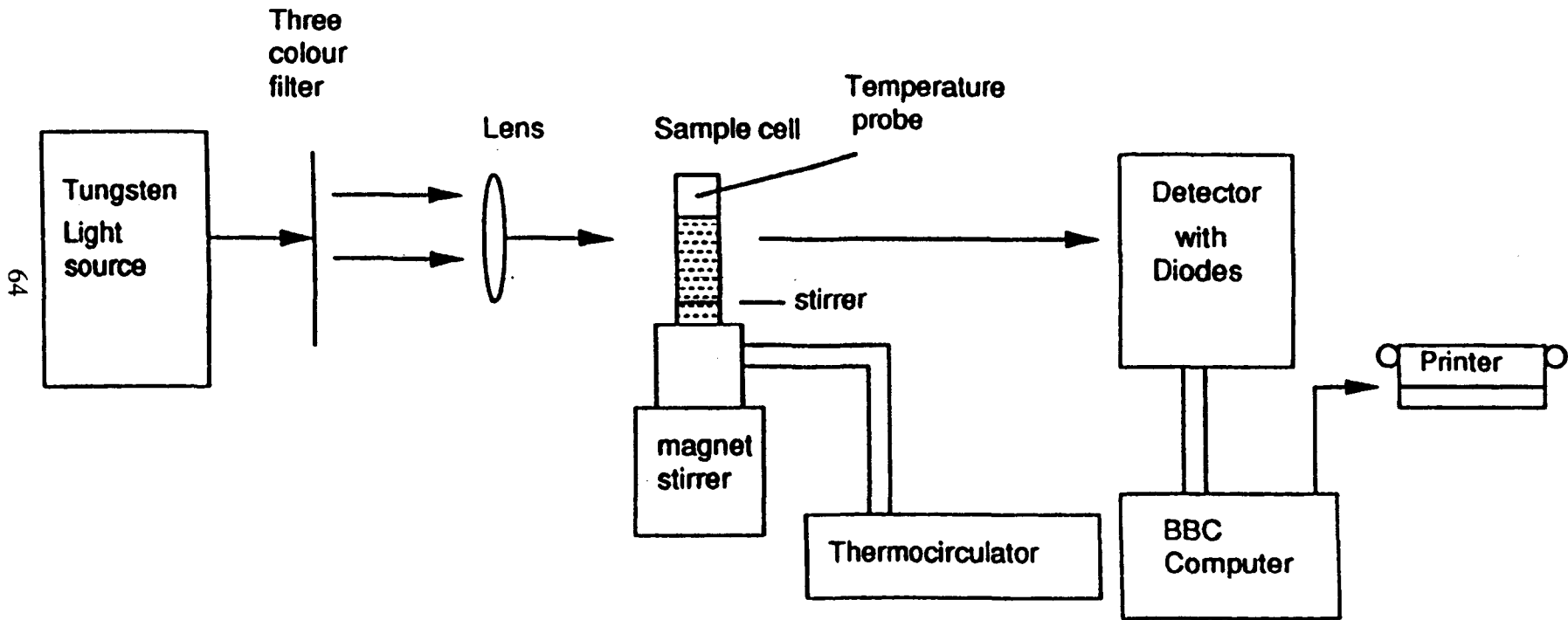


Figure 2.1 – Turbidimeter for Cloud Point Measurement

and changes in turbidity with increased temperature (10 °C/minute) were monitored up to an upper limit of 80 °C (the limit of the apparatus). Photocell and temperature probe outputs were fed to a computer (Acorn, U.K.) for data storage, handling and display.

CHAPTER THREE

PHYSICOCHEMICAL CHARACTERISATION AND SIZE ANALYSIS OF PLA-PEG SYSTEMS

3.1 INTRODUCTION

The physicochemical properties of a potential drug delivery system will influence the ability of the system to carry drug, release the drug and the destination of both the drug and carrier *in vivo*. As discussed previously in chapter one, the diameter of the micelle/particle system used greatly influences the destination of the particles *in vivo* and it is therefore essential that this important parameter is known for a potential drug targeting system. It is also important that this diameter should be reproducible; that is that the micellar/particulate system should be relatively monodisperse and that the method of preparation should give similar micelles/particles with each preparation. This reproducibility will be important for the drug release and performance *in vivo* of the potential drug delivery system. This chapter therefore explores the purity, composition, size and shape of PLA-PEG systems and compares their properties with other copolymers that have been studied as potential drug delivery systems, mainly the poloxamers and poloxamines discussed in sections 1.5 and 1.9. In particular, Poloxamer 407 has been compared, as the molecular weights of the two PEO chains of this copolymer are 4000 each, which is intermediate between the 2000 and 5000 PEG chain lengths on the PLA-PEG copolymers studied in this thesis. Poloxamer 407 has also shown promising *in vivo* results in previous work (section 1.5.2). PLGA particles have also been compared in some studies, as an example of a “solid” biodegradable particle system.

3.2 COMPOSITION OF PLA-PEG COPOLYMERS

3.2.1 Size Exclusion Chromatography

The PLA-PEG copolymers produced for this work consisted of a PEG block of defined molecular weight, linked to a PLA block, the size of which is determined by the input

of PLA to the reaction mixture. Characterisation of these copolymers by SEC in dimethyl formamide gave polydispersity indices in the range 1.09 to 1.2 (calculated from M_w/M_n) showing a narrow distribution of PLA block sizes (Table 2.1). From Table 2.1, it appears that the more PLA present in the sample, the more polydisperse the copolymer. This will be considered in more detail in section 3.3. The polydispersity values compare favourably with values for PLA-PEG copolymers and other copolymers achieved by other groups (Table 3.1).

3.3 PURIFICATION OF AQUEOUS DISPERSIONS OF PLA-PEG COPOLYMERS

3.3.1 Gel Permeation Chromatography (GPC)

Gel permeation chromatography (GPC) is usually used for aqueous systems, whereas size exclusion chromatography (SEC) is usually used for organic systems. Gel permeation chromatography (also known as gel filtration) is a separation method that works on the basis of molecular size. This means that soluble molecules of large molecular weight can be separated from molecules of small molecular weight by this method. The technique involves a porous gel, which is tightly packed into a column and completely filled with solvent. The sample is then passed down the column in the same solvent and the small molecules diffuse into the pores of the gel whereas the large molecules, which are too large to diffuse into the pores, remain in the interstitial fluid and pass straight through the gel column. Smaller molecules, which are diffusing in and out of the pores, are eluted later. Thus separation is achieved between the differently sized molecules, and a high molecular weight molecule, such as a micelle or a particle, can be separated from any smaller molecules that are not part of the aggregates.

This technique has been widely used to purify block copolymers, including poly(oxyethylene-oxypropylene-oxyethylene) (PEO-PPO-PEO) copolymers (Luo *et al.*, 1983; Ding *et al.*, 1991; Sun *et al.*, 1991; Yu *et al.*, 1992) and poly(oxyethylene-oxybutylene-oxyethylene) copolymers (Nicholas *et al.*, 1993). GPC can be used as a preparative technique to purify the sample, or as an analytical technique to provide information on the molecular weight and volume of particles. This latter use of GPC is usually carried out by HPLC (high performance liquid chromatography) using two columns in series to provide a more accurate analysis (Lesieur *et al.*, 1993; Yokoyama

et al., 1993).

Sepharose CL-4B is a cross-linked agarose gel with good thermal and chemical stability, which can be used in aqueous media of pH range 3-14 (Pharmacia, 1982). It is also stable in a variety of solvents, including acetone and ethanol, and as the gel-forming fibres are relatively stiff bundles of polysaccharide chains, the solvents have little effect on pore size. Its molecular weight fractionation range is approximately 3×10^4 g/molecular to 5×10^6 g/molecular and a similar gel, Sepharose CL-2B has been used previously with poly(lactic acid) nanoparticles in the 50-200 nm size range, and other Sepharose gels have been used with liposomes (Szoka and Papahadjopoulos, 1980; Allen, 1984). Sepharose CL-4B was chosen for all the GPC experiments on the PLA-PEG copolymers as the expected molecular weights of the micelles/particles produced from PLA-PEG copolymers and the copolymer molecules themselves would be around the opposite limits of the fractionation range.

3.3.2 The Gel Permeation Chromatography of PLA-PEG Copolymers

Data for aqueous gel permeation chromatography (GPC) were derived from preparative runs on a column of sepharose CL-4B (2.6 x 30 cm) as described in section 2.4.2. Samples (10ml) were loaded at a concentration of 1% w/v and eluted at 80 ml/h with distilled water to investigate the composition of the PLA-PEG copolymers in aqueous solution.

Although the polydispersity data from SEC studies suggests a narrow distribution of the copolymer molecular weight, initial work with these block copolymers indicated that they were not homogenous (unpublished data). Subsequent gel permeation chromatography of the PLA-PEG copolymer dispersions on a sepharose CL-4B matrix in aqueous media, resulted in a clear separation into two peaks (Figures 3.1 and 3.2).

A similar case has been reported for the Poloxamer 407, which also gave a bimodal distribution on GPC separation (Yu *et al.*, 1992; Nicholas *et al.*, 1993). To determine the relative proportions of each of these peaks, a 1% w/v dispersion of each PLA-PEG was separated by GPC as described in section 2.4.2, using a known weight of copolymer. The fractions were collected, freeze-dried and weighed to allow calculation of the proportion of the starting material in each peak. The results are given in Table 3.2.

The results highlight the decrease in the amount of peak two material in the starting

Figure 3.1a – Gel Permeation Chromatograph of 1.5:2 PLA-PEG

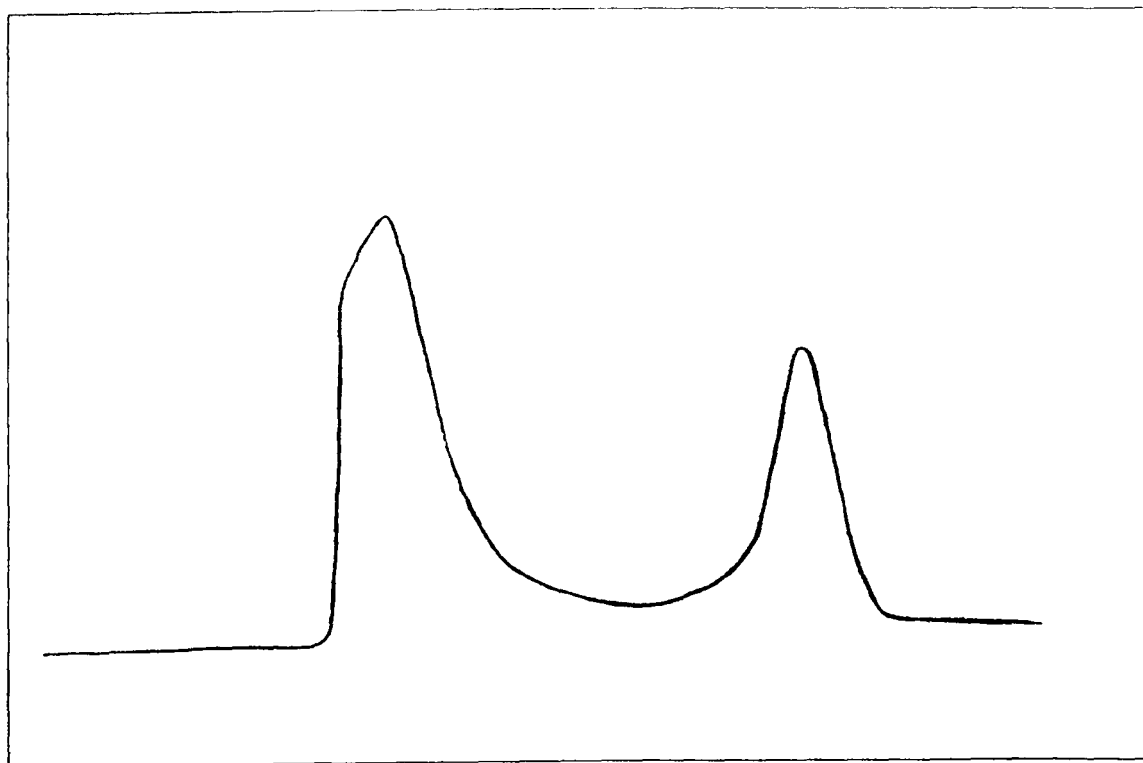


Figure 3.1b – Gel Permeation Chromatograph of 2:5 PLA-PEG

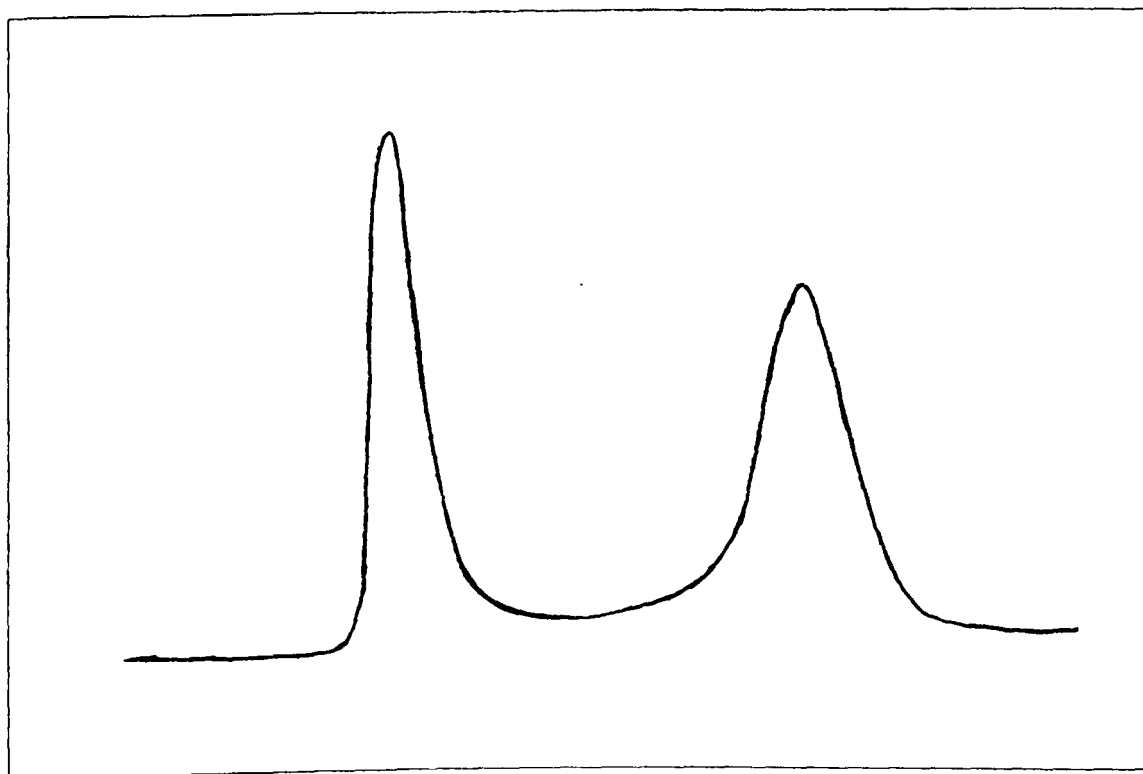


Figure 3.2a – Gel Permeation Chromatograph of 4:2 PLA-PEG

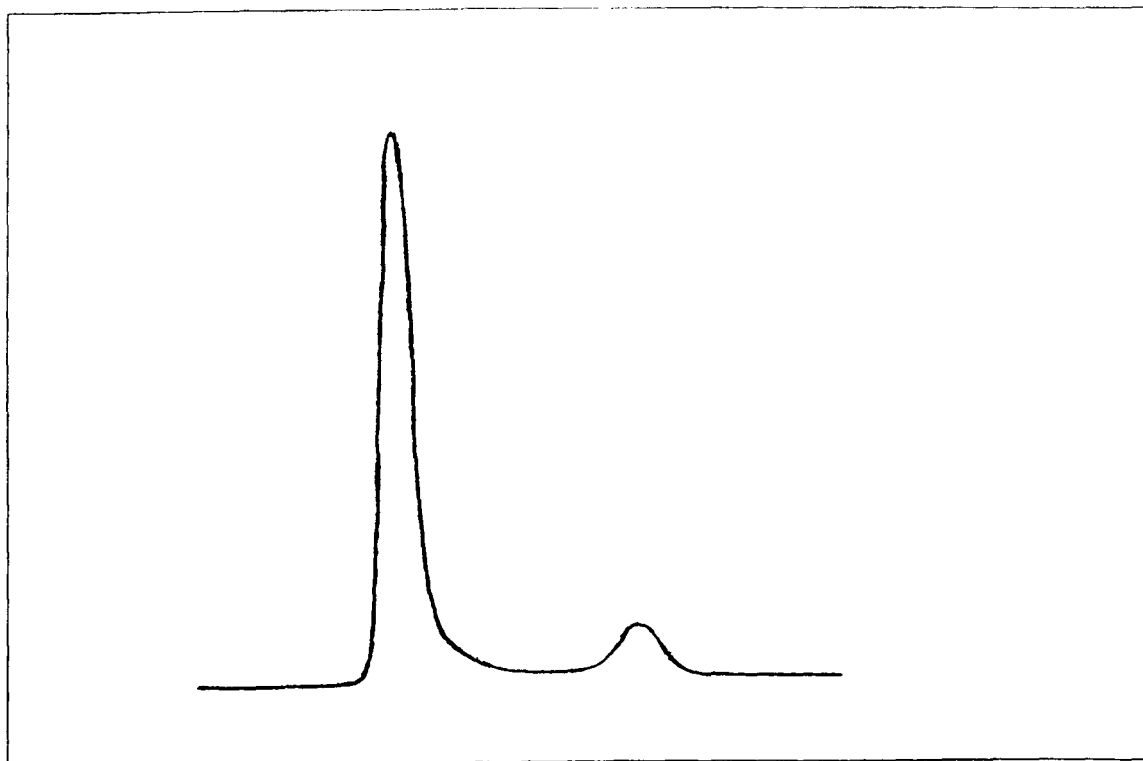


Figure 3.2b – Gel Permeation Chromatograph of 6:2 PLA-PEG

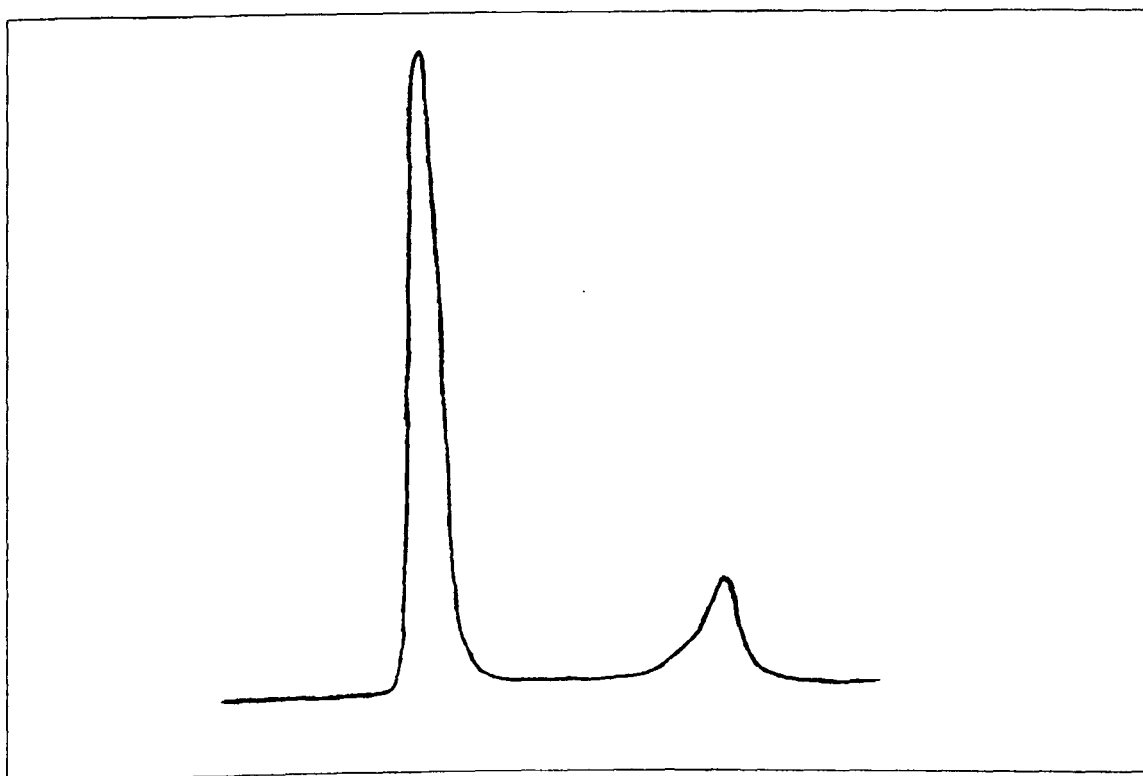


Table 3.1

Polydispersity of PLA-PEG and Related Copolymers After Synthesis

Copolymer Sample	Polydispersity Range	Reference
PLA-PEO	1.4-1.6	<i>Zhu et al (1986)</i>
Star-PEO-PLA	1.3-1.7	<i>Zhu et al (1989)</i>
PLA-PEG	2.0-2.7	<i>Zhu et al (1990)</i>
LPLA-PEG	1.5-2.5	Hu and Liu (1994)
LPLA-PEO-LPLA	1.18-1.55	Youxin and Kissel (1993)
LPLA-PEO-LPLA	1.48-1.80	Youxin <i>et al</i> (1994)
PLA-PTMG	2.58-3.00	Xiong <i>et al</i> (1995)
POE-POB	1.04-1.11	Bedells <i>et al</i> (1993)
PEO-PPO-PEO	<1.1	Reddy <i>et al</i> (1990)

copolymer with the 4:2 and 6:2 PLA-PEG copolymers compared with the water soluble 1.5:2 and 2:5 PLA-PEG copolymers, with the 1.5:2 LPLA-PEG copolymer result falling between the two groups.

The peak one and peak two material resulting from aqueous GPC was subsequently analysed by SEC as detailed in section 2.2.2. Table 3.3 shows the weight average molecular weight of the block copolymer and the PEG component, relative to polystyrene standards, as estimated by SEC, before and after purification by aqueous GPC.

The PLA-PEG copolymers produced for this work consisted of a PEG block of defined molecular weight, linked to a PLA block, the size of which is determined by the input of PLA to the reaction mixture. Therefore it is to be expected that some variation in the amount of PLA attached to the PEG block will occur, and that the actual molecular weight will vary from the theoretical molecular weight predicted from the input of starting materials. This has been noted for PLA-PEG particles previously (Bazile *et al*, 1995).

In the majority of cases, the second peak has a lower molecular weight than the first peak from GPC, with the molecular weight for the unfractionated material having an “average” molecular weight between the two. This would be expected from the method of SEC where the molecular weight deduced is the peak of an approximately Gaussian distribution. The data shows that the molecular weight of material from the first GPC peak was close to that expected from the synthesis, whereas the molecular weight of material from the second GPC peak was significantly lower. This indicates that the second peak is low in PLA content (‘PLA-depleted’) as the PEG chain is completely defined by the starting materials. This data therefore shows that the material produced from the two different peaks differ in molecular weight and the two materials may therefore have different characteristics from each other in aqueous solution. Further information is therefore needed to identify the roles of each of these two materials.

3.3.3 Nuclear Magnetic Resonance (NMR) of PLA-PEG Copolymers

NMR analysis of the freeze-dried material obtained from the two peaks produced by GPC for 1.5:2 PLA-PEG, 2:5 PLA-PEG and 1.5:2 LPLA-PEG (Table 3.4 and Appendix 1) was carried out by Zeneca Pharmaceuticals (Alderley Park, Macclesfield). Table 3.4

shows the expected lactic acid to ethylene glycol ratio as predicted from the input of the starting materials, assuming the PEG molecular weight to be 2000 gmol^{-1} for 1.5:2 PLA-PEG and 1.5:2 LPLA-PEG, and 5000 gmol^{-1} for 2:5 PLA-PEG. Similarly, the values for the lactic acid to ethylene glycol ratio as calculated from the molecular weight values from the NMR studies are shown in Table 3.4. This analysis confirmed that the first peak had a similar ratio of lactic acid groups to ethylene oxide groups to that predicted from the relative proportion of starting materials for the synthesis, but again, the second peak appeared to be low in PLA content ('PLA-depleted'). There was good agreement between the values of molecular weight calculated from the NMR data and the values obtained experimentally by SEC, except for the 1.5:2 LPLA-PEG (Table 3.4).

3.3.4 Calibration of the GPC Sepharose CL-4B Column

A simple calibration was performed using lactic acid, poly(ethylene glycol) standards and PLGA (polylactide-co-glycolic acid) particles in order to determine where the components of the PLA-PEG dispersions should elute. Solutions of PLGA particles (1% w/v, 2 ml) were employed to simulate micelle/particle formation. Two polymer standards of PEG Mw 5600 and Mw 10300, of similar molecular weight to the monomers were chosen to simulate monomer elution, and free lactic acid used to detect where residual lactic acid from the synthetic process would be expected to elute. The method was as described in section 2.4.2 and the results, compared with the values for the PLA-PEG copolymers are shown in Table 3.5.

It can be seen from Table 3.5 that the PLGA particles elute fairly quickly in the void volume of the column, as they are large enough to be excluded from the gel pores. Comparing the elution volume for PLGA particles with the first peak produced with the PLA-PEG copolymers, it can be seen that the values of V_e for all the copolymers are very similar. As the molecular weight of the gel-exclusion volume is much higher than the molecular weights of the individual copolymer molecules (Table 3.5), this supports the idea that micelles are formed from the first peak.

The second peaks produced from the PLA-PEG copolymers eluted with a similar V_e to the standard PEG polymers. Any free monomer should be eluted in the second peak. The amount of free monomer present would depend on the concentration of the micellar solution, with dissociation decreasing with increase in concentration, but trace amounts

Table 3.2

Relative Proportions of the Two Peaks Produced by Aqueous GPC

Copolymer	% Peak One	% Peak Two	% Recovery
1.5:2 PLA-PEG	69.8	26.8	96.6
2:5 PLA-PEG	53.8	41.1	94.9
1.5:2 LPLA-PEG	58.2	20.2	78.4*
4:2 PLA-PEG	86.5	8.3	97.2
6:2 PLA-PEG	87.4	10.2	97.6

* - Low recovery thought to be due to losses on the GPC column.

Table 3.3

Characterisation of PLA-PEG Copolymers by Size Exclusion Chromatography (SEC) Before and After Aqueous Gel Permeation Chromatography (GPC)

Sample	Elution Peak	PEG Chain (Mw)	Experimental Mw	Theoretical Mw	Polydispersity
1.5:2 PLA-PEG	-	2000	3518	3500	1.09
1.5:2 PLA-PEG	1	2000	3947	3500	1.07
1.5:2 PLA-PEG	2	2000	2519	3500	1.03
2:5 PLA-PEG	-	5000	6307	7000	1.09
2:5 PLA-PEG	1	5000	6987	7000	1.10
2:5 PLA-PEG	2	5000	5547	7000	1.09
1.5:2 LPLA-PEG	-	2000	3446	3500	1.08
1.5:2 LPLA-PEG	1	2000	3840	3500	1.08
1.5:2 LPLA-PEG	2	2000	-	3500	-
4:2 PLA-PEG	-	2000	6433	6000	1.24
4:2 PLA-PEG	1	2000	-	6000	-
4:2 PLA-PEG	2	2000	-	6000	-
6:2 PLA-PEG	-	2000	7798	8000	1.20
6:2 PLA-PEG	1	2000	7017	8000	1.18
6:2 PLA-PEG	2	2000	7770	8000	1.13

Table 3.4

Comparison of NMR Peak Integration for Fractionated PLA-PEG Copolymers

Copolymer	PEG Mw	Expected Lactic acid/Ethylene glycol ratio	Elution peak	Molecular weight (SEC)	Molecular weight (NMR)	Experimental Lactic acid/Ethylene glycol ratio (NMR)
1.5:2 PLA-PEG	2000	1:2.1	1	3947	3455	1:2.1
1.5:2 PLA-PEG	2000	1:2.1	2	2519	2386	1:8.3
2:5 PLA-PEG	5000	1:4.0	1	6987	6818	1:4.4
2:5 PLA-PEG	5000	1:4.0	2	5547	5500	1:16.0
1.5:2 LPLA-PEG	2000	1:2.2	1	3840	4909	1:1.1
1.5:2 LPLA-PEG	2000	1:2.2	2	-	2464	1:6.9

would be expected as the separation process during GPC leads to dissociation of the micelles from their monomers (Coll, 1971; Wang *et al*, 1993).

Free lactic acid was also eluted later indicating that if any was present resulting from the synthesis it would be with or after the second peak.

From GPC theory, the ratio of elution volume to void volume (the liquid phase) is linearly related to the logarithm of molecular weight (Squire, 1964; Determann and Michel, 1966; Billmeyer Jr. and Altgelt, 1971). Thus, the samples with the higher molecular weight would be expected to have higher V_e . However, a linear relationship is only present in the fractionation range of the sepharose gel and the samples, apart from peak one of the PLA-PEG copolymers and the PLGA particles, are outside this range. Therefore, the standard PEG copolymers (and hence the PLA-PEG monomers) and the lactic acid all elute with similar V_e . These results show that the material in the first GPC peak is of a much higher molecular weight than the standard polymers (and hence the monomers) and the free lactic acid.

3.3.5 Assessment of Stability using GPC

It was considered possible that the second peak was a decomposition product of the copolymer. To test this hypothesis, experiments were carried out to investigate the effects of storage on the fractionated copolymer dispersions, in aqueous environment, and determining any degradation. This was achieved by passing 1% w/v dispersions of the water soluble polymers (1.5:2 PLA-PEG and 2:5 PLA-PEG) down the Sepharose CL-4B column, to separate the polymers into two peaks. A dispersion of material isolated from the first peak was kept under different storage conditions (4°C and room temperature) in water for a period of two weeks, before analysis on the column as described in section 2.3.2. An accelerated study was also performed by incubating the dispersion in water, at 37°C, for one week then refractionating by GPC. Sodium azide was added at a concentration of 0.02% w/v to prevent microbial degradation.

Only a single peak resulted for samples kept at 4°C, room temperature and 37°C, suggesting that the second peak shown in the initial GPC analysis was not due to degradation. For the 4°C and room temperature samples, a single peak was obtained at a similar elution volume to the micelles. For the accelerated sample kept at 37°C, the elution volume was greater than that noted with the other samples, suggesting a lower

molecular weight, but still less than the elution volume for the second GPC peak. This implies that some degradation has in fact occurred, but the initial GPC chromatograph of two peaks was not reproduced.

A further experiment performed at Zeneca Pharmaceuticals, where a PLA-PEG copolymer was dialysed in distilled water at room temperature for fifteen days, also showed no change in the molecular weight properties of the PLA-PEG copolymer when reanalysed by NMR and SEC.

3.3.6 Discussion

From the above results, it is clear that two species exist in aqueous media for all PLA-PEG copolymers. The GPC chromatographs in Figures 3.1 and 3.2 show the two peaks, with the GPC calibration data showing that the first peak corresponds to aggregates similar in size to PLGA particles, which are therefore likely to be micelles or nanoparticles (depending on the copolymer batch). This first peak shows tailing with the micelle-forming copolymers, which is thought to be due to the continuous establishment of an association equilibrium on the column (Katime *et al*, 1994). As the micelles and free copolymer chains are applied to the column they are separated, and some micelles disassociate to re-establish the equilibrium of free copolymer molecules in the micelle peak. This allows the free copolymer chains to move into the gel pores to be eluted later (Wang *et al*, 1993; Yokoyama *et al*, 1993; Katime *et al*, 1994).

The material in the second peak was shown by NMR and SEC studies to have less PLA attached to the PEG block (PLA-depleted) than the material in the first peak. As a lower amount of PLA in a copolymer molecule makes association into a micelle or particle less likely (El Eini *et al*, 1976), this provides an explanation as to the presence of this second peak, rather than all the material being converted into micelles/particles. The NMR data on the second peak indicated that the PLA chain length was about five to seven PLA residues. It can therefore be assumed that copolymer molecules with at least five PLA residues are necessary to allow association into micellar/particulate systems. This also leads to an explanation for the larger proportion of second peak material separated by GPC for the micelle-forming PLA-PEG copolymers (1.5:2 PLA-PEG and 2:5 PLA-PEG) and LPLA-PEG, compared with the more hydrophobic PLA-PEG copolymers (4:2 and 6:2 PLA-PEG) (Table 3.2). As smaller blocks of PLA are grown onto the PEG

Table 3.5

Results of Calibration of Sepharose CL-4B Column (2.6 x 40 cm)

Sample	Elution Peak	Elution Volume, V_e	$W_{1/2}$
PLGA Particles	-	43	4.5
PEG 5600	-	115	12
PEG 10300	-	115	13
Free Lactic Acid	-	133	7
1.5:2 PLA-PEG	1	46, 52	18
1.5:2 PLA-PEG	2	124	12
2:5 PLA-PEG	1	43	11
2:5 PLA-PEG	2	114	18
1.5:2 LPLA-PEG	1	49	8
1.5:2 LPLA-PEG	2	122	13
4:2 PLA-PEG	1	42	10
4:2 PLA-PEG	2	112	20
6:2 PLA-PEG	1	47	10
6:2 PLA-PEG	2	131	16

$W_{1/2}$ gives the width of the peak at 50 % of the peak height and is a measure of the molecular weight distribution within the peak.

blocks for 1.5:2 PLA-PEG, 1.5:2 LPLA-PEG and 2:5 PLA-PEG (constituting approximately 1500, 1500 and 2000 gmol^{-1} respectively), more of the PLA-depleted copolymer molecules will be formed than for the 4:2 and 6:2 PLA-PEG, where the 4000 and 6000 gmol^{-1} PLA blocks aimed for contain significantly more than the five PLA blocks required for incorporation into a micelle/particle.

Thus, there are more likely to be copolymer molecules produced with depleted PLA for the 1.5:2 PLA-PEG, 2:5 PLA-PEG and 1.5:2 LPLA-PEG than for 4:2 and 6:2 PLA-PEG. This is reflected in the increased amount of the second peak seen on GPC of these copolymers.

The question therefore remains of the origin of the material in the second peak. There are two likely theories: firstly that the second peak is a result of degradation of the copolymer, and secondly that the second peak is a by-product of the synthesis. The literature provides examples of both scenarios. Recent papers by other authors studying the PLA-PEG copolymers have shown that on studying the degradation of these systems, a bimodal distribution was produced with SEC studies. Hu and Liu (1993) note that the higher the PEG content of PLA-PEG copolymers, the faster the rate of hydrolysis, which would correlate with the 1.5:2 and 2:5 PLA-PEG copolymers (which have a higher proportion of PEG) having a greater peak two content. They also observed a change from unimodal to bimodal distribution using SEC (with chloroform as eluent) in studies up to 510 hours of hydrolysis. During this period, the GPC peak area for the higher molecular weight species decreased and that for the lower molecular weight species increased in parallel. Similar results are discussed in a second paper by the same authors, where a bimodal distribution was also observed after hydrolysis (Hu and Liu, 1994). However, the results described in section 3.3.5 make this explanation unlikely. Samples stored at 4°C and room temperature, clearly showed a single peak after 14 days when rechromatographed, indicating that no significant degradation had occurred. Samples kept at 37°C also gave a single peak on rechromatographing, although the elution volume was larger than for the first peak of the original sample. This is likely to be the result of some degradation, as would be expected with a biodegradable copolymer. However, the elution volume of this peak was also different from that of the second peak of the original sample, indicating that whilst some degradation had occurred, the molecular weight was still greater than the peak two material and

micelles/particles were still likely to be present. It is unlikely that degradation of the PLA-PEG copolymers is a significant factor in producing the second peak seen with aqueous GPC.

The second theory, that the second GPC peak is a by-product of the synthesis, appears more likely. Kricheldorf and Meier-Haack (1993) noted that in their production of 1.5:2 LPLA-PEG triblock copolymers, there was likely to be a few percent of diblock copolymers present. Similar reports have been reported with poloxamers, where with Synperonic F127 (a PEO-PPO-PEO copolymer), a bimodal distribution was observed with SEC (with *N,N*-dimethylacetamide as eluent). This was thought to be due to the presence of diblock copolymers originating from the introduction of moisture to the transfer reaction in the anionic polymerisation of propylene oxide and homopoly(oxyethylene) (Luo *et al*, 1983; Yu *et al*, 1992). Malmsten and Lindman (1992) also reported the existence of two peaks on GPC, of which the slowest peak decreased on increasing the temperature and so was attributed to polymer impurities. Linse (1994) also investigated the presence of polymer impurities with poloxamers, particularly the effects of diblock copolymer, PEO homopolymer and PPO homopolymer impurities produced from the synthetic process on the properties of the resultant micelles. Thus impurities resulting from the synthetic production of block copolymers are well documented and it seems likely that this is the cause of the PLA-PEG material with the depleted PLA block, which separates out by aqueous GPC in peak two. Block copolymers are not monodisperse and even though the PLA-PEG copolymers discussed here have very low polydispersity values (Table 2.1), the distributions are still broad in comparison with low molecular weight surfactants (Zhou and Chu, 1987; Linse, 1994). Therefore, even with the best polydispersity value of 1.08 there will still be a variation in the PLA chain lengths of the copolymer molecules. Hence, this explanation for the presence of peak two in the aqueous GPC is probable. The polydispersity values from the SEC analysis do not show a great difference for peak one material compared with the unfractionated material for most of the PLA-PEG copolymers (Table 3.3). This is likely to be due to a lack of sensitivity in the SEC technique. The increase in polydispersity with increased PLA content (i.e. for 4:2 and 6:2 PLA-PEG) indicates a wider variation in the molecular weight of the PLA-PEG copolymer molecules. This reflects a greater distribution of the PLA chain length (as the PEG Mw is fixed), with

the greater input of lactide into the starting materials leading to a greater range of PLA chain lengths.

The presence of impurity that is not associating into micelles can affect the micellar properties. For the poloxamer series, the presence of diblock impurities resulting from the synthesis has led to widely differing estimates in the critical micelle concentration (CMC) of the micelles produced which will be discussed in section 3.6. Also, the diblock impurities and PPO homopolymer can affect the association number and the ability of the micelles to solubilise drugs (Linse, 1994). Given this problem, the remaining characterisation was carried out on the first micelle-forming fraction of material purified by GPC, except where the role of the second fraction in micelle formation was being addressed.

3.4 MICROSCOPY

3.4.1 Analysis of Micelles/Particles by Microscopy

Microscopy is a technique widely used to study the shape, size and characteristics of micelles/particles. The two types of microscopy discussed here are high resolution techniques that are used with samples in the nanometre size range. They can give an estimate of micelle/particle diameter, confirm the shape, and indicate the polydispersity of the distribution and, with atomic force microscopy (AFM), can also show the topography of the surface. As the diameter of the micelles/particles is important for the distribution *in vivo*, it is useful to be able to obtain an estimate of diameter by a variety of methods. Microscopy is able to give a visible estimate of diameter, which can then be compared with other methods.

3.4.2.1 Transmission Electron Microscopy (TEM)

Electron microscopes have superior resolution over light microscopes due to the very short wavelengths of the high-energy electrons (Thomas and Goringe, 1979). The transmission electron microscope has an electron beam, focused by highly concentrated magnetic fields formed between soft-iron pole pieces and generated by currents flowing through annular coils (Cowley, 1988). This electron beam illuminates the specimen (usually with an illuminating system of lenses) and interacts with the thin metallised

sample and is scattered elastically. This scattered radiation is then focused by an objective lens onto a fluorescent screen, where further magnifying (or projector) lenses form an image of the sample of a suitable size. This image can be photographed.

3.4.2.2 Calibration of TEM

A platinum calibration grid was purchased (Agar Aids, UK) and examined using the Jeol 1200 EX12 transmission electron microscope (Jeol, Tokyo, Japan). The grid was photographed at a magnification of 200,000 diameters, which allowed the accuracy of the scale bar for the TEM photographs to be determined by comparing the actual measurements of the grid with the calculated measurements as given by the scale bar. This showed that using the measurement bar for the photographs gave an error of approximately 17 %, such that all measurements need to be scaled up by a factor of 17 % to give the actual size.

3.4.2.3 TEM of PLA-PEG Micelles

Figures 3.3 and 3.4 show transmission electron micrographs of fractionated 1.5:2 and 2:5 PLA-PEG copolymers respectively, with the scale bar corresponding to 58.5 nm. This scale bar value is corrected as described above (section 3.4.2.2), but there may be a minor discrepancy due to the difference in the magnification (the calibration was performed at 200,000 diameters, whereas the Figures shown were taken at 100,000 diameters). These clearly indicate the presence of micelles in the material from the first peak for both copolymers, as shown by light spherical entities surrounded by the darker staining. With the material from the second peak, only the background of the coated grid is seen, with no micelles present for either copolymer (Figure 3.5).

The micelle diameters were measured using a micrograph at 200 K magnification, using the scale bar as a reference with the above correction, and taking a sample size of 200 micelles to give a statistically valid mean and standard deviation. This gave micelle diameters in the material from the first GPC peak of 7.2 nm for 1.5:2 PLA-PEG and 17.0 nm for 2:5 PLA-PEG, which were smaller than micelles seen with the unfractionated copolymer ($8.3 \text{ nm} \pm 1.5 \text{ nm}$ and $20.4 \text{ nm} \pm 8.0 \text{ nm}$ respectively). The electron micrograph obtained for a 0.5% w/v solution of Poloxamer 407 (unfractionated) exhibited similar features to those found in PLA-PEG specimens (data not shown) and

Figure 3.3 – Transmission Electron Micrograph of Fractionated 1.5:2 PLA-PEG Micelles (Magnification = 100K)

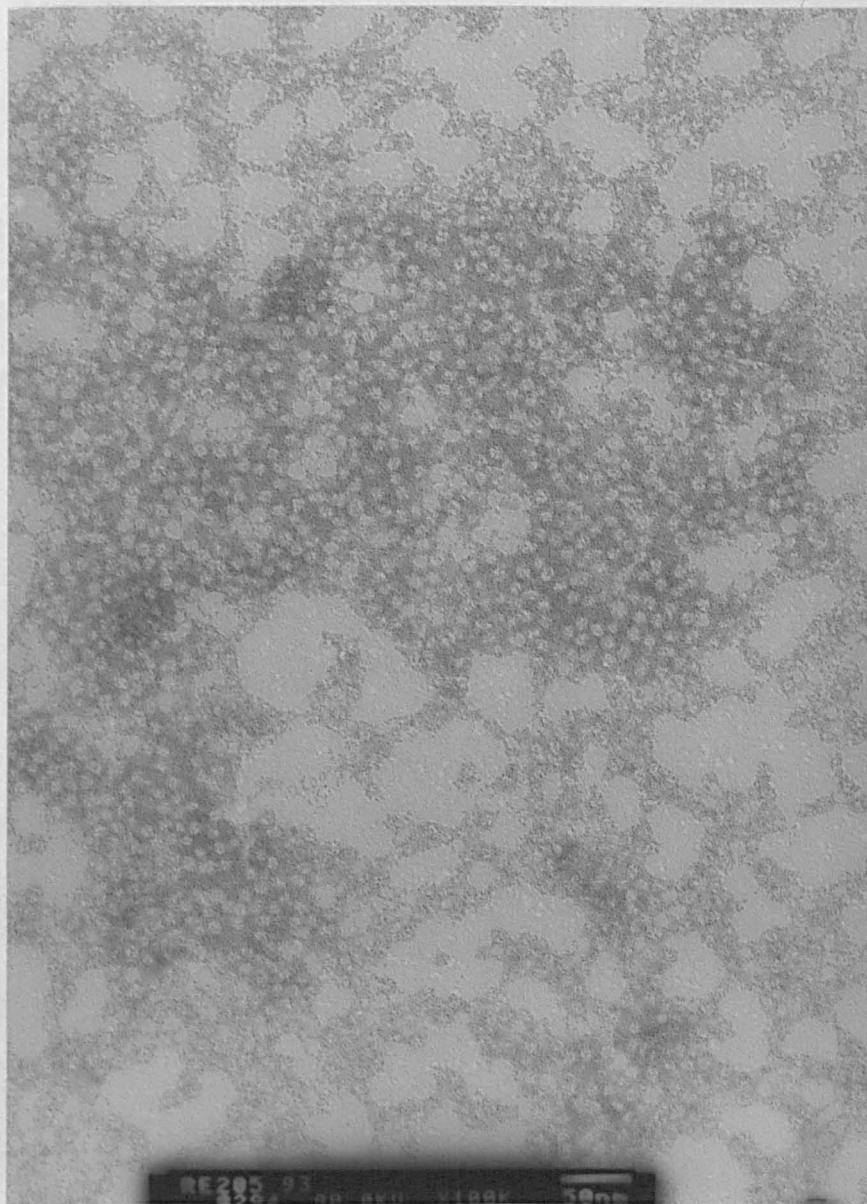


Figure 3.4 – Transmission Electron Micrograph of Fractionated 2:5 PLA-PEG Micelles
(Magnification = 100K)

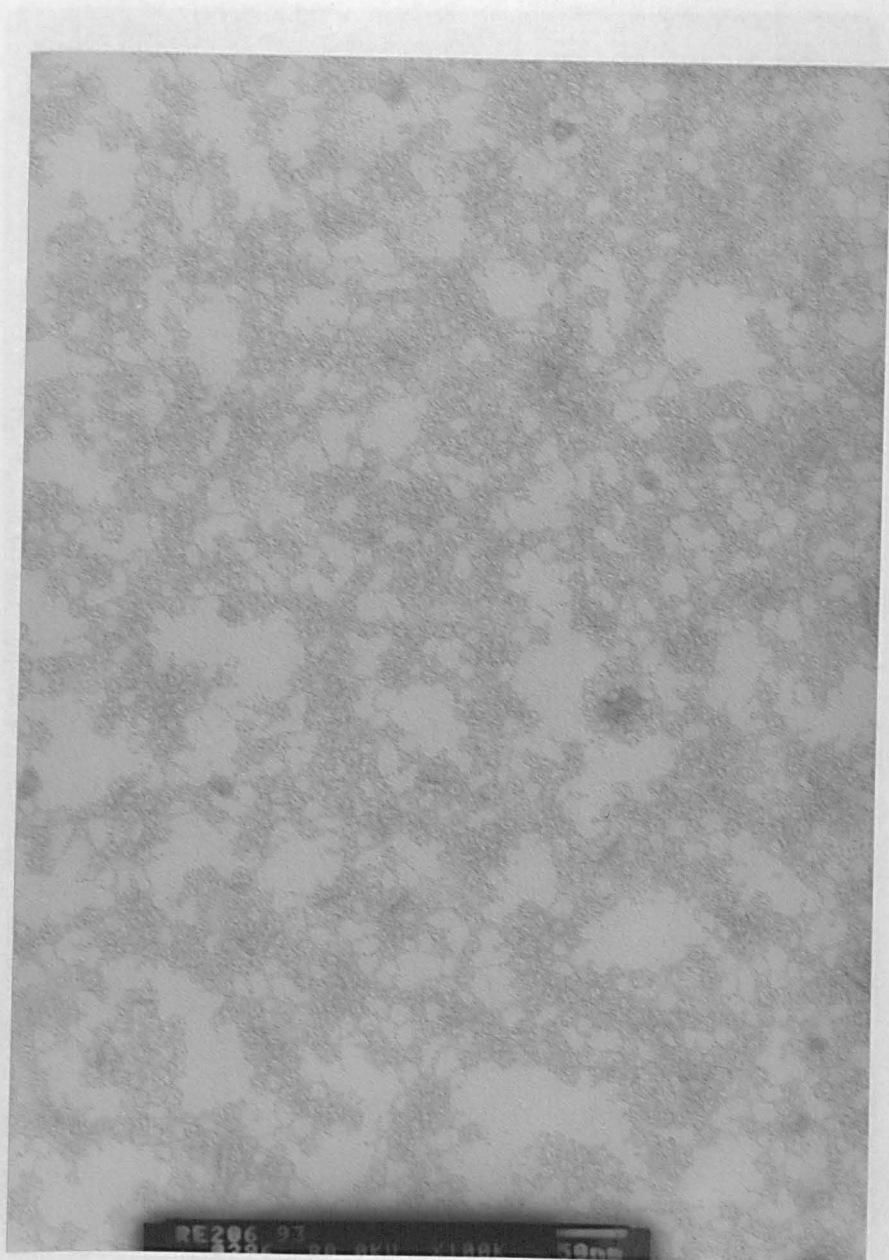
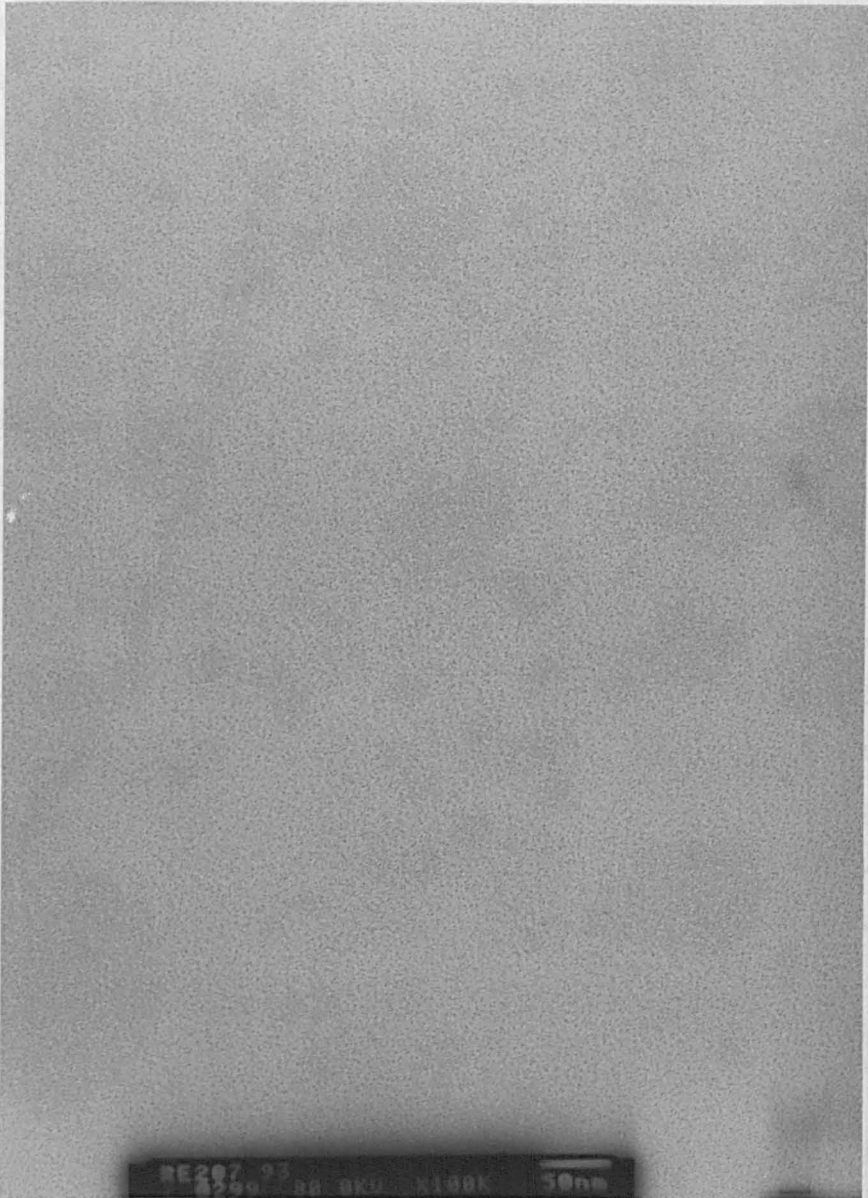


Figure 3.5 – Transmission Electron Micrograph of Peak Two Material from 1.5:2 PLA-PEG Copolymer (Magnification = 100K)



with micelles which were 12.6 nm in diameter.

3.4.2.4 TEM of PLA-PEG Particles

Figures 3.6 and 3.7 show the TEM photographs of fractionated 4:2 and 6:2 PLA-PEG particles respectively. These pictures clearly show the presence of particles as the white spherical entities surrounded by the grey staining. The particles have a narrow size distribution, giving measurements of $11.3 \text{ nm} \pm 1.9 \text{ nm}$ for 4:2 PLA-PEG particles and $15.1 \text{ nm} \pm 3.2 \text{ nm}$ for 6:2 PLA-PEG particles.

PLA-PEG particles have previously been viewed using TEM by Zhu *et al* (1989), where star-PLA-PEG copolymers were examined after preparation from solutions of the copolymers in chloroform. Spherical entities in the size range 40 to 100 nm were seen.

These structures were prepared from a solution in chloroform, so it is expected that the PEG groups would form the core in this instance, with the PLA groups forming the outer shell. The increased molecular weight (M_n values between 20100 and 41500) probably accounts for the larger size of these star-PLA-PEG structures.

3.4.2.5 TEM of 1.5:2 LPLA-PEG Particles

TEM studies have been performed on the 1.5:2 LPLA-PEG particles after cleaning by GPC. Figure 3.8 shows a typical TEM photograph for fractionated 1.5:2 LPLA-PEG particles. This picture is much less conclusive, with fewer discrete particles being observed. Moreover, it can be seen that string-like entities are present along with a few particles. LPLA is more crystalline than DLPLA, which leads to 1.5:2 LPLA-PEG also being more crystalline than the other PLA-PEG copolymers. It was therefore possible that these string-like entities could have been crystals due to the LPLA, but after closer examination under the electron microscope, it was clear that they were strings of particles joined together.

Experiments were performed to attempt to break down these strings of particles. Initially, a sonic bath (Decon FS100, Decon Ultrasonics Ltd., Sussex, England) was employed, with the sample being sonicated for up to thirty minutes. However, TEM showed that this had little effect on breaking down the particle chains. Therefore, the 1.5:2 LPLA-PEG samples were subjected to higher energies of sonication by using a sonic probe (Type 7532-1A, Dawes Instruments Ltd., England) and different energy

Figure 3.6 – Transmission Electron Micrograph of Fractionated 4:2 PLA-PEG Particles
(Magnification = 100K)

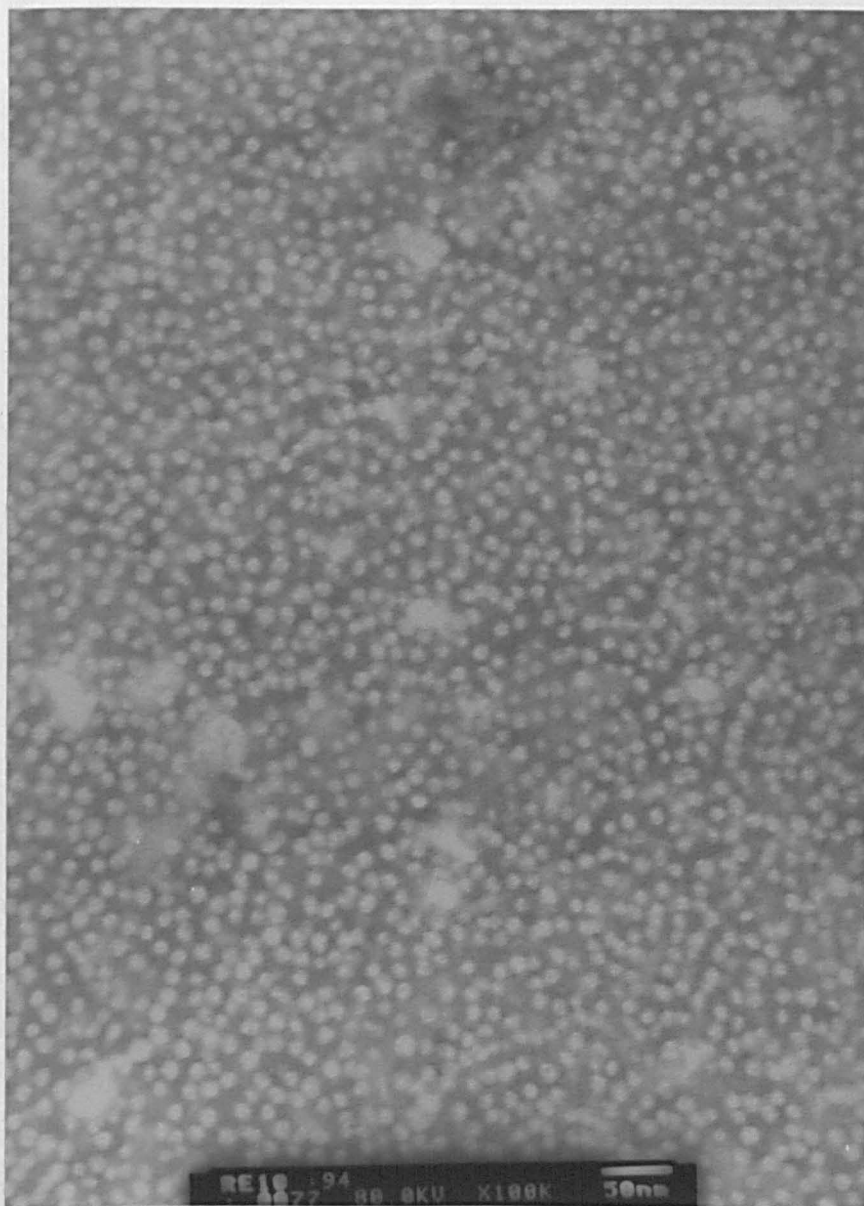


Figure 3.7 – Transmission Electron Micrograph of Fractionated 6:2 PLA-PEG Particles (Magnification = 100K)

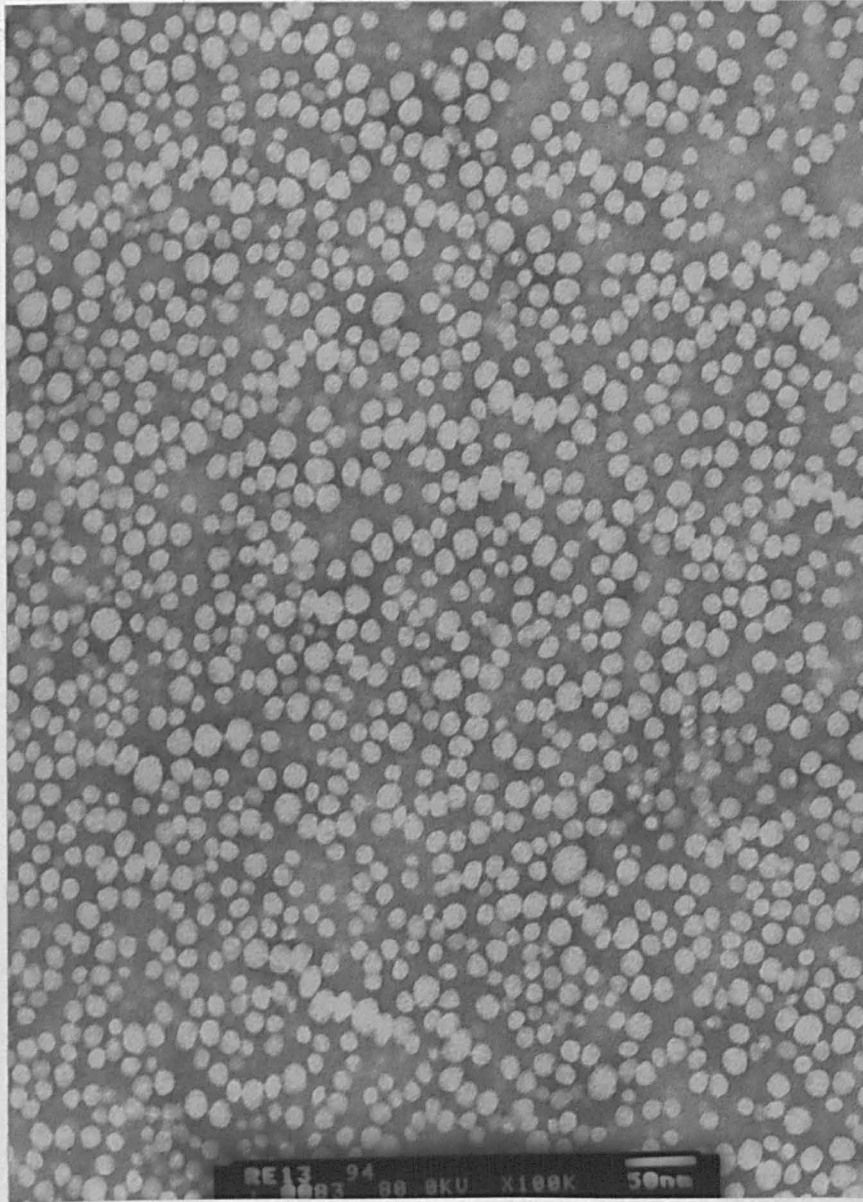
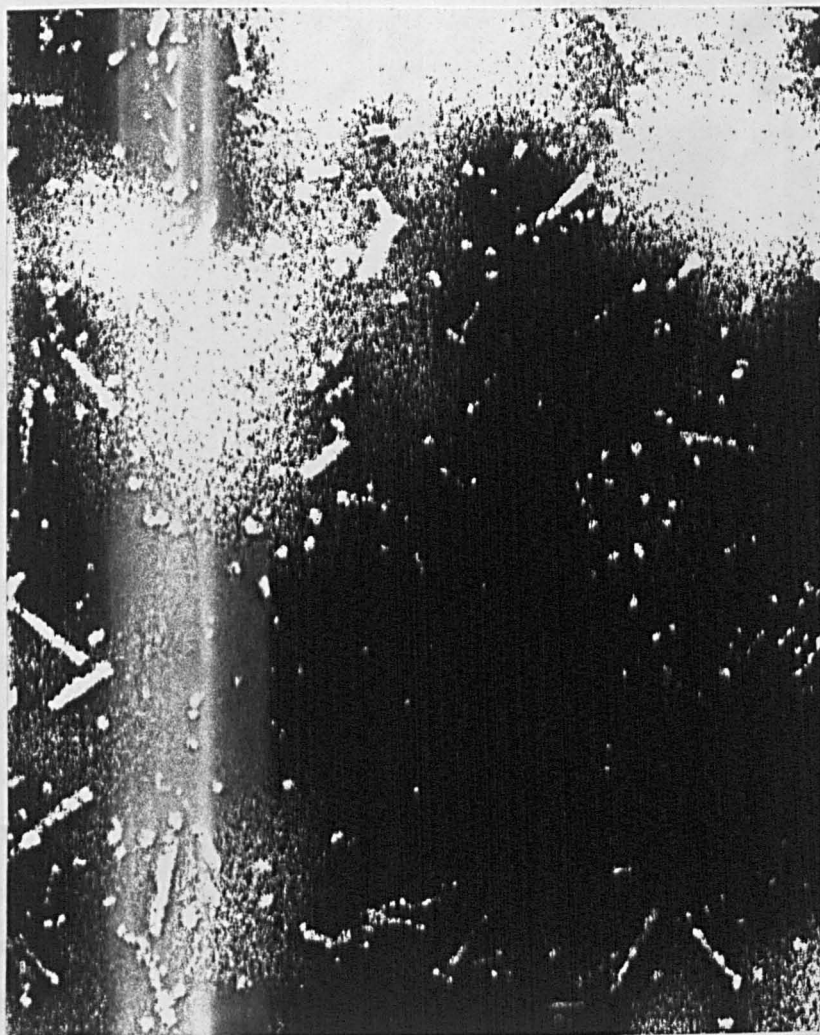


Figure 3.8 – Transmission Electron Micrograph of Fractionated 1.5:2 LPLA-PEG Particles Before Sonication (Magnification = 100K)



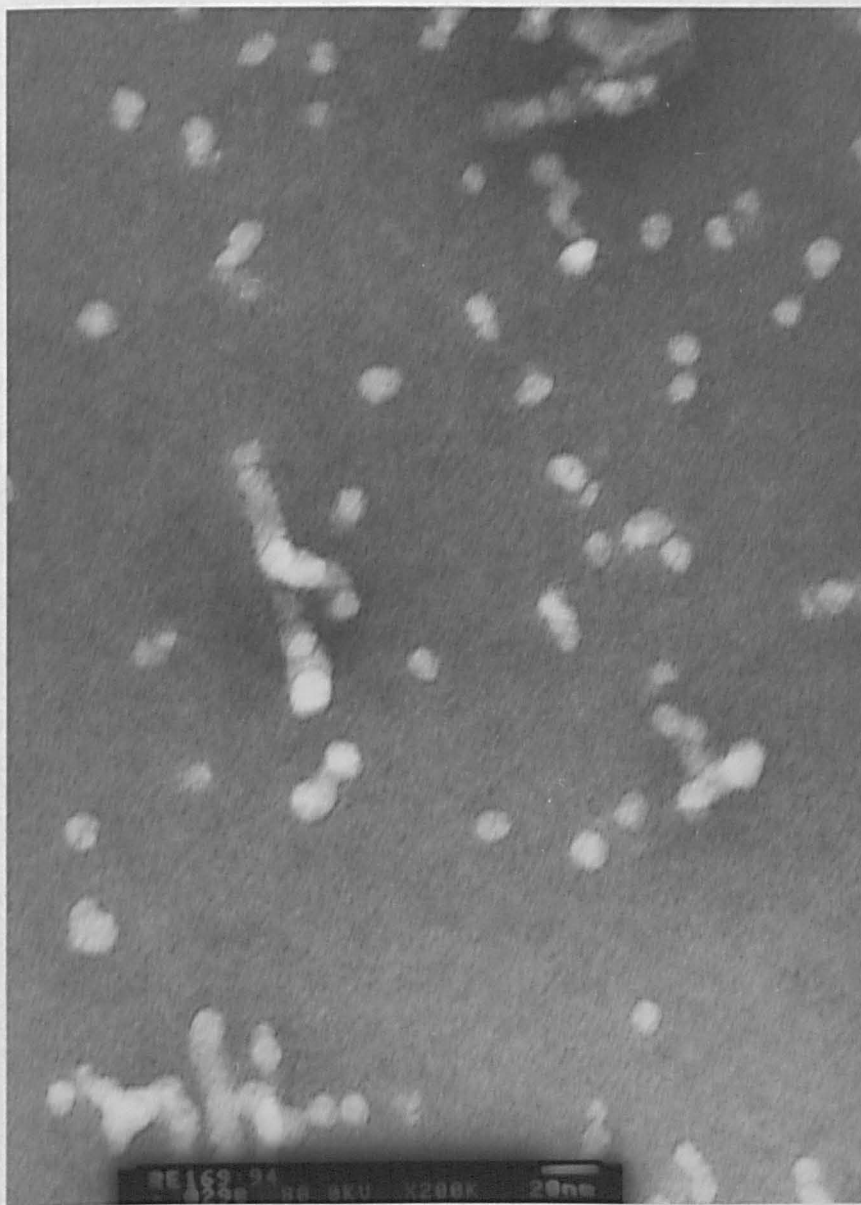
outputs of pulsed sonication. The samples were also sonicated for different lengths of time (up to ten minutes). On analysis by TEM, the best results were seen with an energy output of level 8 on the sonic probe. A distinct improvement was seen with output 7 compared with the lower energy outputs (1-6), and further improvement was seen with output 8, which showed a large number of discrete particles. Chains of particles were still seen, but these had decreased in number when compared with the TEM photographs taken following the use of the lower energy outputs from the sonic probe. At the higher outputs of 9 and 10, there was no significant improvement in the number of discrete.

1.5:2 LPLA-PEG samples were therefore sonicated using the sonic probe at output 8 for 4, 7 and 10 minutes. Examination by TEM of the samples showed an improvement with time, such that the sample sonicated for 10 minutes gave the best result, with the highest number of discrete particles and lowest number of chains present (Figure 3.9). However, the difficulty in obtaining single, discrete particles shows that the particles containing L-PLA, as opposed to DL-PLA appear to be much less sterically stable, and due to this and the polydispersity of the particle distribution, they are not likely to be useful as a drug delivery system. These particles were therefore only considered for comparison of the physicochemical properties, and not for drug loading or biodistribution.

3.4.3.1 Atomic Force Microscopy (AFM)

The atomic force microscope can be used to image the surface of materials and produce topographic images. A tiny, sharp probe is employed which is mounted on a flexible cantilever and when this probe is applied to the sample surface, the forces experienced between the probe and the surface allows topographs to be generated of the material (Shakesheff *et al*, 1994). The AFM works by focusing laser light on a cantilever, which bounces off toward a photodiode. This detects the deflection of the cantilever by sensing the location of the reflected beam. A feedback loop keeps the position of the reflected beam and thereby the force on the sample constant, by moving the sample up and down as the sample is scanned (Drake *et al*, 1989).

Figure 3.9 – Transmission Electron Micrograph of Fractionated 1.5:2 LPLA-PEG After Sonication (Energy Level = 8; 10 minutes) (Magnification = 200K)



3.4.3.2 Atomic Force Microscopy (AFM) of PLA-PEG Particles

This experiment was performed as described in section 2.5.2 on 4:2 PLA-PEG and 6:2 PLA-PEG. High concentrations cause “sweeping” of the particles to occur, i.e. there was movement of the particles as the probe scanned across them (Figure 3.10). This prevented the acquisition of surface images (Roberts *et al*, 1992) and to prevent this phenomenon, a low concentration of particles (0.001 %w/v) was employed.

Figures 3.11 and 3.12 show the pictures produced for 4:2 and 6:2 PLA-PEG particles respectively, which show the particles in two and three dimensions, with a cross section of the particle shown below the image (line profile). The images are represented as grey-scale, so that the height of the image is shown by the shade of the pixels, with black pixels representing the lowest points on the topography and white pixels the highest points, with shades of grey indicating intermediate heights (Shakesheff *et al*, 1994). The 4:2 PLA-PEG particles showed an even distribution and spherical particles as seen in Figure 3.11. Figure 3.12 clearly shows a single particle of 6:2 PLA-PEG, which is again spherical. The three-dimensional picture shows that some compression of the particle has occurred, making the height of the particle appear less than in reality, usually about half the actual value, as the tip of the AFM probe pushes down onto the particle.

The line profiles show image "broadening" due to the interaction between the AFM probe and the sample. This occurs when the AFM generates an image of a rough surface of similar magnitude to the AFM tip itself, causing the side of the probe to become involved in the image generation (Shakesheff *et al*, 1994). The image produced therefore begins with a self-image of the probe, as the AFM probe contacts with the curvature of the particle. The next stage in the image is then of the particle itself as the probe scans the upper part of the particle surface giving real surface data. Finally, another self-image of the probe completes the scan as the reverse side of the probe contacts with the particle. This gives an increase in the apparent particle diameter, giving an apparent particle diameter of about 40 nm, whereas the true diameter of the particle can be estimated by the equation:-

$$\text{broadened particle diameter} = 2w = 4(Rr)^{1/2}$$

where w is the distance between the centres of the particle and the tip, R is the radius of

Figure 3.10 – Sweeping of 4:2 PLA-PEG Particles Using an Atomic Force Microscope

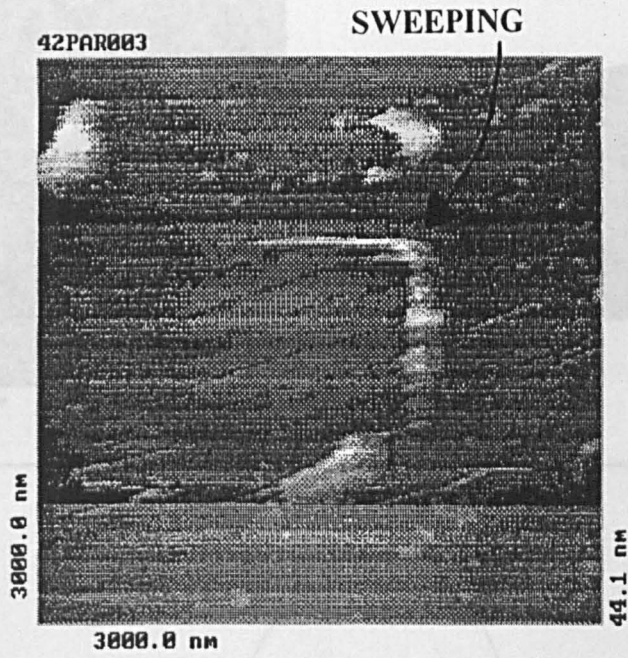


Figure 3.11 – 4:2 PLA-PEG Particles as Imaged Using Atomic Force Microscopy (AFM)

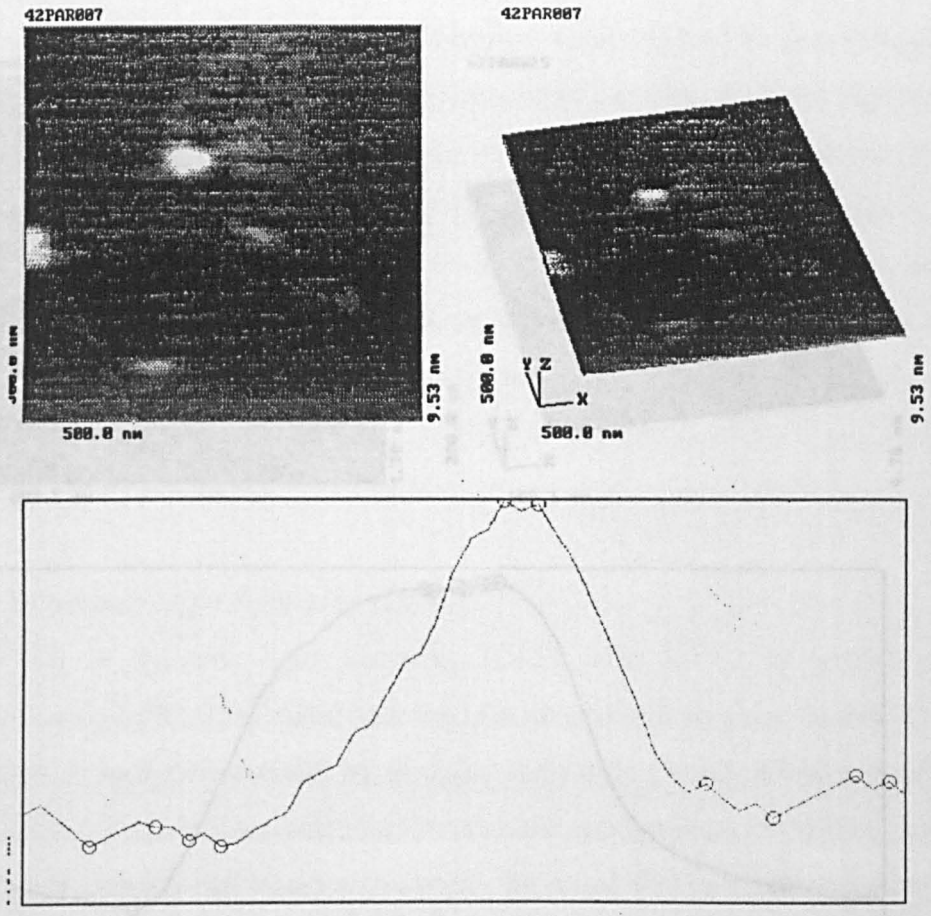
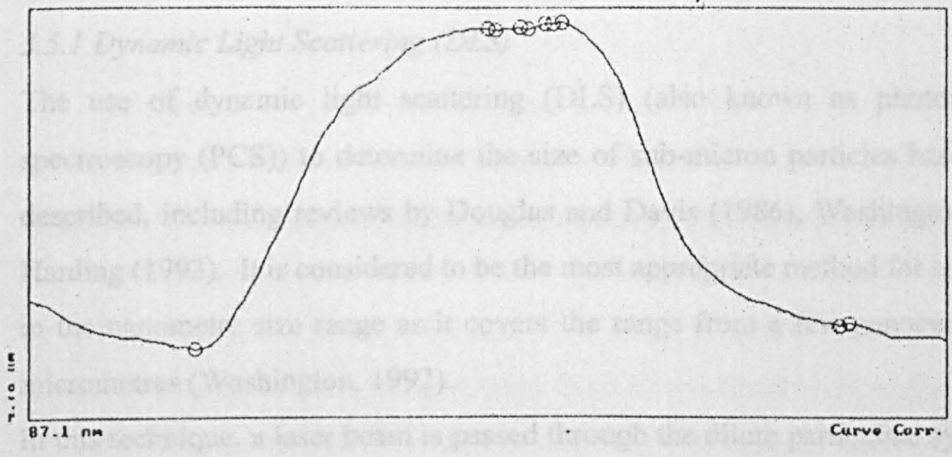
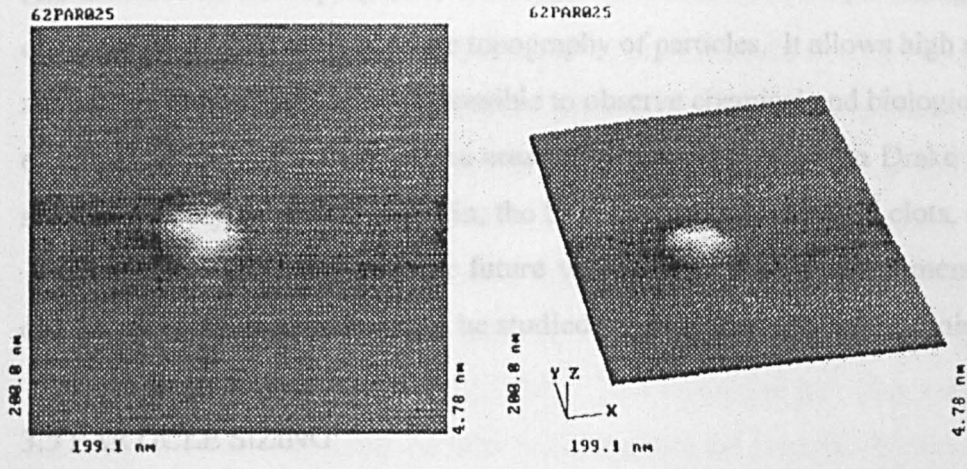


Figure 3.12 – 6:2 PLA-PEG Particles as Imaged Using Atomic Force Microscopy (AFM)

as 10 nm and the broadened particle diameter is taken as 36 nm for 4:2 PLA-PEG and 40 nm for 6:2 PLA-PEG. After calculation, this gives an estimated actual particle size of 16.2 nm for 4:2 PLA-PEG and 20.0 nm for 6:2 PLA-PEG. These results compare reasonably with TEM results.

Atomic force microscopy (AFM) is therefore a suitable tool for providing an estimate of the topography of particles. It allows high resolution of images to be obtained of biological processes (Duke et al (1989)). The use of AFM to image particles is also possible, where the future of the technology is seen, where the



random Brownian motion of the particles causes fluctuations in the intensity of the scattered light. Small particles will diffuse rapidly giving rapid fluctuations in the scattered light, whereas large particles will diffuse more slowly giving light scattering fluctuations over a longer timescale. A photomultiplier then measures the intensity of the scattered light and feeds the information to an autocorrelator. The correlator then calculates the normalized intensity correlation function $g^{(2)}(\tau)$ as a function of the delay time τ . A plot of $2\tau(g^{(2)}(\tau) - 1)$ against τ will then give the diffusion coefficient, D , with the plot being fitted to a linear, quadratic or cubic photo to supply the best fit (Harding, 1991). The hydrodynamic radius, r_h , can then be calculated using the Stokes-Einstein

the tip and r is the radius of the particle. In this experiment, the radius of the tip can be taken as 10 nm and the broadened particle diameter is taken as 36 nm for 4:2 PLA-PEG and 40 nm for 6:2 PLA-PEG. After calculation, this gives an estimated actual particle size of 16.2 nm for 4:2 PLA-PEG and 20.0 nm for 6:2 PLA-PEG. These results compare reasonably with TEM results.

Atomic force microscopy (AFM) is therefore a suitable tool for providing an estimate of particle size and for viewing the topography of particles. It allows high resolution of a naked particle surface and it is possible to observe chemical and biological processes occurring in real time on the same area of surface, such as when Drake *et al* (1989) studied the polymerisation of fibrin, the basic component of blood clots, using AFM. Thus, there is the possibility for future work on PLA-PEG copolymers, where the degradation of the particles could be studied in real time using this technique.

3.5 PARTICLE SIZING

3.5.1 Dynamic Light Scattering (DLS)

The use of dynamic light scattering (DLS) (also known as photon correlation spectroscopy (PCS)) to determine the size of sub-micron particles has been widely described, including reviews by Douglas and Davis (1986), Washington (1992) and Harding (1993). It is considered to be the most appropriate method for sizing particles in the nanometre size range as it covers the range from a few nanometres to a few micrometres (Washington, 1992).

In this technique, a laser beam is passed through the dilute particulate system and the random Brownian motion of the particles causes fluctuations in the intensity of the scattered light. Small particles will diffuse rapidly giving rapid fluctuations in the scattered light, whereas large particles will diffuse more slowly giving light scattering fluctuations over a longer timescale. A photomultiplier then measures the intensities of the scattered light and feeds the information to an autocorrelator. The correlator then calculates the normalised intensity correlation function $g^2(\tau)$ as a function of the delay time (τ). A plot of $\ln(g^2(\tau) - 1)$ against τ will then give the diffusion coefficient, D , with the plot being fitted to a linear, quadratic or cubic plot to supply the best fit (Harding, 1993). The hydrodynamic radius, r_h , can then be calculated using the Stokes-Einstein

equation,

$$r_h = kT / 6\pi\eta D$$

where k is the Boltzmann constant, T is the absolute temperature, η is the viscosity of the solvent and D is the diffusion coefficient. The diameter can thus be determined by multiplying the radius by a factor of two.

Light scattering techniques are widely used for characterisation of colloidal particles.

Static light scattering can be employed to give information on the shape, radius of gyration and molecular weight of a micelle/particle, whereas the technique of dynamic light scattering (DLS) discussed here can give the particle size and an indication of the particle size distribution to a reasonable degree of accuracy (Lodge, 1994). DLS has the advantages of being applicable over a wide size range (5-3000 nm), having a rapid analysis time (usually around a minute), and requiring no prior knowledge of the concentration (Douglas and Davis, 1986). This technique provides a hydrodynamic diameter, which is a hydrated diameter including both the core and the surrounding PEG shell.

3.5.2 Determination of the Hydrodynamic Radius of PLA-PEG Micelles and Particles

DLS measurements have been performed as described in section 2.6.1, on triplicate samples of fractions of both peaks produced from GPC, and also on the unfractionated copolymer dispersions and Poloxamer 407, for comparison (Table 3.6). The fractionated 1.5:2 PLA-PEG and 2:5 PLA-PEG material from the first GPC peak resulted in micelles which were smaller than those formed from freeze-dried unfractionated material. Micelles were not detected by DLS measurement in material eluted in peak two, in agreement with the GPC and TEM results. The polydispersity of the samples is also shown in Table 3.6. The reproducibility between the triplicate samples of each system was reasonable for all of the micellar systems, giving low standard deviations.

This shows that the micelles produced from the unfractionated material are about 4 nm larger for 1.5:2 PLA-PEG and over 6 nm larger for the 2:5 PLA-PEG than those produced with the fractionated material. The polydispersities are similar between the fractionated and unfractionated samples for the 1.5:2 PLA-PEG, but for the 2:5 PLA-PEG, the unfractionated PLA-PEG sample polydispersity is noticeably larger than that for the fractionated sample.

Dynamic light scattering size analysis has also been performed on triplicate samples of 4:2 and 6:2 PLA-PEG particles. The particle size and polydispersity results are shown in Table 3.7. This shows that despite forming particle distributions with low polydispersity (confirmed by TEM), there is a wide size distribution between samples, even though the samples were prepared under the same conditions.

3.5.3 Determination of the Hydrodynamic Radius of 1.5:2 LPLA-PEG Particles

Due to the difficulty in obtaining discrete particles of 1.5:2 LPLA-PEG copolymer, the samples had first to be treated with the sonic probe as described above in section 3.4.2.4.

Dynamic light scattering (DLS) was then performed on the samples in triplicate as described in section 2.6.1. This gave a particle size value of $14.5 \text{ nm} \pm 0.8 \text{ nm}$ for the fractionated 1.5:2 LPLA-PEG particles.

3.5.4 Discussion

Table 3.8 shows that there is a general agreement between the different methods of particle sizing. The agreement between the calculated AFM and the DLS results for the 4:2 and 6:2 PLA-PEG particles is particularly good, with the TEM results being of a similar magnitude but lower. The smaller micelle/particle size measured from TEM can be explained by the sample preparation technique, which involves a drying process causing a collapsing of the hydrophilic PEG shell onto the surface of the particle (Bahadur *et al.*, 1985; Polverari and van de Ven, 1994). In contrast, the size obtained from DLS is a hydrated size and therefore includes the hydrated PEG shell and the solvent associated with it (Bedells *et al.*, 1993) and will thus reflect the length of the hydrated PEG chains as well as the particle core.

The data in Table 3.6 showed a larger micelle size for the unfractionated micelles over the fractionated micelles. This increase in size is presumably due to the presence of the second peak material in the sample. It is possible that interaction between the micelles and the second peak material (which is PLA-depleted and therefore, predominantly PEG) causes a decrease in the diffusion coefficient, D , which is inversely proportional to the particle size. Thus, the PEG chains of the micelles could undergo transient entanglements with the PEG chains of the peak two material (Nicholas *et al.*, 1993), which would give a slower diffusion coefficient and hence an increased particle size.

Table 3.6

Dynamic light scattering results for 1.5:2 and 2:5 PLA-PEG Micelles

Copolymer	Size (nm)	Polydispersity
1.5:2 PLA-PEG Unfractionated	19.8 ± 0.6	0.19 ± 0.02
1.5:2 PLA-PEG Peak One	15.6 ± 0.9	0.22 ± 0.07
1.5:2 PLA-PEG Peak Two	-	-
2:5 PLA-PEG Unfractionated	25.3 ± 0.6	0.68 ± 0.01
2:5 PLA-PEG Peak One	18.9 ± 1.6	0.28 ± 0.01
2:5 PLA-PEG Peak Two	-	-
Poloxamer 407	29.1 ± 0.5	0.12 ± 0.06

Table 3.7

Dynamic light scattering results from 4:2 and 6:2 PLA-PEG Particles

Sample	Size (nm)	Polydispersity
4:2 PLA-PEG (1)	18.9 ± 0.1	0.103 ± 0.019
4:2 PLA-PEG (2)	15.3 ± 0.3	0.171 ± 0.062
4:2 PLA-PEG (3)	10.5 ± 0.3	0.325 ± 0.054
4:2 PLA-PEG (mean)	15.1 ± 3.5	0.200 ± 0.106
6:2 PLA-PEG (1)	25.2 ± 0.2	0.102 ± 0.025
6:2 PLA-PEG (2)	21.1 ± 0.1	0.148 ± 0.015
6:2 PLA-PEG (3)	16.1 ± 0.2	0.264 ± 0.038
6:2 PLA-PEG (mean)	20.8 ± 3.8	0.171 ± 0.074

This is supported by the greater difference between unfractionated and fractionated 1.5:2 LPLA-PEG particles at the higher concentration of 10% w/v, which is discussed in section 4.2.4, where there would be an increased amount of peak two material present and therefore, a greater chance of interaction.

The above theory suggests an “unreal” effect, where the particle size is not increased but the experimental technique makes it appear so. However, it is possible that the increase in particle size is a “real” effect. The second peak material, as already established, is predominantly PEG. These PEG chains from this species could become entangled with the palisade layer of the micelles, the “primary” layer of PEG. Polverari and van de Ven (1994) have illustrated this, by adding more PEO to a dispersion of latex particles previously coated with PEO. They showed that a “secondary” layer of PEO was able to adsorb onto the primary layer by entanglement of the polymer chains of the excess PEO into the loops of the primary layer. The polymer in the secondary layer would be in equilibrium with the free polymer chains in solution.

Finally, it is also feasible that some of the peak two material separated out by GPC, can incorporate into micelles. This means that some of the material in the second peak from GPC would be able to incorporate in a transient manner into micelles in the unfractionated dispersions. The peak two material would be in equilibrium, with a more rapid exchange relative to the higher PLA-containing material of peak one. This could cause an increased association number, thus increasing micelle size by increasing the micelle core size and possible also increasing the PEG chain length as the tighter-packed PEG chains repulse each other and stretch out closer to a tail conformation (Polverari and van de Ven, 1994). This theory is supported by the TEM results, where a small increase in size is also observed, which due to the drying process discussed above, cannot be due to an increase in the hydrophilic PEG chain length alone.

Comparing the different PLA-PEG copolymers, it can be seen that the particle size varies relatively little with the change in PLA to PEG ratio. Generally, increasing PEG chain length results in increased size of micelles and particles (El Eini *et al.*, 1975; Güveli *et al.*, 1981; Almgren *et al.*, 1995). However, this is not reflected in the results for the fractionated PLA-PEG copolymers, as 2:5 PLA-PEG micelles (with a PEG chain length of 5000 as opposed to 2000 for the other PLA-PEG copolymers) are no larger than the other PLA-PEG micelles/particles. Considering the hydrophobic chain length,

Arnarson and Elworthy (1981) observed that for surfactants containing long hydrocarbon chains, there was an increase in micellar size with increasing hydrocarbon chain length. Bahadur *et al* (1985) also noticed that micelle size increased with an increase in the size of the insoluble component of a block copolymer and an increase of the total molecular weight of the copolymer. Again, the PLA-PEG copolymers do not appear to follow these generalities. Despite the differences in hydrophobic chain length between the PLA-PEG copolymers, with theoretical PLA contents of 1500, 4000 and 6000 for 1.5:2 PLA-PEG, 4:2 PLA-PEG and 6:2 PLA-PEG respectively, 6:2 PLA-PEG, there is little difference between the sizes of the micelles and particles formed from these copolymers. Therefore, it appears that a greater increase in the molecular weight of the hydrophilic PEG block and/or hydrophobic PLA block would be necessary to give a significant increase in micelle or particle size.

The PLA-PEG copolymer micelles and particles are of the expected size range considering their block lengths and results quoted for similar copolymers, such as the poloxamers (Pluronic), diblock copoly(oxybutylene/oxyethylene), B_xE_y , copolymers and triblock copoly(oxyethylene/oxybutylene/oxyethylene), $B_xE_yB_x$, copolymers (Table 3.9).

In the only comparable DLS results from the literature, the PLA-PEG particles were prepared by different methods and had different ratios of PLA to PEG to the copolymers discussed here, and are therefore not directly comparable. However, the Me.PEG-PLA particles produced by Bazile *et al* (1995) were in the nanometre size range (56 - 112 nm).

3.6 DETERMINATION OF CMC OF PLA-PEG SYSTEMS

3.6.1 Methods for Determining Critical Micelle Concentration (CMC)

The critical micelle concentration is defined as the concentration at which the experimental method used can just detect the presence of micelles in the system. If micelles are to be used as drug delivery systems, it is imperative that their stability on dilution in an *in vivo* situation can be established. The cmc is thus a useful thermodynamic parameter for characterising micelle stability on dilution (Kabanov *et al*, 1995).

Table 3.8

Summary of Particle Size Analysis by Dynamic Light Scattering and Microscopy

Copolymer	Diameter, DLS (nm)	Diameter, TEM (nm)	Diameter, AFM (nm)
1.5:2 PLA-PEG	15.6 ± 0.9	7.2	-
2:5 PLA-PEG	18.9 ± 1.6	17.0	-
1.5:2 LPLA-PEG	14.5 ± 0.8	11.1	-
4:2 PLA-PEG	15.1 ± 3.5	11.3	16.2
6:2 PLA-PEG	20.8 ± 3.8	15.1	20.0
Poloxamer 407	29.1 ± 0.5	12.6 ± 6.0	-

Table 3.9

Micellar Sizes of Similar Copolymers as Measured by DLS

Copolymer	Theoretical PEO Mw	Temperature (°C)	Size (nm)	Reference
Poloxamer 407	4000 (x2)	25	29.1 ± 0.5	-
EO ₂₅ -PO ₃₉ -EO ₂₅ (P85)	1125 (x2)	37	14.6 ± 0.6	Kabanov <i>et al</i> , 1995
EO ₁₄₄ -PO ₅₆ -EO ₁₄₄ (F108)	6480 (x2)	37	35.0 ± 5.0	Kabanov <i>et al</i> , 1995
B ₃₃ E ₁₃₅	6075	25.3	45.0	Sun <i>et al</i> , 1991
B ₁₃ E ₅₀	2250	20	17.2	Bedells <i>et al</i> , 1993
E ₅₈ B ₁₇ E ₅₈	2610 (x2)	30	13.8 ± 0.6	Nicholas <i>et al</i> , 1993

Critical micelle concentrations (cmcs) can be determined by several different methods. Some of these methods involve the concept of solubilisation, whereby a hydrophobic compound is chosen which can be solubilised into the core of micelles. Thus, an increase in the solubility of a hydrophobic compound indicates the formation of micelles. Examples of this method are given by Goodhart and Martin (1962), who used benzoic acid as the solubilise, Furton and Norelus (1993), who used the oil-soluble dye, 1-(2-pyridylazo)-2-naphthol, and Schmolka and Raymond (1965), who used the dye benzopurpurin 4B. A similar method involves the solubilisation of a hydrophobic fluorescent probe, such as that described by Alexandridis *et al* (1994). Here, the fluorescence efficiency of diphenylhexatriene, DPH, in different Pluronic copolymers was studied. The fluorescence efficiency of DPH in a hydrophilic environment is zero, whereas that in a hydrophobic environment (such as a micelle core) is unity, providing a sensitive indicator of when micelles are formed. These experiments were also corroborated with differential scanning calorimetry (DSC). Güveli *et al* (1981), Reddy *et al* (1990) and Wanka *et al* (1990) have employed static light scattering studies to determine the cmc value, and Wanka *et al* (1990) also performed interfacial tension studies for comparison, whilst Güveli *et al* (1981) compared with viscosity measurements. These last three groups have also used surface tension studies to elicit cmc values, which is the method that will be performed on the PLA-PEG micelles and is described below.

The dye solubilisation method described above (either with fluorescent probe or hydrophobic dye) and the surface tension method of determining cmc are the most widely used. The dye solubilisation method has the drawback that partial exhaustion of the dye can occur, so that the results need careful analysis (Schmolka and Raymond, 1965). Also the presence of the dye/probe could theoretically affect the cmc result, although providing the solubilise is hydrophobic, it should be located in the micelle core and should therefore have a negligible effect on the cmc value (Furton and Norelus, 1993). However, the measurement of surface tension avoids this potential problem. The surface tension method works on the theory that an increase in surfactant concentration leads to a decrease in surface tension according to the Gibbs' isotherm of adsorption, with micelle formation at the cmc causing a break in this dependence (Kabanov *et al*, 1995). The cmc value is therefore determined by plotting the logarithm

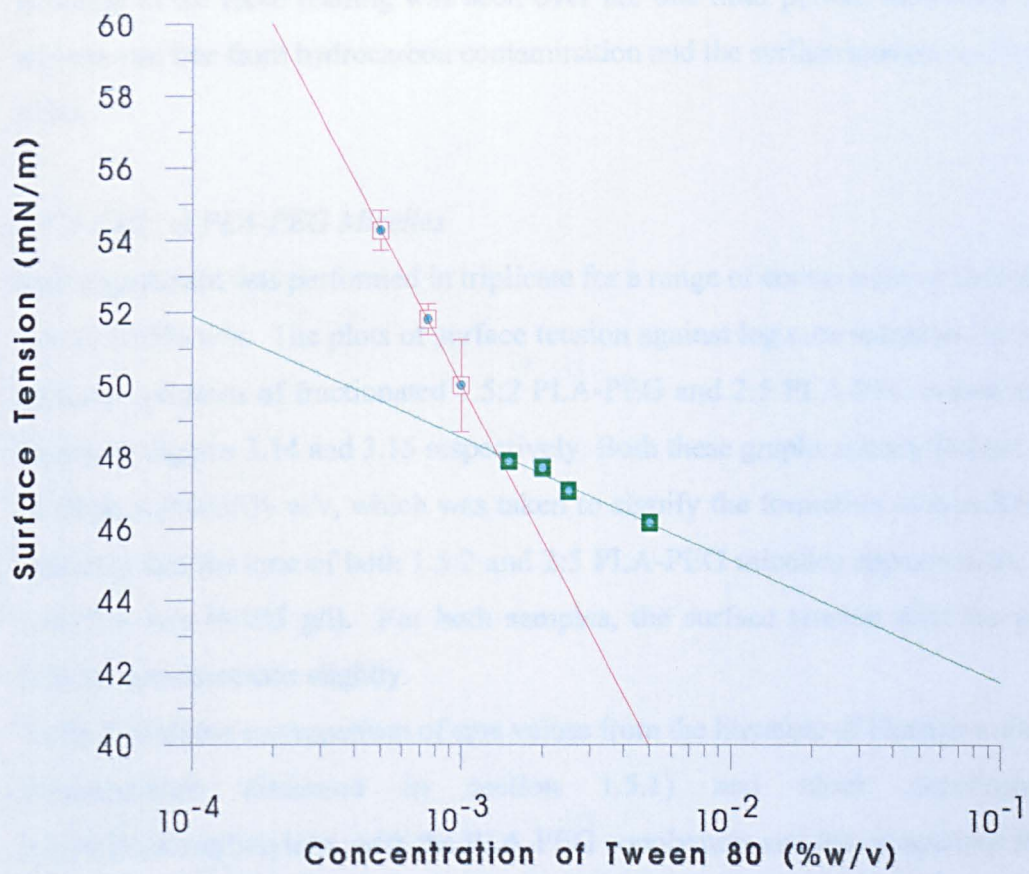
of the concentration against the surface tension, which should give two straight lines before and after the break in dependence. The point at which this break occurs, and therefore where the two lines cross, is the cmc. The method employed to find the cmc by this method has been described previously by many authors (including Bedells *et al.* 1993; Alexandridis *et al.*, 1994) and is outlined in section 2.7.1.

However, it must be remembered in this experiment that due to the nature of block copolymers, no sharp cmc value is observed, as even those with a narrow distribution of molecular weight still have some appreciable heterogeneity (see section 3.3.5). Also, large differences may be noted between cmc values determined by different methods, as their sensitivity to unimers and micelles and the nature of the average quantity estimated can be quite different (Zhou and Chu, 1987).

3.6.2 CMC of Polysorbate (Tween) 80 Micelles

The cmc of Tween 80 was determined using surface tension measurements to provide a control for the experimental determination of the cmc of the 1.5:2 and 2:5 PLA-PEG micelles. Polysorbate 80 was chosen as a surfactant where the literature value of the cmc was readily available (Wan and Lee, 1974) and as it had a similar HLB value to the PLA-PEG micelles (HLB of polysorbate 80 = 15.0; 2:5 PLA-PEG = 14.3; 1.5:2 PLA-PEG = 11.5). Solutions of Tween 80 were prepared using HPLC grade water and chromic acid cleaned glassware at concentrations ranging from 0.0005% w/v to 0.005% w/v. The results are shown in Figure 3.13 as the logarithm of the concentration against surface tension. This shows that there is a definite change in slope between the concentrations 0.001% w/v and 0.0015% w/v. The point of intersection of the two lines is at 0.00135% w/v, which becomes 0.0014% w/v (to two significant figures). A literature value stated by Wan and Lee (1974) is also 0.0014 %w/v for the cmc of Polysorbate 80, showing very good agreement. It is interesting to note that the surface tension values after the point of intersection still show a slight decrease, whereas they would be expected to remain constant, as the surface excess concentration of surfactant molecules is expected to be approximately constant in the presence of micelles. This could perhaps be due to experimental error or to "ageing" of the sample due to hydrocarbon contamination, which would cause the surface tension readings to appear lower than for a pure sample, and also cause a decrease of surface tension with time. To

Figure 3.13 - Plot of Log Concentration of Tween 80 against Surface Tension for the Determination of the CMC



test for this, a further control experiment was performed on solvent used (the HPLC grade water), with the glass slide held at zero immersion for a period of one hour. No decrease in the force reading was seen over the one hour period, indicating that the solvent was free from hydrocarbon contamination and the surface tension readings were valid.

3.6.3 CMC of PLA-PEG Micelles

This experiment was performed in triplicate for a range of concentrations from 0.001% w/v to 0.05% w/v. The plots of surface tension against log concentration (% w/v) for aqueous solutions of fractionated 1.5:2 PLA-PEG and 2:5 PLA-PEG copolymers are shown in Figures 3.14 and 3.15 respectively. Both these graphs show a distinct change in slope at 0.0035% w/v, which was taken to signify the formation of micelles. This indicates that the cmc of both 1.5:2 and 2:5 PLA-PEG micelles appears to be around 0.0035% w/v (0.035 g/l). For both samples, the surface tension after the point of intersection decreases slightly.

Table 3.10 shows a comparison of cmc values from the literature of Pluronic copolymers (nomenclature discussed in section 1.5.1) and block copolymers of oxyethylene/oxybutylene, with the PLA-PEG copolymers and the comparison between authors and techniques. The table clearly shows the discrepancy between the different authors and different techniques, with that between the authors showing the larger variation. One of the reasons for these variations is the difficulty in interpreting results.

With the Pluronic copolymers, for surface tension experiments two inflection points can often be seen, and sometimes a step-like curve between these points that can be smoothed out as the temperature is increased. It is therefore necessary to attempt to explain what causes these steps/inflections, and which one corresponds to the cmc. Different authors have advanced several theories. Prasad *et al* (1979) suggested that the first point of inflection is due to the formation of unimolecular micelles in the bulk due to the collapse of the PPO chains, so that the PPO chains were shielded from the aqueous environment by the PEO chains. However, Alexandridis *et al* (1994 (2)) has pointed out that this has no apparent thermodynamic reasoning at low concentrations and is therefore very unlikely. Also, the increase in temperature should increase the likelihood of these unimolecular micelles, whereas the curve is smoothed out at higher

Figure 3.14 - Determination of the CMC of 1.5:2 PLA-PEG Copolymer using Surface Tension Measurements

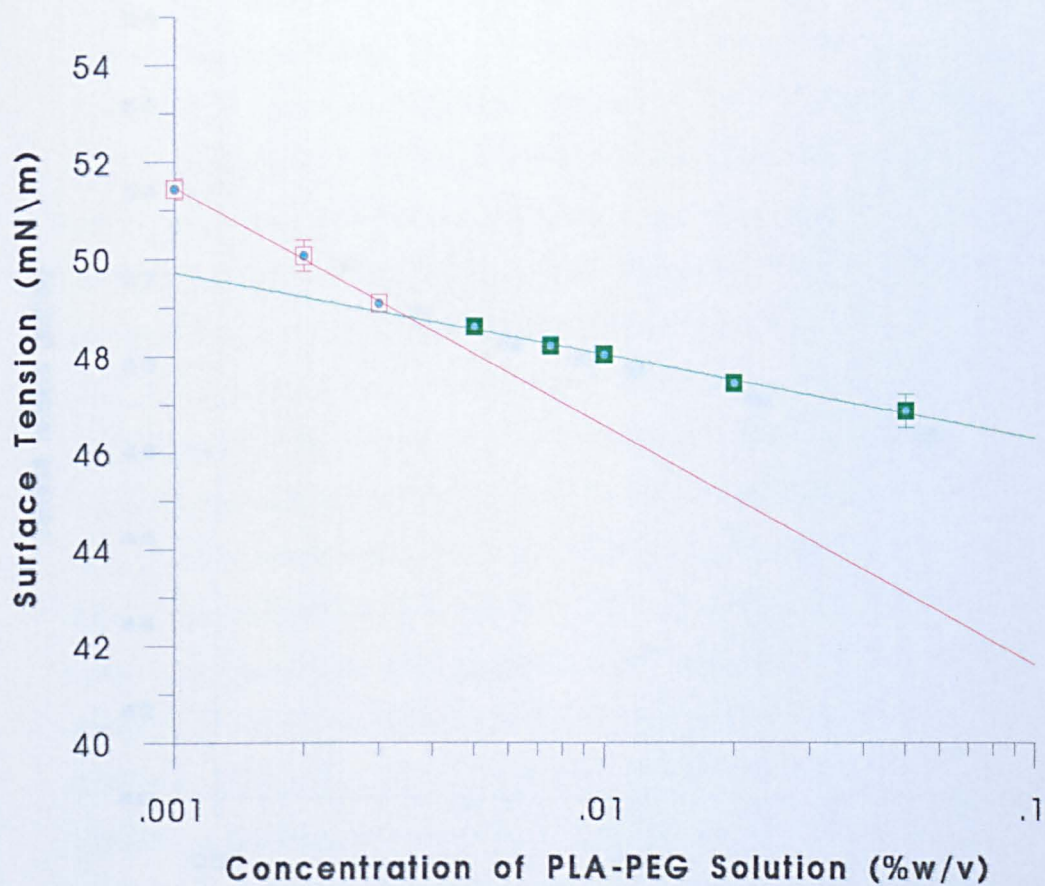
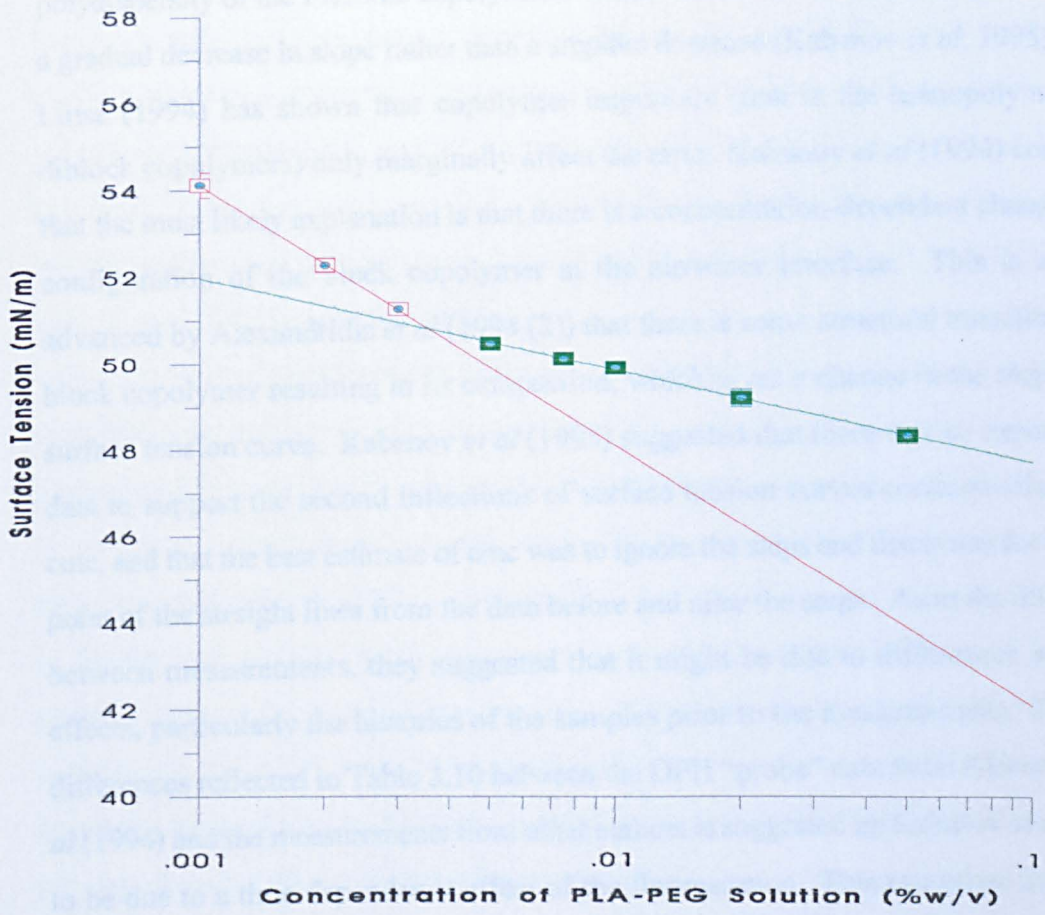


Figure 3.15 - Determination of CMC of 2:5 PLA-PEG Micelles using Surface Tension Measurements



temperatures and not therefore consistent with this theory (Bloß *et al*, 1992). Another possibility discussed by Hecht and Hoffmann (1994) is that the steps are due to polydispersity of the Pluronic copolymers. If this were the reason, then there should be a gradual decrease in slope rather than a steplike decrease (Kabanov *et al*, 1995). Also, Linse (1994) has shown that copolymer impurities (that is the homopolymers and diblock copolymers) only marginally affect the cmc. Kabanov *et al* (1994) concluded that the most likely explanation is that there is a concentration-dependent change in the configuration of the block copolymer at the air/water interface. This is a theory advanced by Alexandridis *et al* (1994 (2)) that there is some structural transition of the block copolymer resulting in its compaction, which gives a change in the slope of the surface tension curve. Kabanov *et al* (1995) suggested that there was no experimental data to support the second inflections of surface tension curves corresponding to the cmc, and that the best estimate of cmc was to ignore the steps and determine the crossing point of the straight lines from the data before and after the steps. As to the differences between measurements, they suggested that it might be due to differences in kinetic effects, particularly the histories of the samples prior to the measurements. The large differences reflected in Table 3.10 between the DPH “probe” data from Alexandridis *et al* (1994) and the measurements from other authors is suggested by Kabanov *et al* (1995) to be due to a time dependence effect of the fluorescence. This can cause the cmc to appear 10 times higher after one hour than after sixteen hours (Alexandridis *et al* (1994) measured their data after three hours). The data at sixteen hours was consistent with other measurements. This “relaxation” of the micellar solutions is thought to be due to the formation of DPH complexes and their complexation/decomplexation during incorporation into the Pluronic micelles.

Another point to consider is that the cmc shows a strong dependence on temperature, especially at low concentrations (Almgren *et al* 1995). For the Pluronics, an increase in temperature decreases the cmc, by decreasing the hydration of the Pluronic chains and thus increasing the hydrophobicity of the micellar core. The micellar cores near the cmc value are very swollen by solvent, and as the concentration or temperature increases, solvent molecules are driven out of the micellar core, resulting in a more hydrophobic, smaller core (Gao and Eisenberg, 1993).

Raymond (1965) noted that although the higher molecular weight copolymers studied decreased in cmc as the ethylene oxide content increased, the lower molecular weight copolymers did not follow this trend, showing a decrease and then an increase with increasing ethylene oxide content. However, El Eini *et al* (1975) observed that the more ethylene oxide in a copolymer, the higher the cmc value. They attributed this to solute-solvent interactions being greater with longer polyethylene oxide chains, so that the solubility of the monomer would be increased and the driving forces that lead to micellisation would also decrease. Several groups, including Schick *et al* (1962) and Güveli *et al* (1981), share this view.

Alexandridis *et al* (1994) compared the values of several different Pluronics and found that the cmc decreased with increasing PPO content (and therefore increasing hydrophobicity), whereas increasing the PEO content increased the cmc but to a much lesser extent. They therefore concluded that the more hydrophilic the copolymer molecule (that is the more PEO), the less likely micellisation was, but the effect on cmc of the hydrophobic PPO group was more pronounced, suggesting that the PPO is the primary factor in the micellisation process. Drawing comparisons with the PLA-PEG copolymers, the 2:5 PLA-PEG has a higher PEG content than the 1.5:2 PLA-PEG, but also has a longer PLA block (2000 Mw compared with 1500). From the PEG groups, the cmc of the 2:5 PLA-PEG would be expected to be higher than that of the 1.5:2 PLA-PEG. This is not the case. It must therefore be assumed that, like the Pluronic copolymers, the influence of the PEG group is less important, and the net effect of this increased PEG molecular weight and increased PLA molecular weight cancel each other out to give the same value for both copolymers. The 2:5 PLA-PEG also has a higher molecular weight, and Alexandridis *et al* (1994) noted that for molecules with the same PPO/PEO ratio, those with higher molecular weight formed micelles more readily. Although the ratio of PLA to PEG in the copolymers is not the same, the higher molecular weight of 2:5 PLA-PEG may still be a contributing factor.

Comparing the values of the cmcs in Table 3.10 for other copolymers with the PLA-PEG copolymers, it can be seen that there is very good agreement with the values for Wanka *et al* (1990), which have similar PEO weight contents to the PLA-PEG copolymers (40% and 70% for P104 and F127 respectively). The much higher value for F127 found by Alexandridis *et al* (1994) is unlikely to be valid, as explained above. The values from

Table 3.10

CMC Values of Related Copolymers

Copolymer	PEO Weight %	Method	Temperature (°C)	CMC (% w/v)	Reference
1.5:2 PLA-PEG	60	ST	20	0.0035	-
2:5 PLA-PEG	70	ST	20	0.0035	-
P123	30	ST	25	0.0015	Wanka <i>et al</i> , 1990
P123	30	Probe	20	0.18	Alexandridis <i>et al</i> , 1994
P103	30	Probe	20	0.7	Alexandridis <i>et al</i> , 1994
P104	40	ST	25	0.003	Wanka <i>et al</i> , 1990
P104	40	Probe	20	2	Alexandridis <i>et al</i> , 1994
P104	40	Dye	25	0.0073	Schmolka and Raymond, 1965
P105	50	Probe	20	2.2	Alexandridis <i>et al</i> , 1994
P84	40	Probe	25	2.6	Alexandridis <i>et al</i> , 1994
P84	40	Dye	25	0.0040	Schmolka and Raymond, 1965
P85	50	Probe	25	4	Alexandridis <i>et al</i> , 1994
P85	50	Dye	25	0.0037	Schmolka and Raymond, 1965
P85	50	ST	25	0.03 - 0.04	Kabanov <i>et al</i> , 1995
P85	50	Probe	25	0.04	Kabanov <i>et al</i> , 1995
F108	80	Probe	25	4.5	Alexandridis <i>et al</i> , 1994
F108	80	Dye	25	0.0073	Schmolka and Raymond, 1965
F108	80	ST	25	0.03 - 0.05	Kabanov <i>et al</i> , 1995

Copolymer	PEO Weight %	Method	Temperature (°C)	CMC (% w/v)	Reference
F108	80	Probe	25	0.03	Kabanov <i>et al.</i> , 1995
F127	70	ST	25	0.004	Wanka <i>et al.</i> , 1990
F127	70	Probe	20	4	Alexandridis <i>et al.</i> , 1994
E ₅₀ B ₁₃	70	ST	20	0.003	Bedells <i>et al.</i> , 1993
E ₅₀ B ₁₃	70	ST	40	0.001	Bedells <i>et al.</i> , 1993
E ₂₄ B ₁₀	60	ST	40	0.0023	Bedells <i>et al.</i> , 1993
E ₁₃₅ B ₃₃	70	ST	25.5	0.0070	Sun <i>et al.</i> , 1991
E ₅₈ B ₁₇ E ₅₈	75	SLS	30	0.030	Nicholas <i>et al.</i> , 1993
E ₁₃₂ B ₅₃ E ₁₃₂	70	SLS	30	<0.002	Nicholas <i>et al.</i> , 1993

Key: “ST” is surface tension technique, “dye” is the dye solubilisation technique and “probe” is the DPH probe solubilisation, as explained in the text.

Bedells *et al* (1993) for the diblock polyoxyethylene/polyoxybutylene copolymers (ExBy) are also in good agreement, being of a similar order of magnitude. The value for E₅₀B₁₃ which has similar hydrophobic and hydrophilic contents to 2:5 PLA-PEG (70% PEO by weight, E₄₄L₂₇) and measured at the same temperature as the PLA-PEG copolymers is very close. It is therefore clear that the cmc values obtained for the PLA-PEG copolymers are reasonable considering their composition.

3.7 ULTRACENTRIFUGATION ANALYSIS

3.7.1.1 Sedimentation Velocity

Analytical ultracentrifugation has been used as a technique for characterising macromolecules for a number of years. Such experiments can give information on the molecular weight of the macromolecule (detailed below in 2.8.2) and on the conformation and homogeneity of the sample with sedimentation velocity experiments.

In sedimentation velocity analytical ultracentrifugation runs, the speed is sufficiently high to cause the macromolecules to sediment, creating boundaries between the sample solution and the solvent, which can be used to give information about the sample macromolecules (Harding, 1993). This experiment is therefore a measure of the velocity of the movement of these boundaries, and as well as showing the homogeneity of the samples, a sedimentation coefficient, *s*, can be calculated, which gives an indication of the size, shape and molecular weight of the aggregates. The sedimentation coefficient, *s*, is defined by:

$$s = \frac{dr/dt}{\omega^2 r} = \frac{v}{\omega^2 r}$$

where ω is the angular velocity (radian s⁻¹) of the rotor,

r is the distance of the boundary, measured from the axis of rotation,

and *v* is the velocity of the boundary.

The sedimentation coefficient is therefore the distance in cm, covered by a macromolecule during 1 second under the effect of a “force” of 10⁻² Nkg⁻¹, and is usually given in Svedbergs, S, where 1 S = 10⁻¹³ s (Price and Dwek, 1986).

The sedimentation coefficient, s , can also be used to calculate the molecular weight of the macromolecule by the Svedberg equation:

$$M = \frac{RTs}{D(1 - v\rho)}$$

where M is the molecular weight,

T is the temperature (Kelvins),

D is the diffusion coefficient (m^2s^{-1}),

v is the partial specific volume (m^3kg^{-1}),

and ρ is the density of the solvent (kg m^{-3}).

However, this experiment assumes that all measurements are performed at infinite dilutions (<0.1% w/v), otherwise corrections are required to give a realistic estimate of the molecular weight. In practice, it is much easier to use sedimentation equilibrium experiments to assess the molecular weight of macromolecules. This process is therefore used for the PLA-PEG copolymers and is outlined in section 2.8.2.

For sedimentation velocity experiments, a specially designed sector shaped cell is used with transparent end windows. The macromolecule solution to be analysed is placed in this cell and a light source positioned below the ultracentrifugation rotor to transmit monochromatic light through the solution and then on to be detected by other appropriate optical components. The moving boundary detected is then recorded and interpreted by computer. A more detailed introduction to this method can be found in van Holde (1985), and Price and Dwek (1986).

3.7.2 Sedimentation Velocity Experiments

Figures 3.16 to 3.19 show the sedimentation velocity absorbance profiles for the PLA-PEG copolymers. All of the PLA-PEG copolymers showed a single sedimenting boundary, indicating homogeneity of the samples.

The sedimentation coefficients will be discussed in section 5.3.

3.7.3 Sedimentation Equilibrium

In contrast with sedimentation velocity experiments, sedimentation equilibrium analysis is not a transport method. In these experiments, a low rotor speed is chosen so that the

Figure 3.16 - Sedimentation Velocity Profiles of 1.5:2 PLA-PEG Micelles at an Absorbance of 231 nm

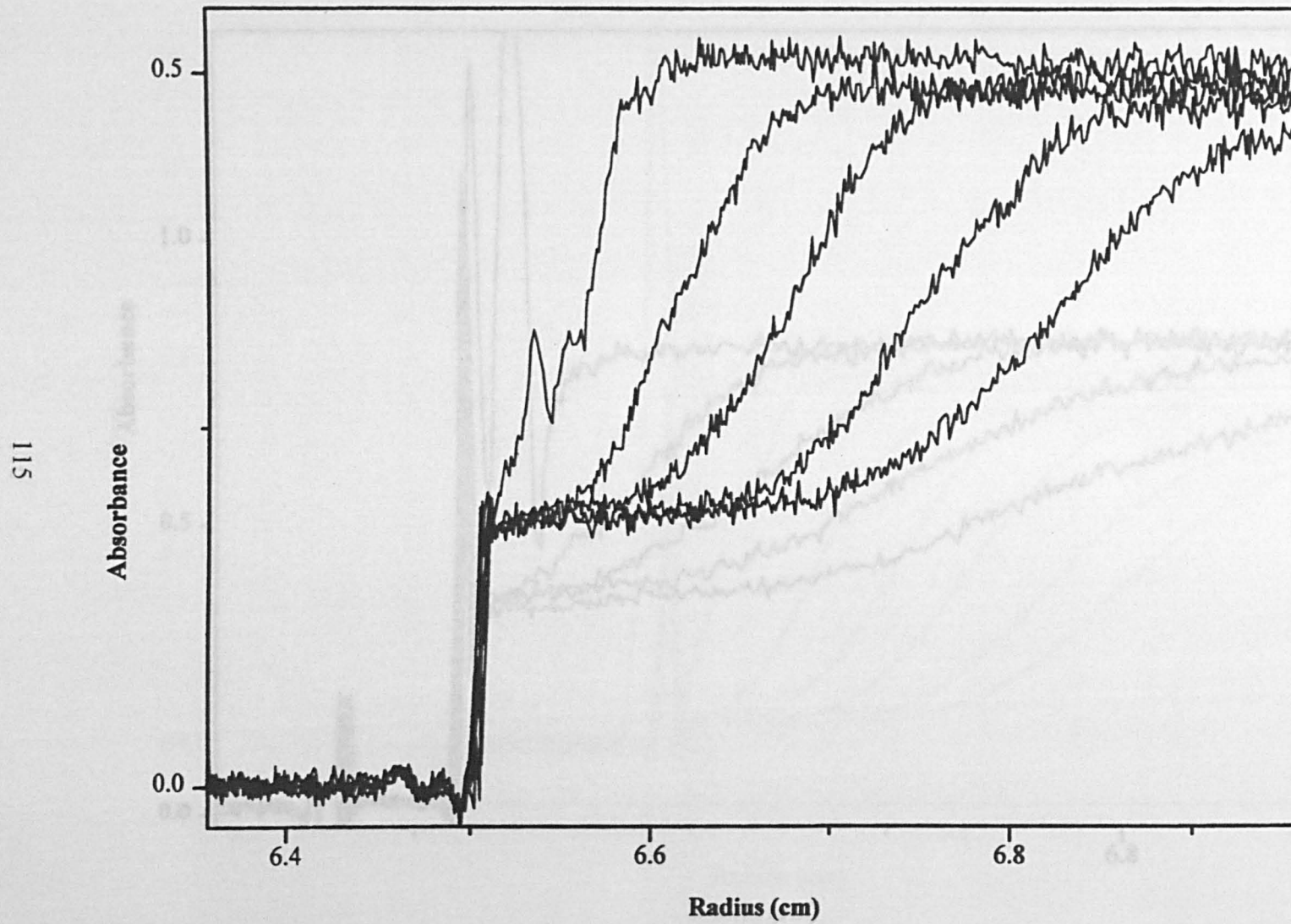


Figure 3.17 - Sedimentation Velocity Profiles for 2:5 PLA-PEG Micelles at an Absorbance of 225 nm

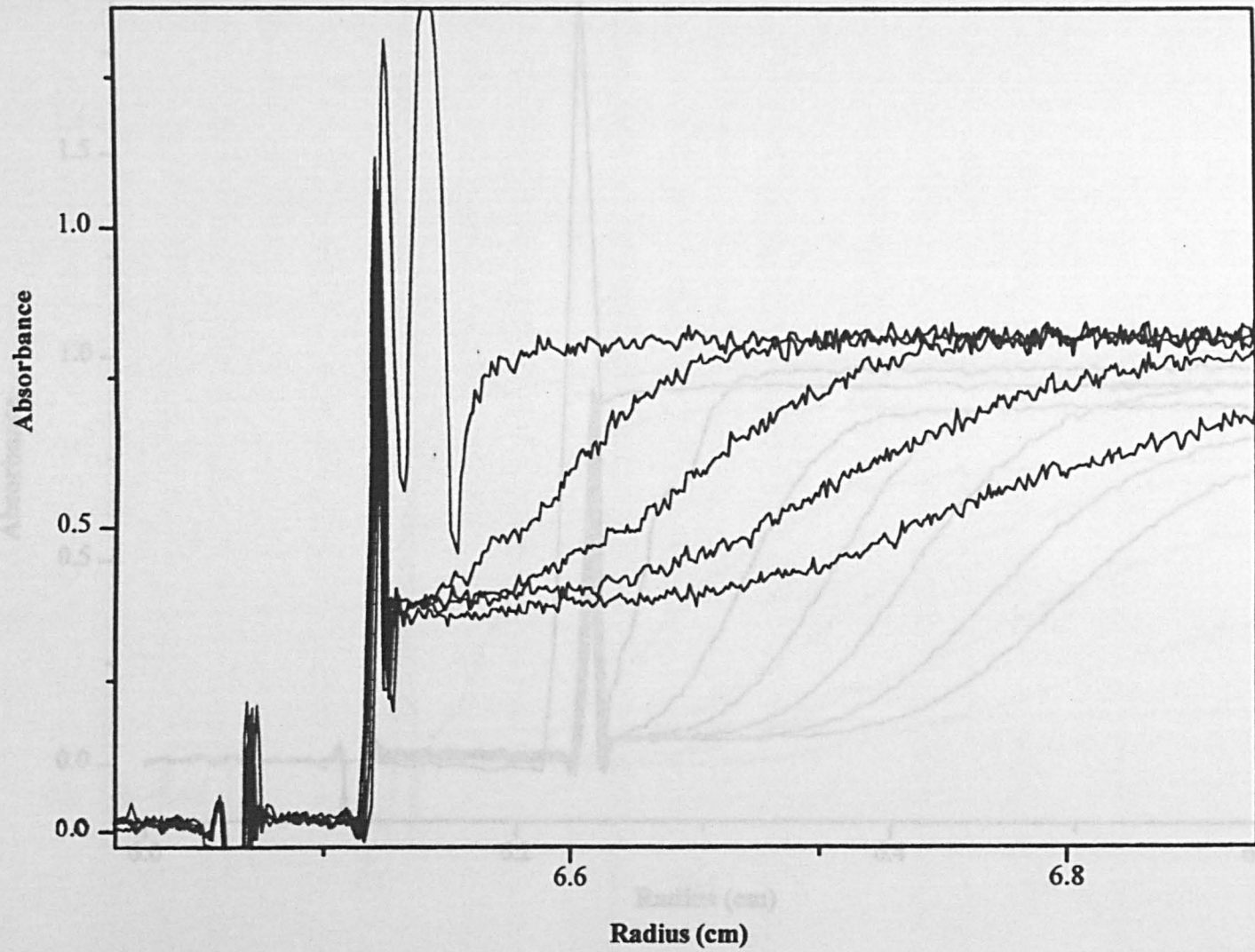


Figure 3.18 - Sedimentation Velocity Profiles of 4:2 PLA-PEG Particles at an Absorbance of 227 nm

117

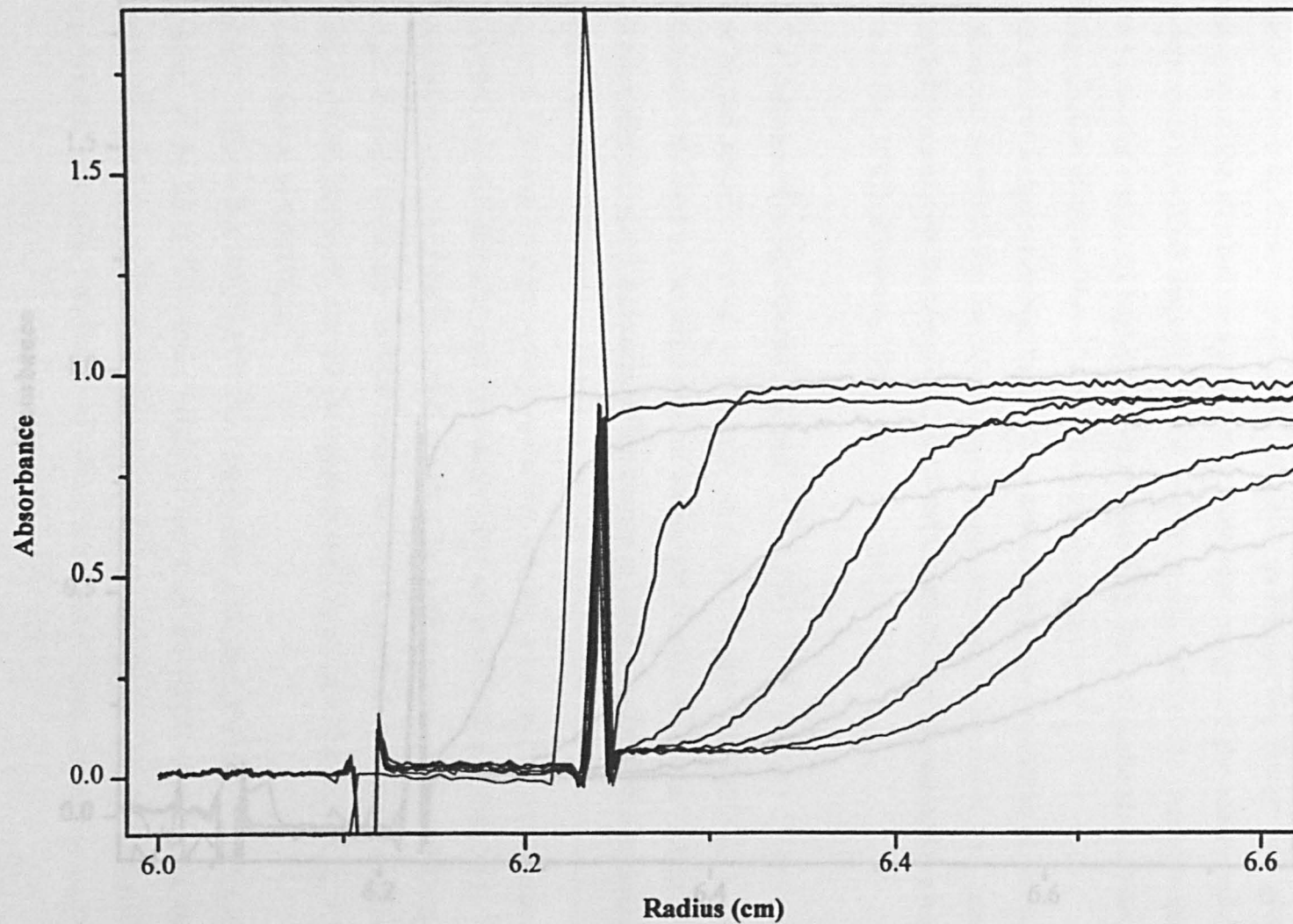
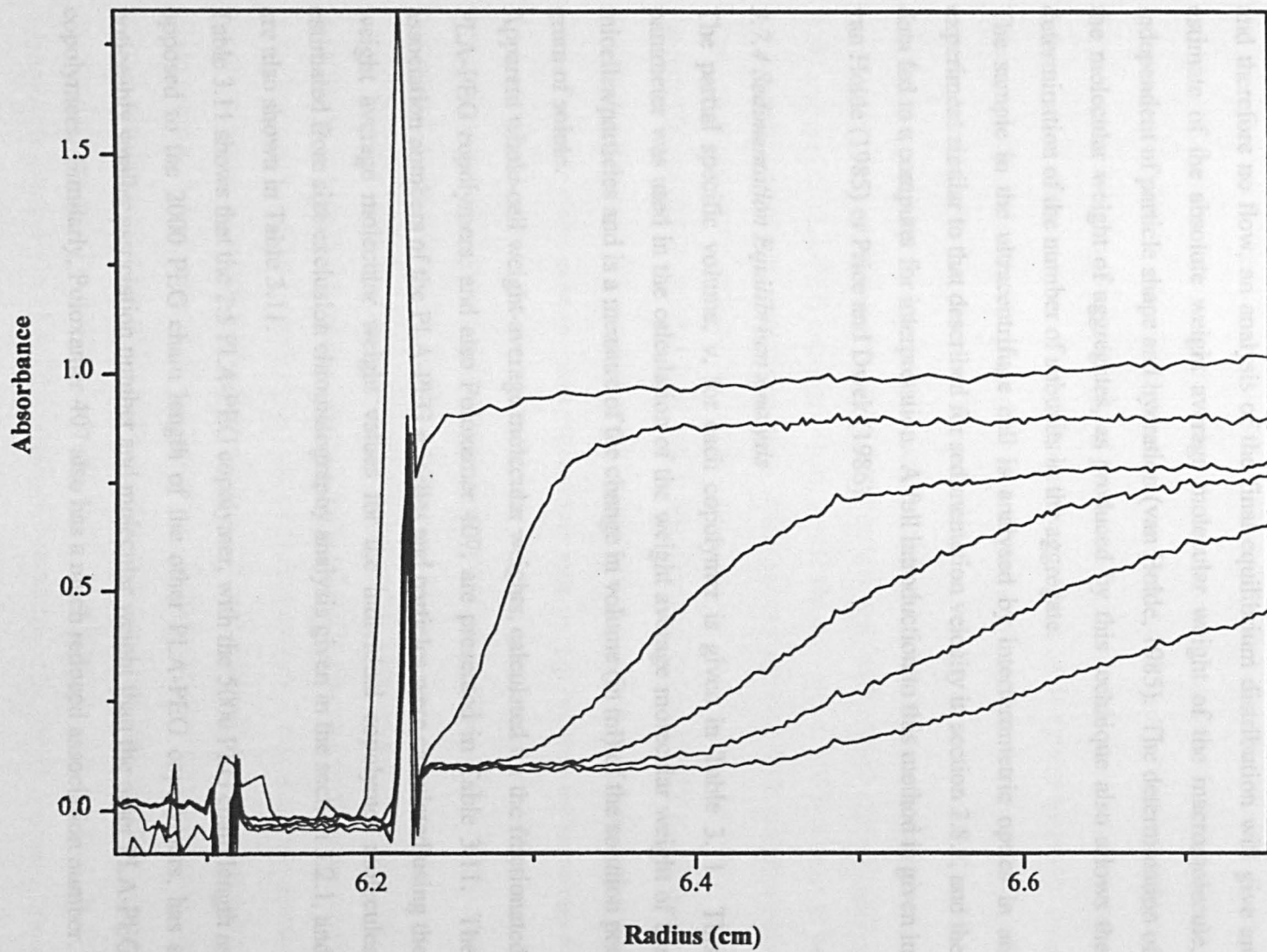


Figure 3.19 - Sedimentation Velocity Profiles of 6:2 PLA-PEG Particles at an Absorbance of 227 nm



forces of sedimentation and diffusion on the macromolecular solute are comparable, and an equilibrium distribution of the solute is achieved (Harding, 1993). This equilibrium distribution can be produced after a period of between 2 and 96 hours depending on the macromolecule, the solvent

and the run conditions. As there is no net transport of matter in the ultracentrifuge cell, and therefore no flow, an analysis of the final equilibrium distribution will give an estimate of the absolute weight average molecular weight of the macromolecule, independent of particle shape and hydration (van Holde, 1985). The determination of the molecular weight of aggregates, as produced by this technique also allows the determination of the number of subunits in the aggregate.

The sample in the ultracentrifuge cell is analysed by interferometric optics in an experiment similar to that described for sedimentation velocity in section 2.8.1, and the data fed to a computer for interpretation. A full introduction to this method is given in van Holde (1985) or Price and Dwek (1986).

3.7.4 Sedimentation Equilibrium Analysis

The partial specific volume, v , for each copolymer is given in Table 3.11. This parameter was used in the calculation of the weight average molecular weight of the micelles/particles and is a measure of the change in volume (in ml) of the solution per gram of solute.

Apparent whole-cell weight-average molecular weights, calculated for the fractionated PLA-PEG copolymers, and also Poloxamer 407, are presented in Table 3.11. The association numbers of the PLA-PEG micelles and particles were calculated using the weight average molecular weight values for the individual copolymer molecules estimated from size exclusion chromatography analysis given in the section 3.2.1, and are also shown in Table 3.11.

Table 3.11 shows that the 2:5 PLA-PEG copolymer, with the 5000 PEG chain length as opposed to the 2000 PEG chain length of the other PLA-PEG copolymers, has a noticeably smaller association number and molecular weight than the other PLA-PEG copolymers. Similarly, Poloxamer 407 also has a much reduced association number.

3.7.5 Discussion

Sedimentation equilibrium is a useful method for determining the molecular weight of micelles/particles. Other methods used include static light scattering (SLS), which involves extrapolation to zero concentration and can be ambiguous in systems showing complex association behaviour (Almgren *et al.*, 1995). SLS can also give association numbers that are too low and incompatible with results from other methods. Another method employed is the time-resolved fluorescence quenching method, TRFQ, but this too has proved difficult with pure Pluronic copolymers due to slow quenching under the conditions used (Almgren *et al.*, 1991). Dye solubilisation has also been attempted for estimation of association numbers, but the results obtained disagreed markedly with other methods. This was thought to be due to the false assumption that at saturation, all micelles would solubilise the same number of dye molecules (Jacobs *et al.*, 1971).

Considering the trend of association numbers of the PLA-PEG copolymers, there is a pronounced decrease between the PLA-PEG copolymers with a PEG chain length of 2000 and the 2:5 PLA-PEG copolymer with a PEG chain length of 5000. This is to be expected for copolymers containing PEG, where groups working with micelles have observed an decreased association number and micellar weight with increased PEG content (Becher, 1961; El Eini *et al.*, 1975; Stubičar and Petres, 1981). Furthermore, Stubičar and Petres (1981) noted that for Tritons with the same hydrophobic group but increasing hydrophilic content, there was a linear relationship between the logarithm of the association numbers and the number of oxyethylene groups. Similarly, Poloxamer 407 with its two PEO groups, and similar PEG content to 2:5 PLA-PEG (~ 70%), also has a much lower association number.

For the hydrophobic groups of micelle-forming polymers, Arnarson and Elworthy (1981) have shown that the association number is linearly related to the number of carbon atoms in the hydrocarbon chain for long chain C_xE_y surfactants, where C represents the number of carbon atoms (x) in the hydrocarbon chain and E represents the number of ethylene oxide groups (y) in the polyethylene oxide chain. Bahadur *et al.* (1985) also found that micelle association number and total micellar weight increased with increased size of the insoluble block for styrene-isoprene block copolymers. An increase in the hydrophobic group of the PLA-PEG copolymer molecules (i.e. the PLA group) would therefore be expected to increase the association number.

Table 3.11

Molecular Weight Data for Copolymer Micelles/Particles obtained from Sedimentation Equilibrium Experiments

Copolymer	Molecular weight	Partial specific volume, v (mlg ⁻¹)	Micelle/particle molecular weight	Association number
1.5:2 PLA-PEG	3947	0.822	520,000 ± 20,000	132 ± 5
4:2 PLA-PEG	6433	0.804	1,000,000 ± 50,000	155 ± 8
6:2 PLA-PEG	7017	0.810	1,500,000 ± 100,000	214 ± 14
2:5 PLA-PEG	6987	0.797	330,000 ± 30,000	47 ± 4
Poloxamer 407	12600	0.808	200,000 ± 10,000	16 ± 1

Combining these data with the DLS data (Table 3.12) shows that the micelles formed with the Poloxamer 407 and 2:5 PLA-PEG copolymers have much lower association numbers per micelle than the 1.5:2 PLA-PEG copolymer, yet with a larger micellar size being detected for Poloxamer 407. This suggests that the Poloxamer 407 micelles form less densely packed micelles relative to the smaller micelles observed with PLA-PEG copolymers. Indeed, Saitō and Satō (1985) noted that an increase in polyoxyethylene chain length led to a decrease in compactness of micelles, which caused an increase in micellar inner polarity. The association number for the 4:2 PLA-PEG particle-forming copolymer is slightly higher than for the 1.5:2 PLA-PEG but with a similar micelle/particle size, indicating still closer packing of the copolymer molecules. The 6:2 PLA-PEG copolymer has a significantly larger association number than the 1.5:2 PLA-PEG and 4:2 PLA-PEG micelles/particles, suggesting further closer packing.

3.8 SUMMARY

The physicochemical properties of copolymers of polylactide and poly(ethylene glycol) (PLA-PEG), which either self disperse in water to form spherical non-ionic micelles (1.5:2 and 2:5 PLA-PEG) or form more “solid-like” particles during the solvent-precipitation process (4:2 and 6:2 PLA-PEG and 1.5:2 LPLA-PEG), have been investigated. These copolymers are defined by the molecular weight ratios of their polylactide to poly(ethylene glycol) components and gave two peaks when purified by gel permeation chromatography (GPC). The first peak consisted of spherical micelles/particles with diameters in the range 14.5 nm and 20.8 nm for the different copolymers as determined by dynamic light scattering (DLS). Analysis by transmission electron microscopy (TEM) and atomic force microscopy (AFM) for 4:2 and 6:2 PLA-PEG copolymers were in good agreement with these values. The second peak produced by GPC was a PLA-depleted species resulting from the synthesis and did not form micelles.

The cmcs of the micelle-forming PLA-PEG copolymers (1.5:2 and 2:5 PLA-PEG) were determined using surface tension measurements and both copolymers formed micelles at 0.0035% w/v, which compares reasonably with values for similar copolymers.

Table 3.12

Summary of DLS and Sedimentation Equilibrium Data

Copolymer	Diameter, DLS (nm)	Micelle/particle molecular weight	Association number
1.5:2 PLA-PEG	15.6 ± 0.9	520,000 ± 20,000	132 ± 5
4:2 PLA-PEG	15.1 ± 3.5	1,000,000 ± 50,000	155 ± 8
6:2 PLA-PEG	20.8 ± 3.8	1,500,000 ± 100,000	214 ± 14
2:5 PLA-PEG	18.9 ± 1.6	330,000 ± 30,000	47 ± 4
Poloxamer 407	29.1 ± 0.5	200,000 ± 10,000	16 ± 1

relatively homogeneous. Molecular weights of the micelles/particles were determined using sedimentation equilibrium experiments. From the molecular weights of the micelles/particles and the molecular weights of the individual copolymer molecules, the number of copolymer molecules per micelle/particle was calculated. These showed the expected trend with the longer chain length of the 2:5 PLA-PEG resulting in a decreased association number and the longer hydrophobic PLA length of the 6:2 PLA-PEG giving a higher association number.

CHAPTER FOUR

SURFACE CHARACTERISATION OF PLA-PEG COPOLYMERS

4.1 INTRODUCTION

The previous chapter concentrated on the properties of the PLA-PEG systems as a whole, considering their purity, and the characteristics of the micelles and particles produced by the different PLA-PEG copolymers. This chapter now studies in more detail a specific part of the PLA-PEG systems, namely the surface characteristics of these systems.

Surface characterisation is a growing tool in the analysis of biomedical polymers, and in this chapter, four different methods of examining the surface of the PLA-PEG copolymers will be discussed. The first technique uses rheological measurements to obtain a value for the length of the PEG layer thickness. Two complementary techniques, static secondary ion mass spectrometry (SIMS) and X-ray photoelectron spectroscopy (XPS), are then discussed, which give chemical and elemental information of the surface and allow some degree of quantification of the surface density of PEG in the samples. Finally, cloud point temperatures, which give an indication of the steric stability of a copolymer system are considered. These four techniques therefore allow different aspects of the PLA-PEG surface to be studied and an overview of the properties of this surface can be obtained. As discussed previously in chapter one, the surface properties of drug delivery systems are very important in determining the *in vivo* biodistribution of the system, by influencing the adsorption of proteins (opsonins and dysopsonins) from plasma. The surface composition can also determine the rate of biodegradation and release of drug molecules *in vivo*, which can have toxicological implications for the patient (Davies *et al*, 1989). The measurements were performed as described in chapter two.

4.2 DETERMINATION OF PEG LAYER THICKNESS BY RHEOLOGICAL MEASUREMENTS

4.2.1 The Significance of the PEG layer Thickness

In chapter one, the potential rapid response from the reticuloendothelial system (RES) to remove colloidal particles injected into the body from the circulation was discussed. This is thought to be due to the adsorption of circulating proteins and blood components (opsonins) onto the particle surface, which causes the recognition and subsequent engulfment by the macrophages of the RES. The steps taken to prevent the extent of uptake were discussed in chapter one and depend on the physicochemical characteristics of the particles, such as their size, surface charge and the presence of a hydrophilic surface layer (for example, polyethylene glycol) to provide steric stabilisation. This steric barrier influences the identity and quantity of the plasma proteins adsorbed, and by that, the interaction of the nanoparticles with the phagocytic cells. This was illustrated by Harper *et al* (1991), who showed a reduction in the uptake of polystyrene microspheres by rat Kupffer cells when polyethylene oxide (PEO) was covalently grafted to the microspheres, or physically adsorbed as Poloxamer 238. The effectiveness of the PEO as a hydrophilic steric barrier has been shown to be affected by both the surface density of the PEO chains and the chain layer thickness of the PEO chains. This was demonstrated by Dunn *et al* (1994), who showed that increased density of PEO chains at the surface of microspheres reduced their uptake by the Kupffer cells in *in vitro* studies, and by the RES in *in vivo* studies in the rat model. Also, Illum *et al* (1987) established that the length of the PEG chains affected the uptake of the particles by mouse peritoneal macrophages, with longer PEG layer thicknesses resulting in less uptake. This was illustrated by relative phagocytic uptake of Poloxamer 407 coated particles with an adsorbed layer thickness of 154 Å being 21.6%, compared with particles coated with Poloxamer 188 with an adsorbed layer thickness of 76 Å giving 95.4% relative phagocytic uptake. The length of the PEG layer thickness is thus an important parameter in determining how effective a potential drug delivery system will be *in vivo* and the knowledge of this value should allow comparison between different copolymer systems in the light of their *in vivo* performance.

4.2.2 Measurement of PEG layer Thickness

In order to design systems that are effective *in vivo*, it is necessary to obtain information on the thickness of the steric barrier, as this gives a direct measure of the extent of the steric repulsion. A DLS measurement will give a value for the hydrodynamic radius of the particle core plus the stabilising PEG layer, but cannot yield any information on the barrier thickness. Previously, when non-biodegradable polystyrene particles were used with copolymers physically adsorbed to the surface, the thickness of the stabilising PEG layer was estimated using DLS. This was achieved from a knowledge of the hydrodynamic radius of the particle in the presence and absence of the polymer layer, such that the adsorbed layer thickness could be obtained by subtraction. This should be further corrected, taking into account the curvature and surface of the particle (Killmann and Sapuntzjis, 1994). Other techniques also allow estimation of the PEG layer thickness, including force-distance measurements between adsorbed layers (Klein and Luckman, 1982; Cohen Stuart *et al*, 1986), small-angle neutron scattering (SANS), which also allows determination of the segment density and the particle core radius (Almgren *et al*, 1995), and viscometry measurements (Cohen Stuart *et al*, 1986). SANS allows the estimation of the PEG layer thickness for block copolymers, by yielding the radius of the aggregate core, thus allowing the PEG layer thickness to be obtained by subtraction from the hydrodynamic radius (Kabanov *et al*, 1995).

Recently, Tadros and collaborators (Liang *et al*, 1992; Miano *et al*, 1992; Pingret *et al*, 1992) have established a simple rheological technique to obtain the thickness of an adsorbed or grafted layer on the surface of a colloidal particle. Basically, parameters such as viscosity or modulus are measured as a function of the volume fraction of the dispersion. When the surface-to-surface distance between the particles approaches twice the adsorbed (or grafted) layer thickness, strong interaction occurs and the system becomes predominantly more elastic than viscous. Thus by measuring the storage (G') and loss (G'') moduli as a function of volume fraction, ϕ , an intersection point is obtained at a critical volume fraction, ϕ_{eff} , which determines the onset of elastic interaction. From a knowledge of ϕ at the crossover point, the adsorbed layer thickness can be calculated. Rheological measurements have also been used to compare between the adsorbed layer thicknesses of poly(ethylene oxide)-poly(propylene oxide) copolymers, with Kim and

Luckham (1992) observing a greater adsorbed layer thickness of Pluronic F127 over Pluronic P105 when adsorbed onto polystyrene particles.

4.2.3 Rheological Data for PLA-PEG Copolymers

Rheological studies were carried out on 1.5:2 PLA-PEG, 1.5:2 LPLA-PEG, 4:2 PLA-PEG, 6:2 PLA-PEG and 2:5 PLA-PEG as described in section 2.8.

Figure 4.1 shows typical strain sweep results (at a frequency of 1 Hz) for a dispersion of 1.5:2 LPLA-PEG with a volume fraction $\phi = 0.148$. The results show a linear region up to a strain value of 0.04. Above this strain value, the complex modulus, G^* , and the storage modulus, G' , decrease, whereas the loss modulus, G'' , increases. This is typical for a viscoelastic system. At this volume fraction, G' is greater than G'' , and this indicates interaction between the PEG layers in the dispersion. Strain sweep results for a range of volume fractions were also obtained showing that the trend obtained depended on the volume fraction. At a volume fraction of $\phi = 0.066$, the loss modulus, G'' , is greater than the storage modulus, G' , showing weak interaction in the dispersion.

Figure 4.2 shows the frequency sweep results for a 1.5:2 LPLA-PEG dispersion with $\phi = 0.148$. It can be seen from this figure that $G' > G''$ over the whole frequency range.

This, as mentioned above, is due to the elastic interaction between the PEG chains on close approach. However, both G^* and G' show significant dependence on frequency.

This implies that the interaction is not sufficient to produce an “elastic gel”. Therefore, it is likely that the PEG chains have undergone some penetration in this case, without any compression.

As the volume fraction of the dispersion is further increased, the frequency dependence of the modulus becomes smaller. This is illustrated in Figure 4.3, which shows the results for $\phi = 0.26$. In this case, $G' \gg G''$ and the slope of the G^* or G' versus frequency is smaller than that shown in Figure 4.2. This implies more penetration of the chains on closer approach. However, there does not seem to be any compression, which in most cases would lead to an “elastic gel”. This is indicated as G^* and G' for LPLA-PEG are still dependent on frequency, even at high volume fractions, whereas if there was compression (and an “elastic gel” formed), there would be little dependence of these parameters on frequency.

Figure 4.1 - Strain Sweep at a Frequency of 1 Hz for 1.5:2 LPLA-PEG with a Volume Fraction of 0.148.

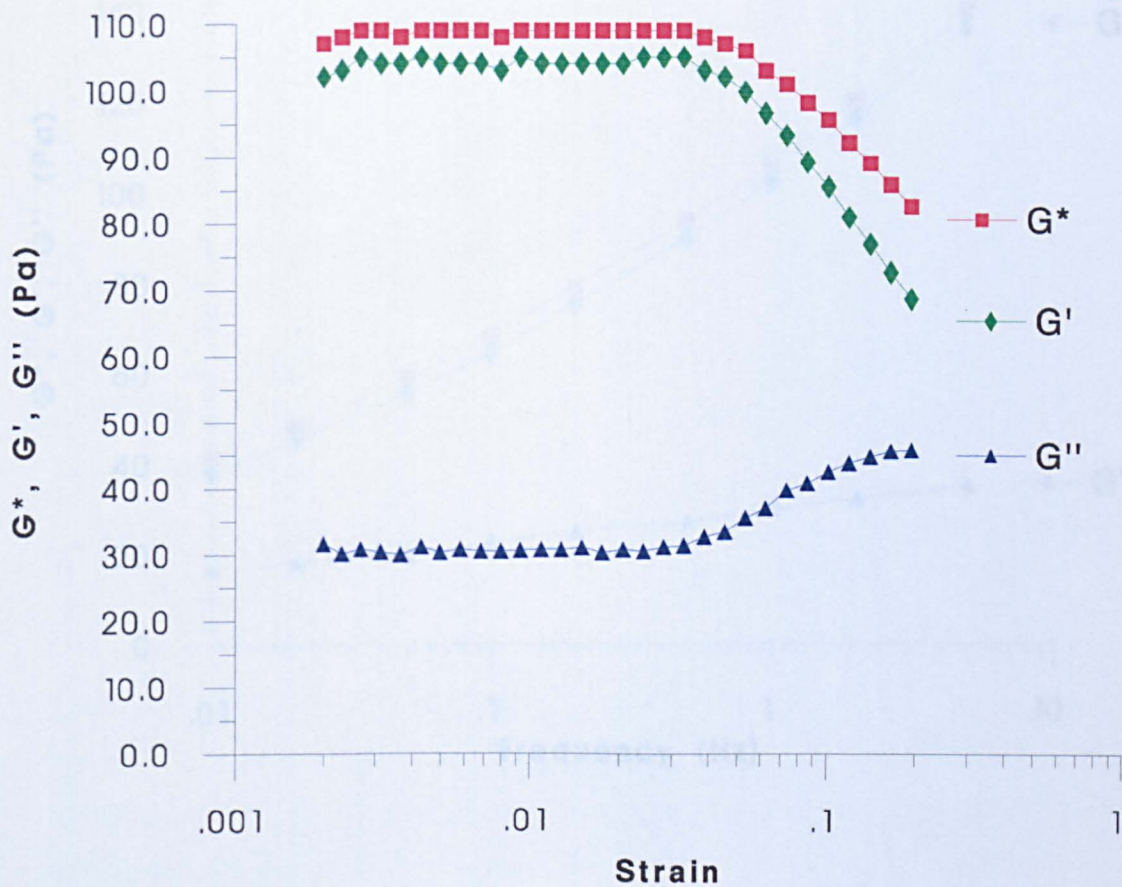


Figure 4.2 - Frequency Sweep for 1.5:2 LPLA-PEG with a Volume Fraction of 0.148

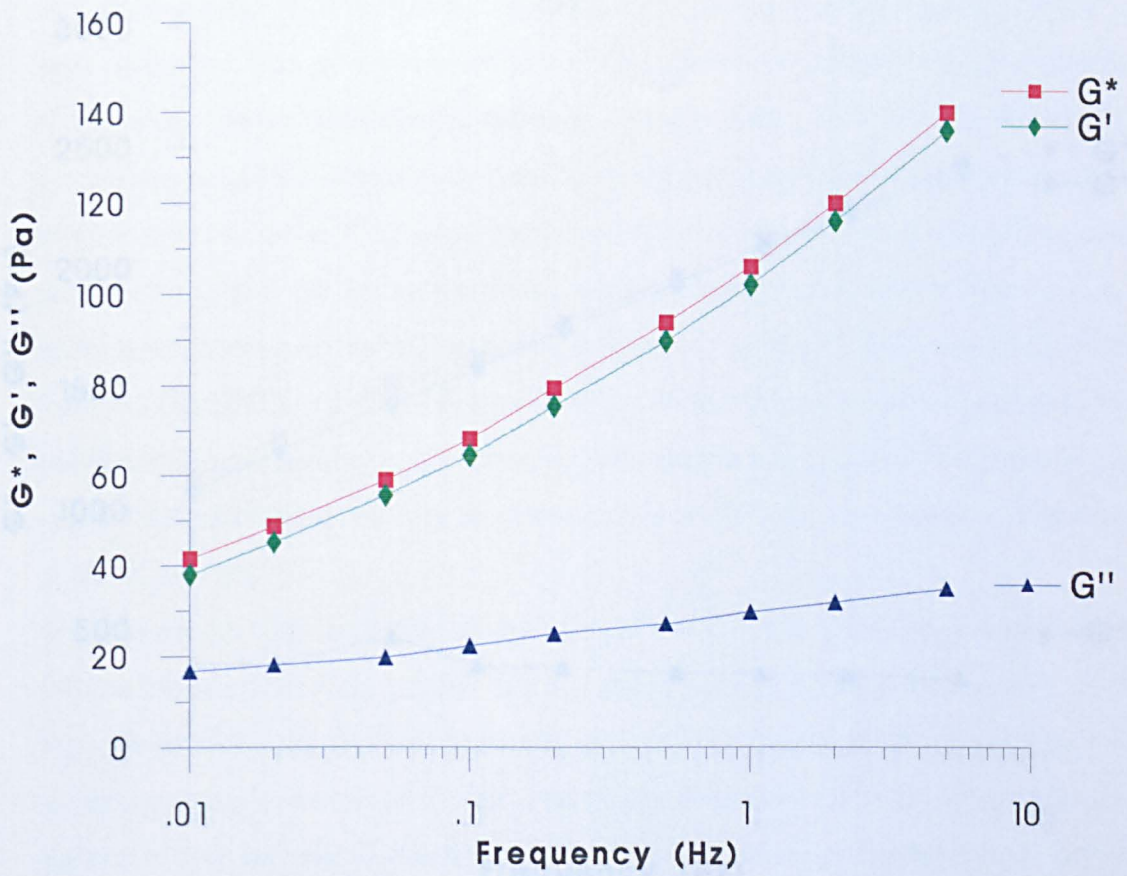


Figure 4.3 - Frequency Sweep for 1.5:2 LPLA-PEG with a Volume Fraction of 0.26

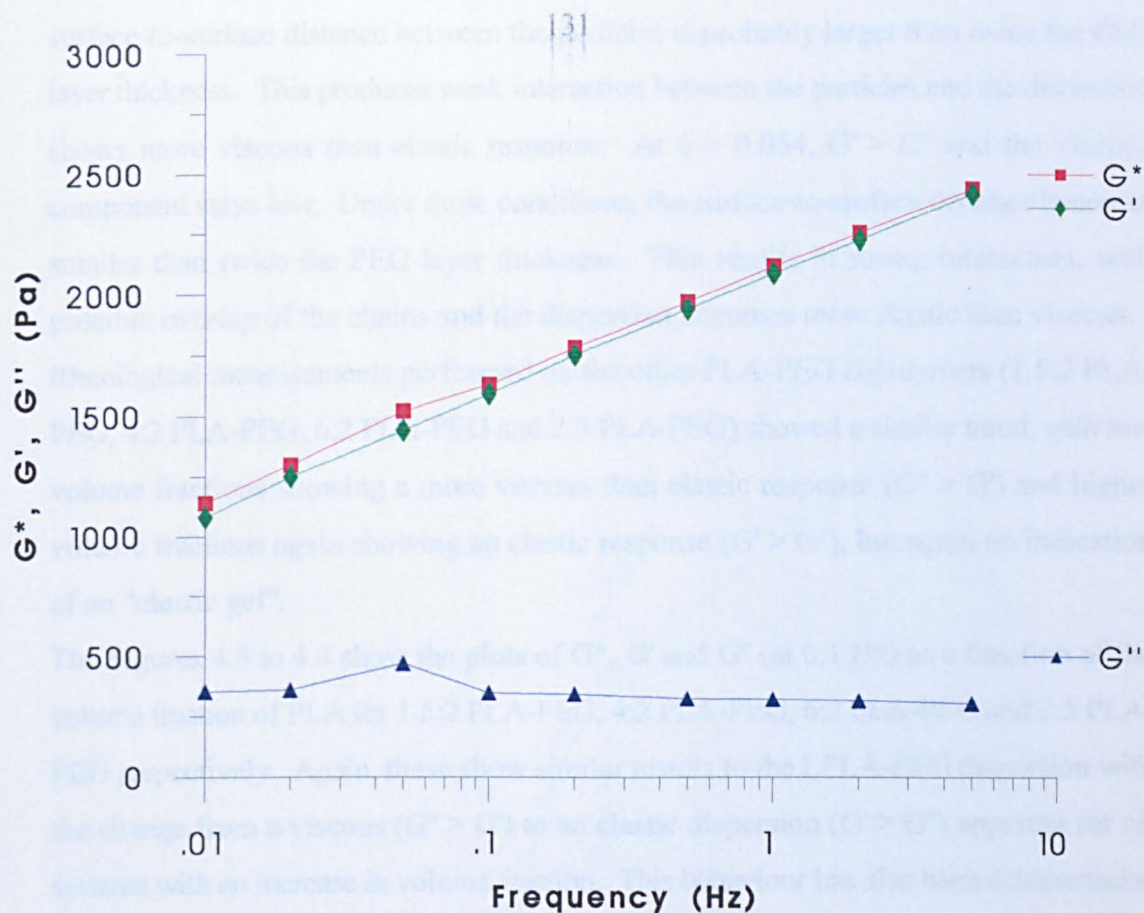


Figure 4.4 shows plots of G^* , G' and G'' (at 0.1 Hz) as a function of the LPLA volume fraction for 1.5:2 LPLA-PEG. At $\phi < 0.054$, $G'' > G'$. Below this volume fraction, the surface-to-surface distance between the particles is probably larger than twice the PEG layer thickness. This produces weak interaction between the particles and the dispersion shows more viscous than elastic response. At $\phi > 0.054$, $G' > G''$ and the viscous component stays low. Under these conditions, the surface-to-surface distance becomes smaller than twice the PEG layer thickness. This results in strong interaction, with possible overlap of the chains and the dispersion becomes more elastic than viscous. Rheological measurements performed on the other PLA-PEG copolymers (1.5:2 PLA-PEG, 4:2 PLA-PEG, 6:2 PLA-PEG and 2:5 PLA-PEG) showed a similar trend, with low volume fractions showing a more viscous than elastic response ($G'' > G'$) and higher volume fractions again showing an elastic response ($G' > G''$), but again no indication of an “elastic gel”.

The Figures 4.5 to 4.8 show the plots of G^* , G' and G'' (at 0.1 Hz) as a function of the volume fraction of PLA for 1.5:2 PLA-PEG, 4:2 PLA-PEG, 6:2 PLA-PEG and 2:5 PLA-PEG respectively. Again, these show similar results to the LPLA-PEG dispersion with the change from a viscous ($G'' > G'$) to an elastic dispersion ($G' > G''$) apparent for all systems with an increase in volume fraction. This behaviour has also been demonstrated by Pluronic P-94 for both increased volume fraction and temperature, with oscillatory measurements (Bahadur and Pandya, 1992).

4.2.4 Dynamic Light Scattering Results for Concentrated PLA-PEG Dispersions

These analyses were carried out for dispersions with concentrations of 10% w/v. Table 4.1 shows the results, after analysis by DLS, of the samples used in the rheological experiments. The values for the PLA-PEG micelles/particles after analysis at this concentration are very similar to those measured at the lower concentration and discussed in section 3.5. Indeed, the values for 1.5:2 PLA-PEG, 2:5 PLA-PEG, 4:2 PLA-PEG and 6:2 PLA-PEG are not significantly different from the values at the lower concentration. No significant dependence of hydrodynamic radius on copolymer concentration has been observed for both poly(oxyethylene/oxypropylene/ oxyethylene)

Figure 4.4 - Plot of G^* , G' and G'' vs Volume Fraction at a Frequency of 0.1 Hz for 1.5:2 LPLA-PEG

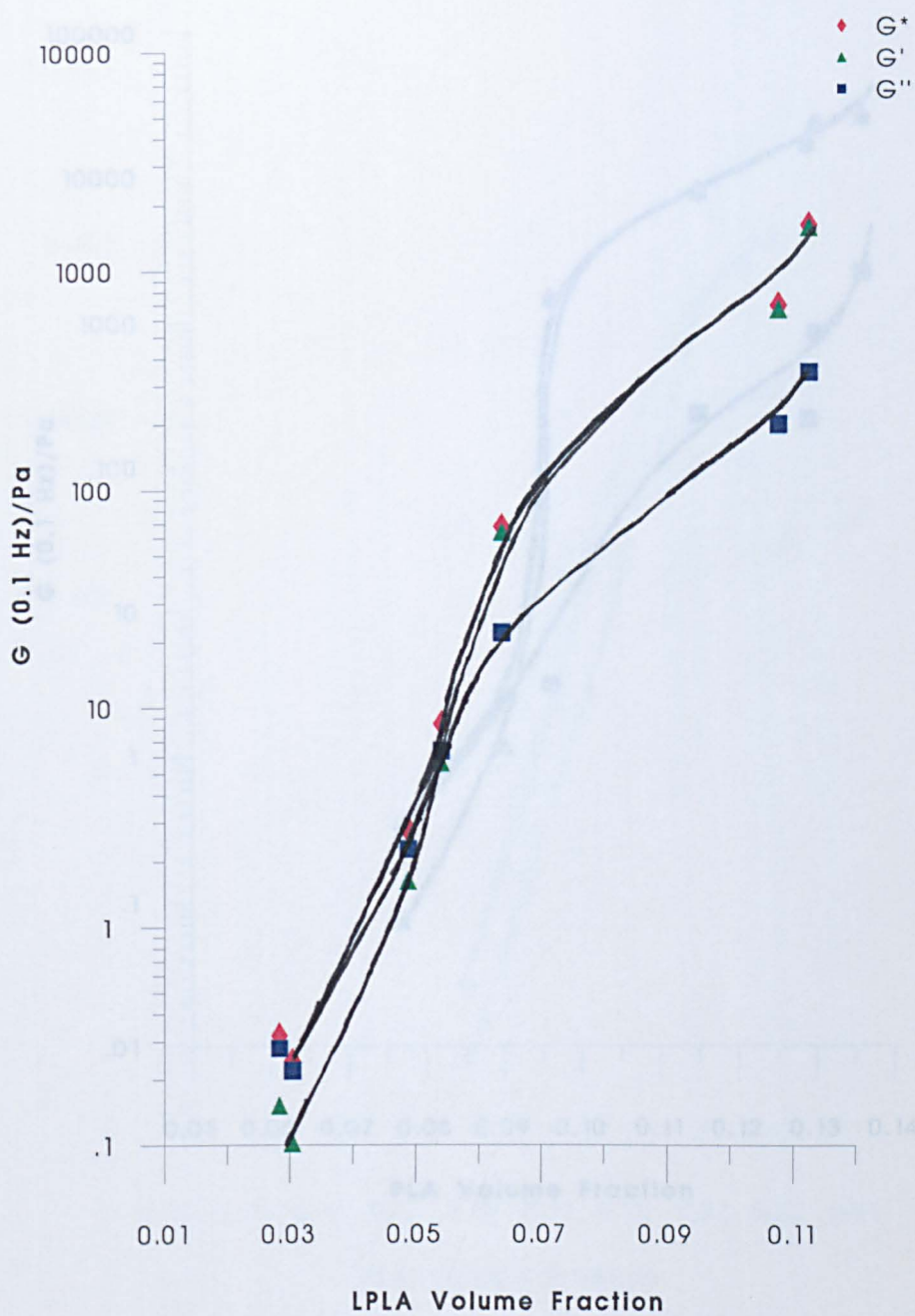


Figure 4.5 - Plot of G^* , G' and G'' vs Volume Fraction at a Frequency of 0.1 Hz for 1.5:2 PLA-PEG

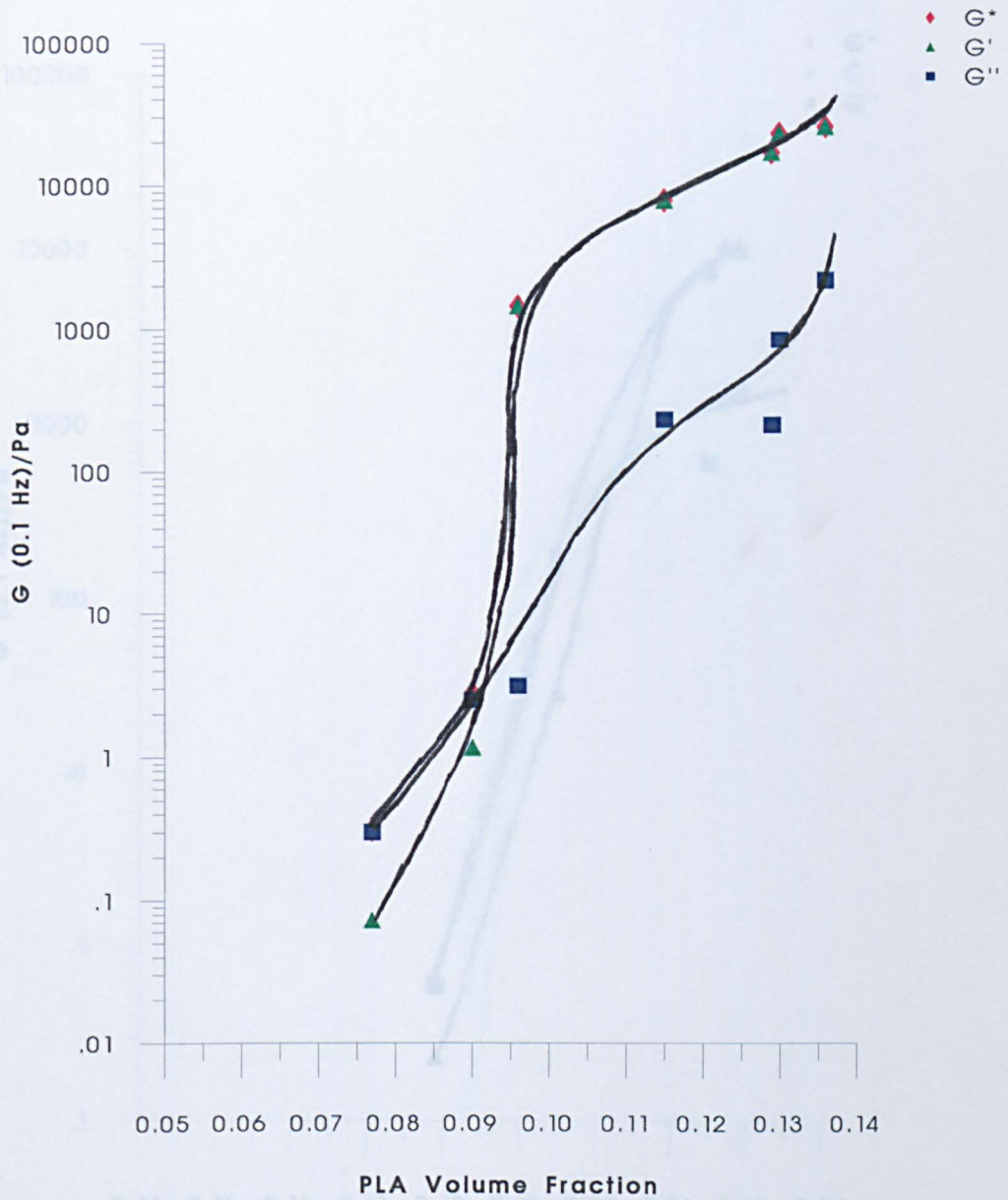


Figure 4.6 - Plot of G^* , G' and G'' vs Volume Fraction at a Frequency of 0.1 Hz for 4:2 PLA-PEG

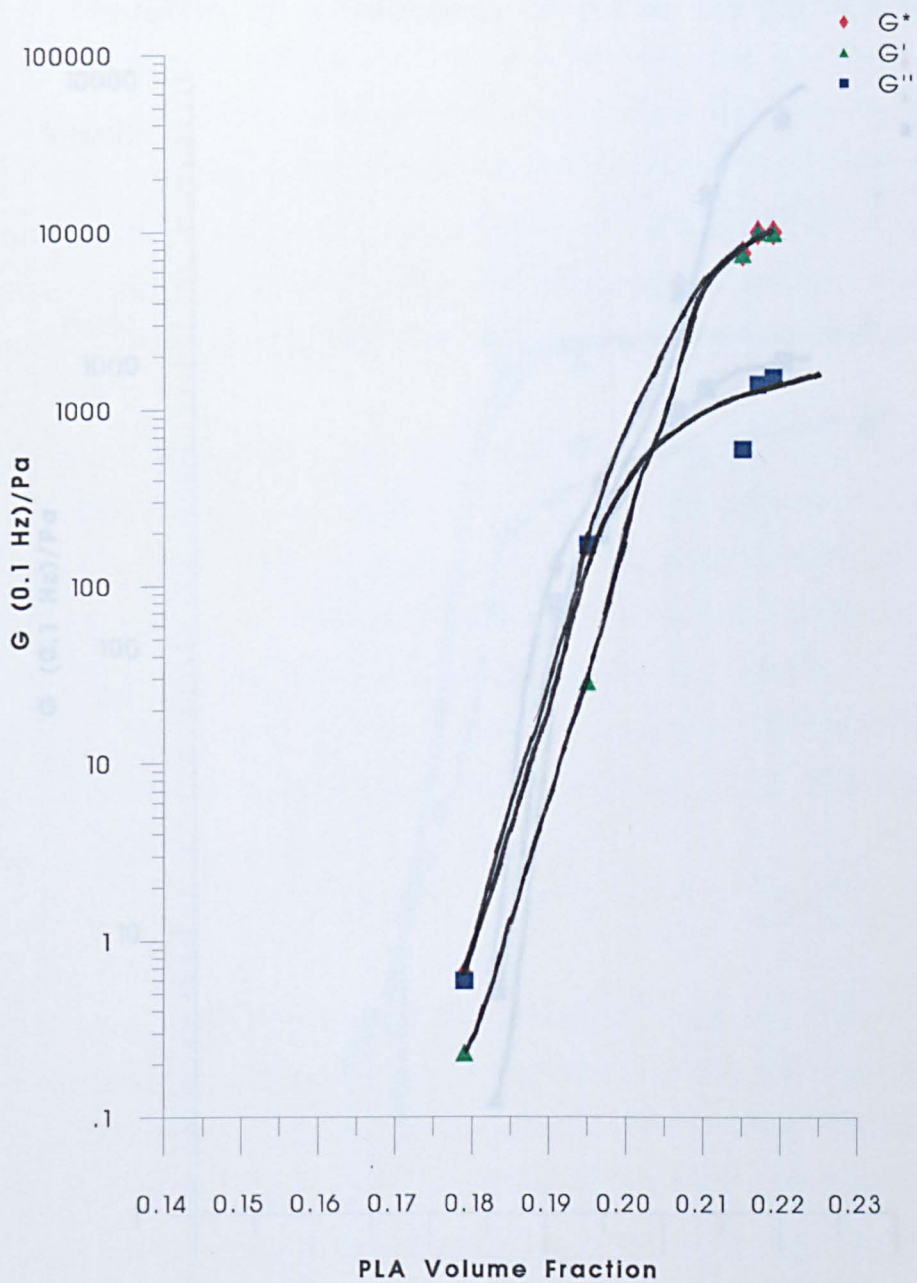


Figure 4.7 - Plot of G^* , G' and G'' vs Volume Fraction at a Frequency of 0.1 Hz for 6:2 PLA-PEG

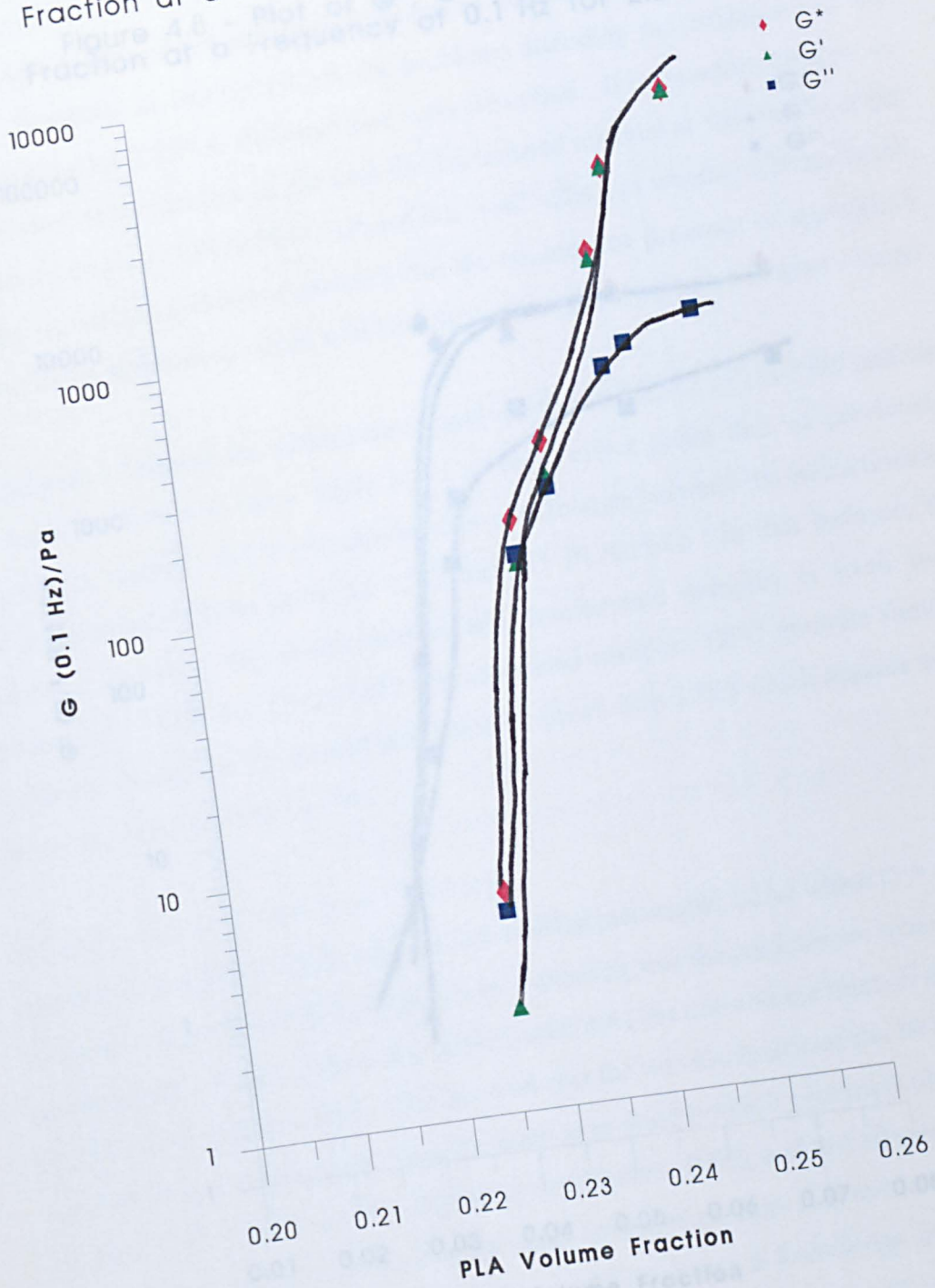
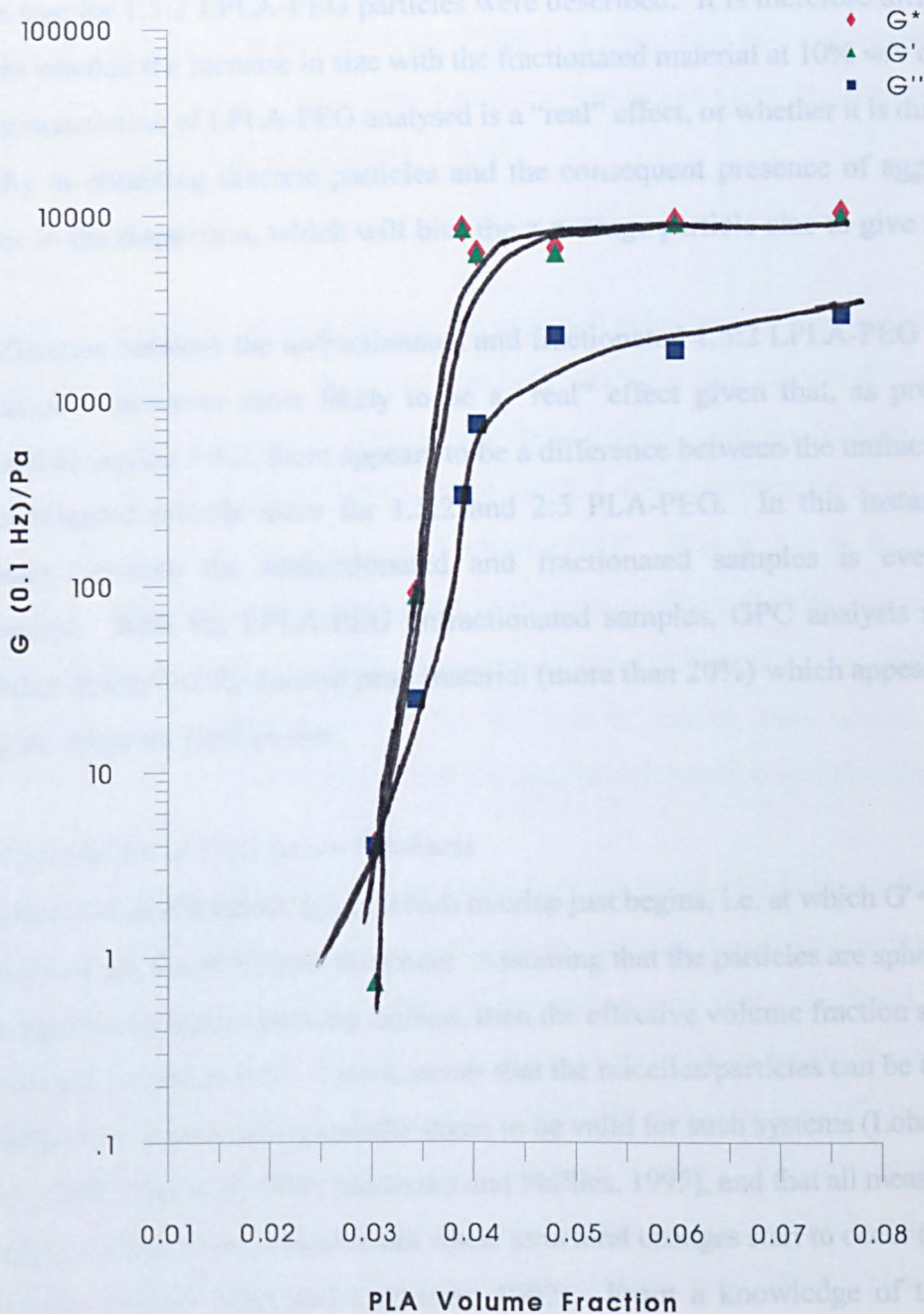


Figure 4.8 - Plot of G^* , G' and G'' vs Volume Fraction at a Frequency of 0.1 Hz for 2:5 PLA-PEG



copolymers (Alexandridis and Hatton, 1995) and poly(oxybutylene/oxyethylene) copolymers (Sun *et al.* 1991).

For 1.5:2 LPLA-PEG, there is a small increase in particle size for the fractionated material. However, in section 3.4.2.5, the problems attending the estimation of the particle size for 1.5:2 LPLA-PEG particles were described. It is therefore difficult to ascertain whether the increase in size with the fractionated material at 10% w/v over the lower concentration of LPLA-PEG analysed is a “real” effect, or whether it is due to the difficulty in obtaining discrete particles and the consequent presence of aggregated particles in the dispersion, which will bias the z-average particle size to give a larger value.

The difference between the unfractionated and fractionated 1.5:2 LPLA-PEG particle size values is however more likely to be a “real” effect given that, as previously discussed in section 3.5.2, there appears to be a difference between the unfractionated and fractionated micelle sizes for 1.5:2 and 2:5 PLA-PEG. In this instance, the difference between the unfractionated and fractionated samples is even more pronounced. With the LPLA-PEG unfractionated samples, GPC analysis shows a significant amount of the second peak material (more than 20%) which appears to be having an effect on particle size.

4.2.5 Calculation of PEG Layer Thickness

The critical volume fraction, ϕ_{eff} , at which overlap just begins, i.e. at which $G' = G''$, can be used to obtain the PEG layer thickness. Assuming that the particles are spherical and are arranged in a random packing fashion, then the effective volume fraction should be approximately equal to 0.64. This assumes that the micelles/particles can be treated as hard spheres, an assumption generally taken to be valid for such systems (Lobaskin and Pershin, 1993; Chu *et al.*, 1994; Streletzky and Phillies, 1995), and that all measurements are carried out below the critical strain where structural changes start to occur (i.e. in the viscoelastic region) (Kim and Luckham, 1992). From a knowledge of the actual maximum volume fraction, ϕ , obtained experimentally from where $G' = G''$ (i.e. the crossover point), and from the hydrodynamic radius, R_h , the PEG layer thickness, Δ , can be obtained from the following equation (Faers and Luckham, 1994): -

$$\phi_{eff} = \phi \left[1 + \frac{\Delta}{R_h - \Delta} \right]^3$$

Using the values for R_h obtained from DLS (Table 4.1), the values of Δ can be calculated and are shown in Table 4.2. All volume fraction values assume that the density of the PLA-PEG copolymers is approximately 1 gcm^{-3} .

4.2.6 Discussion

All PLA-PEG copolymer systems showed the expected behaviour of low moduli values at low volume fractions, with a rapid increase in G^* and G' as the volume fraction was increased. The increased volume fraction also brings about a change from viscous to elastic flow (i.e. from $G'' > G'$ to $G' > G''$) for all the PLA-PEG copolymers at the critical volume fraction, ϕ_c (the crossover point) where $G' = G''$. This is due to the start of repulsive interaction between the PEG layers of adjacent particles/micelles, caused by the loss of configurational entropy and/or an increase in the enthalpy of mixing of the PEG chains (Faers and Luckham, 1994). An increase in moduli thus occurs as the particles/micelles are not able to relax from the applied deformation and therefore store the energy elastically.

The crossover point is affected by the composition of the copolymer being studied, with the molecular weight of an adsorbing copolymer at the particle surface playing a role, particularly the length of the PEG chain. It has been shown that the critical volume fraction (where $G' = G''$) decreases with an increase in PEG chain length (Liang *et al*, 1992; Pingret *et al*, 1992; Faers and Luckham, 1994) for particles with PEO adsorbed or grafted to their surface. This occurs as the increased number of EO units in the chain causes an increase in the PEG layer thickness, which leads to stronger steric interactions at greater separation distances between the particles (Pingret *et al*, 1992). The increase in PEG layer thickness with increased number of ethylene glycol units has been demonstrated by several authors, including Pingret *et al* (1992), and Faers and Luckham (1994). Thus, the thicker the adsorbed/grafted layer of PEG, the more elastic the polymer system (Tadros, 1992), as the steric repulsion becomes longer in range.

Table 4.1

DLS Analysis of 10% w/v PLA-PEG Dispersions

Copolymer Sample	Diameter Size (nm)	R _h (nm)
1.5:2 LPLA-PEG Unfractionated	30.4 ± 0.8	15.2
1.5:2 LPLA-PEG Fractionated	21.0 ± 1.8	10.5
1.5:2 PLA-PEG	17.2 ± 0.7	8.6
4:2 PLA-PEG	14.1 ± 0.9	7.1
6:2 PLA-PEG	16.8 ± 0.8	8.4
2:5 PLA-PEG	23.8 ± 1.5	11.9

Table 4.2

PEG layer Thickness Measurements Estimated from Rheological Measurements

Copolymer	PEG Chain Length	Hydrodynamic Radius (R _h) (nm)	Volume Fraction of Core at Crossover (Φ)	PEG Layer Thickness (Δ) (nm)
1.5:2 LPLA-PEG	2000	15.2	0.054	8.53
1.5:2 PLA-PEG	2000	8.6	0.091	4.11
4:2 PLA-PEG	2000	7.05	0.202	2.25
6:2 PLA-PEG	2000	8.4	0.233	2.40
2:5 PLA-PEG	5000	11.9	0.033	7.47

Applying this to the PLA-PEG copolymers, it can be seen that the volume fraction at the crossover point for 2:5 PLA-PEG is less than for the other copolymers, as would be expected due to its longer PEG chain length of 5000 over 2000 for the other PLA-PEGs. The value of the PEG layer thickness for 2:5 PLA-PEG is also much greater than for the other PLA-PEG copolymers, except for the 1.5:2 LPLA-PEG.

The seemingly anomalous result with the 1.5:2 LPLA-PEG is most likely due to the pronounced increase in size with increase in concentration seen with this copolymer that did not occur with the other PLA-PEG copolymers (with the possible exception of 2:5 PLA-PEG). Increased particle size has been shown to affect the PEG layer thickness, Δ . For example, for polystyrene particles grafted with PEO chains, an increase in particle core size gave an increased value of Δ for constant PEO chain length (Liang *et al*, 1992).

Also, the LPLA-PEG used in this experiment was unfractionated, and the presence of a significant amount of peak two material (which is predominantly PEG) in the sample will probably have affected the results.

The difference between the values of Δ for 4:2 and 6:2 PLA-PEG particles is negligible, considering that the value of Δ is derived from the hydrodynamic radius, R_h , measured by DLS. However, the 4:2, 6:2 and 1.5:2 PLA-PEG copolymers all have a PEG chain of 2000, yet the chain layer thickness of the 1.5:2 PLA-PEG micelles is slightly larger.

This is also reflected in the lower value of the volume fraction of 1.5:2 PLA-PEG at the crossover point. This may be due to a conformational difference between the micellar structure of 1.5:2 PLA-PEG, and the more stable particle structure of 4:2 and 6:2 PLA-PEGs.

Table 4.3 shows comparative values of PEG layer thickness, Δ , for similar polymer systems, but obtained by different methods. Also shown in this table are values for the micelle/particle core radii, R_c , which were calculated for the PLA-PEG copolymers from the numerical difference between the hydrodynamic radius obtained by DLS and given in section 4.2.4, and the PEG layer thickness, Δ (i.e. the shell thickness of the micelles/particles).

Considering the core radii values of the PLA-PEG copolymers, the values for 1.5:2 PLA-PEG and 4:2 PLA-PEG are very similar, in common with their similar size but despite the increased molecular weight of the PLA block of 4:2 PLA-PEG. 1.5:2 PLA-PEG

PEG differs in showing a larger PEG layer thickness, as illustrated by the value of Δ . Comparing the similar 4:2 and 6:2 PLA-PEG copolymers shows that while the values of Δ are very similar, the core radius is slightly larger with 6:2 PLA-PEG, which may be expected due to the larger PLA component, and indeed, the ratios of the core radii to the PEG layer thickness for 4:2 and 6:2 PLA-PEG copolymers are similar to the ratios of the component blocks.

However, there seems to be no definite trend between the PLA-PEG copolymers, possibly as a result of the different structures of the “micelles” with the more stable “particle” structures. A wider range of copolymers within the micellar or particular range may reveal a clearer trend.

Comparing the PLA-PEG copolymers with some of the Pluronic copolymer range (Table 4.3), which are also known to form micelles, shows that the values of R_c and Δ are of a similar magnitude for all systems. Pluronic P85 compares well with 1.5:2 PLA-PEG, which has similar hydrophilic and hydrophobic block contents, whereas 2:5 PLA-PEG compares well with Pluronics F108 and F68, with both the block sizes and the value of Δ for 2:5 PLA-PEG lying between the respective values for the two Pluronic copolymers. A triblock copoly(oxyethylene/oxybutylene/oxyethylene) also shows a similar value for PEG layer thickness, Δ , but has a lower value for the core radius, which may reflect the difference in conformation of triblock copolymers over diblock copolymers. All values for core radii are likely to be on the low side, as the method of calculation used (Zhou and Chu, 1988a) neglects the possible penetration of water and PEO into the micellar core. Thus the value of the core volume, from which the radius is calculated, is at the lower limit (Zhou and Chu, 1988b). Mortensen and Pedersen (1993) showed, to a good approximation, that the micellar core of Pluronics could be thought to consist of completely dehydrated propylene oxide units, covered by a dense monolayer of ethylene oxide units. Linse and Malmsten (1992) found similar behaviour, but also noted the presence of some EO inside the core. The core sizes of the PLA-PEG copolymers are possibly also at the lower limit, as again the contribution of PEG and water to the core is not taken into consideration.

The PEG layer thickness values for 4:2 and 6:2 PLA-PEG are smaller than those seen with 1.5:2 PLA-PEG and the copolymers considered in Table 4.3. As the copolymers

Table 4.3

Comparison of PEG layer Thicknesses of PLA-PEGs with Similar Copolymer Systems

Copolymer	PEG Mw	PLA or PPO or PB Mw	Temp (°C)	R _h (nm)	R _c (nm)	Δ (nm)		Reference
						By Rheology	By Other Method	
1.5:2 LPLA-PEG	2000	1500	25	15.2	6.7	8.5	-	-
1.5:2 PLA-PEG	2000	1500	25	8.6	4.5	4.1	-	-
4:2 PLA-PEG	2000	4000	25	7.1	4.8	2.3	-	-
6:2 PLA-PEG	2000	6000	25	8.4	6.1	2.4	-	-
2:5 PLA-PEG	5000	2000	25	11.9	4.4	7.5	-	-
Pluronic P85	1150x2	2200	37	7.3	3.7	-	3.6 ^a	Kabanov <i>et al</i> , 1995
Pluronic F108	6640x2	3250	37	17.5	2.5	-	15.0 ^a	Kabanov <i>et al</i> , 1995
Pluronic F68	3580x2	1740	54	7.8	2.5	-	5.3 ^a	Kabanov <i>et al</i> , 1995
E ₄₀ B ₁₅ E ₄₀	1800x2	1200	20.5-22.5	6.7	1.7	-	5.0 ^a	Luo <i>et al</i> , 1993
Polystyrene/ P103	900x2	3250	20	44.0	33.5	8.9	10.5 ^b	Faers and Luckham, 1994
Polystyrene/ P105	1665x2	3250	20	46.0	33.5	9.3	12.5 ^b	Faers and Luckham, 1994
Polystyrene/ F108	5800x2	3250	20	47.0	33.5	10.3	13.5 ^b	Faers and Luckham, 1994

R_c = core radius of micelle/particle.R_h = hydrodynamic radius of micelle/particle.

Δ = PEG layer thickness.

^a Estimated by calculation as described by Zhou and Chu (1988a).^b Estimated by DLS.

considered in Table 4.3 are micelle-forming (except for the polystyrene coated particles), this again suggests difficulty in correlating between these two different structures.

Above it was noted that for particles with adsorbed or grafted PEO on the surface, the longer the PEO chain, the greater the adsorbed layer thickness (i.e. Δ). Table 4.3 illustrates this, with the Δ values for polystyrene particles coated with physically adsorbed Pluronics increasing with increasing ethylene oxide chain length (while PPO remains constant). Generally, the PEG layer thicknesses appear greater for copolymers physically adsorbed onto the surface of polystyrene particles, compared with PEG layer thicknesses for self-forming micelles and particles with similar PEG chain lengths. This may be a function of the increased particle size of the polystyrene particles ($R_h=44 \text{ nm} - 47 \text{ nm}$) over the much smaller copolymer micelles and particles ($R_h=6.7 \text{ nm} - 17.5 \text{ nm}$), which can affect Δ (Liang *et al*, 1992), or could be due to conformational differences in the PEG chains.

Faers and Luckham (1994) also compared the values of Δ acquired from the rheology work with values measured by DLS, as shown in Table 4.3. The DLS-measured values were slightly higher, which may be expected as this measurement is sensitive to the distal regions of the adsorbed copolymer. Pingret *et al* (1992) also noted comparable values between DLS and rheological measurements for adsorbed layer thicknesses, Δ .

Table 4.4 shows further calculations of the dimensions of the PEG chains of the PLA-PEG copolymers. The number of ethylene glycol (EG) units, b , was calculated by dividing the PEG molecular weight ($M_w=2000$ or 5000) by the molecular weight of a single ethylene glycol unit, $M_w=45$, and the association number of copolymer molecules in a micelle/particle, N_w , was determined as described in section 3.7.2. Using the hydrodynamic radius, R_h , and the core radius, R_c , from Table 4.3, this allowed the mean volume occupied by a PEG chain, v_{PEG} , and the mean volume occupied by an ethylene glycol unit, v_{EG} , in the micelle/particle shell to be determined by the following equations (Luo *et al*, 1993; Kabanov *et al*, 1995): -

$$v_{PEG} = \frac{4\pi(R_h^3 - R_c^3)}{3N_w}$$

$$v_{EG} = \frac{4\pi(R_h^3 - R_c^3)}{3bN_w} = \frac{v_{PEG}}{b}$$

These equations assume that the micelles/particles are spherical, a reasonable assumption from the TEM data discussed in section 3.4.2. No values could be calculated for 1.5:2 LPLA-PEG as the association number was not determined for this copolymer.

The values for the PLA-PEG copolymers of v_{EG} are of a similar magnitude to those quoted by Kabanov *et al* (1995) for the Pluronic P85 (0.49 nm³), Zhou and Chu (1988b) for Pluronic F68 (0.19 nm³) and Luo *et al* (1993) for E₄₀B₁₅E₄₀ (1.29 nm³ at 20.5 - 22.5 °C). The corresponding value for v_{EG} in unswollen liquid poly(ethylene glycol), assuming that the density of PEG ≈ 1.0 gcm⁻³, is $v_E = 0.073$ nm³ (Luo *et al*, 1993). As this value is an order of magnitude smaller than the values calculated for the PLA-PEG copolymers, this indicates that the PEG shell of the micelles/particles is swollen and has an open structure that can physically trap water molecules, in addition to the two molecules that can bind by hydrogen bonding to the ether oxygen of each EG unit (Zhou and Chu, 1988a; Luo *et al*, 1993; Kabanov *et al*, 1995). The average number of water molecules, N_{water} , that are associated with each ethylene glycol unit can be calculated from the values of v_{EG} by taking the mean volume occupied by a water molecule as $v_{water} \approx 0.030$ nm³, and using the following equation (Luo *et al*, 1993):-

$$N_{water} = \frac{v_{EG} - v_E}{v_{water}}$$

Table 4.4 shows the resulting values, calculated for the PLA-PEG copolymers, from this

equation. The values of v_{PEG} , v_{EG} and N_{water} clearly show a difference between the micelle-forming 1.5:2 and 2:5 PLA-PEG copolymers and the particle-forming 4:2 and 6:2 PLA-PEG copolymers. It is apparent from Table 4.4 that the PEG shells of the 1.5:2 and 2:5 PLA-PEG micelles are much more hydrated than the corresponding PEG shells of the 4:2 and 6:2 PLA-PEG particles. The hydration is more noticeable with 2:5 PLA-PEG which, from the rheology results, has the longest PEG layer thickness, Δ . Conversely, the 4:2 and 6:2 PLA-PEG particles are only slightly more hydrated than would be expected due to the hydrogen bonding that occurs with the ether oxygen molecules of PEG (i.e. there are three water molecules associated per EG unit rather than two).

The value for v_{EG} can also give some indication of the configuration of the PEG chains in the micelles/particles. Two models are considered to represent the possible configurations of PEG chains. These are the “zig-zag” model and the “meander” model. In the “zig-zag” model, the PEG chain is fully extended, with the length and width of an ethylene glycol unit being 3.6 and 2.5 Å respectively, whereas in the “meander” model, the PEG chain is twisted into an expanded helical coil form with the ethylene glycol unit length and width being 2.0 and 4.5 Å respectively. If the PEG chains were presumed in the zigzag form, then the PEG layer thickness would be expected to be about 16 nm for 2000 PEG copolymers and about 40 nm for 5000 PEG copolymers, which are much larger than any of the values observed. If a meander configuration is assumed, the PEG layer thickness values would be about 9 nm for 2000 molecular weight PEG chains and 22 nm for 5000 molecular weight PEG chains, which while still larger than the values measured, are more reasonable. Also, it is thought that for an aqueous solution of PEG chains, with more than ten ethylene glycol units per chain, the meander configuration predominates (Rosch, 1967). Faers and Luckham (1994) observed that the increase in Δ with ethylene oxide chain length scaled with $n\text{EO}^{1/2}$ (where n is the number of EO units in the PEO chain), which showed that the EO chains were arranged as elongated coils in the adsorbed layer, rather than as linear chains (which would scale with $n\text{EO}$). It seems likely therefore that the meander configuration of the PEG chains in the PLA-PEG micelles/particles is the best approximation.

Table 4.4

Molecular Dimensions of PLA-PEG Micelles/Particles

Copolymer	Number of EG units, b	Association number, N_w	R_h (nm)	Volume of PEG chain, v_{PEG} (nm ³)	Volume of EG unit, v_{EG} (nm ³)	Number of H ₂ O Molecules Associated with each EG, N_{water}
1.5:2 PLA-PEG	44	132	8.6	17.3	0.39	11
4:2 PLA-PEG	44	155	7.05	6.7	0.15	3
6:2 PLA-PEG	44	214	8.4	7.2	0.16	3
2:5 PLA-PEG	111	47	11.9	142.6	1.28	40

4.3 ANALYSIS OF SURFACE CHEMISTRY AND STRUCTURE

4.3.1 *Static Secondary Ion Mass Spectrometry (SSIMS)*

Static secondary ion mass spectrometry (SSIMS) is the mass spectrometry of particles emitted by a surface when that surface is bombarded by energetic primary particles, which may be electrons, ions, neutrals or photons (Vickerman, 1988). The secondary ions that are detected are either emitted from the surface in ionised state, or emitted as neutrals and post-ionised before analysis. Static SIMS uses a primary beam with a very low current density so that secondary ions are emitted from areas not previously damaged and the surface monolayer lifetime is much greater than the time needed for analysis (Vickerman, 1988). This process is described in detail by Vickerman (1988) and Briggs (1986, 1991).

Static SIMS allows both the elemental composition and chemical structure of the surface to be studied, as cluster ions are emitted as well as elemental ions, to give a surface mass spectrum (Vickerman, 1988). This is produced by directing a noble gas ion beam (usually of Ar^+ or Xe^+) at the sample surface, which causes material to be sputtered into an ultra-high vacuum (Briggs, 1986). When this beam interacts with the surface atoms, energy is transferred and the atoms in the near-surface region undergo collision sequences. Some of these collisions cause the energy to be dissipated in the bulk sample, whereas others return to the surface causing the emission of secondary ions, atoms or molecules (Vickerman, 1989). These secondary emissions are then extracted into a mass spectrometer and are analysed in terms of their mass/charge ratio (m/z) to provide in sequential experiments, the positive and negative secondary ion mass spectra respectively (Briggs, 1986). It has been shown that the detected secondary ions emerge from a depth of about 10 Å, indicating that SIMS is highly surface specific (Hearn *et al*, 1987; Briggs, 1989).

4.3.2 *Static Secondary Ion Mass Spectrometry (SSIMS) of PLA-PEG Particles*

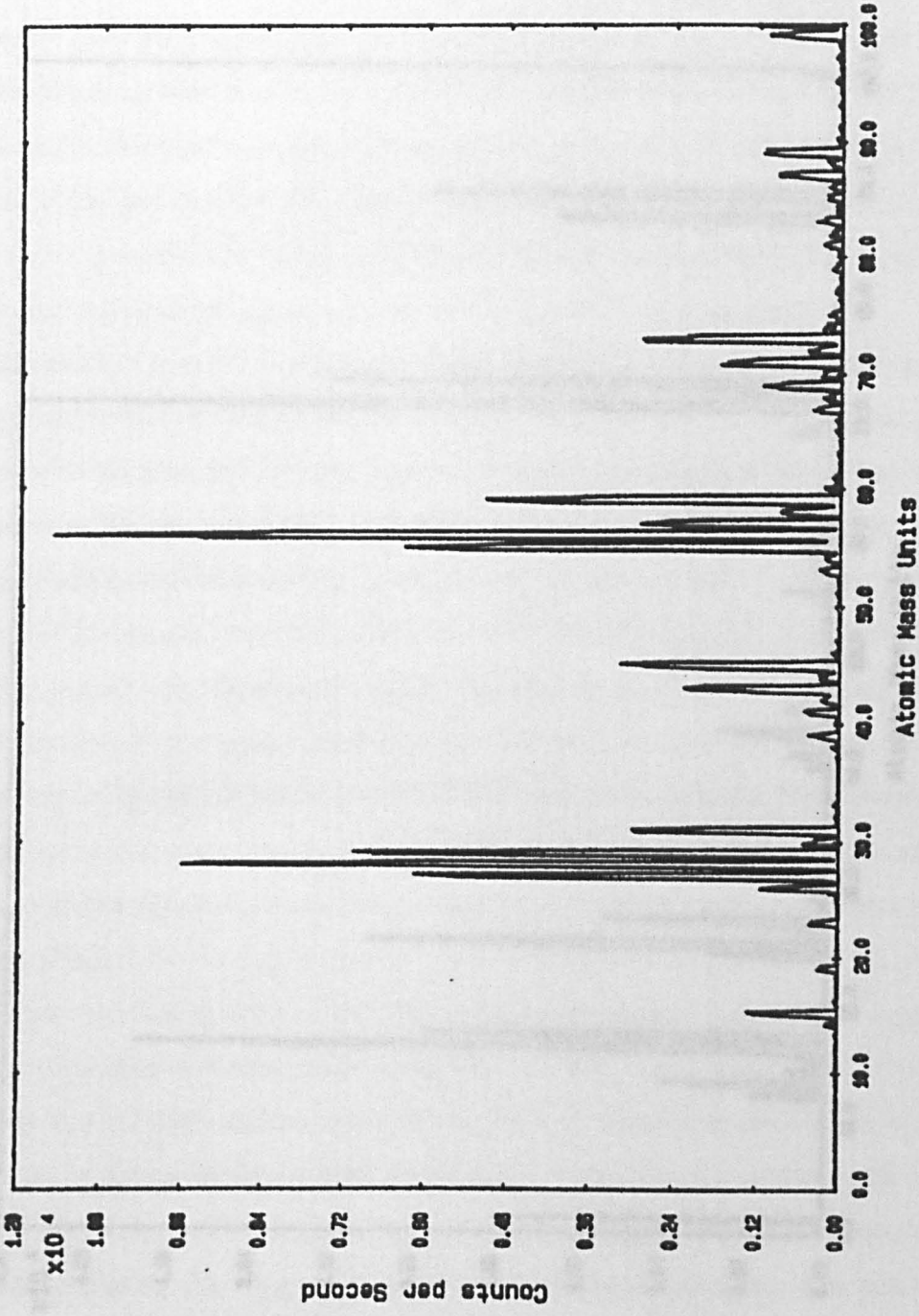
In recent years, SIMS has been employed as a tool for studying polymers considered as potential drug delivery systems, including copolymers (Davies and Lynn, 1990a and 1990b). SIMS was noted as being able to provide a “fingerprint” of chemical information

about both pure polymers and copolymers to a high degree of molecular specificity (Davies *et al*, 1987), and this “fingerprint” also allows the detection of homopolymers within a copolymer structure (Davies and Lynn, 1990a). Therefore, the SIMS spectra of the PLA-PEG copolymers would be expected to show ions from both monomer units. The PLA-PEG copolymers (4:2 and 6:2 PLA-PEG) were analysed as described in section 2.9.1. The analysis was performed on both the unfractionated copolymer dissolved in acetone, and on nanoparticles in aqueous dispersion. The spectra produced in each case were identical between the solutions of the copolymer in chloroform and as nanoparticles in aqueous solution. Figures 4.9 and 4.10 show the positive and negative ion spectra respectively for 4:2 PLA-PEG nanoparticles for m/z of 0 to 100, where m/z is mass/charge. The results represent a combination of the PLA and PEG homopolymer spectra, with diagnostic peaks from both polymers present in the PLA-PEG spectra. On analysis by SIMS, most polymers produce multiple ions that correspond to structures arising from the intact monomer unit, its side chain (if present) and fragments of these species (Davies and Lynn, 1990a). PLA and PEG are no exception to this, and in the following discussion, “M” is used to denote the appropriate monomer repeat unit.

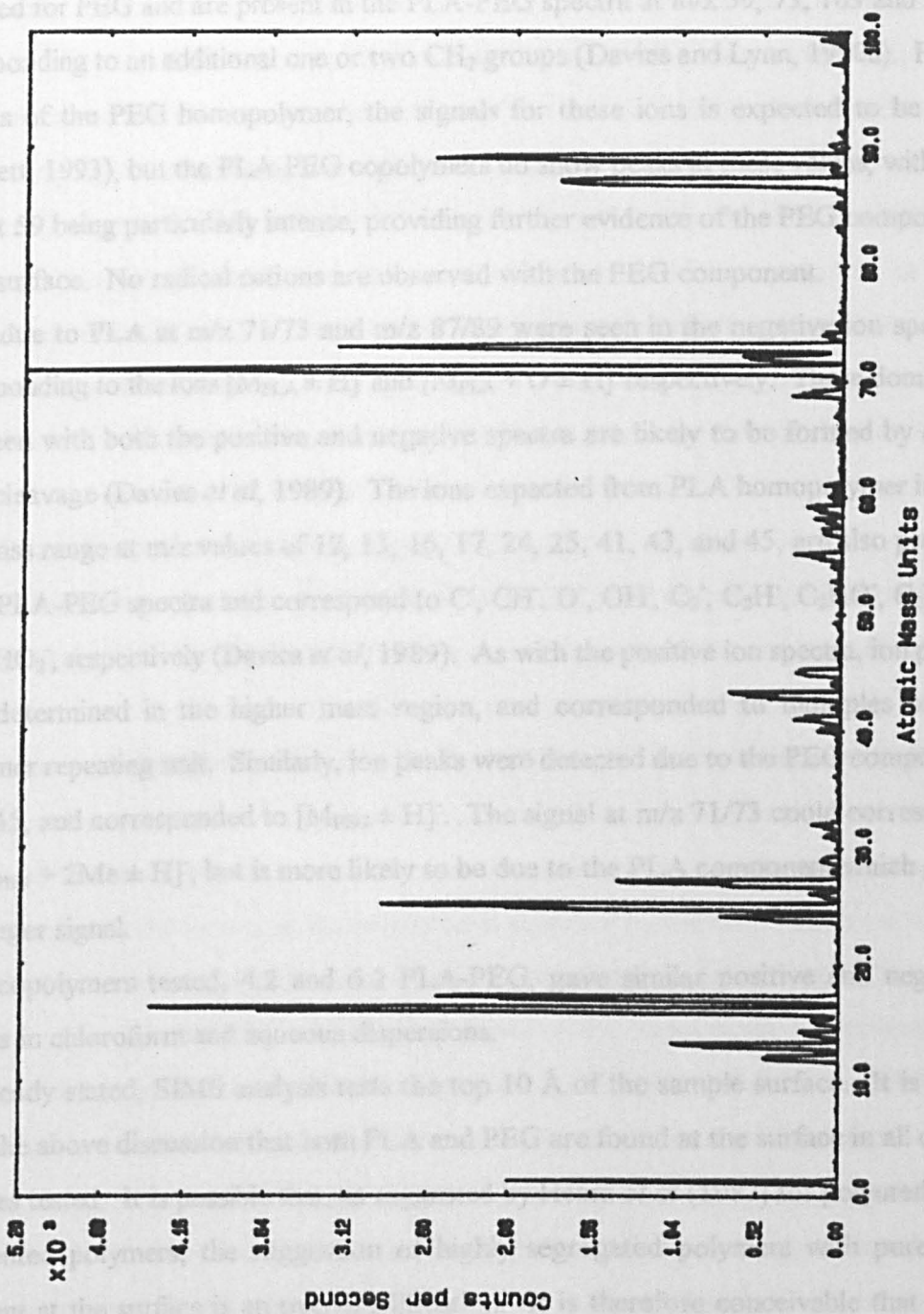
In the low mass region of the positive ion spectra, ion peaks corresponding to PLA are seen at m/z 71/73 due to $[M_{\text{PLA}} \pm H]^+$ and m/z 55 due to $[M_{\text{PLA}} - OH]^+$. PLA also forms an intense cluster at m/z 99/100/101, which corresponds to $[2M_{\text{PLA}} - CO_2 - H]^+$, $[2M_{\text{PLA}} - CO_2]^+$ and $[2M_{\text{PLA}} - CO_2 + H]^+$ (Davies *et al*, 1989) and is seen in the PLA-PEG spectra. Ion peaks are also readily detected in the higher mass region ($m/z > 100$) from the PLA block showing monomer multiples of these ions, for example $[nM_{\text{PLA}} \pm H]^+$ for $n = 1$ to 4.

Most positive ions detected are of the “even electron” type where there is loss of a bonding electron during fragmentation. However, “odd electron” ions were also formed where the electron lost in the formation of an ion was a non-bonding electron, i.e a radical cation (Davies and Lynn, 1990a). With PLA homopolymer, radical cations are seen at m/z of 128, 200 and 272, corresponding to $[nM_{\text{PLA}} - O]^+$ for $n=2 - 4$. As strong peaks are noted in the PLA-PEG spectra at all these values, it seems likely that these cations are formed on SIMS analysis of the PLA-PEG samples.

Figure 4.9 – Positive Ion SIMS Spectrum for 4:2 PLA-PEG Nanoparticles



Figures 4.10 Negative Ion SIMS Spectrum for 4:2 PLA-PEG Nanoparticles



The presence of PEG in the positive ion spectra was detected by the ion peaks at m/z 43/45, which corresponds to $[M_{\text{PEG}} \pm H]^+$. Although peaks are expected for PLA also at m/z 43/45, with PLA homopolymer the peak at 43 would be dominant, whereas in the PLA-PEG spectra, the peak at m/z 45 is dominant indicating PEG. Ions are also expected for PEG and are present in the PLA-PEG spectra at m/z 59, 73, 103 and 117, corresponding to an additional one or two CH_2 groups (Davies and Lynn, 1990a). From analysis of the PEG homopolymer, the signals for these ions is expected to be low (Bridgett, 1993), but the PLA-PEG copolymers do show peaks at these values, with the peak at 59 being particularly intense, providing further evidence of the PEG component at the surface. No radical cations are observed with the PEG component.

Peaks due to PLA at m/z 71/73 and m/z 87/89 were seen in the negative ion spectra corresponding to the ions $[M_{\text{PLA}} \pm H]^-$ and $[M_{\text{PLA}} + \text{O} \pm H]^-$ respectively. These dominant ions seen with both the positive and negative spectra are likely to be formed by ester chain cleavage (Davies *et al*, 1989). The ions expected from PLA homopolymer in the low mass range at m/z values of 12, 13, 16, 17, 24, 25, 41, 43, and 45, are also present in the PLA-PEG spectra and correspond to C^- , CH^- , O^- , OH^- , C_2^- , C_2H^- , C_2HO^- , $\text{C}_2\text{H}_3\text{O}^-$ and CHO_2^- , respectively (Davies *et al*, 1989). As with the positive ion spectra, ion peaks were determined in the higher mass region, and corresponded to multiples of the monomer repeating unit. Similarly, ion peaks were detected due to the PEG component at 43/45, and corresponded to $[M_{\text{PEG}} \pm H]^-$. The signal at m/z 71/73 could correspond to $[M_{\text{PEG}} + 2\text{Me} \pm H]^-$, but is more likely to be due to the PLA component which gives a stronger signal.

Both copolymers tested, 4:2 and 6:2 PLA-PEG, gave similar positive and negative spectra in chloroform and aqueous dispersions.

As already stated, SIMS analysis tests the top 10 Å of the sample surface. It is clear from the above discussion that both PLA and PEG are found at the surface in all of the samples tested. It is possible that, as suggested by Hearn *et al* (1987) for polyurethanes segmented polymers, the suggestion of highly segregated polymers with pure soft segment at the surface is an oversimplification. It is therefore conceivable that there could be PLA groups at the surface of the PLA-PEG systems, in addition to PEG. However, the chloroform-dissolved samples also show PEG at the surface, indicating

that the surface orientation of this component is still towards the surface, even when the surface chemistry is disrupted (Brindley *et al*, 1992).

Although SIMS gives good molecular specificity of chemical structure, quantitation of the surface composition remains difficult due to matrix effects influencing secondary ion yields and hence ion intensities (Davies *et al*, 1989). These factors that are responsible for matrix effects include the polymer film thickness and uniformity, sample charging (during analysis) and the type of substrate used (Davies *et al*, 1989). Quantitation has been attempted by comparing the relative intensities of ions characteristic to the individual components of a copolymer (Davies and Lynn, 1990a; Brindley *et al*, 1992). However, this would also prove difficult with the PLA-PEG copolymers as the diagnostic ion usually used for PEG, $m/z=45$, also has a contribution from PLA. The complementary technique of X-ray photoelectron spectroscopy (XPS) is usually employed to provide quantitative data and will therefore now be discussed.

4.3.3 X-Ray Photoelectron Spectroscopy (XPS)

X-ray photoelectron spectroscopy (also known as ESCA or electron spectroscopy for chemical analysis) is the application of energy analysis to the electrons emitted from a surface illuminated by X-rays and exhibiting a photoelectric effect (Smith, 1994). The process has been described in detail by Watts (1990a) and Smith (1994) and has been used for surface analysis of biodegradable copolymers in conjunction with SIMS (Davies and Short, 1988). In this technique, X-rays are applied to the sample surface and the energy carried by the incoming X-ray photon is absorbed by the target atom and raises it into an excited state. The atom relaxes again by emitting a photoelectron, and as these photoelectrons are emitted from all energy levels of the target atom, a characteristic electron energy spectrum is produced for that atom type (Smith, 1994) by analysis by an electron spectrometer. The spectrometer measures the kinetic energy of the electron, but as this is not an intrinsic property of the material, this value is converted into the binding energy, which identifies the electron specifically, both in terms of its parent element and atomic energy level (Watts, 1990a). Lines in the spectrum can then be labelled according to which energy level they originated from.

The intensities of the photoelectron lines produced are important and allow quantification

of the material, so that XPS allows quantitative as well as qualitative analysis. The precise energy and shape of a particular line of the spectrum also reflects the local environment and chemical state of the emitting element (Smith, 1994). Any effect that alters the energy levels of atoms in the surface region will also alter the XPS spectrum, giving rise to chemical shifts in energy.

Therefore, XPS provides element and chemical state identification for atoms in the top few atomic layers of the sample (the top 10 - 100 Å in depth are studied depending on the electron take-off angle (Ratner, 1988)), and can also give some structural information under certain conditions. XPS is therefore not as surface specific as SIMS.

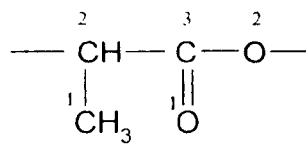
4.3.4 X-ray Photoelectron Spectroscopy of PLA-PEG Particles

XPS can be used to provide evidence that PEG is present at the surface of the PLA-PEG samples, and the samples (4:2 and 6:2 PLA-PEG) were analysed as described in section 2.9.2. This was illustrated by Brindley *et al* (1992), who prepared polystyrene particles with PEG grafted to the surface. Subsequent XPS analysis of these particles showed two main carbon environments due to the hydrocarbon carbon, \underline{C} -C/ \underline{C} -H, attributable to the polystyrene backbone, and the ether carbon, \underline{C} -O, arising from the PEG groups at the surface with a small contribution from the sulphate end groups on the polystyrene chains.

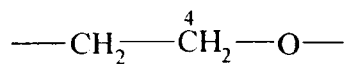
Brindley *et al* (1994) also noted an increase in the ether carbon content with an increase in PEG density. Similarly, Lee and Andrade (1988) have observed an increase in the ether carbon peak with an increase in the amount of PEO-PPO-PEO surfactant adsorbed onto dimethyl dichloro silane (DDS) surfaces.

Dunn *et al* (1994) have mentioned the difficulty in obtaining PEG density values for grafted particles (and hence block copolymers) compared with physically adsorbed systems, where the density of PEG on a particle surface can be calculated from the plateau levels of adsorption isotherms. However, XPS measurements allow a comparative indication of the amount of PEG at the surface by measuring the percentage of \underline{C} -O bonds within the 1s carbon spectra for different systems. XPS has been performed on the 4:2 and 6:2 PLA-PEG copolymers prepared from fractionated material as nanoparticles in water and as unfractionated copolymer in chloroform. Figure 4.11 gives the structures of the PLA and PEG monomers, with the carbon atoms numbered

Figure 4.11 – Structures of the PLA and PEG Monomers (carbon and oxygen atoms numbered to aid interpretation)



PLA Monomer



PEG Monomer

Figure 4.12 – Carbon C 1s Envelopes for XPS Analysis of 4:2 PLA-PEG Nanoparticles

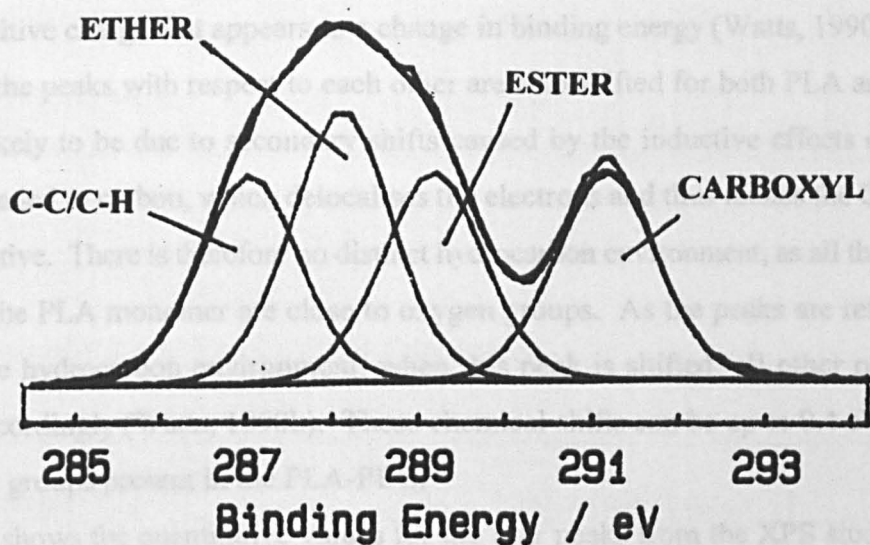


Figure 4.12 shows the carbon C 1s envelopes for XPS analysis of 4:2 PLA-PEG nanoparticles. This clearly shows the presence of both PLA and PEG at the surface. The three peaks expected for PLA are present, corresponding to hydrocarbon (CH₂-CH) (1), ester (C-(CH₂)C=O) (2) and carboxyl (C-O-C=O) (3) environments, as well as the peak expected for PEG, corresponding to the ether environment (C-C-O-C) (4). However, the binding energy values of these peaks are different to the expected values for PLA homopolymer and PEG homopolymer, as shown in Table 4.5. This is probably as a result of the inductive properties of the copolymers. When X-rays are fired at the copolymer samples, electrons are emitted and collected, and this can leave the sample with a positive charge, which causes a change in binding energy (Watts, 1990b). The values of the peaks with respect to each other are shifted for both PLA and PEG. This is likely to be due to the inductive effect caused by the inductive effects of the O groups being more electronegative than the C atoms, which makes the C atoms more negative. There is also a slight shift in the ester peak, as all the carbon atoms in the PLA monomer are in ester groups. As the peaks are referenced against the hydrocarbon peak, the ester and ether peaks are shifted accordingly. Table 4.6 shows the quantitative results from the XPS studies, and demonstrates from the values of carbon in the ether carbon environment, C-C-O-C, that there is more PEG at the surface of the 4:2 PLA-PEG than the 6:2 PLA-PEG. Table 4.6 also clearly shows the hydrocarbon contamination present in the re-fractionated samples prepared in chloroform by the greatly increased CH₂-CH environment detected for the PLA with respect to the carbon detected for the other carbon groups present in PLA (all should be equal), and also with respect to the corresponding values for samples in water. Hydrocarbon contamination has previously been noted with PLA samples (Davies *et al.*, 1989), and varies from sample to sample. It is likely that the GPC process removes this contamination and hence, no raised hydrocarbon values are seen with the PLA-PEG samples in water prepared from fractionated material. Tables 4.7 and 4.8 show the stoichiometry results for the 4:2 and 6:2 PLA-PEG copolymers, for carbon and oxygen present from the C 1s and O 1s spectra respectively.

to aid interpretation.

Figure 4.12 shows the carbon C 1s envelopes for XPS analysis of 4:2 PLA-PEG nanoparticles. This clearly shows the presence of both PLA and PEG at the surface. The three peaks expected for PLA are present, corresponding to hydrocarbon ($\underline{\text{C}}\text{H}_3\text{-CH}$) (1), ester ($\text{C-(CH}_3\text{)}\underline{\text{C}}\text{-O}$) (2) and carboxyl ($\text{C-O-}\underline{\text{C}}\text{=O}$) (3) environments, as well as the peak expected for PEG, corresponding to the ether environment ($\text{C-}\underline{\text{C}}\text{-O-C}$) (4). However, the binding energy values of these peaks are different to the expected values for PLA homopolymer and PEG homopolymer, as shown in Table 4.5. This is probably as a result of the insulating properties of the copolymers. When X-rays are fired at the copolymer samples, electrons are emitted and collected, and this can leave the sample with a positive charge that appears as a change in binding energy (Watts, 1990b). The values of the peaks with respect to each other are also shifted for both PLA and PEG. This is likely to be due to secondary shifts caused by the inductive effects of the O groups bonded to carbon, which delocalises the electrons and thus makes the O groups more negative. There is therefore no distinct hydrocarbon environment, as all the carbon atoms in the PLA monomer are close to oxygen groups. As the peaks are referenced against the hydrocarbon environment, when this peak is shifted, all other peaks are shifted accordingly (Watts, 1990b). These chemical shifts can be up to 0.4 eV for the functional groups present in the PLA-PEG.

Table 4.6 shows the quantitative values for the four peaks from the XPS studies, and demonstrates from the values of carbon in the ether carbon environment, $\text{C-}\underline{\text{C}}\text{-O-C}$, that there is more PEG at the surface of the 4:2 PLA-PEG than the 6:2 PLA-PEG. Table 4.6 also clearly shows the hydrocarbon contamination present in the unfractionated samples prepared in chloroform by the greatly increased $\underline{\text{C}}\text{H}_3\text{-CH}$ environment detected for the PLA with respect to the carbon detected for the other carbon groups present in PLA (all should be equal), and also with respect to the corresponding values for samples in water. Hydrocarbon contamination has previously been noted with PLA samples (Davies *et al.*, 1989), and varies from sample to sample. It is likely that the GPC process removes this contamination and hence, no raised hydrocarbon values are seen with the PLA-PEG samples in water prepared from fractionated material.

Tables 4.7 and 4.8 show the stoichiometry results for the 4:2 and 6:2 PLA-PEG copolymers, for carbon and oxygen present from the C 1s and O 1s spectra respectively.

Table 4.5

Binding Energy Values for PLA and PLA-PEG Copolymers

Sample	PLA C 1s Binding Energy (eV)			PEG C 1s Binding Energy (eV)
	(1)	(2)	(3)	
PLA Homopolymer	285.0	287.0	289.0	-
PEG Homopolymer	-	-	-	286.5
4:2 PLA-PEG in water	287.0	289.2	291.2	288.1
6:2 PLA-PEG in water	287.0	289.0	291.1	288.0

Table 4.6

XPS Analysis of 4:2 and 6:2 PLA-PEG Copolymers

Sample	XPS C 1s Envelope Ratios (%)			
	$\underline{\text{C}}\text{H}_3\text{-CH}$ (1)	$\text{C-}\underline{\text{C}}\text{-O-C}$ (4)	$\text{C-}(\text{CH}_3)\underline{\text{C}}\text{-O}$ (2)	$\text{C-O-}\underline{\text{C}}\text{=O}$ (3)
4:2 PLA-PEG in water	23	30	23	23
4:2 PLA-PEG in chloroform	37	30	17	17
6:2 PLA-PEG in water	26	21	26	26
6:2 PLA-PEG in chloroform	55	19	13	13
Pure PLA	33.3	-	33.3	33.3
Pure PEG	-	100	-	-

Table 4.7

Stoichiometry of 4:2 and 6:2 PLA-PEG for Carbon from XPS Carbon 1s Spectra

Sample	% C from Polylactide: experimental (theoretical)	% C from Polyethylene Glycol: experimental (theoretical)
4:2 PLA-PEG in water	69 (65)	30 (35)
4:2 PLA-PEG in chloroform	71 (65)	30 (35)
6:2 PLA-PEG in water	78 (73)	21 (27)
6:2 PLA-PEG in chloroform	81 (73)	19 (27)

Table 4.8

Stoichiometry of 4:2 and 6:2 PLA-PEG for Oxygen from XPS Oxygen 1s Spectra

Sample	% O from Polylactide: experimental (theoretical)	% O from Polyethylene Glycol: experimental (theoretical)
4:2 PLA-PEG in water	78 (71)	22 (29)
4:2 PLA-PEG in chloroform	67 (71)	34 (29)
6:2 PLA-PEG in water	82 (78)	18 (21)
6:2 PLA-PEG in chloroform	72 (78)	29 (21)

These show reasonable agreement with the theoretical values obtained for the nanoparticles, with the PEG values being slightly lower. From Table 4.8 it appears that more PEG is present at the surface in the chloroform samples than in water. However, this may be due to the second PLA-depleted (PEG-rich) species present in the unfractionated material in chloroform that would not be present in the fractionated material used to prepare the nanoparticles. Table 4.9 shows a comparison of the two PLA-PEG nanoparticle samples with previous results for polystyrene particles grafted with PEG 2000 (Dunn *et al*, 1994) and PLGA particles coated with physically adsorbed poloxamer 407 and poloxamine 908 (Scholes, 1994). Surface density of PEG is an important factor for a potential drug delivery system as it has been shown to be related to the uptake of nanoparticles by the reticuloendothelial system (RES) in *in vivo* studies (Dunn *et al*, 1994). These studies were performed using the polystyrene (PS)-PEG 2000 particles, where the PEG was grafted to the polystyrene particle surface with different densities of PEG denoted as a to d, where a was equivalent to the lowest density and d the highest. Decreasing uptake of particles by the liver was seen with increasing surface density, with PS-PEG 2000a particles giving little reduction in liver uptake whereas a significant decrease in uptake is seen with PS-PEG 2000 particles b, c and d. The authors noted that little significant improvement was seen with PS-PEG 2000d particles over PS-PEG 2000c particles and concluded that only a certain density of PEG on the particle surface was necessary to give the desired result (Dunn *et al*, 1994). The PLA-PEG nanoparticles could be expected to be similar to the grafted PS-PEG particles, and it can be seen from Table 4.9 that the % C-O lies between the results seen for PS-PEG 2000b particles and PS-PEG 2000c particles. The surface density of the PLA-PEG copolymers could therefore be expected to be sufficient to prevent uptake by the liver, but this is only one of a number of important factors which determines the biodistribution profile of nanoparticles, and the implications will be discussed further in section 6.3. Similarly, extended blood circulation times have been noted *in vivo* for PLGA nanoparticles coated with poloxamer 407 and poloxamine 908 and the % C-O for the ether environment seen is similar to that obtained for the PLA-PEG nanoparticles (Dunn *et al*, 1994; Scholes, 1994).

Table 4.9

Comparison of PLA-PEG Nanoparticles with Coated PLGA Nanoparticles and Polystyrene Particles with Grafted PEG 2000 of Differing Surface Densities

Sample	XPS C 1s % Ether Carbon (% C-O)
4:2 PLA-PEG nanoparticles	30
6:2 PLA-PEG nanoparticles	21
PLGA coated with Poloxamer 407 ¹	29
PLGA coated with Poloxamer 407 ²	31
PLGA coated with Poloxamine 908 ¹	28
PLGA coated with Poloxamine 908 ²	25
Polystyrene-PEG 2000a	8
Polystyrene-PEG 2000b	15
Polystyrene-PEG 2000c	41
Polystyrene-PEG 2000d	51

¹ - particles produced by the Fessi method followed by physical adsorption of surfactant to the surface of the nanoparticle.

² - particles produced by the Fessi method in the presence of surfactant.

a - d indicates increased surface density of PEG 2000 from a to d, due to differing input molar ratios of styrene to ethylene glycol.

4.4 THE STABILITY OF PLA-PEG AQUEOUS DISPERSIONS TO ADDED SALT

4.4.1 Theory of Cloud Point Testing

When the temperature of an aqueous solution of non-ionic surfactant micelles is raised, the solution becomes turbid over a narrow temperature range. The temperature of the onset of this turbidity is known as the cloud point, T_c (or also the critical flocculation temperature in certain cases). Above the cloud point, the system separates into two isotropic phases, one of which is an almost micelle-free dilute solution of the surfactant, with the other phase being a concentrated surfactant phase which only occurs above the cloud point (Hinze and Pramauro, 1993). This phase separation is usually reversible on cooling, when a clear solution is again formed.

The cloud point temperature is a function of the structure of the aggregate, and is affected by the size of both the hydrophilic and hydrophobic chain length, and the chain packing density, surface coverage and molecular structure of the hydrophilic chain (usually polyethylene glycol (PEG)) (Tadros and Vincent, 1980). Therefore, T_c gives an indication of the steric stability of the aggregate and thereby its performance *in vivo*, where the properties of the hydrophilic PEG chain are important in determining the biodistribution (Illum *et al*, 1987).

Cloud point temperatures are affected by the presence of other materials, and certain electrolytes are used to decrease the cloud point. This feature is utilised in the measurement of the cloud point temperatures of PLA-PEG micelles/particles to ensure that the T_c values are in the measurable temperature range of the instrument.

4.4.2 Mechanism of Clouding of PEG-Stabilised Aggregates

Cloud points are usually more influenced by the anions of added electrolytes than the cations (Tokiwa and Matsumoto, 1975). The effect of electrolytes on the steric stability of nonionic micelles/particles can be considered in terms of two factors: -

- i) the hydration of ions, with the consequent change of the nearby water structure, which affects the affinity of the water molecules for the ether oxygens of the amphiphile, and
- ii) the binding of ions or salts of polyvalent metals to ether oxygens via cation complexation at high concentrations, leading to an increase in amphiphile solubility

(Schott, 1973).

In the first category, are the anions such as sulphates, chlorides, iodides and thiocyanates, whereas in the second category, are cations, such as dioxane (Schott and Han, 1976).

The effect of an additive on the cloud point can be assessed by its lyotropic number, where the lower the lyotropic number below 11.7 (Schott and Han, 1976), the greater the depression of the cloud point (otherwise known as salting out). Similarly, higher lyotropic numbers indicate an elevation of the cloud point. Sodium sulphate was chosen for the determination of PLA-PEG cloud points due to its low lyotropic number of 1.60 (Firman *et al*, 1985).

Several theories have been advanced throughout the years to account for cloud points (the onset of flocculation). Flocculation is generally thought to be due to the decreasing solvency of the dispersion medium for the stabilising PEO chains. This results in contacts between molecules of the dispersion medium and between PEO chains becoming energetically more favourable than dispersion medium-PEO chain contacts (Napper, 1968; Napper, 1970a). Suggestions have been made that this may be due to a competitive binding process between the ions and the polymer for the water molecules; as ion hydration increases, less solvent is available to dissolve the PEO chains (Boucher and Hines, 1976; Napper, 1970b). However, this theory does not explain all observations, which led to a further suggestion that to explain clouding in the presence of electrolyte, the structure of the water must be considered. In the presence of an electrolyte, water consists of three regions (Boucher and Hines, 1976; Napper, 1970b).

Region A consists of the innermost polarised water molecules around the ion, which move with the ion. Region B is partially ordered by the electric field of the ion, concentric with the ion and contains water molecules with greater mobility compared with pure water, as the hydrogen bonding is destroyed. Region C behaves as bulk water with hydrogen bonding present. The extent of region B compared with A and C is a measure of the structure-breaking ability of the ion. As region A is impenetrable to the PEO chains, only regions B and C are available to dissolve the PEO, which leads to decreased solvency for the PEO. The flocculating ability of an added salt is due to how the salt affects the bulk water, the water-polymer interaction and the polymer-polymer interactions. Therefore with sulphate ions, which are powerful flocculants, a large B

region is seen with negligible A region (Tadros and Vincent, 1980), whereas chlorides are highly hydrated (large A region) and need increased concentration to be effective. Although this theory has been generally accepted, there is still debate within the literature about the cause of clouding. Rupert (1992) studied clouding in terms of a Flory-Huggins approach, and concluded that clouding was the result of a change in the balance between the hydrophobic and hydrophilic interactions of a micelle with its surroundings with increasing temperature. The theory suggested that the unfavourable interactions between hydrophobic groups and water were responsible for clouding, and not a sudden dehydration. Another theory proposed is that clouding is caused by a change in PEO head group conformation, which reduces the dipole moment of an ethylene oxide group and makes the head group less hydrophilic (Karlström, 1985).

4.4.3 Cloud Point Temperatures of PLA-PEG Micelles/Particles

Poloxamer 407 was chosen as a comparable species to the "PLA-rich" fraction (peak one). PEG 8000 is comparable to the total PEG content of Poloxamer 407, and was chosen so that the contribution of PEG to the micelle stability could be determined. PEG 8000 also serves as a comparator to the PEG portion of the PLA-PEG copolymers (Mw 2000 and 5000), and to the "PLA-depleted" fraction of the PLA-PEG copolymers. The experiments were performed as described in section 2.10.

For PEG 8000 solutions, a sharp increase in turbidity was seen, as the temperature increased, followed by a plateau region, extending to the end point of the experiment (80°C) (Figure 4.13a). This turbidity was reversible, clearing rapidly on cooling of the solution. Reversibility is generally noted for this type of incipient phase separation in polymer solutions (Napper, 1969; Hinze and Pramauro, 1993). No further phase separation was observed for PEG 8000 solutions during testing to 80°C.

Poloxamer 407 showed a different pattern of behaviour compared with PEG 8000. A sharp increase in absorbance at the cloud point (T_c) was followed by a plateau region, as with PEG 8000. However, a marked fall in absorbance was then observed corresponding to separation of a solid phase (Figure 4.13b). Examination of samples at 80°C, after testing, revealed a collection of solids at the surface of clear liquid, with reversibility exhibited at all stages of turbidity. The point of decrease in turbidity after

Figure 4.13a – Cloud Point Curve of PEG 8000 Solution

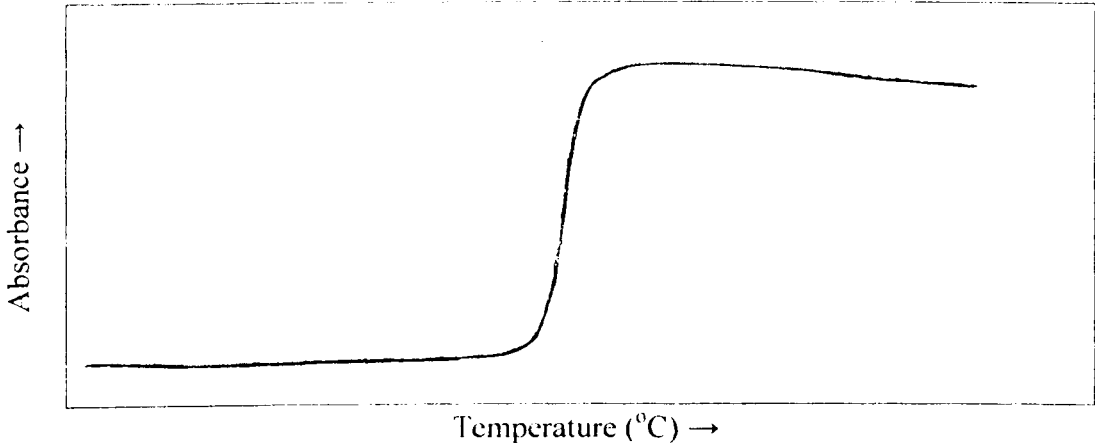


Figure 4.13b – Cloud Point Curve of Poloxamer 407 Dispersion

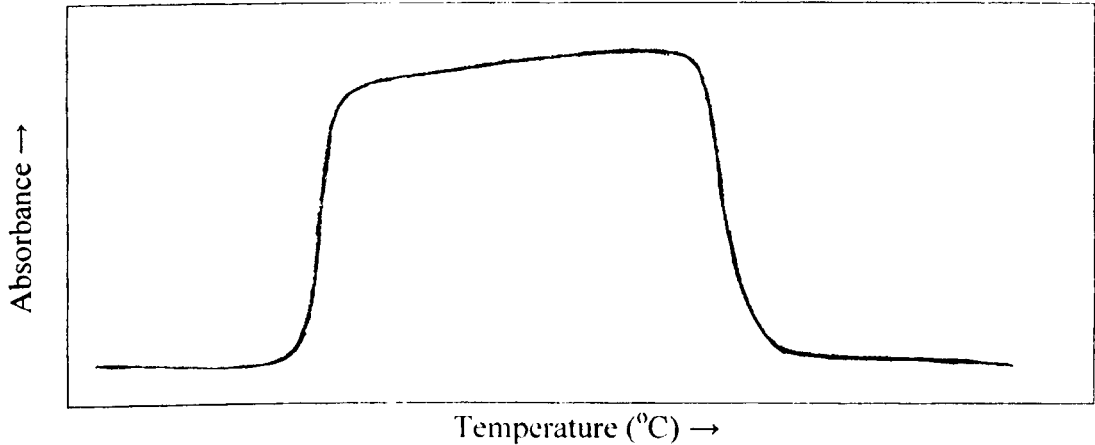
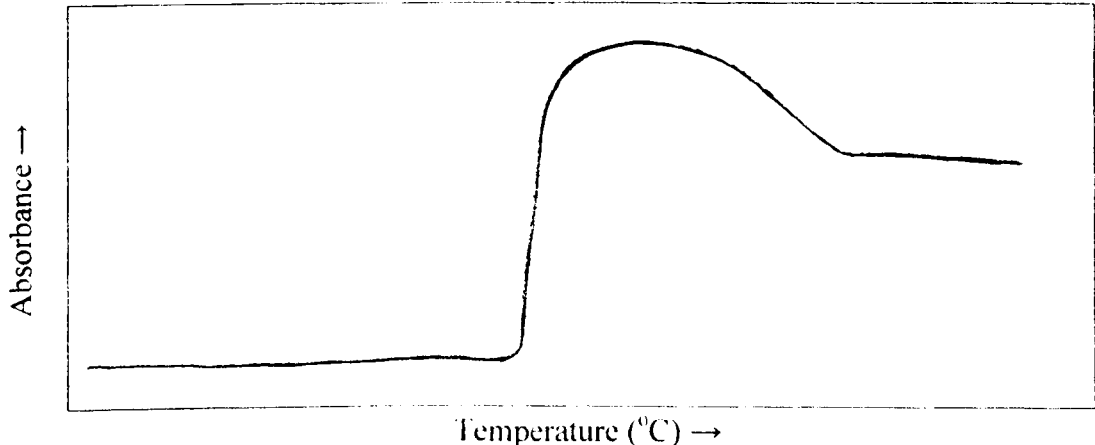


Figure 4.13c – Cloud Point Curve of Unfractionated 1.5:2 PLA-PEG Dispersion



the plateau region allowed the assignment of a solid phase separation temperature (T_s) for the surfactant. The unfractionated PLA-PEG materials showed similar behaviour to Poloxamer 407, albeit with lower associated cloud point temperatures (T_c). Retained background turbidity gave rise to a second stable plateau region, which is considered to be due to the PLA-depleted species within the material and therefore appeared to behave similarly to the PEG 8000 homopolymer (Figure 4.13c). The cloud point curves for the fractionated PLA-PEG micelle forming materials were again similar, but showed a larger drop in turbidity to the second plateau region relative to the unfractionated PLA-PEG copolymers. Reversibility was displayed for both fractionated and unfractionated PLA-PEG copolymers.

Table 4.10 shows that the cloud point temperatures (T_c) and the solid phase temperatures (T_s) for the fractionated PLA-PEG copolymers, the unfractionated 1.5:2 PLA-PEG copolymer, and Poloxamer 407, decreased with increasing salt concentration in line with the expected behaviour of PEG-containing copolymer solutions. Cloud point temperatures are lower than those measured for PEG 8000 by approximately 30 °C. It is interesting to note the very much reduced rate of decline of T_s compared with T_c with salt addition for the block copolymer. This could indicate that the thermodynamic factors which drive the separation of solid phase have a weaker temperature dependence than the "salting out" process of the hydrophilic PEG component which leads to the cloud point.

The lower cloud point temperatures (T_c) seen with the 1.5:2 and 2:5 PLA-PEG micelles, compared with Poloxamer 407, indicate reduced solvency of the stabilising PEG component associated with PLA-PEG relative to that in Poloxamer 407 (Table 4.10). This implies that the Poloxamer 407 micelles have greater "steric" stability than the 1.5:2 PLA-PEG micelles. This may be expected due to the higher proportion of the stabilising PEG moiety in the poloxamer 407, which has two PEG chains of M_w 4000, as opposed to the one PEG chain (M_w 2000 or 5000) on the PLA-PEG copolymers.

Table 4.11 shows the cloud point temperatures for the unfractionated 1.5:2 and 2:5 PLA-PEG copolymers compared with the material from both GPC peaks. There was little difference between the T_c 's of unfractionated and fractionated micelle forming species. Comparison of the 1.5:2 and 2:5 PLA-PEG fractionated micelle forming material

Table 4.10

Cloud Point Temperatures (T_c) for 1% w/v PLA-PEG Copolymers in the Presence of Na_2SO_4

Na ₂ SO ₄ Conc. (M)	1.5:2 PLA-PEG Unfractionated		1.5:2 PLA-PEG Fractionated		2:5 PLA-PEG Fractionated		Poloxamer 407		PEG 8000
	T _c (°C)	T _s (°C)	T _c (°C)	T _s (°C)	T _c (°C)	T _s (°C)	T _c (°C)	T _s (°C)	T _c (°C)
0.1	77.6	-	76.7	-	81.8	-	-	-	-
0.2	68.2	75.6	62.7	73.7	69.4	80.5	74.4	-	-
0.3	58.7	69.3	55.4	67.2	56.6	74.6	61.5	73.4	-
0.4	42.7	65.7	43.4	65.6	39.8	70.3	48.8	65.3	73.1
0.5	24.0	52.8	26.4	59.4	27.3	65.0	31.7	59.5	58.2

Table 4.11

Comparison of Cloud Point Temperatures for Fractionated and Unfractionated PLA-PEG

Sample	Elution Peak	Na ₂ SO ₄ Concentration (M)				
		0.1	0.2	0.3	0.4	0.5
1.5:2 PLA-PEG	-	77.6	68.2	58.7	42.7	24.0
1.5:2 PLA-PEG	1	76.7	62.7	55.4	43.4	26.4
1.5:2 PLA-PEG	2	83.3	71.2	61.6	49.3	44.5
2:5 PLA-PEG	-	83.2	70.5	56.2	45.3	21.4
2:5 PLA-PEG	1	81.8	69.4	56.6	39.8	27.3
2:5 PLA-PEG	2	87	74.9	60.9	48.6	36.4
Poloxamer 407	-	-	74.4	61.5	48.8	31.7
PEG 8000	-	-	-	-	73.1	58.2

revealed that the difference between these copolymers was not significant. However, the material from peak two (PLA-depleted) from GPC analysis shows significantly higher cloud points than the micelle-forming materials but not as high as the PEG 8000 control.

The values are intermediate between the two types of sample (micelle-forming and PEG 8000 solutions), as would be expected for a sample with an increased PEG content (Ganong and Delmore, 1991). Cloud point temperatures have been shown to be affected by the structure of the nonionic species (Hinze and Pramauro, 1993), with an increase in the number of EO groups increasing the cloud point, and to also be affected by the length of the hydrophobic chain (Rupert, 1992), with a decrease in hydrophobe chain increasing the cloud point for a homologous series of surfactants (Hinze and Pramauro, 1993).

Similar cloud point studies were performed with 4:2 and 6:2 PLA-PEG particles. The cloud point curve was similar to that seen previously with the 1.5:2 and 2:5 PLA-PEG copolymers and also Poloxamer 407. After clouding and flocculation had occurred, reversibility was not seen and the dispersions remained cloudy/flocculated. This could be due to the lack of solubility in water or due to the attractive forces between the particles being stronger than the attraction of the PEG chains for the dispersion media.

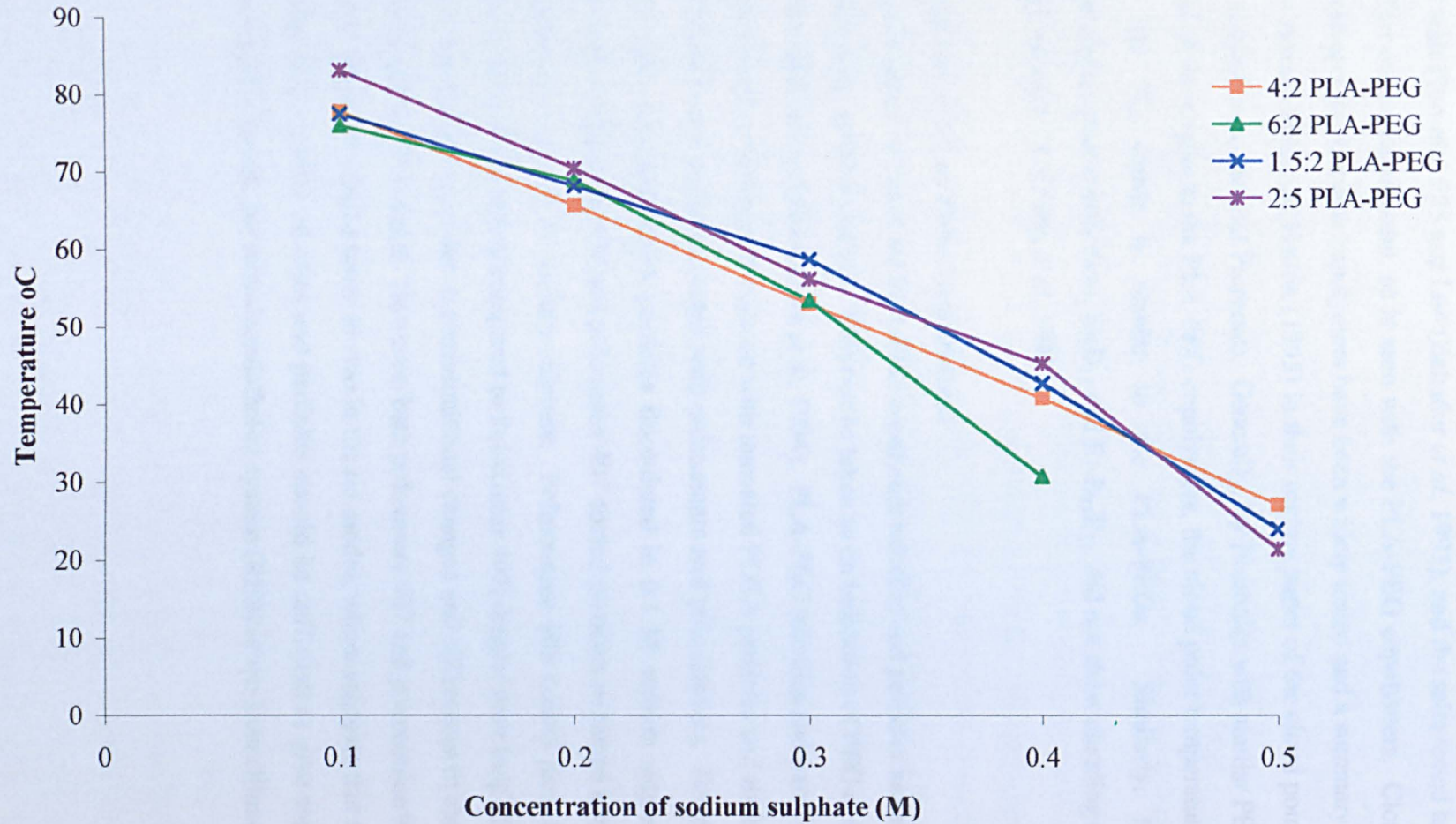
It could also indicate incomplete coverage of the PLA groups by the surface PEG (Napper, 1970a). The structure of the micelles/particles at the cloud point and beyond is not clear, and the concentration at which they change structure (if such a change occurs) is also not yet known.

Figure 4.14 shows the cloud point temperatures for the 4:2 and 6:2 PLA-PEG dispersions against 1.5:2 and 2:5 PLA-PEG for comparison. This shows that the cloud point temperatures for the 4:2 and 6:2 PLA-PEG particles are very similar to 1.5:2 PLA-PEG at the lower sodium sulphate concentrations. This may be expected as the molecular weight of the PEG chain is 2000 for all three copolymers, so the steric stability is expected to be similar. At 0.4 M sodium sulphate, the 6:2 PLA-PEG shows a greater decrease in stability in the presence of salt compared with the 4:2 and 1.5:2 PLA-PEG.

This could indicate that the 6:2 PLA-PEG particles are less sterically stable than the 4:2, 1.5:2 and 2:5 PLA-PEG particles and micelles.

Considering the change in the cloud points of the PLA-PEG micelles/particles with

Figure 4.14 - Comparison of cloud point temperatures for 1.5:2 and 2:5 PLA-PEG dispersions with 4:2 and 6:2 PLA-PEG dispersions



increasing sodium sulphate concentration, Figure 4.14 shows that the decrease in cloud point appears to be approximately linear for each copolymer. A linear change has also been noted with Pluronic P85 and L64 (Bahadur *et al*, 1993), and the salts tested had a strong effect on the cloud point, as is seen with the PLA-PEG copolymers. Cloud point temperatures for Pluronic copolymers have been widely tested and a summary is provided by Alexandridis and Hatton (1995) in their review paper of the cloud points of 1% w/v dispersions of several Pluronics. Generally, for Pluronics with similar PEG contents and chain lengths to the PLA-PEG copolymers, the cloud point temperatures are over 100 °C, which is similar to the PLA-PEGs. Similarly, the oxyethylene/oxybutylene copolymers, E₃₈B₁₂ and E₂₁B₁₁E₂₁, did not show clouding up to a testing limit of 95 °C (Yang *et al*, 1995).

4.4.4 Implications of Cloud Point Temperatures

The cloud point temperatures of the PLA-PEG copolymer micelles and particles indicate steric stability in the presence of salt. This can be taken as an indication of PEG at the surface of the micelles/particles (Maste *et al*, 1994). PLA-PEG micelles and particles show increased steric stability as compared with uncoated PLGA particles and similar steric stability to PLGA particles coated with poloxamers and poloxamines. Scholes (1994) noted that uncoated PLGA particles flocculated in 0.1 M sodium sulphate solution, at room temperature, whereas poloxamer 407 coated particles remained stable to salt addition of up to 0.5 M sodium sulphate. Poloxamine 908 coated particles showed reduced stabilising ability compared to Poloxamer 407, despite their long PEG length. This was thought to be due to conformational changes and differences in chain packing density of the PEO chains. However, both poloxamer 407 and poloxamine 908 give extended blood circulation times *in vivo* in the rat model, which suggests that the steric stability of PLA-PEG micelles and particles should be sufficient to give some degree of protection against the reticuloendothelial system (RES) of the liver (Illum *et al*, 1987).

4.5 SUMMARY

This chapter has discussed four different methods of studying the surface of the PLA-PEG copolymers. Surface analysis studies of SIMS and XPS have indicated that PEG is indeed present on the surface of these structures and that the density of the PEG is equivalent to that previously achieved with systems that have shown promising *in vivo* studies. Cloud point temperatures have further confirmed the presence of PEG at the micelle/particle surface by the illustration of steric stability on addition of sodium sulphate to all systems.

Rheological measurements allowed the PEG layer thickness to be calculated for the PLA-PEG systems. Differences in the resulting values were seen, with the micelle-forming 1.5:2 and 2:5 PLA-PEG copolymers having longer PEG layer thicknesses than the particle-forming 4:2 and 6:2 PLA-PEG copolymers. This may prove an important factor in the *in vivo* behaviour of these copolymers.

CHAPTER FIVE

DRUG LOADING POTENTIAL OF PLA-PEG MICELLES AND PARTICLES

5.1 INTRODUCTION

So far, the physicochemical properties of the PLA-PEG systems have been considered with respect to their suitability as drug delivery systems, and their possible use in drug targeting by avoidance of the reticuloendothelial system (RES) *in vivo*. The ability of the PLA-PEG systems to incorporate drug molecules must now be considered, so that the drug loading and hence drug delivery potential of the micelles and particles can be assessed. Comparing quantitatively the incorporation of two model drugs of different hydrophobicity between the PLA-PEG systems will do this. An *in vitro* release study in phosphate buffered saline (PBS) under physiological conditions of pH 7.4 and 37 °C is then described for one of these systems.

5.2 “MODEL” DRUGS

5.2.1 Sudan Black B

Sudan Black B (SBB) (Mw 456.6) is the most popular of the Sudan azo dyes. It has been used for many years as a universal lipid stain in histology and pathology, where it stains both apolar (neutral) lipids and polar (phospho-) lipids (Tas *et al*, 1980). The structure of SBB is shown in Figure 5.1a and consists of five aromatic rings and two secondary amine groups that give it basic properties (Pfüller *et al*, 1977; Horobin, 1981).

Sudan black B has previously been used in ultracentrifugation studies on micellar systems due to its ease of incorporation and useful absorbance spectrum. It has also been used as a model drug with PLA and PLGA implants (Katayama *et al*, 1995). The water solubility of SBB is very low due to its high lipophilicity and SBB would therefore be expected to incorporate in the core of a PLA-PEG micelle or particle, with little present in the aqueous solution. A log P value of 7.6 has been calculated for SBB (Saunders, 1993), using the CLogP computer program (version 3.54), and is similar to

another calculated value of 3.2 found in the literature (Juarroz *et al.*, 1986). Determining values of log P above 7.0 experimentally is not feasible (Craig, 1990).

3.2.2 Testosterone

Testosterone is a steroid hormone that is responsible for the development and maintenance of the male sex characteristics and secondary sex characteristics. It has a steroid structure, which is shown in Figure 5.1b. Testosterone is a hydrophobic steroid drug to give an example of a pharmaceutically relevant compound of lower hydrophobicity than SBB. Other groups (Thakkar and Hull, 1967; Malcolmson and Lestrade, 1997) have also previously incorporated testosterone into micelles and particles.

Figure 5.1a – Structure of Sudan Black B

Similarly to Sudan Black B, the hydrophobicity of testosterone was assessed by determination of its octanol/water partition coefficient (log P). The calculated value of 3.35 compared well with the experimentally determined value of 3.32 (Craig, 1990).

5.3 DRUG LOADING OF TESTOSTERONE AND SUDAN BLACK B INTO PLA-PBG MICELLES AND PARTICLES

5.3.1 Method of Drug Incorporation

Testosterone (10 mg/ml) and Sudan Black B (SBB) (20 mg/ml) in acetone were added to preformed dispersions of the 1:5:2 and 2:5 PLA-PBG micelles (1% w/v for testosterone, 0.25% w/v for SBB), and 4:2 and 6:2 PLA-PBG particles (0.25% w/v for both drugs). The higher copolymer concentration used with the PLA-PBG micelles was part of earlier studies, where a higher PLA-PBG concentration was used to ensure adequate solubility of the incorporated testosterone on UV analysis. As the results are reported as weight of drug over weight of polymer, the studies were not repeated at the lower concentration. The acetone was allowed to evaporate during incubation overnight at 35 °C. The copolymer/drug dispersions were then centrifuged using a Centaur 2 (840g, Sorvall, U.K.) centrifuge (340 minutes), followed by a Micro Centaur (950g, Sorvall, U.K.) centrifuge (31,600 g, five minutes). After removal of the supernatant, the precipitate of drug that had not been incorporated into the

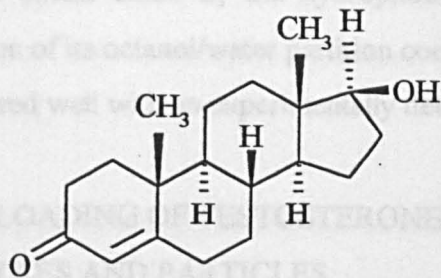
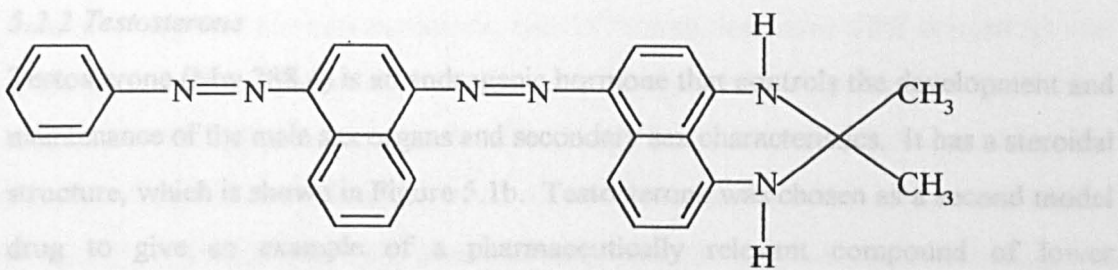


Figure 5.1b – Structure of Testosterone

another calculated value of 7.2 found in the literature (Juarranz *et al*, 1986). Determining values of log P above 7.0 experimentally is not feasible (Craig, 1990).

5.2.2 Testosterone

Testosterone (Mw 288.4) is an androgenic hormone that controls the development and maintenance of the male sex organs and secondary sex characteristics. It has a steroidal structure, which is shown in Figure 5.1b. Testosterone was chosen as a second model drug to give an example of a pharmaceutically relevant compound of lower hydrophobicity than SBB. Other groups (Thakkar and Hall, 1967; Malcolmson and Lawrence, 1993) have also previously incorporated testosterone into micelles and particles.

Similarly to sudan black B, the hydrophobicity of testosterone was assessed by determination of its octanol/water partition coefficient (log P). The calculated value of 3.35 compared well with an experimentally determined value of 3.32 (Craig, 1990).

5.3 DRUG LOADING OF TESTOSTERONE AND SUDAN BLACK B INTO PLA-PEG MICELLES AND PARTICLES

5.3.1 Method of Drug Incorporation

Solutions of testosterone (1 mg/ml) and sudan black B (SBB) (20 mg/ml) in acetone were added to fractionated dispersions of the 1.5:2 and 2:5 PLA-PEG micelles (1% w/v for testosterone, 0.25% w/v for SBB), and 4:2 and 6:2 PLA-PEG particles (0.25% w/v for both drugs). The higher copolymer concentration used with the PLA-PEG micelles was part of earlier studies, where a higher PLA-PEG concentration was used to ensure adequate absorbance of the incorporated testosterone on UV analysis. As the results are expressed as weight of drug over weight of polymer, the studies were not repeated at the lower concentration. The acetone was allowed to evaporate during incubation overnight at 25 °C. The copolymer/drug dispersions were then centrifuged using a Centaur 2 (MSE, Sussex, U.K.) centrifuge (840 g, ten minutes), followed by a Micro Centaur (MSE, Sussex, U.K.) centrifuge (11,600 g, five minutes). After removal of the supernatant, the precipitate of drug that had neither incorporated into the

micelles/particles nor dissolved in the supernatant was dissolved in ethanol (SBB) or purified water (testosterone). The absorbance of each solution was measured by UV spectroscopy (Uvikon, Kontron Instruments, Tegimenta, Switzerland) at 257 nm to determine testosterone concentrations, and 587 nm to determine SBB concentrations.

Testosterone concentration was determined at a longer wavelength than the λ_{max} ($\lambda=240$ nm), as the PLA-PEG dispersions also absorb significantly at this wavelength. Similarly, the second maximum for SBB in ethanol was evaluated and used for measurements, due to PLA-PEG absorbance at the first maximum ($\lambda \sim 230$ nm). Aqueous solubility was determined similarly by adding a solution of drug in acetone (1 ml) to water and then centrifuging off the excess. The absorbance of the supernatant was then measured. This sample also acted as a control. Extinction coefficients for testosterone and SBB were calculated from the absorbance of aqueous dilutions of ethanolic stock drug solutions.

The amount of drug incorporated was then calculated by subtraction, as described below in section 5.3.3.

5.3.2 Verification of Drug Loading by Sedimentation Velocity Experiments

5.3.2.1 Method

This experiment was performed as described in section 2.8.1, but with testosterone and sudan black B (SBB) incorporated into dispersions of fractionated PLA-PEG material. For 1.5:2 and 2:5 PLA-PEG solutions, PLA-PEG/testosterone-loaded dispersions were prepared by adding a solution of testosterone in acetone (1 ml, 0.5 mg/ml) dropwise to an aqueous solution of fractionated PLA-PEG (5ml, 0.2% w/v). The dispersions were stirred overnight to remove the solvent by evaporation. Sudan black B (10 mg) was incorporated by addition of the SBB directly to an aqueous solution of fractionated PLA-PEG (5 ml, 0.2% w/v) and sonicating for ten minutes at room temperature. The different loading methods used to incorporate SBB and testosterone in this experiment reflect earlier work on drug loading performed before the work described in this thesis. The resulting suspensions were then filtered through a 0.2 μm filter to remove excess testosterone/sudan black B. Earlier control experiments showed that the entire free drug, apart from that dissolved in solution, was removed by the filtration process (data not shown). The runs were performed at 20°C, with the PLA-PEG/testosterone system run

at 40,000 revs/minute and the PLA-PEG/SBB system at 30,000 revs/minute. Both these dispersions were scanned at two wavelengths, the first to detect the micelles plus model drug, and the second, where the micelles are transparent, to evaluate whether sedimentation boundaries were still produced. For the testosterone systems, 1.5:2 PLA-PEG was scanned at 232 nm (λ_1) and 258 nm (λ_2), and 2:5 PLA-PEG was scanned at 226 nm (λ_1) and 258 nm (λ_2). For the SBB system, 1.5:2 PLA-PEG was scanned at 231 nm (λ_1) and 510 nm (λ_2) and 2:5 PLA-PEG at 225 nm (λ_1) and 510 nm (λ_2). Sedimentation coefficients (s_{20}) were then determined for all the samples (Harding, 1984), where s_{20} represents the sedimentation coefficient at 20 °C.

Similarly, the experiment was performed for 4:2 and 6:2 PLA-PEG particles with testosterone (1ml, 1 mg/ml) and sudan black B (SBB) (1 ml, 10 mg/ml) incorporated into 0.25% w/v dispersions. In this experiment, the drugs were incorporated as described above in section 5.3.1. Dilution of the PLA-PEG/SBB samples by a factor of fifty (to an approximate concentration of 0.005% w/v) was needed to give suitable absorbance values of the sedimenting boundaries. The runs were then performed at 20°C and 20,000 revs/minute. Again, these dispersions were scanned at two wavelengths. For testosterone, the dispersions were scanned at 226 nm (λ_1) and 258 nm (λ_2), and for sudan black B, at 226 nm (λ_1) and 599 nm (λ_2). Sedimentation coefficients (s_{20}) were then determined for all the samples.

5.3.2.2 Calculation and Implications of Sedimentation Coefficients

The sedimentation coefficients (s_{20}) (in Svedbergs (S), where 1S=1x10⁻¹³ seconds) calculated for the fractionated PLA-PEG copolymers alone are listed in Table 5.1, along with the micelle/particle molecular weights estimated from the sedimentation equilibrium experiments, as described in section 3.7. The sedimentation coefficient values show an increase with increased micelle/particle molecular weight.

Sedimentation coefficients, s , are related to molecular weight by the following equation:-

$$s = \frac{M(1 - \bar{v}\rho)}{N_A f}$$

where M is the molecular weight,
 v is the partial specific volume (m^3g^{-1}),
 ρ is the density of the solvent (kg m^{-3}),
 N_A is Avogadro's number, and
 f is the frictional coefficient (kg s^{-1}).

This implies that s is linear with molecular weight. However, since f is related to the effective hydrodynamic radius of the micelle/particle, which in turn depends on the cubic root of the micelle/particle volume, then if all other parameters are constant, it is more true to say that s varies with $M^{2/3}$ for micelles or particles of similar shape, solvation and partial volume (Rowe, 1992).

This relationship between a molecular weight and sedimentation coefficient depends, however, on the sedimentation coefficient being corrected for pressure effects and being extrapolated to zero concentration (Suzuki, 1992). These corrections have not been performed for the PLA-PEG copolymer systems. This method of calculating molecular weight assumes that each species sediments independent of the others, an assumption that is not supported by experimental data (Suzuki, 1992). Therefore, absolute values of the molecular weight cannot be obtained from the sedimentation coefficient. Hence, although the sedimentation coefficients will follow this relationship in an approximate manner, deviations are expected to occur, but the plot of sedimentation coefficient against $M^{2/3}$ is approximately linear.

The sedimentation coefficients (s_{20}) (in Svedbergs (S), where $1\text{S}=1\times 10^{-13}$ seconds) calculated for the fractionated 1.5:2 and 2:5 PLA-PEG copolymers alone and in the presence of the two model drugs, testosterone and SBB, are listed in Table 5.2. Figure 5.2a illustrates an example of the single sedimenting boundary observed for 2:5 PLA-PEG material alone, indicating homogeneity. Both PLA-PEG dispersions with testosterone also showed single boundaries at the wavelength scanned for PLA-PEG (λ_1), but a significant amount of material was found to be absorbing but not sedimenting with these systems. This is most likely due to free testosterone dissolved in the aqueous solution, or testosterone bound to free non-associated copolymer, which had too low a molecular weight to sediment under the experimental conditions. At the testosterone specific wavelength, sedimenting boundaries were not observed, suggesting that the

Figure 5.2a - Sedimentation Velocity Profiles for 2:5 PLA-PEG Micelles at an Absorbance of 225 nm

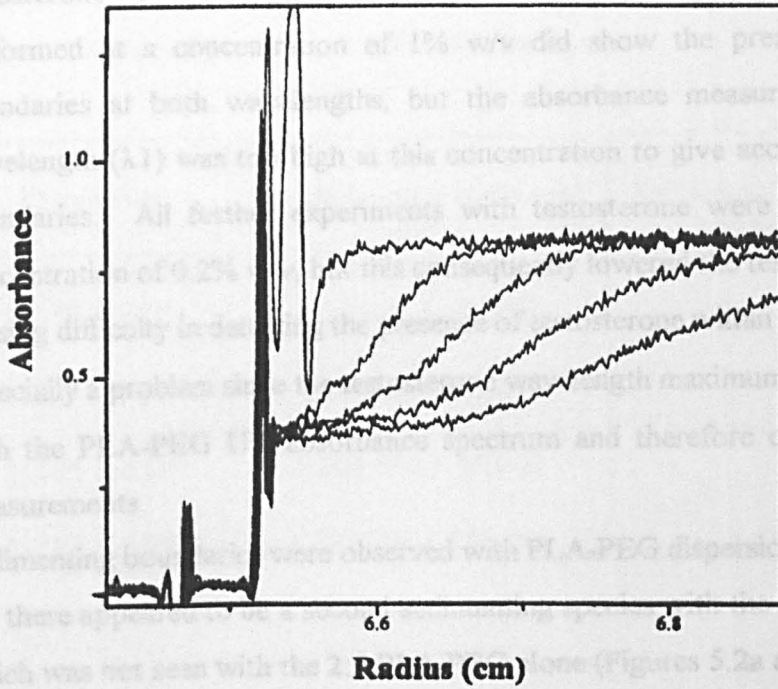
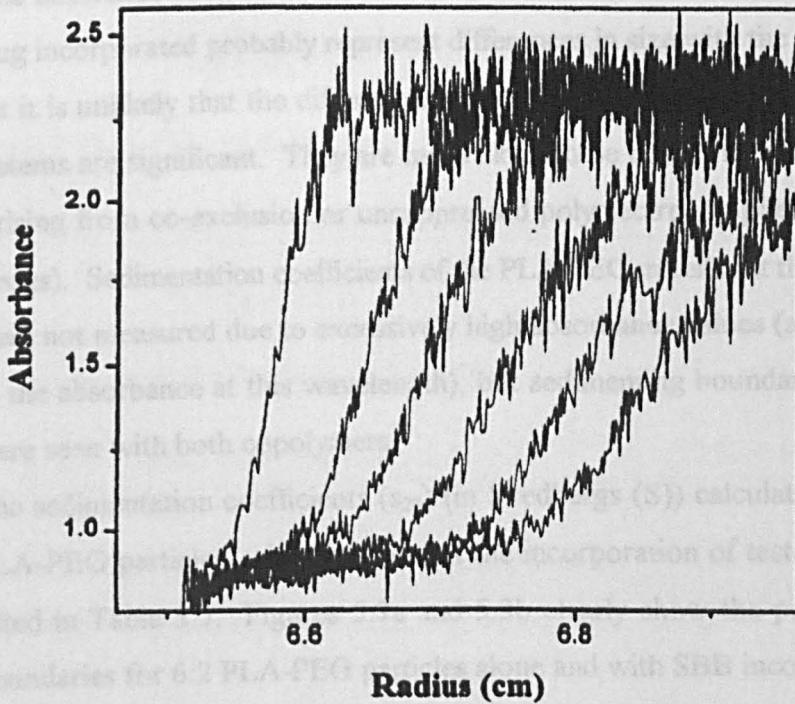


Figure 5.2b – Sedimentation Velocity Profiles for 2:5 PLA-PEG Particles with Sudan Black B Incorporated at an Absorbance of 599 nm



testosterone was not incorporated into the micellar core. However, earlier experiments performed at a concentration of 1% w/v did show the presence of sedimenting boundaries at both wavelengths, but the absorbance measured at the PLA-PEG wavelength (λ_1) was too high at this concentration to give acceptable sedimentation boundaries. All further experiments with testosterone were thus conducted at a concentration of 0.2% w/v, but this consequently lowered the testosterone absorbance, causing difficulty in detecting the presence of testosterone within the micelles. This was especially a problem since the testosterone wavelength maximum ($\lambda=240$ nm) overlaps with the PLA-PEG UV absorbance spectrum and therefore could not be used for measurements.

Sedimenting boundaries were observed with PLA-PEG dispersions incorporating SBB, but there appeared to be a second sedimenting species with the 2:5 PLA-PEG system, which was not seen with the 2:5 PLA-PEG alone (Figures 5.2a and b). This behaviour pattern may suggest polydispersity of the micelles. Assuming the conformations of the PLA-PEG/SBB and PLA-PEG systems are the same (spherical micelles), it can be speculated that the differences in sedimentation coefficient (Table 5.2) reflect differences in molecular weight, M (for spherical particles s_{20} is approximately proportional to $M^{2/3}$).

The difference between the sedimentation coefficients of the polymer alone and with drug incorporated probably represent differences in size with the 2:5 PLA-PEG system, but it is unlikely that the differences between these s_{20} values for the 1.5:2 PLA-PEG systems are significant. They are more likely to be due to thermodynamic non-ideality (arising from co-exclusion or unsuppressed polyelectrolyte phenomena from the PLA blocks). Sedimentation coefficients of the PLA-PEG micelles at the first wavelength (λ_1) were not measured due to excessively high absorbance values (as the SBB contributed to the absorbance at this wavelength), but sedimenting boundaries indicating micelles were seen with both copolymers.

The sedimentation coefficients (s_{20}) (in Svedbergs (S)) calculated for the fractionated PLA-PEG particles, with and without the incorporation of testosterone and SBB, are listed in Table 5.3. Figures 5.3a and 5.3b clearly show the presence of sedimenting boundaries for 6:2 PLA-PEG particles alone and with SBB incorporated and measured at λ_2 (599 nm). Similar results were seen with 4:2 PLA-PEG, and the SBB has plainly

Table 5.1

Sedimentation Coefficients of PLA-PEG Copolymers

Copolymer	Micelle/particle molecular weight	Sedimentation Coefficient, s_{20} (S) (Mean \pm s.e., n = 3)
2:5 PLA-PEG	330,000 \pm 30,000	7.99 \pm 0.38
1.5:2 PLA-PEG	520,000 \pm 20,000	8.51 \pm 0.14
4:2 PLA-PEG	1,000,000 \pm 50,000	16.0 \pm 0.27
6:2 PLA-PEG	1,500,000 \pm 100,000	34.4 \pm 0.99

Table 5.2

Sedimentation Velocity Analysis of Fractionated PLA-PEG Micelles

Copolymer Sample	Sedimentation Coefficient (S), s_{20} (Mean \pm s.e., n = 3)
1.5:2 PLA-PEG	8.51 \pm 0.14
1.5:2 PLA-PEG with Testosterone (λ_1)	9.57 \pm 0.11
1.5:2 PLA-PEG with Sudan Black B (λ_2)	9.76 \pm 0.20
2:5 PLA-PEG	7.99 \pm 0.38
2:5 PLA-PEG with Testosterone (λ_1)	7.36 \pm 0.10
2:5 PLA-PEG with Sudan Black B (λ_2)	10.88 \pm 0.18; 6.55 \pm 0.14

λ_1 –wavelength for detecting PLA-PEG and drug.

λ_2 – wavelength specific for detecting incorporated drug.

Figure 5.3a - Sedimentation Velocity Profiles of 6:2 PLA-PEG Particles at an Absorbance of 227 nm

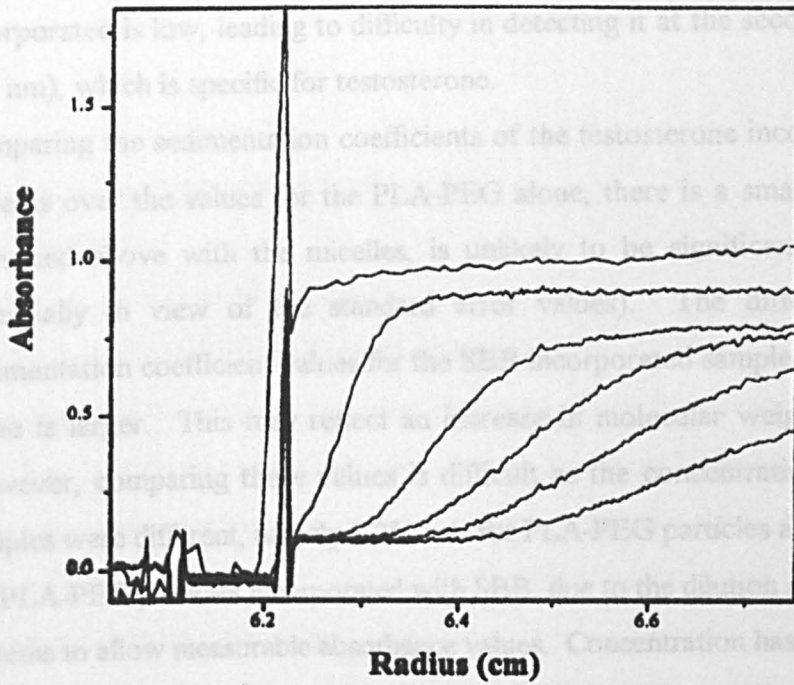
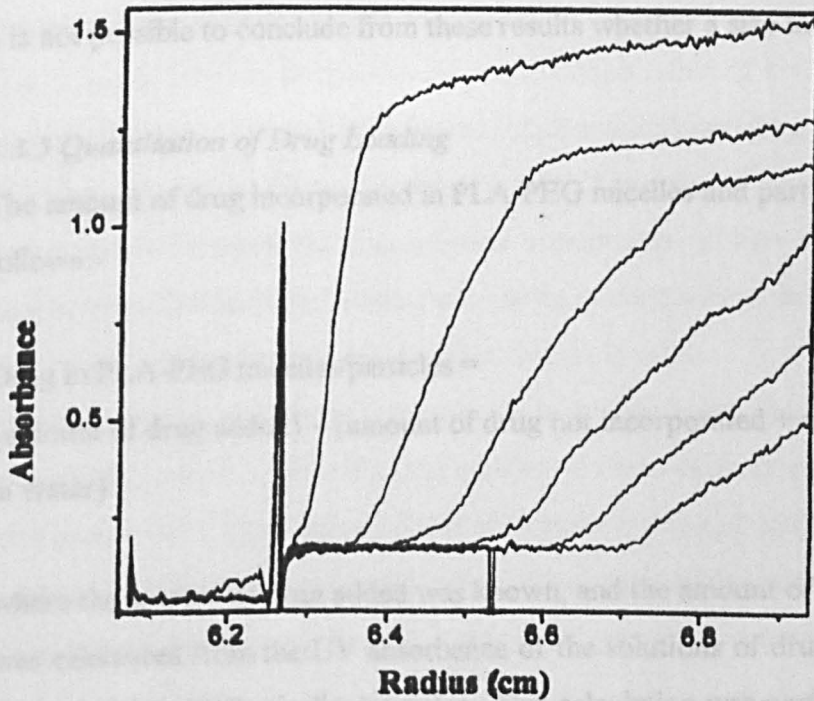


Figure 5.3b - Sedimentation Velocity Profiles for 6:2 PLA-PEG Particles with Sudan Black B Incorporated at an Absorbance of 599 nm



been incorporated into the particles and is sedimenting with them. As seen with the micelle-forming copolymers, these studies show that the absorbance of the testosterone incorporated is low, leading to difficulty in detecting it at the second wavelength ($\lambda = 257$ nm), which is specific for testosterone.

Comparing the sedimentation coefficients of the testosterone incorporated PLA-PEG systems over the values for the PLA-PEG alone, there is a small difference that, as discussed above with the micelles, is unlikely to be significant for this technique (especially in view of the standard error values). The difference between the sedimentation coefficient values for the SBB incorporated samples over the PLA-PEG alone is larger. This may reflect an increase in molecular weight of the particles. However, comparing these values is difficult as the concentrations of the measured samples were different, namely 0.2% w/v for PLA-PEG particles alone and 0.005% w/v for PLA-PEG particles incorporated with SBB, due to the dilution necessary for the SBB systems to allow measurable absorbance values. Concentration has been shown to affect sedimentation coefficients, with increased polymer concentration leading to a decrease in sedimentation coefficient (Lavrenko *et al*, 1992). The sedimentation coefficient values measured for the more concentrated PLA-PEG dispersions are lower than the corresponding values for the more dilute dispersions with SBB incorporated. Therefore, it is not possible to conclude from these results whether a size increase has occurred.

5.3.3 Quantitation of Drug Loading

The amount of drug incorporated in PLA-PEG micelles and particles was calculated as follows:-

Drug in PLA-PEG micelles/particles =

{amount of drug added} - {amount of drug not incorporated + amount of drug soluble in water}

where the amount of drug added was known, and the amount of drug not incorporated was calculated from the UV absorbance of the solutions of drug precipitate excluded from the PLA-PEG micelles/particles. This calculation was performed using the Beer-

Lambert equation: -

$$c = \frac{A}{l\varepsilon}$$

where c is the concentration (mol cm^{-3}),

A is absorbance,

l is the length of the cell (cm), and

ε is the molar extinction coefficient of the drug ($\text{cm}^2 \text{mol}^{-1}$).

Aqueous solubilities for testosterone and sudan black B were also calculated from the Beer-Lambert equation, and were found to be 23 mg cm^{-3} and 1.2 mg cm^{-3} respectively. From the concentration and aqueous solubility of each drug, the mass of drug not incorporated was calculated, allowing the %w/w drug loading of the PLA-PEG micelles and particles to be determined.

Table 5.4 shows the results of the drug loading into the PLA-PEG micelles and particles. Values are also given for the percentage of added drug incorporated, which is also known as the incorporation “efficiency”, and is a measure of how effectively the system takes up the available drug. It is dependent on both the concentration of the copolymer and the amount of drug added to the dispersion. Comparison of this value can therefore only be made between samples at the same concentration of both copolymer and drug. So, the efficiency of PLA-PEG micelles (1.5:2 and 2:5) in taking up testosterone cannot be compared with the efficiency of the PLA-PEG particles (4:2 and 6:2), but comparison can be made between the two micellar copolymers or between the two particular copolymers. Similarly, no comparison can be made between the testosterone and SBB results, but comparing between the SBB values is valid.

Another measure of the effectiveness of incorporating drug is the molar incorporation ratio (MIR), which is defined as the number of moles of drug incorporated per mole of copolymer, for a given drug. From this molar ratio and the association number of copolymer molecules in a micelle/particle, the number of drug molecules associated with the micelle or particle can be calculated, and these values are also given in Table 5.4.

Table 5.3

Sedimentation Velocity Analysis of Fractionated PLA-PEG Particles

Copolymer Sample	Copolymer Concentration (% w/v)	Sedimentation Coefficient, s_{20} (S) (Mean \pm s.e.)
4:2 PLA-PEG	0.2	16.0 \pm 0.27
4:2 PLA-PEG + Testosterone λ_1	0.2	18.1 \pm 0.01
4:2 PLA-PEG + SBB λ_1	0.005	28.8 \pm 0.50
4:2 PLA-PEG + SBB λ_2	0.005	31.2 \pm 0.38
6:2 PLA-PEG	0.2	34.4 \pm 0.99
6:2 PLA-PEG + Testosterone λ_1	0.2	30.0 \pm 0.82
6:2 PLA-PEG + SBB λ_1	0.005	45.6 \pm 1.04
6:2 PLA-PEG + SBB λ_2	0.005	45.4 \pm 1.31

λ_1 – wavelength for detecting PLA-PEG and drug.

λ_2 – wavelength specific for detecting incorporated drug.

5.3.4 Discussion

The results in Table 5.4 show that higher drug loading was observed for the particle-forming 4:2 and 6:2 PLA-PEG copolymers compared with the micelle-forming 1.5:2 and 2:5 PLA-PEG. Clearly, the sudan black B (SBB) incorporated was significantly higher than testosterone for all copolymers. For both drugs, a general trend between the percentage of drug incorporated by weight (%w/w) and the molecular weight of the micelle or particle is seen (as determined from sedimentation equilibrium experiments in section 3.7.2.). This trend shows an increase in drug loading with an increase in micelle/particle molecular weight, particularly the PLA molecular weight. A decrease in %w/w drug loading is seen with the increased PEG content, when 2:5 PLA-PEG is compared with the other PLA-PEG copolymers (1.5:2, 4:2 and 6:2 PLA-PEG).

Previously with Pluronic micelles, increased drug loading of hydrophobic drugs has been observed with increased hydrophobicity of copolymer (i.e. an increase in PPO) (Hurter and Hatton, 1992; Kabanov *et al*, 1995). Increase in polyoxyethylene chain length has previously shown a decrease in % w/w drug loading, for micelle-forming polyoxyethylene stearates (Goodhart and Martin, 1962) and for polyoxyethylene cetyl ethers and monostearates (Saitō and Satō, 1985). Thus it can be observed, particularly with testosterone, that the drug loading increases as follows: -

$$2:5 \text{ PLA-PEG} < 1.5:2 \text{ PLA-PEG} < 4:2 \text{ PLA-PEG} < 6:2 \text{ PLA-PEG}$$

The differences in the drug loadings of SBB between the copolymers are not as pronounced as the differences seen with the testosterone.

From the fourth column of Table 5.4, which lists the molar incorporation ratio (MIR), it may seem curious that with SBB, the value of MIR for 2:5 PLA-PEG is greater than that for 1.5:2 PLA-PEG. This reversal has also been noted by other authors (Goodhart and Martin, 1962; Gouda *et al*, 1970; Saitō and Satō, 1985; Goldenberg *et al*, 1993).

The MIR for 2:5 PLA-PEG implies that the solubilising efficiency of this copolymer is greater than that for 1.5:2 PLA-PEG and comparable with 4:2 PLA-PEG, despite the greater hydrophilicity of 2:5 PLA-PEG. This contradiction with the %w/w drug loading values has been attributed to the decrease in micelle molecular weight that occurs when

Table 5.4

Drug Incorporation Studies of Testosterone and Sudan Black B into Fractionated PLA-PEG Micelles and Particles

Copolymer	%w/w Drug incorporated	% Added drug incorporated	MIR*	Number of drug molecules per micelle/particle
1.5:2 PLA-PEG + Testosterone	0.74 ± 0.01	73.9 ± 0.7	0.10 ± 0.0	13 ± 0
4:2 PLA-PEG + Testosterone	0.93 ± 0.09	23.7 ± 1.9	0.21 ± 0.0	33 ± 3
6:2 PLA-PEG + Testosterone	1.96 ± 0.31	49.1 ± 7.1	0.48 ± 0.1	102 ± 16
2:5 PLA-PEG + Testosterone	0.34 ± 0.02	34.2 ± 2.3	0.08 ± 0.0	4 ± 1
1.5:2 PLA-PEG + SBB	63.9 ± 0.1	79.8 ± 0.0	5.5 ± 0.0	729 ± 0
4:2 PLA-PEG + SBB	68.9 ± 0.1	86.1 ± 0.1	9.7 ± 0.0	1505 ± 2
6:2 PLA-PEG + SBB	70.9 ± 0.6	88.6 ± 0.7	10.9 ± 0.1	2332 ± 19
2:5 PLA-PEG + SBB	59.0 ± 0.9	73.7 ± 1.1	9.0 ± 0.1	424 ± 6

* - MIR is the molar incorporation ratio, i.e. the number of moles of drug incorporated per mole of copolymer.

the PEG chain length is increased. This causes a decrease in the amount of drug per micelle, but is compensated for by an increase in the number of micelles present (Barry and El Eini, 1976). The higher amount of SBB incorporated in 1.5:2 PLA-PEG micelles over 2:5 PLA-PEG micelles is clearly illustrated in the last column of Table 5.4, which shows the number of drug molecules associated with each micelle or particle. The difference in MIR for testosterone between the two copolymers is much less pronounced and ANOVA statistical analysis performed at the 5% confidence level shows that the difference is not significant.

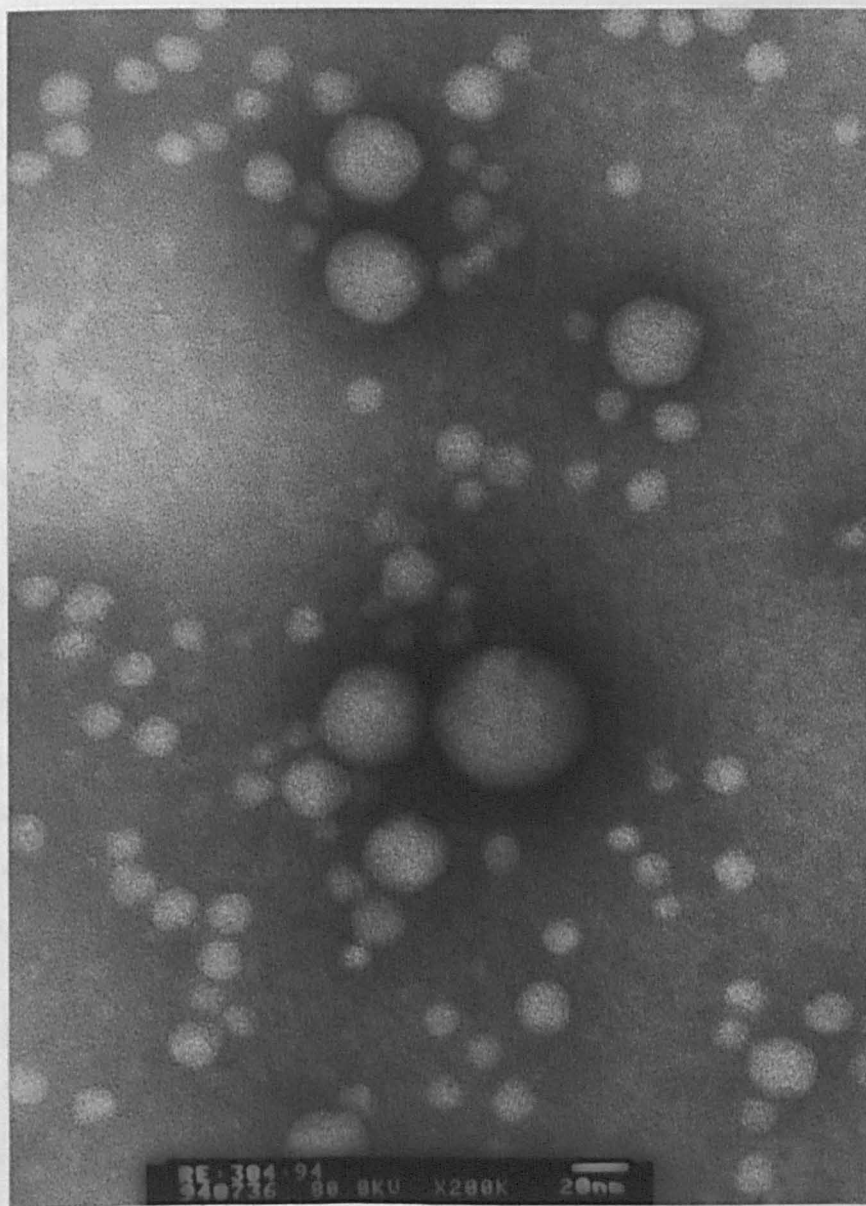
Drug uptake into the particle-forming 4:2 and 6:2 PLA-PEG is greater than that with the micelle-forming 1.5:2 and 2:5 PLA-PEG copolymers for both drug compounds. As well as the increased hydrophobicity of these copolymers (i.e. more PLA), this may be partly due to the greater stability of the 4:2 and 6:2 PLA-PEG particles over the micelles formed with 1.5:2 and 2:5 PLA-PEG. It should be remembered that the number of drug molecules per micelle is an average value for the micellar solution. The micelle can act as a dynamic entity, with a fluctuating size, and drug molecules can therefore pass back and forth between the micelle and the aqueous solution (Jacobs *et al*, 1972). This may make micelles potentially less able to retain drug than the more stable particles.

The effect of incorporating drug on the properties of PLA-PEG micelles and particles must be considered. Mukerjee (1980) observed that the presence of a solubilise inside a micelle can affect the monomer-micelle equilibria, the stability and the size of the micelle to various degrees. A solubilised substance will generally increase the size of micelles, not only by its incorporation but also by causing an increase in association number of copolymer molecules in the micelle. An increased micelle size was noted with poloxamers, when hexane was solubilised (Al-Saden *et al*, 1982) and was concluded to be due to an increased association number. Size increases have been observed with other micelles when substances have been incorporated into their cores (Oranli *et al*, 1985; Goldenberg *et al*, 1993; Quintana *et al*, 1995). It may be expected that the incorporation of testosterone and SBB would increase the micelle/particle size. DLS studies on PLA-PEG micelles and particles with testosterone incorporated showed no significant increase in particle size over PLA-PEG alone, and these results were confirmed by TEM studies. DLS studies were not possible on micelles and particles incorporated with SBB, but

Figure 5.4 shows a typical TEM picture for PLA-PEG particles after incorporation with SBB. This picture clearly shows the presence of some structures that are larger than the majority of particles present. It is unclear as to whether these structures are particles, aggregated SBB or artefacts of the TEM process. Mukerjee (1980) refers to the presence of swollen spheroidal micelles in a system where aromatic solubilisates are used at high concentrations of surfactant. However, before these spheroidal structures were seen, the system became highly viscous, then less viscous when the swollen micelles predominated. Therefore, this is unlikely to be the reason for these large structures as the concentration of the PLA-PEG micelles and particles is fairly low and no change in viscosity is observed. However, Bjerrum *et al* (1980) incorporated SBB into Triton X-100 micelles, and when this system was analysed by GPC, two populations of micelles were seen to be associated with SBB. The first population had a higher molecular weight than the micelles alone, and the second population were of similar molecular weight to the micelles without SBB. In section 5.3.2.2, the sedimentation velocity results showed the presence of two species for 2:5 PLA-PEG micelles. This could confirm that there is heterogeneity of the PLA-PEG samples with SBB incorporated, similar to that noted by Bjerrum *et al* (1980). However, two sedimenting species were not apparent with the other PLA-PEG copolymers (1.5:2, 4:2 and 6:2), whereas larger structures are still noted on the TEM picture. This may be due to the dilute solutions used for 4:2 and 6:2 PLA-PEG particles (~0.005% w/v), and the lower concentration of SBB in the 1.5:2 PLA-PEG micelles of the sedimentation velocity experiment (~1-2 % w/w) compared with the drug loading experiments. The larger structures seen in the TEM picture are in the minority, and therefore may not be visible in sedimentation velocity experiments, especially at the lower concentrations. Otherwise, these large structures may be artefacts of the TEM process and would not exist to be detected by sedimentation velocity.

The only other possibility for these large structures is that some SBB is not incorporated in the micelles and particles and has aggregated. This is unlikely, as control experiments for the *in vitro* release studies described below showed no significant difference in the UV absorbance of SBB/PLA-PEG particles measured before and after chromatographing on a hydrophobic propyl agarose gel column. If free SBB were present as aggregates, it would have bound to the hydrophobic gel leading to a change in absorbance.

Figure 5.4 – TEM picture of 4:2 PLA-PEG Particles with SBB Incorporated (Magnification = 200K)



From the above, drawing any definite conclusions regarding these large structures seen after the incorporation of SBB is difficult. The majority of the particles and micelles are similar in size to those observed without the presence of SBB, implying that any increase in size due to increased association number is small, as expected for small micelles (Mukerjee, 1980). Fessi *et al* (1989) also noted that the size of poly(D,L-lactide) nanocapsules loaded with indomethacin did not change.

Drug loading in micelles is usually low, as indicated by Barry and El Eini (1976). They investigated the solubility of several steroids, including testosterone, in long chain polyoxyethylene surfactants (polyoxyethylated cetyl alcohols), showing that only 2 - 9 molecules were associated with each micelle at 25 °C, representing a maximum of 3 % of the micellar weight. This is similar in magnitude to the results observed for the incorporation of testosterone into the PLA-PEG micelles, but the values for SBB are considerably greater. A much increased drug loading was achieved with the hydrophobic dye SBB over the steroid testosterone, which is apparent with all PLA-PEG copolymers.

This may be partly explained by the greater hydrophobicity of SBB over testosterone. SBB has a log P (octanol/water) of 7.2 compared with a log P for testosterone of 3.35 (calculated values, CLogP version 3.54). However, from the above results, it is unclear how significant the hydrophobicity is in determining the drug loading into PLA-PEG micelles/particles. Further studies have been performed to investigate this factor by using a range of testosterone esters of varying hydrophobicity but similar structure, in order to define how important hydrophobicity is for drug loading into PLA-PEG copolymers. A strong correlation between the micelle-water partition coefficient and log P has been described previously for Pluronic (Hurter and Hatton, 1992).

5.4 INFLUENCE OF HYDROPHOBICITY ON DRUG LOADING

5.4.1 Testosterone Esters

To investigate the effect of hydrophobicity on drug loading, testosterone esters were chosen for incorporation into 4:2 PLA-PEG particles. These compounds have differing hydrophobicity but similar chemical structures, and provide a continuation of the testosterone result already measured. Furthermore, testosterone esters have been

employed to study the effect of drug hydrophobicity previously (Noguchi *et al*, 1985; Malcolmson and Lawrence, 1993). The testosterone esters chosen for this experiment were testosterone propionate (log P=4.88), testosterone isocaproate (log P=6.34) and testosterone enanthate (log P=7.0). Log P values for the testosterone esters are for octanol/water, and are calculated values (Daylight, version 3.6) (Shute, 1995). Figure 5.5 shows the chemical structures of the testosterone esters.

5.4.2 Quantitation of Drug Loading of Testosterone Esters

A range of testosterone esters (1 ml, 1 mg/ml in acetone) were incorporated into 4:2 PLA-PEG particles (0.25% w/v) by the method described previously in section 5.3.1.

Aqueous solubility and extinction coefficients in ethanol of the testosterone esters were also determined as before. The unincorporated drug was dissolved in ethanol and the UV absorbance measured at 241 nm for all three drugs. The drug loading into the 4:2 PLA-PEG particles was then calculated as described in section 5.3.3 and the results are given in Table 5.5. ANOVA (analysis of variance) statistical analysis was performed on the testosterone ester results at the 5% confidence level.

5.4.3 Discussion

Table 5.5 shows that although the more hydrophobic testosterone enanthate incorporates more readily than the other testosterone esters (that are less hydrophobic than testosterone enanthate), the incorporation is not of the same magnitude as that seen with SBB (Table 5.4). No obvious trend is seen between the hydrophobicity (as measured by log P values) of the testosterone esters and the drug loading into PLA-PEG particles.

ANOVA statistical analysis shows that the difference between the incorporation of testosterone propionate and testosterone isocaproate is not significant. The difference in drug loading between these two esters and testosterone is also not significant.

However, the difference between the testosterone enanthate and the other testosterone esters and testosterone is significant. Therefore, the hydrophobicity of the drug molecule is not the major factor in influencing uptake into PLA-PEG particles, although it may still have a small role.

A different explanation is therefore needed to account for the much higher drug loading

Table 5.5
Drug Incorporation Studies of Testosterone Esters into Fractionated 4:3 PLA-PEG Particles

Drug Incorporation	Drug P	% w/w Drug	Incorporation Efficiency (%)
Testosterone	3.35	0.93 ± 0.09	23.7 ± 2.7
Testosterone Propionate	4.53	0.55 ± 0.06	13.9 ± 1.6
Testosterone Isocaproate	6.34	0.57 ± 0.04	14.3 ± 0.9
Testosterone Enanthate	7.0	2.52 ± 0.11	62.9 ± 2.8
Solulan Black B	5.7	0.9 ± 0.1	36.1 ± 0.1

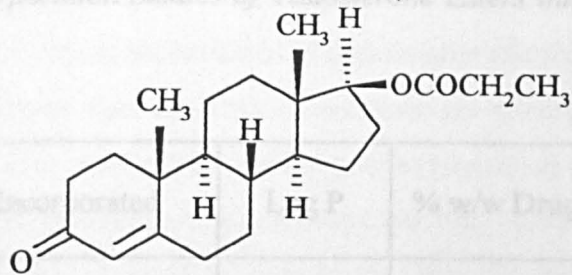


Figure 5.5a – Structure of Testosterone Propionate

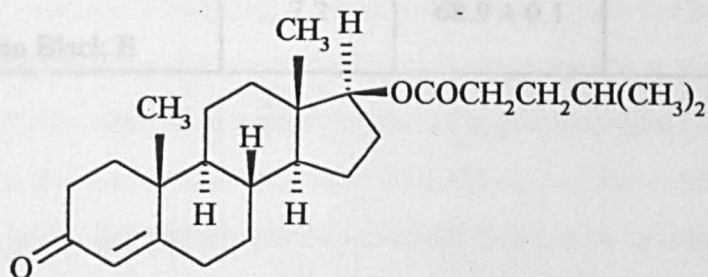


Figure 5.5b – Structure of Testosterone Isocaproate

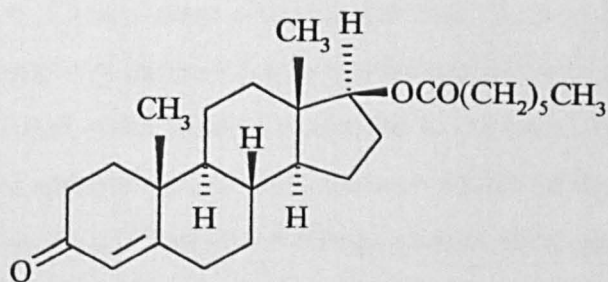


Figure 5.5c – Structure of Testosterone Enanthate

Table 5.5

Drug Incorporation Studies of Testosterone Esters into Fractionated 4:2 PLA-PEG Particles

Drug Incorporated	Log P	% w/w Drug	Incorporation Efficiency (%)
Testosterone	3.35	0.93 ± 0.09	23.7 ± 2.7
Testosterone Propionate	4.88	0.55 ± 0.06	13.9 ± 1.6
Testosterone Isocaproate	6.34	0.57 ± 0.04	14.3 ± 0.9
Testosterone Enanthate	7.0	2.52 ± 0.11	62.9 ± 2.8
Sudan Black B	7.2	68.9 ± 0.1	86.1 ± 0.1

achieved with SBB compared with testosterone and its esters. Examination of the chemical structures of the drugs (Figures 5.1 and 5.5) provides a probable explanation of this result. These show that SBB is more aromatic than testosterone and its esters. It has been shown that aromatic compounds are solubilised in greater quantities and selectively over more aliphatic compounds (Nagarajan *et al*, 1986), and whereas SBB contains five aromatic rings, testosterone only contains unsaturated bonds. The difference in the magnitude of drug loading between the aromatic benzene and aliphatic hexane for poly(ethylene oxide-propylene oxide) micelles (Nagarajan *et al*, 1986), is similar to that seen between testosterone and SBB into the PLA-PEG systems. They explained this greatly increased drug loading with the aromatic compounds as due to the lower interfacial tension against water of aromatic molecules compared with aliphatic molecules. This leads to a lower free energy of formation per unit area of the micellar core-water interface. Therefore, a larger micelle-or particle can be formed, containing more aromatic molecules compared with aliphatic molecules of similar size, for a given free energy of formation and a given number of copolymer molecules. It is also possible that the aromatic planar structure of the SBB allows the SBB molecules to stack flat on each other, increasing the number of molecules that can be incorporated.

Even between aromatic molecules, there is selectivity of how much drug compound is incorporated into micelles or particles. Kumar and Singh (1992) showed that sudan IV was solubilised into Triton X-100 micelles preferentially to anthracene. Sudan IV is a hydrophobic dye, similar in structure to sudan black B, but with one less aromatic ring, an OH group and no secondary amine groups. Anthracene consists of three fused aromatic rings. They explained this selectivity by concluding that the drugs were solubilised into different areas of the micellar core. Sudan IV was thought to incorporate in the outer region of the core due to hydration of its hydroxyl group, whereas the more hydrophobic anthracene would be confined to the centre of the core. Sudan black B could also be incorporated in the outermost region of the core due to hydration by possible hydrogen bonding of the nitrogen atoms of its amine groups with the water present in the PEG shell. However, compared with the effect of the aromatic ring, this is unlikely to contribute significantly to the increased drug loading of SBB over testosterone, as testosterone and its esters also have hydrophilic groups (carboxyl and

hydroxyl groups), which could hydrogen bond to water.

5.5 COMPARISON OF DRUG LOADING BETWEEN PLA-PEG AND SIMILAR SYSTEMS

Micelles and particles have been widely researched in recent years as possible drug delivery systems. The PLA-PEG micelles and particles compare favourably with drug loading into micellar systems reported in the literature. Several groups have exploited the ability of micelles to solubilise hydrophobic substances, which would otherwise be insoluble in aqueous media. Saito *et al* (1994) showed that the solubility of estriol was increased when Pluronic L-64 was added to the system. Another drug substance, diazepam, has also been solubilised into Pluronic L-64, with a drug loading of 2.28% w/w at 40 °C. Kabanov *et al* (1989) achieved a drug loading of 7% w/w with haloperidol into Pluronic P85 micelles, and subsequently showed an increase in the neuroleptic activity of this drug when injected intraperitoneally into mice. Similarly, incorporation of salicylic acid into poly(oxyethylene/oxybutylene/oxyethylene) (E₄₀B₁₅E₄₀) gel gave a drug loading of 3.6% w/w (Luo *et al*, 1993). These last three drugs have some aromatic character, which may facilitate their uptake into these micellar systems. Another example of drug loading into micelles is of adriamycin, an anti-cancer drug, into poly(ethylene oxide-co-β-benzyl L-aspartate) (PEO-PBLA) micelles, where a drug loading of 10% w/w of adriamycin was achieved (Kwon *et al*, 1995). The PLA-PEG systems thus show comparable drug loading to that achieved with these systems, and much higher drug loading with SBB.

A direct comparison can be made with work performed by Malcolmson and Lawrence (1993), where the incorporation of testosterone and its esters was studied for micelles and microemulsions prepared from the surfactant Brij 96 (polyoxyethylene-10-oleyl ether). In this work, Brij 96 micelles were studied at concentrations of 10, 15 and 20% w/w, with these concentrations also used to prepare microemulsions. The PLA-PEG copolymers compare well with the results of this paper, with the drug loading for testosterone being slightly higher than that seen with the Brij micelles for all PLA-PEG systems. Drug loading for testosterone into the 4:2 and 6:2 PLA-PEG particles is also

higher than for the microemulsions. The drug loadings of the esters are similar between the Brij micelles, microemulsions and 4:2 PLA-PEG particles for testosterone propionate and slightly better for the Brij micelles and microemulsions for testosterone enanthate.

However, an increased drug loading with the 4:2 PLA-PEG particles might be expected if the experiment were performed at the higher concentrations used for the Brij surfactant studies.

Table 5.6 shows an overview of drugs that have previously been loaded into PLA and PLGA particles. Wide ranges of drug compounds have been incorporated by different authors, with widely varying drug loadings. There is no obvious trend in the results, with aromatic compounds not being loaded significantly more than aliphatic compounds. An example of this is the work by Gref *et al* (1994), where the aromatic lidocaine gave similar drug loading to the steroid prednisolone, in studies in PLGA-PEG particles. However, comparing all these compounds directly with the PLA-PEG systems is difficult, due to their widely differing size distributions and the different methods of preparation of the drug loaded particles.

5.6 *IN-VITRO* RELEASE OF SUDAN BLACK B FROM 4:2 PLA-PEG PARTICLES

5.6.1 *Introduction*

In this chapter, it has been shown that drug loading of PLA-PEG systems is possible and relatively high loading can be achieved. It is now important to determine whether this drug can be released from the PLA-PEG system, and the duration of this release. The *in-vitro* release study described below is similar to that usually employed to elucidate the release of drug from particles and micelles, and will provide a basis for future work in this area.

5.6.2 *Method of In-Vitro Release*

The hydrophobic interaction gel, propyl agarose (Sigma Chemical Company, St. Louis, USA), was packed into a PD10 column, using phosphate buffered saline (PBS) (pH 7.4 at 25 °C, 0.01 M phosphate buffer) as the eluent. A dispersion of 4:2 PLA-PEG particles in PBS (0.25% w/v, 1 ml) was passed down the column, and the fractions collected and

Table 5.6

Review of Drug Loading into PLA and PLGA Particles

Drug	Polymer	Log P ^a	Aromatic ^b	Drug Loading (% w/w)	Approximate Size (nm)	Reference
Savoxepine	DL-PLA	6.55 (C)	✓	0.2 - 16.5	230 - 680	Allémann <i>et al.</i> 1993
Triamcinolone acetonide	DL-PLA	2.53 (M), 2.70 (C)	x	7.8	500	Krause <i>et al.</i> 1985
Triamcinolone acetonide	DL-PLA	2.53 (M), 2.70 (C)	x	2.9	710	Krause <i>et al.</i> 1985
Rifampicin	DL-PLA	2.39 (C)	✓	5.7	1310	Denkbaş <i>et al.</i> 1994
Bupivacaine	DL-PLA	3.38 (C)	✓	20.7-23.1	1000 - 5000	Le Corre <i>et al.</i> 1994
Beclomethasone dipropionate	DL-PLA	4.2 (C)	x	24.3	2600 - 4200	Wichert and Rohdewald, 1993
5-Fluorouracil	DL-PLA	-0.89 (M)	x	9.4	4300	Çiftçi <i>et al.</i> 1994

Drug	Polymer	Log P ^a	Aromatic ^b	Drug Loading (% w/w)	Approximate Size (nm)	Reference
Piroxicam	DL-PLA	0.26 (M)	✓	9.9	5000	Wagenaar and Müller, 1994
Diazepam	DL-PLA	2.80 (M), 3.18 (C)	✓	6.8/29.8	6480/7760	Pavanetto <i>et al.</i> 1994
Diazepam	DL-PLA	2.80 (M), 3.18 (C)	✓	21.1	8000 - 70000	Bodmeier and McGinity, 1987
Hydrocortisone	DL-PLA	1.61 (M), 1.86 (C)	x	12.4	8000 - 70000	Bodmeier and McGinity, 1987
Progesterone	DL-PLA	3.87 (M), 3.85 (C)	x	20.8	8000 - 70000	Bodmeier and McGinity, 1987
Quinidine	DL-PLA	3.44 (M), 3.20 (C)	✓	5.1	8000 - 70000	Bodmeier and McGinity, 1987
Cis-Platin	DL-PLA	*	x	31.7	20000 - 50000	Spenehauer <i>et al.</i> 1986
Lomustine	DL-PLA	2.83 (M), 2.76 (C)	x	19.9	58200	Benito <i>et al.</i> 1984
Progesterone	DL-PLA	3.87 (M), 3.85 (C)	x	31.7	160000	Benito <i>et al.</i> 1984
Phenobarbitone	L-PLA	1.47 (M), 1.36 (C)	x	9.35	20490	Jail and Nixon, 1989
Indomethacin/Benzyl benzoate	DL-PLA/F68/ phospholipid	4.27 (M), 4.23 (C) (Indomethacin)	✓	5.0	229	Fessi <i>et al.</i> 1989

Drug	Polymer	Log P ^a	Aromatic ^b	Drug Loading (% w/w)	Approximate Size (nm)	Reference
Taxol	DL-PLA/F68/ phospholipid	2.32 (C)	✓	2.4	260	Fessi <i>et al.</i> , 1989
Vitamin K	DL-PLA/F68/ phospholipid	*	✓	75	270	Fessi <i>et al.</i> , 1989
Dexamethasone	DL-PLA/F68/ phospholipid	1.83 (M), 2.2 (C)	x	0.96	300	Fessi <i>et al.</i> , 1989
Taxol	50:50 DL- PLA:EVA	2.32 (C)	✓	0.6	10000-30000	Burt <i>et al.</i> , 1995
Cyclosporin A	PLGA	*	x	5.98	298	Sánchez <i>et al.</i> , 1993
Roxithromycin	PLGA	*	x	4.4	354	Julienne <i>et al.</i> , 1989
Indomethacin	PLGA	4.27 (M), 4.23 (C)	✓	7.24	2400	Conti <i>et al.</i> , 1995
Timolol maleate	PLGA	1.91 (M), 1.63 (C)	x	2.2	9000	Sturesson <i>et al.</i> , 1993
Nifedipine	PLGA	2.40 (C)	✓	18.8	9700	Sansdrap and Moës, 1993

Drug	Polymer	Log P ^a	Aromatic ^b	Drug Loading (% w/w)	Approximate Size (nm)	Reference
Lidocaine	PLGA-PEG	2.26 (M), 1.98 (C)	✓	up to 45	90 - 150	Gref <i>et al.</i> 1993

Key to Table 5.6

* - Not calculable due to a missing fragment or uncommon structural feature.

^a - Log P values for octanol:water taken from Craig (1990). except for ^c which was from Juarranz *et al* (1986).

(M) - Measured experimentally; (C) - Calculated value.

^b - Aromatic defined, in this context, as possessing at least one aromatic ring.

analysed by UV spectroscopy to determine the elution volume of the PLA-PEG particles. A solution of SBB in acetone (1ml, 10mg/ml) was added to 4:2 PLA-PEG particles (0.25% w/v) as before, and the excess drug centrifuged off as described above in section 5.3.1. The supernatant was collected and the absorbance of the dispersion determined at 587 nm after appropriate dilution with PBS. PLA-PEG particles loaded with SBB were then passed down the PD10 column as a control experiment, and the UV absorbance of the dispersion at 587 nm remeasured. The change in absorbance between the two samples was negligible, showing that all the SBB was incorporated stably in the particles.

The 4:2 PLA-PEG particles with SBB were then incubated for 3 hours, 1 day, 3 days, 7 days, 14 days and 28 days in a water bath at 37 °C under conditions, with stirring throughout using a magnetic stirrer. A comparative sample of the unincubated particles was measured by UV to provide the absorbance of the SBB in the particles before release, A_1 . After incubation for the required time, the samples were removed and 1 ml passed down the propyl agarose packed PD10 column. The particle fractions were collected from the column, pooled and assayed by UV spectroscopy at 587 nm to give the absorbance of SBB remaining in the particles, A_2 . This allowed the percentage of SBB remaining in the PLA-PEG particles to be calculated by the following equation: -

$$\% \text{ of SBB released} = \frac{A_1 - A_2}{A_1} \times 100$$

The propyl agarose column was regenerated between samples by washing sequentially with 0.5 M sodium hydroxide solution, 0.1 M sodium acetate solution (pH 4.5), purified water, 2 M sodium chloride solution and purified water.

5.6.3 Results and Discussion of In-Vitro Release Study

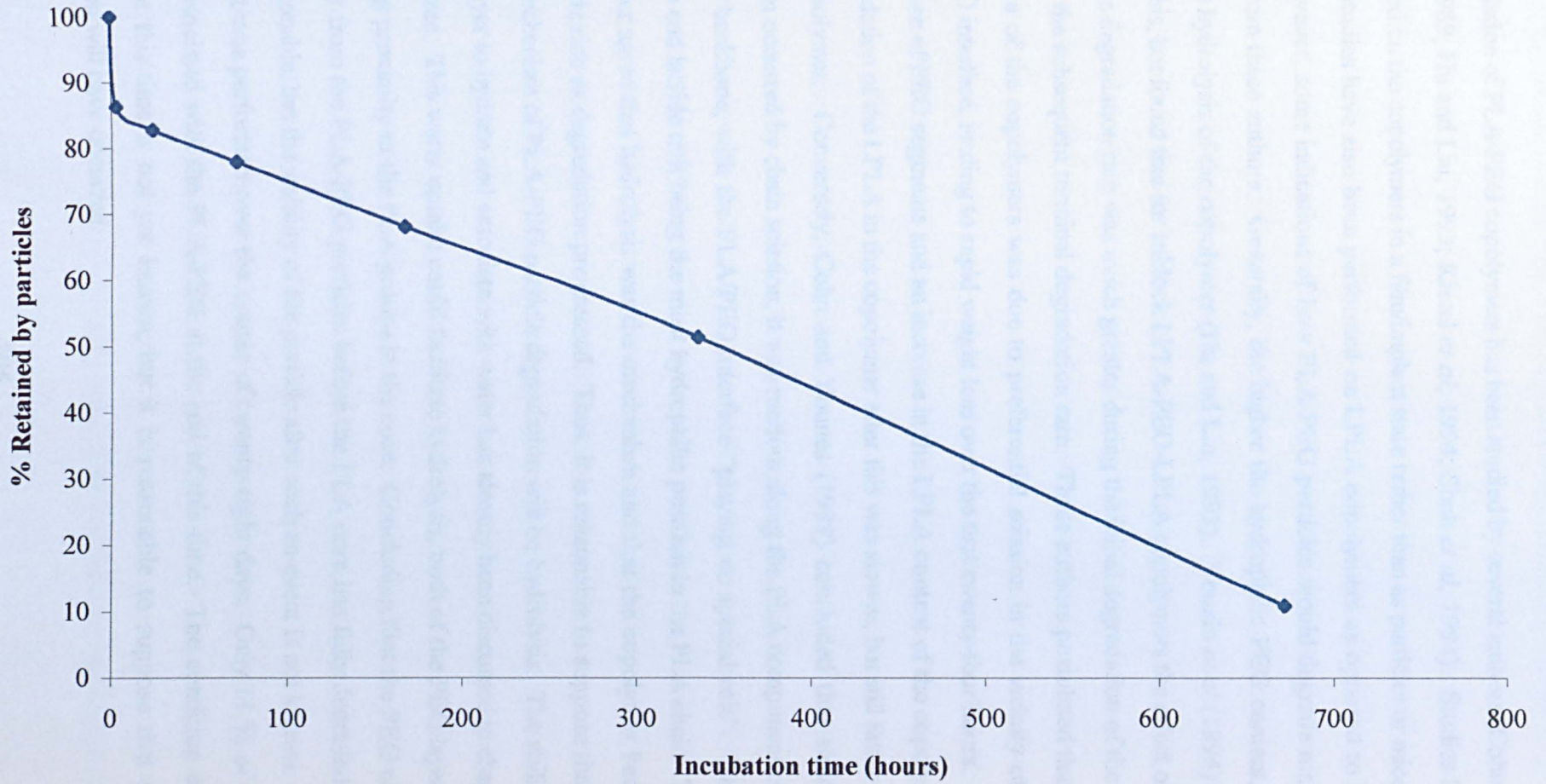
Figure 5.6 shows the results of the in-vitro release of SBB from 4:2 PLA-PEG particles

in PBS at 37 °C. This shows a small “burst” effect, with about 14 % of SBB being released in the first three hours of the study. The release from three hours onwards is linear, corresponding to zero order kinetics, with a low release rate of about 0.1 % perhour, which offers the possibility of PLA-PEG systems being used for sustained release. This type of release has been seen previously with PLA particles (Aso *et al*, 1993; Gupta *et al*, 1993; Allémann *et al*, 1994; Conti *et al*, 1994; Le Corre *et al*, 1994), with the durations of the two phases varying with different drugs, particle size, preparation method and the release media used.

The small burst release observed may be due to drug at the surface of the particles. If the mechanism of this initial release was diffusion from the core of the particles, the *in-vitro* release profile should usually show a lag time before release commences (Bodmeier and McGinity, 1987). This lag time would allow the buffer media to penetrate into the particles. Although no such effect is evident from the in-vitro profile of the PLA-PEG particles, it cannot be totally discounted as there is no time point before three hours. However, considering that the PLA-PEG particles are already hydrated due to their PEG chains, it is unlikely that a significant lag period would occur. In Bodmeier and McGinity's data (1987), the lag periods for the release of quinidine from PLA microspheres are of the order of 25 to 50 hours, which do not occur with the PLA-PEG particles. They considered that after the penetration of the buffer during the lag period, the burst release was then due to a rapid leaching of drug through the pores and channels formed by the buffer. For the PLA-PEG particles, it is more likely that the burst release is due to drug adsorbed at the surface of the particles, which has been concluded by other authors (Krause *et al*, 1985; Allémann *et al*, 1994; Pavanetto *et al*, 1994). Some SBB may be associated with the PEG chains due to the presence of its amine groups, and with the outer region of the PLA core. This SBB would therefore be able to diffuse out more rapidly than the SBB within the PLA core.

In the linear phase, the drug release may be due to degradation of the particles, drug diffusion through the copolymer or both. The linear relationship followed zero-order kinetics, and gave a much closer linear fit than the alternative release trend displayed by some PLA systems of release directly proportional to the square root of time (Spenlehauer *et al*, 1986; Çiftçi *et al*, 1994; Wagenaar and Müller, 1994).

Figure 5.6 - In Vitro Release Profile of Sudan Black B from 4:2 PLA-PEG Particles



The degradation of PLA-PEG copolymers has been studied by several authors (Cohn and Younes, 1989; Hu and Liu, 1993; Kissel *et al*, 1994; Shah *et al*, 1994). Studies have concentrated on the copolymers in a film/implant state rather than as particles or micelles, and most studies have also been performed on LPLA copolymers as opposed to DL-PLA. However, some indications of how PLA-PEG particles would degrade may be deduced from these authors. Generally, the higher the hydrophilic PEG content, the greater the hydrolysis of the copolymer (Hu and Liu, 1993). Youxin *et al* (1994) also observed this, but found that for triblock LPLA-PEO-LPLA copolymers the effect of the PEO on the degradation rate was much greater during the initial degradation of the first week than the subsequent terminal degradation rate. These authors postulated that the degradation of the copolymers was due to preferential scission in the vicinity of the LPLA/PEO interface, leading to rapid weight loss over the first twenty-four hours. This led to release of PEO segments and an increase in the LPLA content of the copolymer. The degradation of the LPLA in the copolymer after this was slower, but still faster than the homopolymer. Conversely, Cohn and Younes (1989) concluded that although degradation occurred by chain scission, it was random along the PLA component of the PLA-PEG backbone, with the PLA/PEO interface “playing no special role”. This is despite the end lactide unit being the most hydrophilic position in the PLA chain. They did however agree that hydrolysis was the mechanism and that the copolymer became more lactide rich as degradation progressed. Thus, it is reasonable to suppose that the primary mechanism of PLA-PEG particle degradation will be hydrolysis. The ability of the PEG layer to hydrate and associate with water has already been discussed in chapters one and three. This water uptake could facilitate hydrolysis, both of the PEG layer and by allowing proximity to the PLA groups in the core. Concluding that the PEG chains will be lost from the PLA-PEG particles before the PLA core has fully degraded also seems reasonable, but the stability of the particle after such an event is not known. This experiment was performed over the course of twenty-eight days. Only 11 % of SBB remains associated with the PLA-PEG at the end of this time. The condition of the particles at this time is not yet known, but it is reasonable to suppose that some degradation will have occurred.

In a study of the release of SBB from PLA implants (PBS containing Tween 80 (0.6% w/v), pH 7.4, 37 °C), the SBB release was very slow over the six-day period studied (Katayama *et al*, 1995). To increase the release rate, a polyoxyethylated castor oil derivative (HCO-60) was formulated into the implant, which increased the release rate to 13.5 % released after six days. If the burst release of the SBB from the PLA-PEG particles is neglected and the linear release considered, this release rate of SBB is in good agreement. The increased release rate of PLA when a hydrophilic component is added has also been observed with LPLA-PEO-LPLA copolymers. Here, the presence of PEO increases water solubility and therefore permeability, leading to an increase in drug release (Youxin *et al*, 1994). With this copolymer, pulsatile release was achieved with bovine serum albumin (BSA), with the BSA release rate varying from zero order release to a lag period where no drug release occurred. The authors concluded that this was due to the destruction of the mechanical properties of the microspheres due to loss of PEO and chain scission in the amorphous region of the PLA phase; that is that the release was degradation controlled.

Several other factors play a role in influencing the rate of release of drug from a copolymer system. The glass transition temperature (T_g), which is dependent on the polymer molecular weight, affects release such that the lower the glass transition temperature, the faster the release of drug (Aso *et al*, 1993; Le Corre *et al*, 1994). A value of T_g for PLA has been found to be 55°C (Bodmeier and McGinity, 1987), but will decrease with the incorporation of hydrophilic polymers. The temperature at which the release study is performed will therefore affect the drug release. For a polymer with a glass transition temperature of 55°C, at temperatures below this, the polymeric matrix will be glassy, whereas at temperatures above T_g , it will be rubbery (Denkbaş *et al*, 1994). A polymer in the rubbery phase degrades much faster, and diffusion of molecules in rubbery polymers is also faster. The glass transition temperature is thus an important factor to consider in release studies.

The drug loading of the particles also influences the rate of release, with higher drug loading leading to faster release (Spenlehauer *et al*, 1986; Bodmeier and McGinity, 1987; Pavanetto *et al*, 1994; Uchida *et al*, 1996). It has been shown that for PLA microspheres, the drug release was inversely proportional to the drug loading level, and

the total percentage of drug released increased with greater drug loading (Bodmeier and McGinity, 1987). The drug loading of the 4:2 PLA-PEG particles in this experiment is high (~ 37% w/w for the 10 mg of SBB loaded). Therefore, the release rate of SBB would be expected to decrease with decreased drug loading.

The pH of the media and its effect on the drug may also affect the drug release, especially with lower molecular weight PLA (Çiftçi *et al*, 1994). Low molecular weight PLA contains high numbers of -COOH and -OH polar end groups, which can lead to swelling during the dissolution of the drug. Any ionisation of the secondary amine groups of SBB and/or ionisation of the carboxyl groups of PLA may also play a role in the release (Le Corre *et al*, 1994). The pH of the media also has a significant effect on degradation, and if the release is degradation-controlled, then the pH will noticeably affect release. This was illustrated by Denkbaş *et al* (1994), who showed that D,L-poly lactide microspheres degraded faster in alkaline media (pH 9.8) than at neutral pH (pH 7.4), with a corresponding increase in the rate of rifampicin release.

However, it must be noted that SBB is very insoluble in aqueous media and it is possible that there is another explanation for the apparent decrease in SBB content of the PLA-PEG particles, as it is difficult for the SBB to diffuse out under such conditions. Generally, the model drug should have some solubility in the dissolution medium in *in vitro* testing, but addition of solvents or lipophilic substances to the media to increase SBB solubility may also affect the results of the study and this was therefore not attempted.

5.7 SUMMARY

Drug loading into both PLA-PEG micelles and particles has been successfully achieved.

The amount incorporated has been determined, and it was shown that the drug loading of the aromatic hydrophobic dye, sudan black B (SBB), was much greater than that of the steroidal testosterone and its esters. There was a general trend of increasing drug loading with increased molecular weight of PLA-PEG copolymer, but this was less pronounced with SBB. A study of the drug loading of testosterone esters of varying hydrophobicity (as measured by Log P octanol/water values) showed no clear

relationship between drug loading and hydrophobicity. It was concluded that the greatly increased drug loading achieved with SBB over testosterone and its esters is most likely due to the aromatic structure of SBB.

An *in-vitro* release study of the drug release of SBB from 4:2 PLA-PEG particles was conducted. This showed that the SBB showed a small burst release over the first three hours, followed by a linear release profile that extended to the end of the experiment at twenty-eight days. The burst release was probably due to SBB incorporated in the PEG layer at the surface of the particles. The linear release may be diffusion or degradation controlled, and further studies are needed to elucidate the mechanism of drug release. Therefore, PLA-PEG micelles and particles have the ability to both load and release drugs, which gives them good potential for future drug delivery systems. The *in-vitro* release profile over one month indicates that they may be employed as sustained release systems.

CHAPTER SIX

IN VITRO AND IN VIVO STUDIES OF PLA-PEG COPOLYMERS

6.1 INTRODUCTION

Previous chapters of this thesis have presented the physicochemical aspects of PLA-PEG micelles and particles, and have shown the presence of PEG at the surface, which is expected to confer “steric stability” to the systems. This chapter will now examine whether this steric stability can prevent the uptake of the systems by the reticuloendothelial system of an animal model, namely the rat. So far, the PLA-PEG systems have shown promise, being of a small size and able to hold and release drug in a controlled manner. This ability to load drugs is now exploited in the radiolabelling of the PLA-PEG systems to allow the distribution of the systems in an *in vivo* model to be assessed. This chapter therefore presents details of the radiolabelling of PLA-PEG systems, the stability of this radiolabel *in vitro* in serum, and the biodistribution of the micelles and particles.

6.2 RADIOLABELLING OF PLA-PEG COPOLYMERS

6.2.1 Radiolabelling of Colloidal Systems

Introducing a radionuclide into the system can assess the fate of parenterally administered particulate systems. The presence of a radionuclide readily allows the monitoring of particle uptake by various organs and the rate of elimination from the body. This can be achieved either by gamma-scintigraphy or scintillation counting after sacrifice and dissection of animals, depending on the nature of the radionuclide emissions.

A limited number of radionuclides are suitable for radiolabelling in drug delivery studies. The factors that affect the choice of radiolabel include the cost, ease of sample preparation and detection, handling risks, the availability of a suitable preparation, and the half-life of the radionuclide. This must be long enough to remain at detectable levels over the course of the experiment. Either beta or gamma-emitting radiation can be used, with gamma radiation preferred due to easier sample preparation for counting. Beta

radiation has been successfully employed to study drug release of carbon-14 labelled-savoxepine from PLA nanoparticles (Allémann *et al*, 1994), which also allows the biodistribution of the nanoparticles to be followed to some extent. Carbon-14 has also been used for labelling poly(alkyl 2-cyanoacrylate) nanoparticles, but problems were encountered in this process with the label, including a tendency for the ^{14}C -labelled monomer to undergo spontaneous polymerisation when isolated during the initial preparation stage, causing a wide particle size distribution (Douglas *et al*, 1987). A stable gamma-emitting technetium ($^{99\text{m}}\text{Tc}$)-dextran complex was therefore developed and covalently bound to the nanoparticles during polymerisation. PLA nanoparticles have also been radiolabelled with technetium for *in vivo* studies in rats (Krause *et al*, 1985) and mice (Çiftçi *et al*, 1994). Technetium-99 has a half-life of 6.02 hours, and is widely used for medical diagnosis.

Another radionuclide that has been employed in medicine is indium-111. This isotope has been complexed with both oxine (8-hydroxyquinoline) and DTPA-SA (the distearyl amide of diethylenetriaminepentaacetic acid). The radiolabelling method is different here, with radiolabelling achieved by incorporation of an indium-111 complex, rather than by covalently attaching the radiolabel as described above for carbon-13 and technetium-99. Indium-111-oxine (or indium-111 8-hydroxyquinoline) is a neutral lipophilic complex consisting of three molecules of oxine chelated with one ion of indium as shown in Figure 6.1. This oxine complex has been used in medical physics, usually for radiolabelling leukocytes and platelets (Thakur and McKenney, 1985). In drug delivery, our group at Nottingham has used indium-111-oxine routinely as a radiolabel. Several different systems have been radiolabelled, including PLA particles (Müller *et al*, 1988) and PLGA particles (Scholes *et al*, 1992; Scholes, 1993). The other complex, In-111-DTPA-SA, has also been used in drug delivery, for radiolabelling liposomes (Klibanov *et al*, 1991; Torchilin *et al*, 1994), and nanoparticles (Gref *et al*, 1994). The half-life of In-111 of 2.8 days is suitable for *in vivo* experiments.

Iodine-131 has been successfully employed for the radiolabelling of polystyrene nanoparticles by an irradiation method where the iodine is covalently attached to the particle surface (Huh *et al*, 1974). However, due to its high energy radiation, high handling risks are associated with this isotope (Müller *et al*, 1988). Difficulties have also been experienced in radiolabelling PLA particles with iodine-131 using this method, with labelling efficiency being low and particle aggregation occurring.

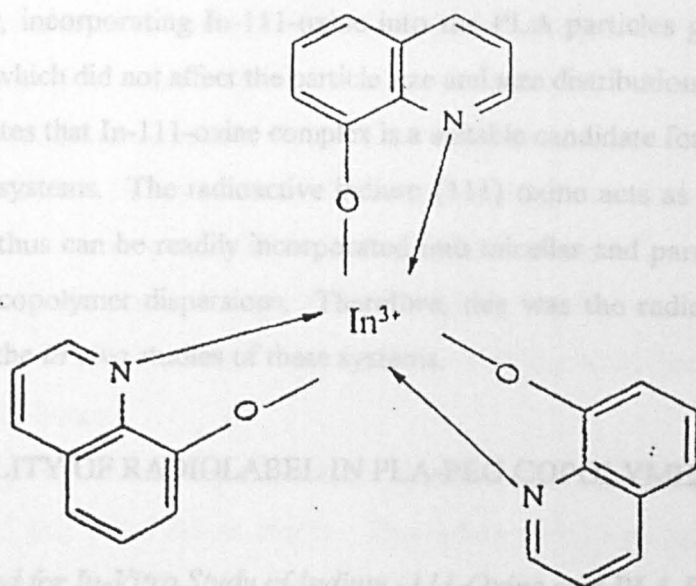


Figure 6.1 – Structure of Indium (111) Oxine Radiolabel

Conversely, incorporating In-111-oxine into PLA particles gave a high labelling efficiency, which did not affect the particle size and size distribution (Muller *et al.*, 1988). This indicates that In-111-oxine complex is a suitable candidate for the radiolabelling of PLA-PEG systems. The radioactive indium-111-oxine acts as a hydrophobic drug model and thus can be readily incorporated into vesicular and particulate forms of the PLA-PEG copolymer dispersion. The reason for this choice was the radionucleide preparation chosen for the purpose of these systems.

6.3 STABILITY OF RADIOLABEL IN PLA-PEG COPOLYMERS

6.3.1 Method for *In-Vitro* Study of Indium-111-Oxine in PLA-PEG Copolymers

Before performing the *in vivo* studies, the stability of the indium-111-oxine label in PLA-PEG micelles and particles was ascertained. This was carried out as follows, by testing how much indium-111-oxine was released by the PLA-PEG particles during *in vitro* incubation at 37 °C in 50% v/v rat serum to simulate *in vivo* conditions.

Indium-111-oxine solution (50 µg/ml) was obtained from Amersham International (Bucks., UK) with radioactivity of 37 MBq ml⁻¹ at the activity reference date. Dispersions of 4.2 and 6.2 PLA-PEG particles (1% w/v) were prepared as described in section 2.1.4 and the indium-111-oxine complex was added with the acetone. Sephadex CL-4B was packed into PD10 columns (10 cm) using phosphate buffered saline (PBS) (pH 7.4 at 25 °C, 0.01 M phosphate buffer) (Sigma Chemical Company, St. Louis, USA) as eluent.

Two initial control experiments were performed, firstly a dispersion of PLA-PEG particles (4.2 and 6.2 PLA-PEG, 1 ml, 1% w/v) was applied to a PD10 column, followed by 0.5 ml aliquots of PBS. The eluted aliquots were collected in quartz UV cells and analysed at 225 nm by UV spectroscopy (U-220, Kontron Instruments, Tübingen, Switzerland) to determine the elution volume of the PLA-PEG particles. Secondly, 50% v/v serum in PBS (1 ml) was applied to a similar column, and the collected fractions analysed at 280 nm, to determine where the serum proteins eluted.

Radiolabelled 4.2 and 6.2 PLA-PEG particles (1 ml) were then applied to PD10 columns, with PBS as the eluent, to separate the radiolabelled particles from any free unincorporated label. The eluted aliquots were collected and the radioactivity assayed using an LKB compugamma gamma counter (Compugamma, LKB, Wallac, Finland).

Conversely, incorporating In-111-oxine into the PLA particles gave a high labelling efficiency, which did not affect the particle size and size distribution (Müller *et al*, 1988).

This indicates that In-111-oxine complex is a suitable candidate for the radiolabelling of PLA-PEG systems. The radioactive indium (111) oxine acts as a hydrophobic drug model and thus can be readily incorporated into micellar and particulate forms of the PLA-PEG copolymer dispersions. Therefore, this was the radionuclide preparation chosen for the *in vivo* studies of these systems.

6.3 STABILITY OF RADIOLABEL IN PLA-PEG COPOLYMERS

6.3.1 Method for In-Vitro Study of Indium -111-Oxine and PLA-PEG Copolymers

Before performing the *in vivo* studies, the stability of the indium-111-oxine label in PLA-PEG micelles and particles was ascertained. This was carried out as follows, by testing how much indium-111-oxine was released by the PLA-PEG particles during *in vitro* incubation at 37 °C in 50% v/v rat serum to simulate *in vivo* conditions.

Indium-111-oxine solution (50 µg/ml) was obtained from Amersham International (Bucks., UK) with radioactivity of 37 MBq ml⁻¹ at the activity reference date.

Dispersions of 4:2 and 6:2 PLA-PEG particles (1% w/v) were prepared as described in section 2.3.4 and the indium-111-oxine complex was added with the acetone. Sepharose CL-4B was packed into PD10 columns (10 cm) using phosphate buffered saline (PBS) (pH 7.4 at 25 °C, 0.01 M phosphate buffer) (Sigma Chemical Company, St. Louis, USA) as eluent.

Two initial control experiments were performed, firstly a dispersion of PLA-PEG particles (4:2 and 6:2 PLA-PEG, 1 ml, 1% w/v) was applied to a PD10 column, followed by 0.5 ml aliquots of PBS. The eluted aliquots were collected in quartz UV cells and analysed at 225 nm by UV spectroscopy (Uvikon, Kontron Instruments, Tegimenta, Switzerland) to determine the elution volume of the PLA-PEG particles. Secondly, 50% v/v serum in PBS (1 ml) was applied to a similar column, and the collected fractions analysed at 280 nm, to determine where the serum proteins eluted.

Radiolabelled 4:2 and 6:2 PLA-PEG particles (1 ml) were then applied to PD10 columns, with PBS as the eluent, to separate the radiolabelled particles from any free unincorporated label. The eluted aliquots were collected and the radioactivity assayed using an LKB compugamma gamma counter (Compugamma, LKB, Wallac, Finland).

From the control experiment, the fractions corresponding to the 4:2 and 6:2 PLA-PEG particles were determined. These also corresponded to the most radioactive fractions indicating good incorporation. From these data, the incorporation efficiency of the indium (111) oxine complex into the PLA-PEG particles was calculated. The three most radioactive fractions were pooled and used for the serum stability experiments by adding rat serum to give a serum concentration of 50% v/v. Samples of the 4:2 and 6:2 PLA-PEG particles in 50% v/v serum were then incubated in a water bath for 5 minutes, three hours and 24 hours.

After the appropriate time had elapsed, the samples were removed and applied to a PD10 column (0.5 ml) with PBS as eluent. The radioactivity was again analysed using a gamma-spectrometer. The stability of the label was then calculated, by expressing the radioactivity left associated with the particles after incubation as a percentage of the particle initial activity.

Further controls were also performed. The PLA-PEG particles were incubated with PBS alone (no serum present) to investigate the effect of the incubation conditions on the PLA-PEG particles in the absence of serum. Free ^{111}In complex was also incubated with serum, to determine where indium-111-oxine released from the PLA-PEG particles would bind (i.e. to which serum proteins). In both of these experiments, the incubation lasted for three hours.

6.3.2 Results and Discussion

Figure 6.2 shows the plot of the control experiments of particles alone (6:2 PLA-PEG) and serum alone. This shows that the PLA-PEG particles are eluted first in the void volume of the column, as would be expected from the GPC work described in chapter three. The serum profile consists of two peaks: one of which has a high molecular weight and is eluted in the void volume (with the particles), and the other which elutes later and is of smaller molecular weight. While most of the serum components elute separately from the PLA-PEG particles, a small proportion overlap and are apparently eluted with the particles. The control experiment of indium and serum will give more insight into the significance of this and is discussed below.

Figure 6.3 shows a typical plot for the radiolabelled PLA-PEG particles (6:2 PLA-PEG). The efficiency of radiolabel incorporation into the particles was good, at $78.1\% \pm 2.2\%$ for 4:2 PLA-PEG and $89.6\% \pm 2.6\%$ for 6:2 PLA-PEG. High efficiencies of uptake

Figure 6.2 - Serum stability control experiment: 6:2 PLA-PEG 1% w/v Particles and 50% v/v Serum Run on a PD10 Column (Sephacrose CL-4B)

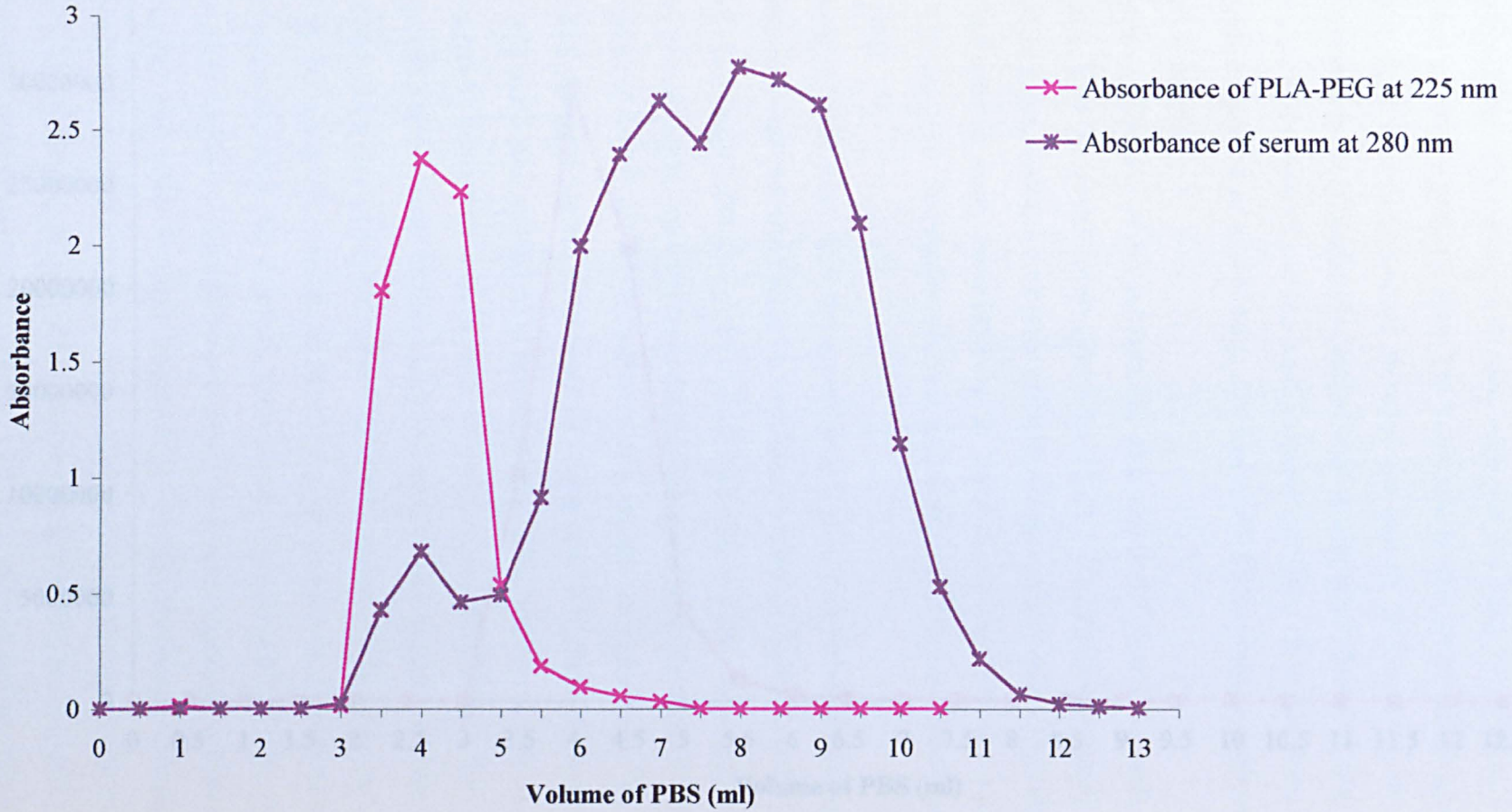
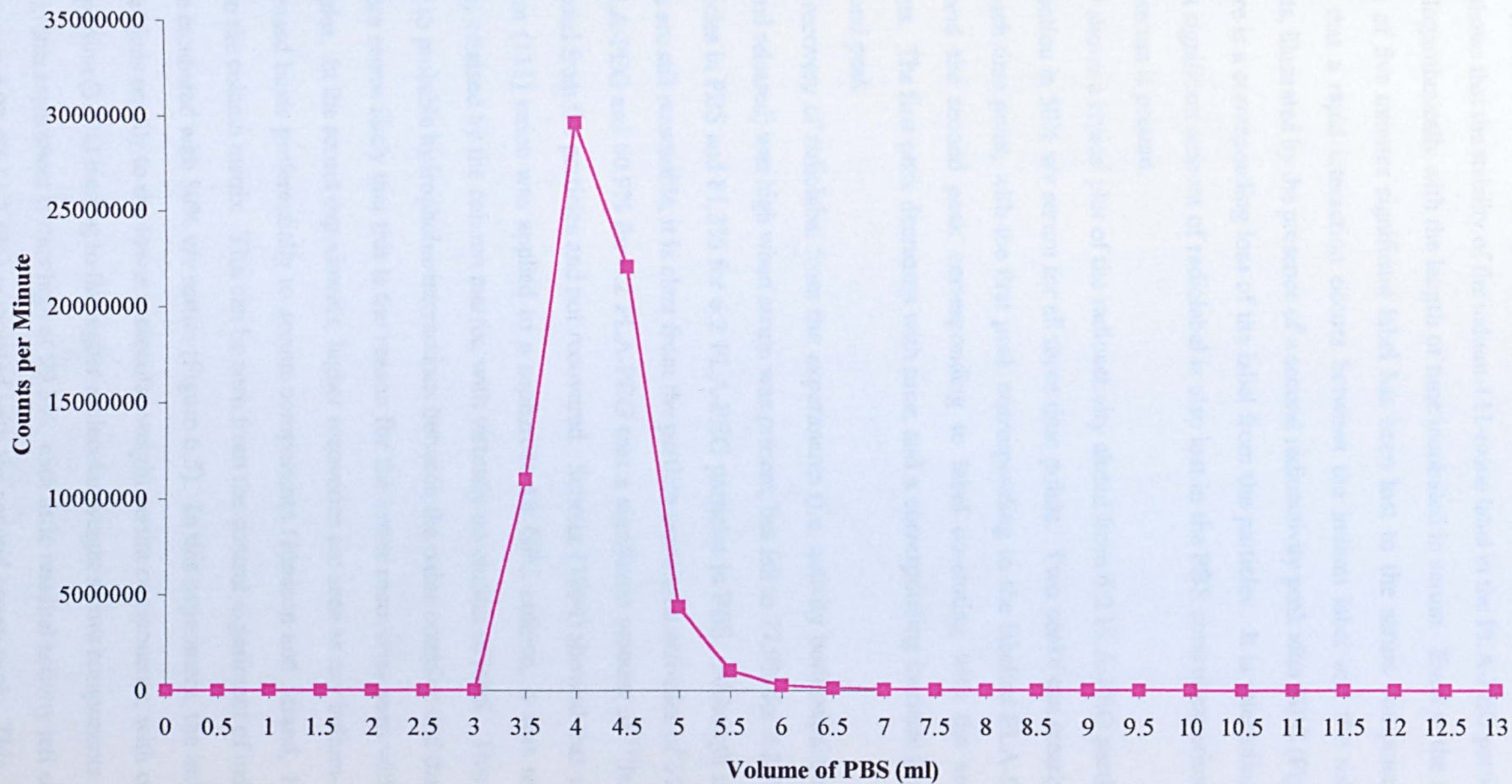


Figure 6.3 - Activity of 1% w/v 6:2 PLA-PEG Particles Radiolabelled with Indium (111) Oxine



could be expected due to the hydrophobic oxine.

Table 6.1 shows that the stability of the indium-111-oxine label in the PLA-PEG particles decreases logarithmically with the length of time incubated in serum. Even at the first time point of five minutes significant label has been lost to the serum components, indicating that a rapid interaction occurs between the indium label and the serum components, illustrated by the presence of a second radioactivity peak after GPC (Figure 6.4). There is a corresponding loss of the label from the particles. It is interesting to note that a significant amount of radiolabel is also lost in the PBS control experiments where no serum is present.

Figure 6.4 shows a typical plot of the radioactivity eluted from 6:2 PLA-PEG particles after incubation in 50% v/v serum for all three time points. Two peaks can clearly be seen for each time point, with the first peak corresponding to the labelled PLA-PEG particles and the second peak corresponding to label co-eluting with the serum components. The first peak decreases with time, and a corresponding increase is seen in the second peak.

The total recovery of radiolabel from the experiments (i.e. activity both remaining in particles and released) was high when serum was present, but fell to 77.9% for 4:2 PLA-PEG particles in PBS and 81.3% for 6:2 PLA-PEG particles in PBS. Although these recoveries are still reasonable, it is clear from the particle associated activities of 55.4% for 4:2 PLA-PEG and 60.9% for 6:2 PLA-PEG that a significant amount of ^{111}In has been released from the particles and not recovered. Scholes (1994) showed that when free indium (111) oxine was applied to a sepharose-4B GPC column, it was nearly completely retained by the column matrix, with virtually no elution of label. This was attributed to probable hydrophobic interactions between the oxine complex and the gel. It therefore seems likely that this is the reason for the lower recoveries seen with the PBS samples. In the serum experiments, higher recoveries are seen as any indium-111-oxine released binds preferentially to serum components (Jönsson and Strand, 1992) rather than the column matrix. This can be seen from the control experiment of indium-111-oxine incubated with 50% v/v serum (Figure 6.5). In this experiment, the indium-111-oxine binds readily to the lower molecular weight serum components, with only a small proportion (3.8%) binding to the higher molecular weight serum components. The recovery in this experiment is thus high at 99.3%, with little residual activity left on the GPC column and 93.4% ($\pm 2.6\%$) associated with the second serum peak. This

Figure 6.4 - Serum Stability Data for 6:2 PLA-PEG Particles Incubated in 50% v/v Serum

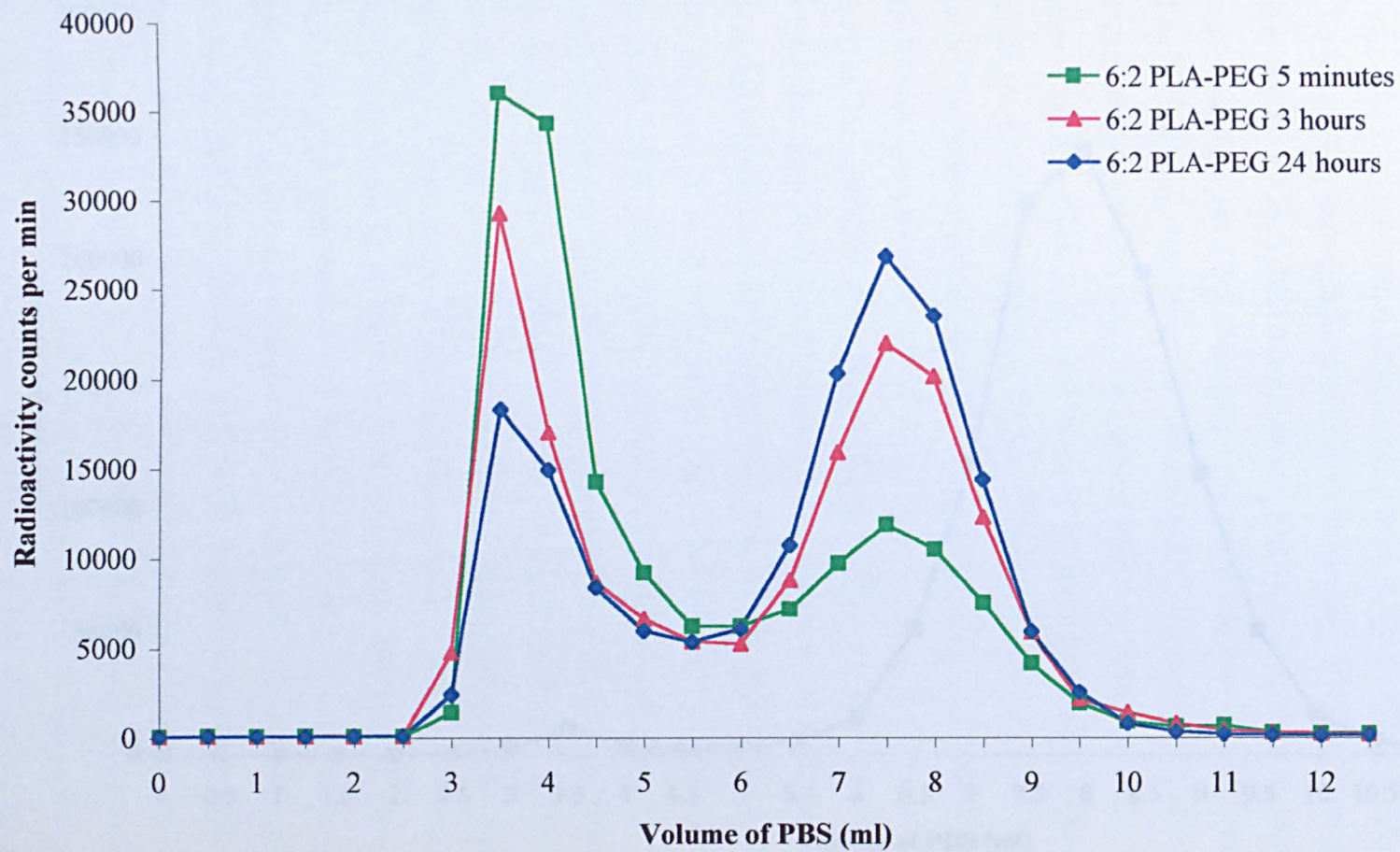
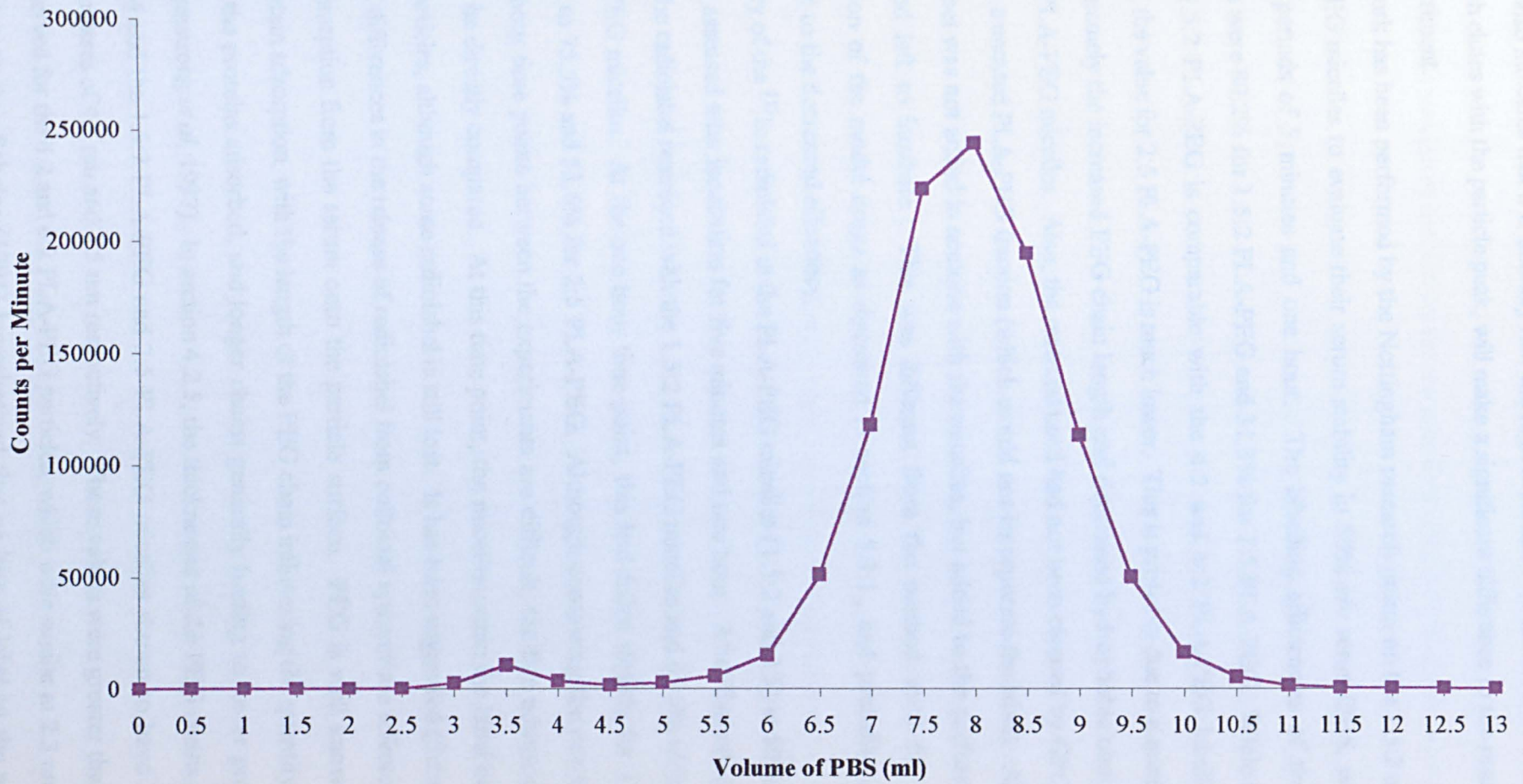


Figure 6.5 - Activity of Indium (111) Oxine After Incubating for Three Hours in 50% v/v Serum



experiment also indicates that it is unlikely that the high molecular weight fraction of the serum, which elutes with the particle peak, will make a significant difference to the results of this experiment.

Previous work has been performed by the Nottingham research group on the 1.5:2 and 2:5 PLA-PEG micelles to evaluate their serum stability in 50% v/v serum/PBS, with incubation periods of 5 minutes and one hour. The labelling efficiencies of these copolymers were 80.2% for 1.5:2 PLA-PEG and 31.3% for 2:5 PLA-PEG. While the value for 1.5:2 PLA-PEG is comparable with the 4:2 and 6:2 PLA-PEG labelling efficiencies, the value for 2:5 PLA-PEG is much lower. This is probably due to a number of factors, namely the increased PEG chain length and decreased hydrophobic content of the 2:5 PLA-PEG micelles. Also, the material used had not been cleaned by GPC to remove the truncated PLA-PEG fraction (which would not incorporate the label). Also, the radiolabel was not added in acetone with the micelles, but added to the preformed micelles and left to incubate. This was different from the method used for the incorporation of the model drugs as discussed in section 5.3.1., and probably also contributed to the decreased efficiency.

The stability of the ^{111}In radiolabel in the PLA-PEG micelles (1.5:2 and 2:5) in 50% v/v serum was assessed after incubation for five minutes and one hour. After five minutes, 77.0% of the radiolabel remained with the 1.5:2 PLA-PEG micelles and 65.6% with the 2:5 PLA-PEG micelles. At the one hour time point, this had fallen slightly for 1.5:2 PLA-PEG to 75.5% and 53.6% for 2:5 PLA-PEG. Although comparing the one hour and three hour time points between the experiments are difficult, the five minute time points can be directly compared. At this time point, the micelles retain the label better than the particles, although some radiolabel is still lost. It has been suggested (Scholes, 1994) that differences in the release of radiolabel from colloidal systems are affected by protein adsorption from the serum onto the particle surface. PEG is well known to reduce protein adsorption, with the length of the PEG chain influencing the quantity and quality of the proteins adsorbed, and longer chains generally leading to lower protein uptake (Armstrong *et al*, 1997). In section 4.2.5, the thicknesses of the PEG chains were determined and the 1.5:2 PLA-PEG and 2:5 PLA-PEG micelles shown to have PEG layer thicknesses of 4.1 nm and 7.5 nm respectively. These values were greater than the values observed for the 4:2 and 6:2 PLA-PEG particles, which were similar at 2.3 nm and 2.4 nm respectively. Scholes (1994) hypothesised that as loss of label to the serum

occurred after protein adsorption to the surface of microspheres, then if protein adsorption was reduced, the loss of label would also be reduced. It is possible therefore that the increased retention of the label by the micelles over the PLA-PEG particles is due to decreased protein adsorption on account of their increased PEG chain layer thicknesses. However, this cannot be the only factor as 1.5:2 PLA-PEG micelles perform better than 2:5 PLA-PEG micelles. From the results, it seems likely that the hydrophobicity and therefore ability of the micelle/particle to retain drug generally is also a factor. The most hydrophobic 6:2 PLA-PEG particles perform significantly better than the 4:2 PLA-PEG particles, and the more hydrophobic 1.5:2 PLA-PEG performs better than 2:5 PLA-PEG. The serum stability of the radiolabel may therefore be partly determined by the ability of the micelles/particles to hold onto the indium-111-oxine through hydrophobic interactions and hydrogen bonding, and the more hydrophobic particles/micelles have a greater proportion of PLA available for such interactions. The results for the PLA-PEG particles are similar to those found with PLGA particles prepared by the solvent precipitation method, radiolabelled with indium-111-oxine and coated with Poloxamer 407 (Scholes, 1994). Here, the radiolabel was also released from the particles, with increasing time of incubation again giving an increase in label release. There was also a considerable release to the PBS in the control sample. This release was attributed to the solvent precipitation method used for preparation of the particles leading to rapid precipitation of the PLGA polymer causing highly porous nanoparticles. As the PLA-PEG particles are also produced by this method, it is reasonable that they would also be porous and that would allow the release of the ^{111}In , even when no serum is present. However, the effect of serum on the release of label from the PLA-PEG particles is still significant, with a further 29.8% released when serum is present for 4:2 PLA-PEG particles, and 20.5% released for 6:2 PLA-PEG particles.

6.3.3 Implications for *In vivo* Experiments

The leakage of the indium label from the PLA-PEG particles suggests that this radiolabel is not ideal, and although *in vivo* studies with indium-111-oxine will give some indication of the biodistribution of the particles, there is likely to be some error. Indium-111-oxine is known to have a low stability in serum, due to the ready formation of a complex between ^{111}In and the plasma protein transferrin (Jönsson and Strand, 1992). This is because the stability constant of the indium-transferrin is greater than that

Table 6.1

Stability of Indium-111-Oxine Radiolabel in 4:2 and 6:2 PLA-PEG Particles (mean \pm s.d.)

Sample	Incubation Media	Incubation Time	Radioactivity Retained by Particles (%)	Recovery (%)
4:2 PLA-PEG	50% v/v Serum	5 minutes	40.6 \pm 3.1	93.0 \pm 0.4
6:2 PLA-PEG	50% v/v Serum	5 minutes	57.9 \pm 6.5	90.6 \pm 3.5
4:2 PLA-PEG	50% v/v Serum	3 hours	25.6 \pm 0.5	98.4 \pm 4.5
6:2 PLA-PEG	50% v/v Serum	3 hours	40.4 \pm 0.0	95.2 \pm 1.9
4:2 PLA-PEG	50% v/v Serum	24 hours	18.8 \pm 0.2	96.2 \pm 0.6
6:2 PLA-PEG	50% v/v Serum	24 hours	34.1 \pm 2.8	98.3 \pm 4.3
4:2 PLA-PEG	PBS	3 hours	55.4 \pm 1.1	77.9 \pm 1.8
6:2 PLA-PEG	PBS	3 hours	60.9 \pm 3.1	81.3 \pm 3.5
Free ¹¹¹ In	50% v/v Serum	3 hours	3.8 \pm 0.4	99.3 \pm 2.3

of indium-oxine (log K's = 30 and 11 respectively) (Thakur and McKenney, 1985; Jönsson and Strand, 1992). Free ionic indium has also been shown to bind quickly with transferrin when injected into the blood (Goodwin *et al*, 1971; Jönsson and Strand, 1992). Therefore, it is important to consider these possible problems when interpreting the *in vivo* data for the PLA-PEG micelles and particles.

6.4 BIODISTRIBUTION OF PLA-PEG MICELLES AND PARTICLES

6.4.1 Introduction

The *in vivo* fate of PLA-PEG micelles and particles will be affected by all the properties discussed so far in this thesis and those outlined in chapter one. These include: -

- 1) the lengths of the hydrophobic PLA block and the hydrophilic PEG block,
- 2) the size of the micelle/particle,
- 3) the length of the PEG chain at the surface of the micelle/particle,
- 4) the density of PEG at the surface, and
- 5) the steric stability of the micelle/particle (as determined by stability in the presence of salt).

The presence of any incorporated drug in the core of the micelles/particles may also affect the biodistribution properties of these copolymers, if it affects the properties of the systems.

Due to the special skills required, the animal studies were performed with other members of the research group who were trained in the methods and carried them out regularly.

6.4.2 Preparation of Radiolabelled PLA-PEG Micelles and Particles for Biodistribution Studies

Biodistribution studies on PLA-PEG micelles were performed in female wistar rats, with the 1.5:2 and 2:5 PLA-PEG copolymers. Two concentrations of the micelle-forming PLA-PEG copolymers were selected on the basis that on dilution in the blood, the lower concentration system would be expected to revert to a non-associated copolymer, while the higher concentration system would be expected to remain above the cmc for a significant period *in vivo*. [Assuming a blood volume of 7.5% of body weight and a 150g rat, the lower concentration (0.2% w/v, 0.1 ml) in blood would be at 0.0008% w/v, and the higher concentration (5.4% w/v, 0.5 ml) would be at 0.24% w/v in the blood initially

($cmc=0.0035\%$ w/v); V_d is not considered in this case since unknown]. For the lower PLA-PEG copolymer concentration (0.2% w/v), an aqueous dispersion (1% w/v) was prepared by adding 100mg of the PLA-PEG copolymer (1.5:2 and 2:5) to 10 ml of water containing a radiolabelled marker, hydrophobic indium-111-oxine complex (0.2 ml, 2.5 MBq) and shaking until the polymer dissolved. For the higher PLA-PEG concentration (5.4% w/v), indium-111-oxine solution (0.005 ml - 0.021 ml) was added to 1% w/v dispersions of fractionated PLA-PEG and left for 30 minutes to equilibrate. For both concentrations, free indium was separated from incorporated indium using a sepharose CL-4B gel permeation column (10 cm) equilibrated with distilled water. At the lower concentration, the PLA-PEG dispersions were collected and diluted to the required concentration. At the higher concentration, the eluent was monitored and the most active fractions pooled for the *in vivo* experiment. Radiolabelled dispersions were then mixed with concentrated fractionated PLA-PEG polymers to give a dispersion of 5.4% w/v. Different preparation methods were used for the two PLA-PEG concentrations studied, as at the higher concentration, experiments showed that the PLA-PEG dispersion would have undergone significant dilution on the PD10 column, and resolution of the GPC technique was also low. Therefore, an unreasonable amount of PLA-PEG material would have been required to prepare the PLA-PEG dispersion this way, and some free indium-111-oxine may not have been separated from the PLA-PEG micelle peak.

Radiolabelled 4:2 and 6:2 PLA-PEG particles (10 ml, 1% w/v, 0.0025 ml ^{111}In) were prepared in water as described in the serum stability experiment (section 6.3.1). Free indium was again separated from labelled particles by GPC using a sepharose CL-4B column (10 cm) and purified water as eluent. The most active fractions were pooled to be injected for the biodistribution studies.

6.4.3 Rat Biodistribution Studies

Radiolabelled 1.5:2 and 2:5 PLA-PEG micelles (0.2% w/v, 0.1 ml; 5.4% w/v, 0.5 ml) were injected into groups of three female Wistar rats (150 g \pm 10 g) via the tail vein. Blood samples (10 μ l) were taken from the tail at 0.25, 0.5, 1, 2 and 3 hours post injection. At 3 hours post-injection the rats were sacrificed and the liver, spleen, lungs, kidneys and one femur removed. The remaining activity in the organs and blood was counted using a gamma spectrometer (Compugamma, LKB, Wallac, Finland), and the

carcass activity determined, for the higher concentration study, using a well counter (EG and G Ortec, Bracknell, UK). Free indium-111-oxine was similarly studied as a control.

This experiment was performed in collaboration with Susan E. Dunn.

4:2 and 6:2 PLA-PEG particles were injected (0.3 ml, 1 mg) into groups of three female Wistar rats (150 g \pm 10 g) via the tail vein. Blood samples (20 μ l) were taken from the tail at 0.25, 0.5, 1, 2 and 3 hours post injection. At 3 hours post-injection the rats were sacrificed and the liver, spleen, lungs, kidneys and one femur removed. The remaining activity in the organs, blood and carcass were counted as for the micelles. Free indium-111-oxine was again studied as a control. This experiment was performed in collaboration with Helen Redhead.

6.4.4 Results of Biodistribution Studies on PLA-PEG Micelles

The biodistribution results are presented in Figure 6.6 and the blood clearance in Figure 6.7, with control values for free indium oxine also included. The results are expressed as a percentage of the injected dose and are a mean of the three rats \pm standard deviation (s.d.). The liver and spleen can be considered to represent the reticuloendothelial system (RES). Data for lung, kidney and femur are not presented, since the radioactivity associated with these organs was found to be negligible.

The free indium oxine was partly taken up by the liver, but also circulated in the blood at a significant level for the three-hour period of the study. At low concentrations, both of the PLA-PEG copolymers appeared to be directed specifically to the liver with no increase in spleen uptake levels. Also, blood levels dropped quite rapidly. In contrast, at the higher concentrations of copolymer in the blood, there were marked differences between the two copolymers. The 2:5 PLA-PEG dispersion showed a similar liver and spleen activity levels to that seen with the lower concentrations. However, the 1.5:2 PLA-PEG exhibited an improved biodistribution, namely a greatly reduced liver uptake in comparison to the lower concentration and a corresponding increase in the circulating blood levels. The 2:5 PLA-PEG copolymer at the higher concentration differed from the lower concentration only by a slightly higher kidney uptake and attainment of a stable blood activity at around 10% of the injected dose.

Table 6.2

Blood Clearance Values for High and Low Concentration PLA-PEG Micelle In vivo Studies

Blood Activity	Percentage of Total Dose Injected (%)				
	Indium-111-Oxine	1.5:2 PLA-PEG 5.4 %w/v	2:5 PLA-PEG 5.4 %w/v	1.5:2 PLA-PEG 0.2 %w/v	2:5 PLA-PEG 0.2 %w/v
After 1 hour	23.7 ± 14.9	22.7 ± 8.4	14.1 ± 4.9	0.0 ± 3.0	14.2 ± 9.3
After 2 hours	11.3 ± 6.1	19.1 ± 5.3	10.9 ± 4.2	0.0 ± 0.0	0.0 ± 0.0
After 3 hours	12.1 ± 9.7	19.3 ± 7.6	10.5 ± 1.8	2.1 ± 0.0	0.0 ± 0.0

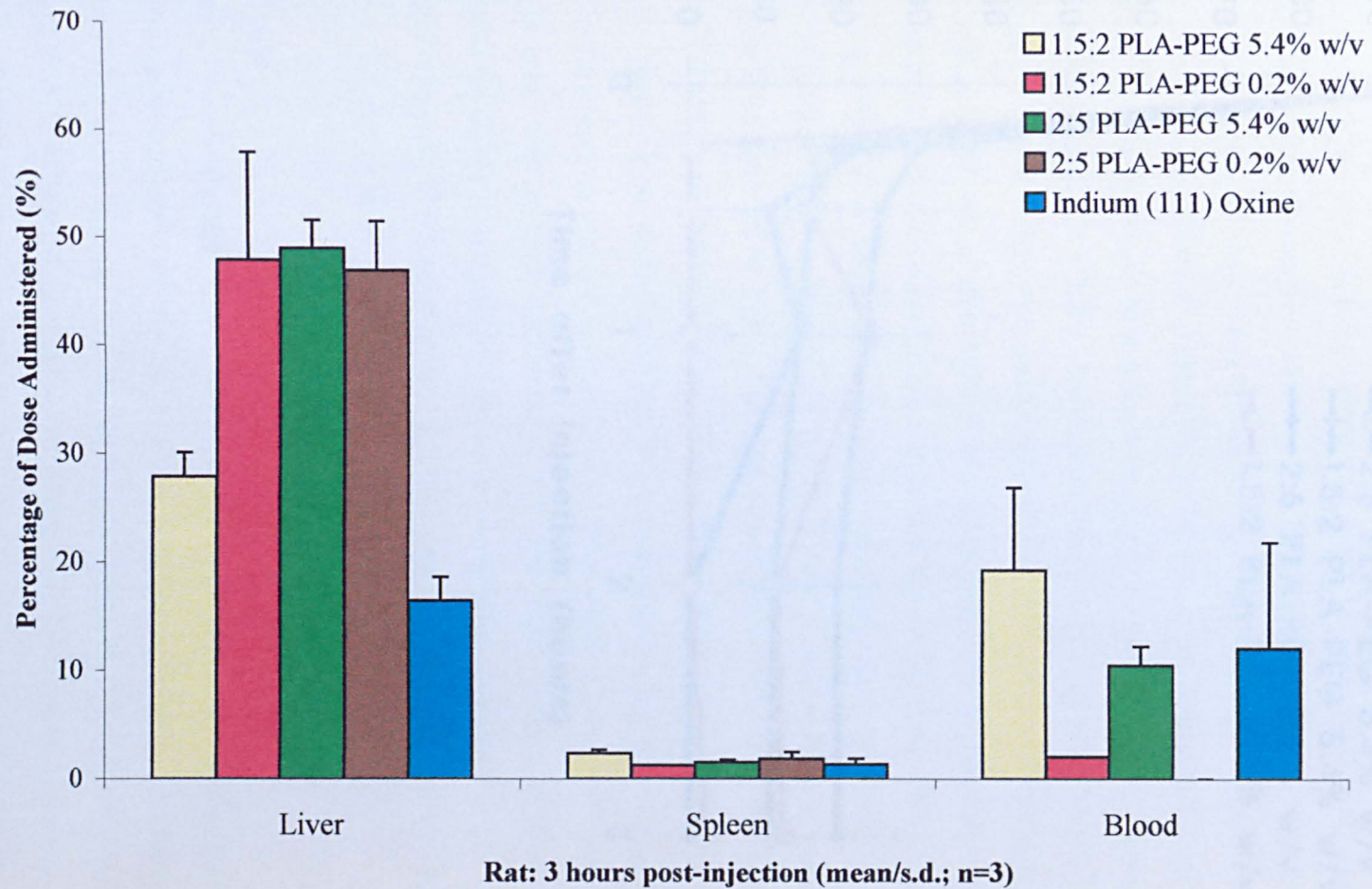
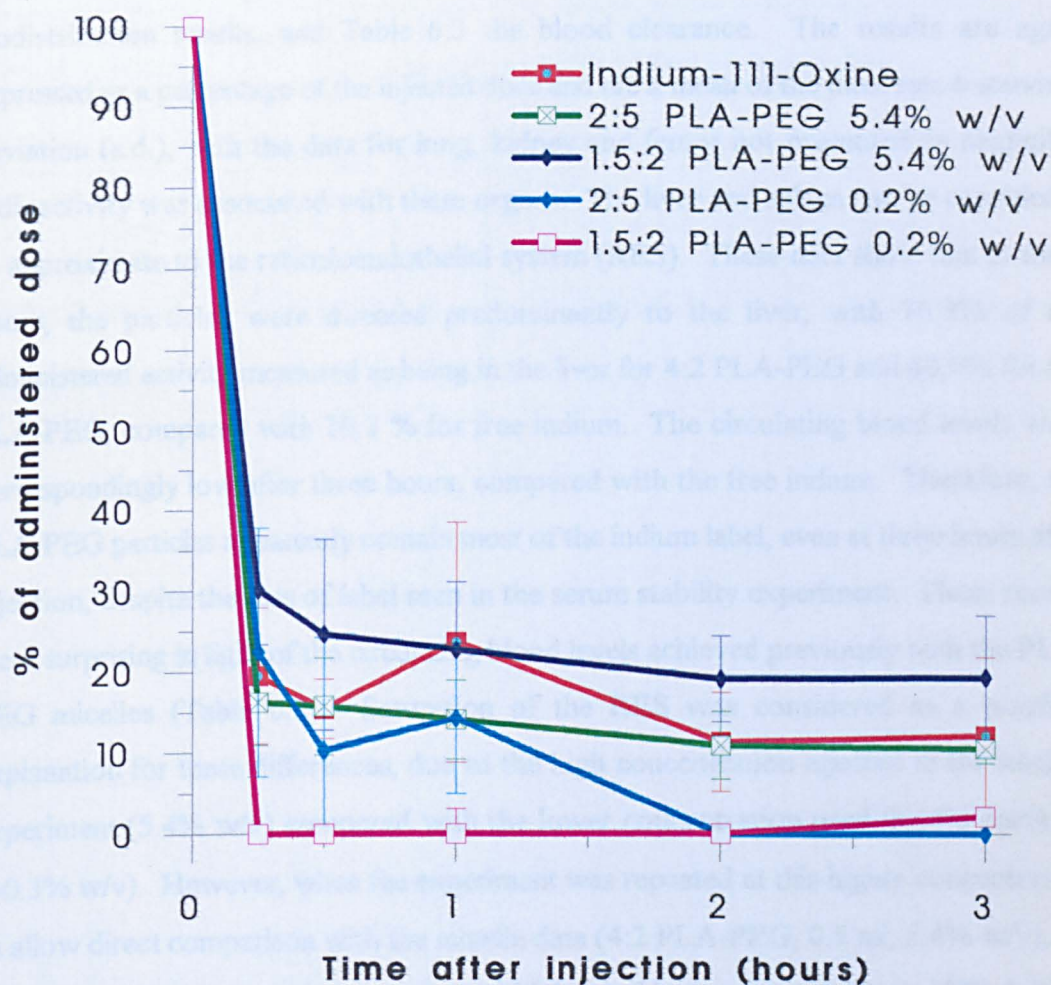
Figure 6.6 - Data from Biodistribution Studies of Purified 1.5:2 and 2:5 PLA-PEG Micelles

Figure 6.7 - Blood Elimination Curves for 1.5:2 PLA-PEG, 2:5 PLA-PEG and Indium-111-Oxine in the Rat Model



6.4.5 Results of Biodistribution Studies on PLA-PEG Particles

The biodistribution study was performed for the 4:2 and 6:2 PLA-PEG particles, labelled with indium (111) oxine, and with free indium as a control. Figure 6.8 shows the biodistribution results, and Table 6.3 the blood clearance. The results are again expressed as a percentage of the injected dose and are a mean of the three rats \pm standard deviation (s.d.), with the data for lung, kidney and femur not presented as negligible radioactivity was associated with these organs. The liver and spleen can be considered to approximate to the reticuloendothelial system (RES). These data show that at three hours, the particles were directed predominantly to the liver, with 76.5% of the administered activity measured as being in the liver for 4:2 PLA-PEG and 68.0% for 6:2 PLA-PEG, compared with 10.1 % for free indium. The circulating blood levels were correspondingly low after three hours, compared with the free indium. Therefore, the PLA-PEG particles apparently contain most of the indium label, even at three hours after injection, despite the loss of label seen in the serum stability experiment. These results were surprising in light of the circulating blood levels achieved previously with the PLA-PEG micelles (Table 6.2). Saturation of the RES was considered as a possible explanation for these differences, due to the high concentration injected in the micelle experiment (5.4% w/v) compared with the lower concentration used for the particles (\approx 0.3% w/v). However, when the experiment was repeated at this higher concentration to allow direct comparison with the micelle data (4:2 PLA-PEG, 0.5 ml, 5.4% w/v), no significant difference was seen between the higher and lower concentrations of PLA-PEG particles. With the higher concentration, 1.9% of the administered dose was found in the blood at three hours and 74.4% in the liver, compared with 2.1% in the blood and 76.5% in the liver for the lower concentration.

6.4.6 Discussion

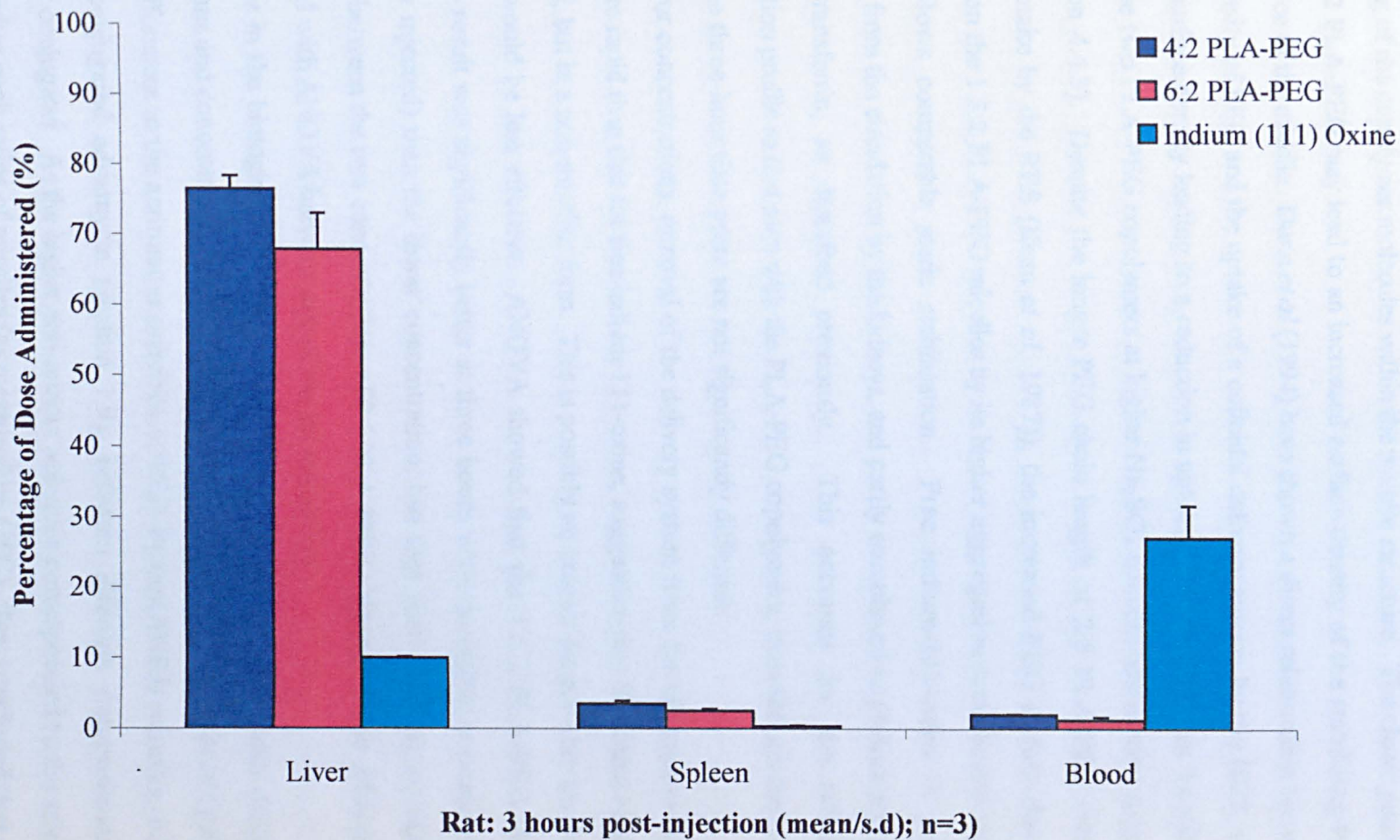
Two different concentrations of PLA-PEG copolymer dispersions were investigated as delivery systems *in vivo* in the rat model. Micelles were expected to be present in the blood at the higher concentration. The biodistribution results showed improved results for the 1.5:2 PLA-PEG compared with the 2.5 PLA-PEG at the higher concentration. ANOVA statistical analysis was performed on the results (Dunn, 1995) and showed that

Table 6.3

Blood Clearance Values for PLA-PEG Particle In vivo Studies

Blood Activity	Percentage of Total Dose Injected (%)		
	Indium-111-Oxine	4:2 PLA-PEG	6:2 PLA-PEG
After 1 hour	37.3 ± 5.7	4.8 ± 0.8	3.3 ± 0.6
After 2 hours	29.8 ± 9.7	2.7 ± 0.2	1.8 ± 0.3
After 3 hours	27.1 ± 4.6	2.1 ± 0.1	1.4 ± 0.4

Figure 6.8 - Data from Biodistribution Studies of Purified 4:2 and 6:2 PLA-PEG Particles



the liver uptake of the higher concentration 1.5:2 PLA-PEG copolymer was significantly improved over both 2:5 PLA-PEG systems and the lower concentration 1.5:2 PLA-PEG.

This difference between the two copolymers probably reflects differences in the stability and packing of the copolymer molecules within the micelle structure. The closer packing of the 1.5:2 PLA-PEG may lead to an increased surface density of the stabilising PEG at the surface of the micelle. Dunn *et al* (1994) have shown a direct relationship between surface density of PEG and the uptake of a colloidal delivery system by the RES, with increased surface density leading to a reduction in uptake. The similarity in T_c values between the two PLA-PEG copolymers at higher Na_2SO_4 concentrations also support this (section 4.4.3). Despite the longer PEG chain length of 2:5 PLA-PEG (which reduces uptake by the RES (Illum *et al*, 1987)), the increased PEG surface density conferred on the 1.5:2 PLA-PEG micelles by its higher aggregation number and closer packing allows comparable steric stabilisation. Free indium-111-oxine is partly eliminated from the circulation by the kidneys, and partly complexed to plasma proteins such as transferrin, as described previously. This accounts for the different biodistribution profile to that seen with the PLA-PEG copolymers, even though the blood levels at the three-hour time point are not significantly different.

At the lower concentrations, removal of the delivery system from the circulation to the liver is more rapid than that for free indium-111-oxine, suggesting that the oxine remains complexed, but in a non-micellar form. This is possibly an unimer form where the steric shielding would be less effective. ANOVA showed that the 1.5:2 PLA-PEG blood circulation result was significantly better at three hours with the higher concentration (5.4% w/v injected) than the lower concentration, but that there was no significant difference between the two concentrations of 2:5 PLA-PEG. No significant differences were found with ANOVA between any of the spleen values.

Differences in the biological behaviour of micelle-forming copolymers with different compositions and concentrations have been noted previously. Yokoyama *et al* (1994d) noticed differences in the antitumour activities of PEG-P(Asp(ADR)) micelles, where ADR is conjugated adriamycin (section 1.9), between different compositions of copolymer conjugates. As the higher anti-tumour activities corresponded to the samples with the higher peak ratios of micelles (as measured by GPC), they concluded that only the compositions of PEG-P(Asp(ADR)) which formed micelles were effectively delivered to the tumours. Non-associated PEG-P(Asp(ADR)) was not effective in inhibiting

tumours in this study and would be expected to exist as free polymer chains and renally clear in less than one hour (Kwon *et al*, 1993). Free polymer chains with a molecular weight of less than 50,000 g mol⁻¹ have been shown to be renally cleared within minutes of intravenous injection (Kwon *et al*, 1994b), although this does not occur with the PLA-PEG copolymer molecules.

The results for the 4:2 and 6:2 PLA-PEG particles show a large accumulation in the liver.

There is no significant difference between the two different copolymer systems. This similarity between the two systems may be expected due to their similar PEG chain layer thicknesses (section 4.2.5) and similar response in the presence of salt (section 4.4.3).

However, the direction of the PLA-PEG particles predominantly to the liver was not expected. Previously in this thesis, the surface characteristics of these particles have been studied, and the presence of PEG identified at the surface of the particles. This PEG has also been shown (by XPS, section 4.3.4) to be of a similar surface density to that of particles coated with poloxamers and poloxamines, and PEG-grafted particles which have avoided the RES. Furthermore, the cloud point experiments (section 4.4.3) demonstrated steric stability in the presence of salt (sodium sulphate), which also suggests possibility for avoidance of the RES. It would therefore be surprising if the particles were unable to avoid RES capture, as is suggested by the high percentage of the injected dose found in the liver in these experiments. A possibility is that the particles have succeeded in extravasating through the fenestrations in the endothelium of the liver (section 1.3.1). If this occurred, the particles may be taken up by the hepatocytes that lie between the sinusoids of the liver. Roerdink *et al* (1984) showed that small unilamellar vesicles (diameter 25-80 nm) composed of sphingomyelin, cholesterol and phosphatidylserine (ratio 4:5:1) were taken up by the liver after intravenous injection into rats. They separated the liver cells into non-parenchymal cells (Kupffer cells), endothelial cells and parenchymal cells (hepatocytes) by elutriation centrifugation analysis. They found that although Kupffer cells were actively involved in the uptake of these vesicles, the parenchymal cells also took up substantial amounts. By comparison, the endothelial cells did not associate with the vesicles. Similarly, it is possible that the PLA-PEG particles are associating with the hepatocytes as their small size may allow them to penetrate through the fenestrations of the endothelial lining of the liver sinusoids. Further experimentation was therefore required to investigate the intrahepatic distribution of the injected PLA-PEG particles.

6.5 LIVER DISTRIBUTION STUDY OF 4:2 PLA-PEG PARTICLES

6.5.1 Method

To discover the fate of the PLA-PEG particles in the rat liver after intravenous injection, an experiment was performed, whereby 4:2 particles were radiolabelled and injected as described previously (section 6.4.2) into two female wistar rats ($150 \text{ g} \pm 10 \text{ g}$). The livers were removed after three hours, and examined using an adaptation of the method for the isolation of non-parenchymal cells described in Dunn (1995). After three hours, each rat was anaesthetised using an intraperitoneal injection of pentobarbitone (0.5 ml , 60 mg/ml) (Sagatal, Rhone Poulenc, Dagenham, UK). Each rat was then secured to a surgical board and the liver exposed, cannulated and perfused with HBSS (Hank's balanced salt solution) buffer ($\text{pH } 7.4$, $37 \text{ }^\circ\text{C}$, 10 ml/min), while massaging the liver to remove residual blood. This was followed by 100 ml of HBSS buffer containing 0.033% w/v collagenase type IV and 0.033% w/v calcium chloride at a slower flow rate of 3.2 ml/min , with continued massaging of the liver to breakdown the liver structure. The liver was then removed and washed with ice cold HBSS, before passing through a nylon gauze to generate the cellular components. The cell suspension was then centrifuged at 50 g for two minutes at $4 \text{ }^\circ\text{C}$ using a Heraeus Christ Minifuge T. Most of the hepatocytes collect as a pellet, so the supernatants were removed and the pellets resuspended and centrifuged for a further two minutes twice at 50g , with the pellets retained, to ensure complete removal of the hepatocytes. The activity in the pellets was then measured with a gamma counter. The combined supernatants were then centrifuged at 2500 rpm for 5 minutes at $4 \text{ }^\circ\text{C}$, with the pellets removed and retained. This was then repeated twice to ensure complete removal of cellular components. The remaining supernatants were then counted for activity using the gamma counter. The pellets were then resuspended in 10 ml of ice cold HBSS buffer. These pellets contained non-parenchymal cells, erythrocytes and other cellular debris. Two tubes containing 7 ml of Nycodenz density gradient (Nycoprep, Nycomed, Sweden) were then taken, and 5 ml of the resuspended pellet added to each tube. The tubes were mixed by inversion and 1 ml of cold HBSS buffer overlaid onto each tube before centrifuging at 2420 rpm for 15 minutes at $4 \text{ }^\circ\text{C}$. The non-parenchymal cells collect at the interface of the density gradient and buffer, and were removed carefully, using a plastic disposable pipette. The pellet, which had collected at the bottom of the Nycodenz tube was separated from the Nycodenz supernatant, and

both were counted for activity. The non-parenchymal cells were then washed with cold HBSS twice (2500 rpm, 5 minutes), resuspended in HBSS and both were counted for activity. The results therefore give a percentage of the activity associated with the cells and the other stages of the process.

This experiment was performed in collaboration with Helen Redhead and Jonathan Neal.

6.5.2 Results

Table 6.4 shows the results of this experiment, separated into parenchymal cells (hepatocytes) and non-parenchymal cells (Kupffer cells and endothelial cells). The difference in the activity in these cells and the total activity in the liver was distributed between the supernatant solutions and sedimented pellets of other liver constituents. These results show that there does not appear to be significant uptake of the PLA-PEG particles by the Kupffer cells of the RES, with less than 2% of the total injected dose measured in these cells. Conversely, there appears to be a significant amount of radioactivity associated with the hepatocytes.

6.6 GENERAL DISCUSSION OF *IN VIVO* STUDIES

The free indium-111-oxine control shows a distinctly different biodistribution pattern from the PLA-PEG micelles and particles. This indicates that indium-111-oxine incorporated in micelles and particles is sufficiently associated with the PLA-PEG polymers throughout the experiments, allowing the polymer micelles or particles to be followed, despite the results of the serum stability experiment. Yokoyama *et al* (1994a) noted a similar change in biodistribution patterns between free adriamycin and adriamycin conjugated to poly(aspartic acid)-poly(ethylene glycol) micelles, with the biodistribution of the adriamycin being noticeably different after micellar incorporation. The blood concentration of adriamycin was significantly lower than that for the micelles conjugated with adriamycin, and the micelles remained circulating in the blood for a much longer time period.

The micelles and particles give distinctly different biodistribution results when comparing the liver values and blood. Particle uptake of the 4:2 and 6:2 PLA-PEG by the liver is noticeably higher than the liver uptake for the 1.5:2 and 2:5 PLA-PEG micelles, although a significant amount of 2:5 PLA-PEG micelles are directed to the

Table 6.4

Location of 4:2 PLA-PEG Particles in the Rat Liver After Differential Centrifugation

Cell Subtype	Percentage of Accumulated Liver Dose (%)		Percentage of Total Dose Injected (%)	
	Liver (1)	Liver (2)	Rat (1)	Rat (2)
Parenchymal cells	33.9	28.1	23.9	21.3
Non-parenchymal cells	2.1	1.4	1.5	1.0
Total dose in liver (%)	-	-	70.5	75.9

liver. The 2:5 PLA-PEG micelles may behave similarly to the 4:2 and 6:2 PLA-PEG particles, considering the significant liver uptake (49.0% of the injected radioactivity dose) and the relatively low blood levels (10.5% of the injected radioactivity dose at three hours).

Analysis of the liver distribution experiment described above looks promising with more than 20% of the injected radioactivity found to be associated with the hepatocytes. Targeting of colloidal carriers to the hepatocytes could lead to better treatments for liver diseases such as cancer and hepatitis. However, the above experiment is very much a starting point, and the technique of centrifugation may not allow total separation of the different groups of cells, which may lead to error. It is also possible that part of the indium-111-oxine label could be released in these *in vitro* conditions, as the stability study above illustrated the significant release of the complex *in vitro*, both in PBS and serum. As no control was done to show the location of free ¹¹¹In in the liver (accumulation in the liver was low in the *in vivo* experiments at 10.1%), there is no guarantee that free indium is not affecting the results. This method of separating hepatocytes has also yet to be fully validated. It is clear therefore that although these results may be promising, further clarification is required.

The possibility that the radioactivity in the liver is due to some uptake by the RES must therefore be considered. It is interesting in the light of the *in vivo* results to note the difference between the 1.5:2 PLA-PEG chain layer thickness and the 4:2 and 6:2 PLA-PEG thicknesses. A PEG chain layer thickness of approximately 5-6 nm is considered reasonable to provide steric stabilisation for colloidal systems (Allen, 1994b). This thickness of the PEG chain would allow a large number of possible conformations of the PEG in aqueous solution, a high transition rate from one conformation to another, with increased mobility of the chains. This would therefore decrease the probability of the proteins in the blood adsorbing to the micelle/particle surface, and hence decrease uptake by the RES. With the smaller PEG layer thicknesses involved with the 4:2 and 6:2 PLA-PEG particles, the mobility, the number of conformations and the transition rate of the PEG chains will be reduced, increasing the risk of protein adsorption. If the uptake is by the RES, this may be significant in considering why the 1.5:2 PLA-PEG micelles circulate for longer time periods in the blood compared with 4:2 and 6:2 PLA-PEG which are quickly taken up by the liver. As already discussed, the PEG chain length and layer thickness has to be of a requisite value before steric repulsion will occur, and the surface

density of the PEG is also important. Although the 4:2 and 6:2 PLA-PEG particles may have the required PEG surface density (shown by the XPS results), the PEG chain layer thickness is shorter and less hydrated than for the 1.5:2 PLA-PEG micelles, despite having the same PEG chain length of 2000. Conversely, the 2:5 PLA-PEG micelles have a significantly longer chain length of 7.47 nm, but due to this higher hydrophilicity (PEG chain length of 5000), it has a lower association number and hence, an expected lower surface density of PEG. As the combination of both PEG chain layer thickness and surface density are thought to be important, it is conceivable that the PLA-PEG micelles and particles are being taken up by the RES.

The high percentage of PLA-PEG particles in the liver at three hours may be related to particle size. It has been illustrated with liposomes composed of phosphatidylcholine, cholesterol and the ganglioside GM₁ with diameters less than 70 nm, that 70% of the injected doses were directed to the liver (Liu *et al*, 1992), which is similar to the PLA-PEG results. The authors concluded that this was presumably due to uptake by the parenchymal cells. Similarly, for PEG-containing liposomes, regardless of the phospholipid composition, it was observed that those with diameters of less than 90 nm were predominantly taken up by the liver (Allen, 1994b). More recently, Litzinger *et al* (1994) used fluorescence microscopy to explore the uptake of smaller liposomes (i.e. less than 70 nm diameter) composed of dioleoyl-N-(monomethoxypoly(ethylene glycol)succinyl)-phosphatidylethanolamine (PEG-PE) by the liver. The liposomes were labelled with DiI (1,1'-dioctadecyl-3,3,3',3'-tetramethylindocarbocyanine perchlorate) and used to examine the intrahepatic distribution. Liposomes of less than 70 nm were not detected in areas corresponding to the parenchymal cells, but were found to be localised in the Kupffer cells. However, it was also considered that due to the spread of the hepatocytes over a relatively large area of the liver, any fluorescence associated with the hepatocytes might be too dispersed to be detected by this technique. Therefore, it could not be conclusively stated that there was no association with hepatocytes by the small liposomes, although it appears that Kupffer cell uptake accounts for at least some of the liver uptake. Furthermore, Liu *et al* (1992) investigated the effects of RES blockade with dextran sulphate 500 on the fate of liposomes containing GM₁. They found no significant difference before and after blockade, whereas if the liposomes were in the Kupffer cells, a decrease in the liver uptake would be expected. Litzinger *et al* (1994) further explored their findings by studying protein adsorption to the PEG-PE liposomes. They found that

the small liposomes bound protein much more avidly than the larger liposomes, with the ratio of protein to lipid increased to approximately 45-fold more for the smaller liposomes than for liposomes of average diameter 151 nm. Experiments where the percentage of PEG-PE in the liposomes was altered and then the liposomes exposed to the protein streptavidin, gave similar results. For the same concentration of PEG-PE, the smaller liposomes bound 20% of the available streptavidin compared with 3% for the larger liposomes (PEG-PE concentration of 5.0 mol%). This greater protein adsorption by the small liposomes was attributed to an increase in their curvature compared with larger liposomes, such that the extended PEG chains splay to a greater degree, allowing protein to penetrate to the more hydrophobic surface. This may also explain why the 1.5:2 PLA-PEG micelles manage to avoid uptake by the liver better than the other PLA-PEG systems. The increased surface density of PEG of the 1.5:2 PLA-PEG micelles over the 2:5 PLA-PEG micelles, combined with the PEG chain layer thickness, prevents protein adsorption. However, the surface density of the 2:5 PLA-PEG micelles is not enough to prevent the proteins from penetrating to the hydrophobic PLA core, despite the longer chain length.

Although the results for the 1.5:2 PLA-PEG copolymer are encouraging, longer circulation times have been obtained with micelles elsewhere. Stable micelles of less than 100 nm in size were prepared from an ABA block copolymer, poly(oxyethylene-b-isoprene-oxyethylene) (POE-PI-POE), by crosslinking the chains in the hydrophobic (polyisoprene) core. These nonbiodegradable micelles were shown to remain in circulation in mice with a half life of more than 50 hours (Rolland *et al*, 1992).

Kwon *et al* (1993) have demonstrated long circulation times in blood in mice using poly(aspartic acid) P(Asp)-poly(ethylene glycol), PEG-P(Asp(ADR)), block copolymer micelles, conjugated with adriamycin. For one copolymer (Mw P(Asp) = 2100, PEG = 12000), approximately 68% and 10% of the injected dose were still present in the blood after four hours and twenty-four hours respectively. A corresponding low uptake in the liver and spleen of 28% and 3.5% at twenty-four hours was observed for this copolymer conjugate. The long circulation of these micelles in the blood was attributed to the low interaction between the PEG corona outer region of the micelles and the biocomponents. They noted that relatively longer PEG block lengths and shorter P(Asp) blocks gave better circulation times and lower RES uptake.

6.7 SUMMARY

Serum stability studies have been performed to investigate the stability of the radioactive label, indium-111-oxine, when incubated in 50% v/v rat serum for five minutes, three hours and 24 hours at 37 °C. These indicated that although the radiolabel was incorporated efficiently into the micelles and particles, a proportion was rapidly released on exposure to the serum. This bound to the serum proteins (illustrated by GPC), probably mostly to transferrin. The percentage of radiolabel bound to the serum proteins increased as the incubation time increased, with a corresponding decrease in the ¹¹¹In associated with the PLA-PEG particles.

However, *in vivo* studies in the rat showed that the indium-111-oxine appeared to remain associated with the PLA-PEG systems, giving markedly different biodistribution results to that of free indium-111-oxine. PLA-PEG micelles demonstrated extended circulation times in the blood during the period of study (three hours). The 1.5:2 PLA-PEG showed increased blood levels and lower uptake of the micelles by the liver compared with the 2:5 PLA-PEG micelles. This is thought to be due to differences in the packing density of the copolymer molecules on the micelle surface.

PLA-PEG particles, however, were directed to the liver. This could be due to their ability to penetrate through the fenestrations of the liver sinusoids and hence associate with the hepatocytes. A liver distribution experiment with the 4:2 PLA-PEG particles showed more than 20% of activity associated with the hepatocyte fraction. However, it is still possible that some RES uptake by the Kupffer cells is occurring, as has been shown previously with PEG-PE-liposomes (Litzinger *et al*, 1994).

CHAPTER SEVEN

OVERVIEW AND FUTURE WORK

7.1 SUMMARY

Previous work in our group in the field of drug targeting has centred mainly on nondegradable particles, such as polystyrene. More recently, other polymers have been explored in an attempt to reproduce the findings of this earlier work with biodegradable polymers. The objectives of the research described in this thesis were to explore the potential of a group of biodegradable polylactide (PLA) and poly(ethylene glycol) (PEG) AB block copolymers for use as drug delivery systems. A range of four copolymers was available and these differed in the ratio of PLA to PEG in each copolymer. These copolymers are therefore defined by the molecular weight ratios of their polylactide to poly(ethylene glycol) components. This research aimed to characterise these copolymers through physicochemical analysis, drug loading and biodistribution in an appropriate animal model.

Copolymers of polylactide and poly(ethylene glycol) (PLA-PEG), which contained a higher proportion of the hydrophilic PEG block than the more hydrophobic PLA block per copolymer molecule, were able to self-disperse in water to form spherical non-ionic micelles. Two peaks were produced when the copolymers, 1.5:2 PLA-PEG and 2:5 PLA-PEG, were purified by gel permeation chromatography (GPC). The first peak was shown by analysis with dynamic light scattering (DLS) and transmission electron microscopy (TEM) to consist of spherical micelles, with a diameter of 15.6 nm for 1.5:2 PLA-PEG micelles and 18.9 nm for 2:5 PLA-PEG micelles. The second peak was a PLA-depleted species resulting from the synthesis, which did not form micelles. These micelle sizes were in the size range required for long circulation in the blood, and were also small enough to pass through the fenestrations in the liver endothelium.

Copolymers of polylactide and poly(ethylene glycol), which contained more of the hydrophobic PLA block than the PEG block per copolymer molecule, formed more stable “solid particle” structures when prepared by the solvent-precipitation method. These

particles were defined as 4:2 and 6:2 PLA-PEG, and again gave two peaks on GPC analysis, of which the first peak formed particles. The second peak was significantly smaller than for the micelle-forming copolymers. After analysis by DLS, particle sizes of 15.1 nm and 20.8 nm were determined for 4:2 PLA-PEG and 6:2 PLA-PEG particles respectively. Particle formation of this magnitude was also noted with TEM and atomic force microscopy (AFM).

Surface analysis studies, by static secondary ion mass spectrometry (SIMS) and X-ray photoelectron spectroscopy, of the particle-forming PLA-PEG copolymers (4:2 and 6:2 PLA-PEG) showed PEG at the surface of both the copolymer in acetone and the particles in aqueous media. PEG surface density was also comparable with polymer systems that have shown avoidance of the reticuloendothelial system (RES) in the rat in *in vivo* studies. This indicated that the PLA-PEG particles should be able to avoid the major RES uptake seen with the hydrophobic PLA and PLGA particles. Stability testing in the presence of salt (sodium sulphate) also suggested that the micelles and particles had sterically stabilised surfaces. The PEG chain layer thicknesses were determined by rheological measurements for all four copolymers and found to vary from 2.3 nm to 7.5 nm. The greatest chain layer thickness of 7.5 nm was seen with 2:5 PLA-PEG, which has a longer PEG chain length of 5000 gmol⁻¹, compared with 2000 gmol⁻¹ for the other three copolymers. Despite having the same chain length of 2000 gmol⁻¹, 1.5:2 PLA-PEG micelles had a larger PEG chain layer thickness and greater hydration than the 4:2 and 6:2 PLA-PEG particles.

Testosterone and Sudan Black B (SBB), which have different hydrophobicities, were used as “model drugs” to evaluate the drug loading ability of the micelles and particles.

Ultracentrifugation sedimentation velocity studies confirmed that the model drugs had been incorporated into the micelles and particles. Higher drug loading was obtained for the 1.5:2 PLA-PEG micelles than for the 2:5 PLA-PEG micelles, and the amounts incorporated into the particle forming PLA-PEG copolymers were higher than for the micelles. A general trend of increased drug loading with increased molecular weight of PLA-PEG copolymers was apparent, but more pronounced for the testosterone loading.

The amount of aromatic SBB incorporated into the PLA-PEG systems was substantial (59.0% w/w and over) compared with the steroidal testosterone, which was significantly

lower than SBB for all copolymers (less than 2% w/w). To investigate the reason for this, a range of testosterone esters of varying hydrophobicity were incorporated into 4:2 PLA-PEG particles, to study if hydrophobicity was the determining factor in drug incorporation. However, the difference in loading between the testosterone esters was small in comparison with the large difference observed with between testosterone and SBB. Therefore, it can be concluded that although hydrophobicity may play a role in drug loading, the aromatic nature of SBB is likely to be the more significant factor. This is because it is energetically more favourable to incorporate aromatic than aliphatic compounds (Nagarajan *et al*, 1986).

In vitro release studies, using 4:2 PLA-PEG particles loaded with SBB (37 °C, phosphate buffered saline, pH 7.4), were performed. These showed that after an initial small burst release over the first three hours of the study (approximately 14% of the SBB incorporated was released), the drug release was linear to the end of the experiment at twenty-eight days (when approximately 89% of SBB had been released). The burst release was probably due to SBB incorporated in the PEG layer at the surface of the particles. The possibility of using PLA-PEG particles as sustained release drug delivery systems is therefore illustrated by these results.

Having established that the PLA-PEG copolymers formed micelles and particles with PEG at the surface, and were able to incorporate and release drug, the *in vivo* fate of the systems was studied. A radioactive marker was needed to allow the biodistribution of the PLA-PEG systems to be determined. Indium-111-oxine was chosen, as it had previously been used with both PLA (Müller *et al*, 1988) and PLGA particles (Scholes *et al*, 1992), and was a lipophilic complex that should easily incorporate. This radiolabel was readily incorporated into the PLA-PEG micelles and particles, with a good incorporation efficiency. However, subsequent stability studies performed, at 37 °C in 50% v/v rat serum, to assess the retention of the label by the particles in simulated *in vivo* conditions, showed that considerable ¹¹¹indium was lost from the PLA-PEG particles.

This became bound instead to serum components (most likely the protein transferrin, with which indium forms a more stable complex than with oxine). Three time points were studied: five minutes, three hours and 24 hours, and the percentage of radiolabel bound to the serum proteins increased as the incubation time increased, with a

corresponding decrease in particle-associated ^{111}In .

However, *in vivo* studies in the rat showed that the indium-111-oxine appeared to remain associated with the PLA-PEG systems, giving markedly different biodistribution results to that of free indium-111-oxine. PLA-PEG micelles, at high concentration, demonstrated extended circulation times in the blood during the period of study (three hours). The 1.5:2 PLA-PEG showed increased blood levels and lower uptake of the micelles by the liver compared with the 2:5 PLA-PEG micelles. This is thought to be due to differences in the packing density of the copolymer molecules on the micelle surface.

The PLA-PEG particles were directed to the liver on intravenous injection into the rat model. Further studies are necessary to elucidate whether the particles have been captured by the reticuloendothelial system or if their small size has allowed them to penetrate through the fenestrations of the liver sinusoids and associate with the hepatocytes. A liver distribution experiment with the 4:2 PLA-PEG particles showed more than 20% of activity associated with the hepatocyte fraction. Some RES uptake by the Kupffer cells may still be occurring, as has been shown previously with PEG-PE-liposomes (Litzinger *et al*, 1994).

7.2 FUTURE WORK

PLA-PEG copolymers have been successfully characterised in this thesis and show promise for the future. The requirements of having sterically stabilised systems with PEG at the surface and a hydrophobic core for drug incorporation have been fulfilled, and the micelles and particles are sub-200 nm in size. Furthermore, substantial model drug has been incorporated, and released from PLA-PEG systems. This work therefore gives a promising basis for further study of these copolymers and the possibility of a biodegradable drug delivery system, which could be used for drug targeting purposes. However, the range of copolymers studied so far has been fairly limited. This has made it difficult in some cases to predict the trends of the data collected. Expanding the range of copolymers will therefore allow more information to be gained from results and increase the understanding of these systems. In some areas, such as the rheological experiments to calculate PEG chain layer thickness, expanding both the particle-forming

systems and the micelle-forming systems would be useful. This would allow insight into the effect of having a micellar or particulate system on the PEG chain layer thickness.

As the micelle-forming copolymers have also been used as coatings for polystyrene or PLGA particles, a comparison of the PEG chain layer thickness values of 1.5:2 PLA-PEG and 2:5 PLA-PEG physically adsorbed onto these particles with the micelle values would give information on the difference between the PEG chain layer thickness of self-forming systems as opposed to coated systems. The density of PLA-PEG copolymers should also be measured to verify the assumption made in the rheology work that the density of PLA-PEG copolymers $\approx 1 \text{ gcm}^{-3}$. Small angle neutron scattering (SANS) could also be performed on the PLA-PEG copolymers to provide comparative values of the hydrophobic core radius, R_c and PEG chain layer thickness, Δ .

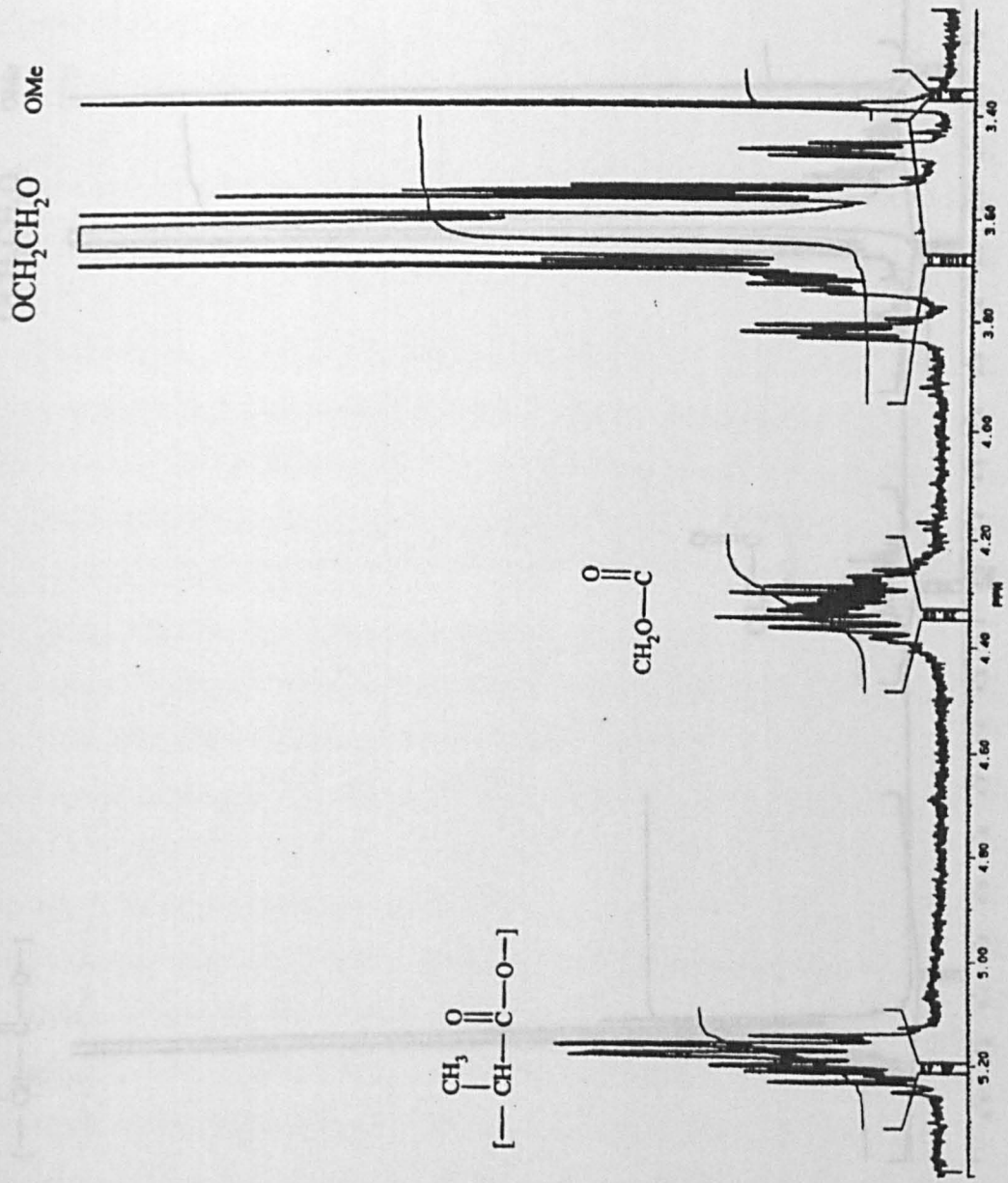
Drug loading of PLA-PEG copolymer systems has been fairly successful so far. However, more pharmaceutically relevant drugs should be explored in later work. The *in vitro* release studies also look promising, and studies performed at different concentrations of SBB are required to study the effect of drug loading on release. Determination of the glass transition temperatures (T_g) of PLA-PEG copolymers by differential scanning calorimetry (DSC) would give a comparison of the release rate between the different PLA-PEG copolymers. The lower the glass transition temperature, the faster the release. Similarly, an in depth degradation study should be performed to determine whether drug release follows degradation of the copolymer. This has implications for *in vivo* fate of the PLA-PEG systems, as the PEG chains could be cleaved by hydrolysis, thus removing the hydrophilic steric shell. An *in vivo* drug release would also be of value.

Although the problems exposed in the serum stability experiment do not appear to have affected the *in vivo* results, finding a radiolabel that is more stable in the presence of serum would be instructive. A possible option is the complex, indium-111-DTPA-SA, (the distearylamine of diethylenetriaminepentaacetic acid), which has successfully been used by other researchers in drug delivery (Klibanov *et al*, 1991; Torchilin *et al*, 1994; Gref *et al*, 1994). The fate of PLA-PEG particles in the liver also needs investigating more closely, as discussed in chapter six, to discover if any of the PLA-PEG particles are associating with the hepatocytes or if the uptake is by the RES. If the RES is the source

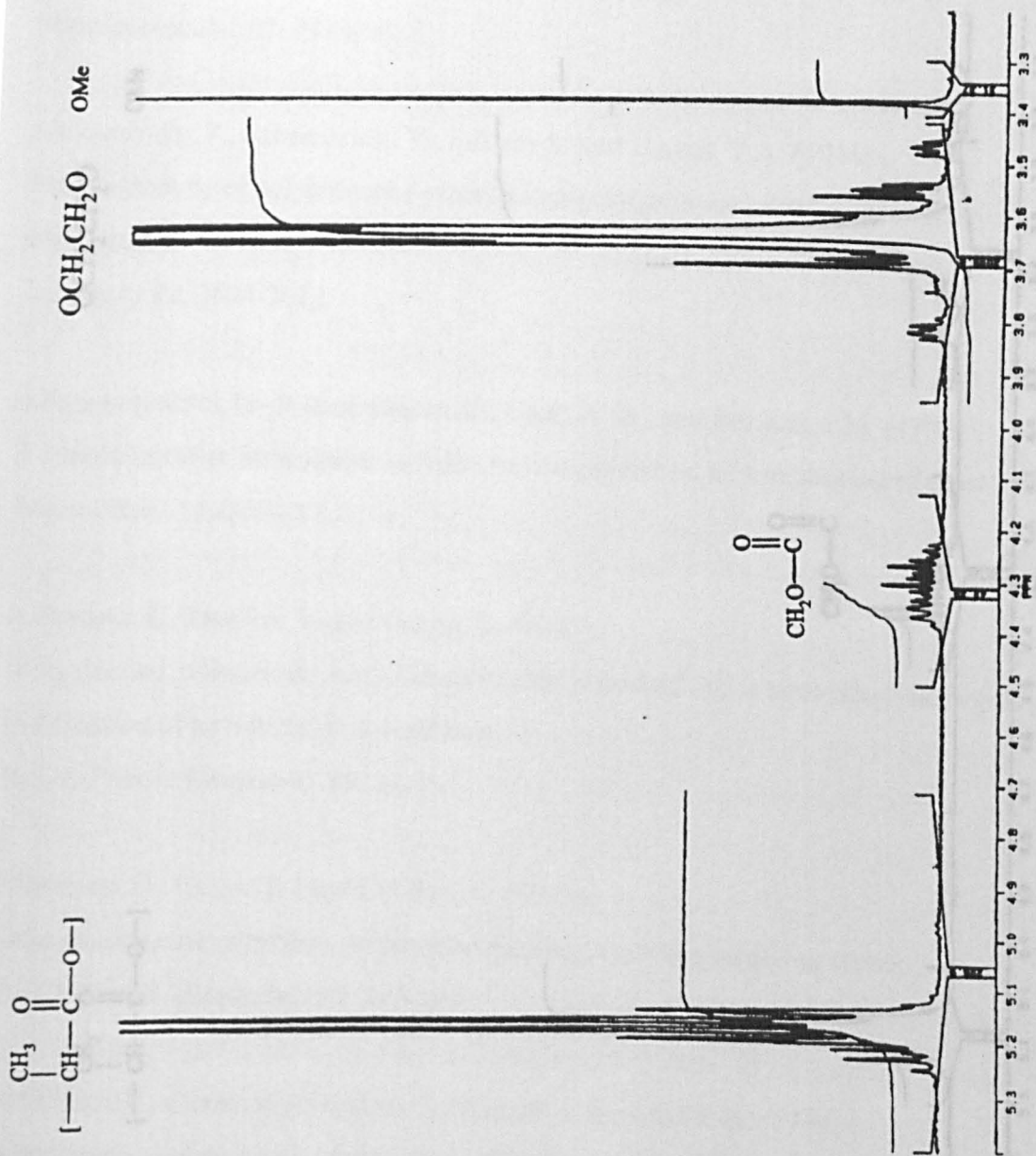
of uptake, then changing the copolymer block lengths or the particle preparation method to produce larger particles (preferably more than 70 nm) may resolve the problem. In conclusion, there is much scope for future work on the PLA-PEG copolymer series. The promise of a biodegradable drug delivery system for drug targeting may not yet be reality, but these systems represent a further step forward.

APPENDIX ONE (continued) (NMR) Trace of Peak One 1.5:2 LPLA-PEG

Nuclear Magnetic Resonance (NMR) Trace of Unfractionated 1.5:2 LPLA-PEG



Nuclear Magnetic Resonance (NMR) Trace of Peak One 1.5:2 LPLA-PEG



REPEATED Nuclear Magnetic Resonance (NMR) Trace of Peak Two 1.5:2 LPLA-PEG

Al-Saden, A.A., Whately, T.L., Florence, A.T. (1982)

Polyoxamer association in aqueous solution

J. Coll. Interface Sci. 90, 303-309

Alexandridis, P., Holzwarth, J.F. and Hatton, T.A. (1994a)

Micellization of poly(ethylene oxide)-poly(propylene oxide) triblock copolymers in aqueous solutions: thermodynamics of copolymer association

Macromolecules 27, 2414-2425

Alexandridis, P., Athanassiou, V., Patsis, S. and Hatton, T.A. (1994b)

Self-assembly activity of poly(ethylene oxide)-*b*-poly(propylene oxide) triblock copolymers

Langmuir 10, 2604-2612

Alkhatib-Gayut, H., Ramakrishnan, S., Chai, H.-B., and Pezzuto, J.M. (1994)

A mixed micellar formulation suitable for the parenteral administration of

Pharm. Res. 11, 206-212

Altomann, E., Doelker, E. and Gurny, R. (1993)

Drug loaded poly(lactic acid) nanoparticles produced by a reversed-phase emulsion process

Particulation of an injectable dosage form

Int. J. Pharm. Biopharm. 39, 13-18

Altomann, E., Gurny, R., and Doelker, E. (1993)

Drug loaded nanoparticles - preparation methods and drug targeting issues

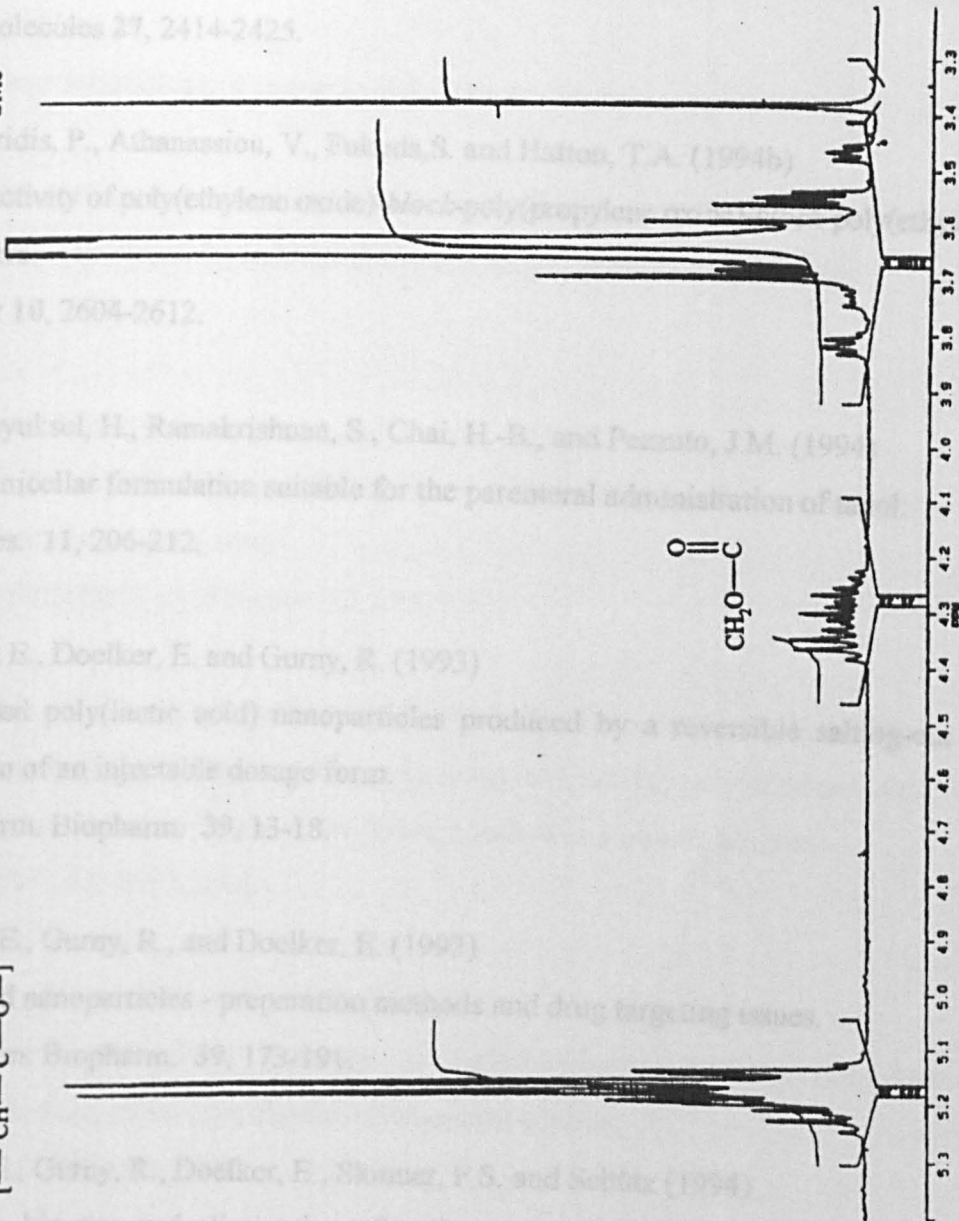
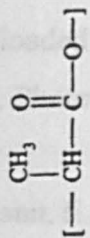
Int. J. Pharm. Biopharm. 39, 173-191

Altomann, E., Gurny, R., Doelker, E., Stauder, F.S. and Seiber (1994)

Distribution, kinetics and elimination of radiolabelled poly(lactic acid) nanoparticles after intravenous and intramuscular

OMe
OCH₂CH₂O

CH₂O-C



REFERENCES

Al-Saden, A.A., Whately, T.L., Florence, A.T. (1982)

Poloxamer association in aqueous solution.

J. Coll. Interface Sci. **90**, 303-309.

Alexandridis, P., Holzwarth, J.F. and Hatton, T.A. (1994a)

Micellization of poly(ethylene oxide)-poly(propylene oxide) triblock copolymers in aqueous solutions: thermodynamics of copolymer association.

Macromolecules **27**, 2414-2425.

Alexandridis, P., Athanassiou, V., Fukuda, S. and Hatton, T.A. (1994b)

Surface activity of poly(ethylene oxide)-*block*-poly(propylene oxide)-*block*-poly(ethylene oxide) copolymers.

Langmuir **10**, 2604-2612.

Alkan-Onyuksel, H., Ramakrishnan, S., Chai, H.-B., and Pezzuto, J.M. (1994)

A mixed micellar formulation suitable for the parenteral administration of taxol.

Pharm. Res. **11**, 206-212.

Allémann, E., Doelker, E. and Gurny, R. (1993)

Drug loaded poly(lactic acid) nanoparticles produced by a reversible salting-out process: Purification of an injectable dosage form.

Eur. J. Pharm. Biopharm. **39**, 13-18.

Allémann, E., Gurny, R., and Doelker, E. (1993)

Drug-loaded nanoparticles - preparation methods and drug targeting issues.

Eur. J. Pharm. Biopharm. **39**, 173-191.

Allémann, E., Gurny, R., Doelker, E., Skinner, F.S. and Schütz (1994)

Distribution, kinetics and elimination of radioactivity after intravenous and intramuscular

injection of ¹⁴C-savoxepine loaded poly(D,L-lactic acid) nanospheres to rats.

J. Contr. Rel. **29**, 97-104.

Allémann, E., Rousseau, J., Brasseur, N., Kudrevich, S.V., Lewis, K., and van Lier, J.E. (1996)
Photodynamic therapy of tumours with hexadecafluoro zinc phthalocyanine formulated in PEG-coated poly(lactic acid) nanoparticles.

Int. J. Cancer **66**, 821-824.

Allen, T.M. (1984)

Chapter 8, 116-119.

In *Liposome Technology*, Volume 1. Ed. Gregoriadis, G.

Allen, T.M. (1994a)

Long-circulating (sterically stabilized) liposomes for targeted drug delivery.

TiPS **15**, 215-220.

Allen, T.M. (1994b)

The use of glycolipids and hydrophilic polymers in avoiding rapid uptake of liposomes by the mononuclear phagocyte system.

Advanced Drug Delivery Reviews **13**, 285-309.

Almgren, M., van Stam, J., Lindblad, C., Li, P., Stilbs, P. and Bahadur, P. (1991)

Aggregation of poly(ethylene oxide)-poly(propylene oxide)-poly(ethylene oxide) triblock copolymers in the presence of sodium dodecyl sulfate in aqueous solution.

J. Phys. Chem. **95**, 5677-5684.

Almgren, M., Brown, W. and Hvidt, S. (1995)

Self-aggregation and phase behavior of poly(ethylene oxide)-poly(propylene oxide)-poly(ethylene oxide) block copolymers in aqueous solution.

Colloid Polym. Sci. **273**, 2-15.

Alonso, M.J., Gupta, R.K., Min, C., Siber, G.R., and Langer, R. (1994)

Biodegradable microspheres as controlled-release tetanus toxoid delivery systems.

Vaccine **12**, 299-306.

Amiji, M. and Park, K. (1992)

Prevention of protein adsorption and platelet adhesion on surfaces by PEO/PPO/PEO triblock copolymers.

Biomaterials **13**, 682-692.

Amiji, M. and Park, K. (1994)

Surface modification of polymeric biomaterials with poly(ethylene oxide) - A steric repulsion approach.

ACS Symp. Series **540**, 135-146.

Andrade, J.D., Smith, L.M. and Gregonis, D.E. (1985)

The contact angle and interface energetics, 263-264.

In Surface and Interfacial Aspects of Biomedical Polymers, Volume 1.

Ed. Joseph D. Andrade Plenum Press, London.

Armstrong, T.I., Davies, M.C., and Illum, L. (1997)

Human serum albumin as a probe for protein adsorption to nanoparticles: Relevance to biodistribution.

J. Drug Targeting **4**, 389-398.

Amarnson, T. and Elworthy, P.H. (1981)

Effects of structural variations of non-ionic surfactants on micellar properties and solubilization: surfactants containing very long hydrocarbon chains.

J. Pharm. Pharmacol. **33**, 141-144.

Aso, Y., Yoshioka, S. and Terao, T. (1993)

Effects of storage on the physicochemical properties and release characteristics of progesterone-

loaded poly(*l*-lactide) microspheres.

Int. J. Pharm. **93**, 153-159.

Attwood, D., Elworthy, P.H., and Kayne, S.B. (1971)

Membrane osmometry of solubilized systems.

J. Pharm. Pharmac. **23**, Suppl., 77S-84S.

Attwood, D. and Florence, A.T. (1983)

Surfactant Systems: Their chemistry, pharmacy and biology.

Chapman and Hall, London.

Bader, H., Ringsdorf, H., and Schmidt, B. (1984)

Watersoluble polymers in medicine.

Angew. Makromol. Chemie **123/124**, 457-485.

Bahadur, P., Sastry, N.V., Marti, S. and Riess, G. (1985)

Micellar behaviour of styrene-isoprene block copolymers in selective solvents.

Coll. Surf. **16**, 337-346.

Bahadur, P. and Pandya, K. (1992)

Aggregation behavior of Pluronic P-94 in water.

Langmuir **8**, 2666-2670.

Bahadur, P., Pandya, K., Almgren, M., Li, P. and Stilbs, P. (1993)

Effect of inorganic salts on the micellar behavior of ethylene oxide-propylene oxide block copolymers in aqueous solution.

Colloid Polym. Sci. **271**, 657-667.

Barry, B.W., El Eini, D.I.D. (1976)

Solubilisation of hydrocortisone, dexamethasone, testosterone and progesterone by long-chain polyoxyethylene surfactants.

J. Pharm. Pharmac. **28**, 210-218.

Bazile, D., Prud'Homme, C., Bassoullet, M.-T., Marland, M., Spenlehauer, G. and Veillard, M. (1995)

Stealth Me.PEG-PLA nanoparticles avoid uptake by the mononuclear phagocytes system.

J. Pharm. Sci. **84**, 493-498.

Becher, P. (1961)

Nonionic surface-active compounds. IV. Micelle formation by polyoxyethylene alkanols and alkyl phenols in aqueous solution.

J. Coll. Sci. **16**, 49-56.

Bedells, A.D., Arafeh, R.M., Yang, Z., Attwood, D., Heatley, F., Padget, J.C., Price, C. and Booth, C. (1993)

Micellisation of diblock copoly(oxyethylene/oxybutylene) in aqueous solution.

J. Chem. Soc. Faraday Trans. **89**, 1235-1242.

Benita, S., Benoit, J.P., Puisieux, F. and Thies, C. (1984)

Characterization of drug-loaded poly(*d,l*-lactide) microspheres.

J. Pharm. Sci. **73**, 1721-1724.

Bergström, K., Österberg, E., Holmberg, K., Hoffman, A.S., Schuman, T.P., Kozlowski, A., and Harris, J.M. (1994)

Effects of branching and molecular weight of surface-bound poly(ethylene oxide) on protein rejection.

J. Biomater. Sci. Polymer Edn. **6**, 123-132.

Billmeyer Jr., F.W. and Altgelt, K.H. (1971)

The sizes of polymer molecules and the GPC separation, 3-12.

In Gel Permeation Chromatography. Edited by K. H. Altgelt and L. Segal. Marcel Dekker, Inc., New York.

Bjerrum, O.J., Bhakdi, S. and Rieneck, K. (1980)

Monitoring of detergent binding to amphiphilic proteins by means of micelles containing the hydrophobic dye sudan black B.

J. Biochem. Biophys. Meth. **3**, 355-366.

Bloß, P., Hergert, W.-D., Wohlfarth, C. and Wartewig, S. (1992)

Viscometric characterization of poly(oxyethylene)-*block*-poly(oxypropylene)-*block*-poly(oxyethylene) in aqueous solution.

Makromol. Chem. **193**, 957-973.

Blume, G., Cevc, G., Crommelin, M.D.J.A., Bakker-Woudenberg, I.A.J.M., Kluff, C., and Storm, G. (1993)

Specific targeting with poly(ethylene glycol)-modified liposomes: coupling of homing devices to the ends of the polymeric chains combines effective target binding with long circulation times.

Biochim. Biophys. Acta **1149**, 180-184.

Bodmeier, R. and McGinity, J.W. (1987)

The preparation and evaluation of drug-containing poly(*dl*-lactide) microspheres formed by the solvent evaporation method.

Pharm. Res. **4**, 465-471.

Bodor, N., Stek, E., Higuchi, T. (1975)

Delivery of a quaternary pyridinium salt across the blood-brain barrier by its dihydropyridine derivative.

Science **190**, 155-156.

Boucher, E.A. and Hines, P.M. (1976)

Effects of inorganic salts on the properties of aqueous poly(ethylene oxide) solutions.

J. Poly. Sci. **14**, 2241-2251.

Bridgett, M.J. (1993)

The control of bacterial adhesion to polymeric surfaces.

PhD Thesis, University of Nottingham.

Briggs, D. (1986)

SIMS for the study of polymer surfaces: a review.

Surf. Int. Anal. **9**, 391-404.

Briggs, D. (1989)

Recent advances in secondary ion mass spectrometry (SIMS) for polymer surface analysis.

British Polymer Journal **21**, 3-15.

Briggs, D., and Hearn, M.J. (1986)

Interaction of ion beams with polymers, with particular reference to SIMS.

Vacuum **36**, 1005-1010.

Brindley, A., Davis, S.S., Davies, M.C. and Watts, J.F. (1994)

Polystyrene colloids with surface grafted poly(ethylene oxide) as model systems for site specific drug delivery. Part 1: Preparation and surface chemical characterisation using SIMS and XPS.

J. Colloid Interface Sci. **171**, 150-161.

Brindley, A., Davies, M.C., Lynn, R.A.P., Davis, S.S., Hearn, J. and Watts, J. (1992)

The surface characterisation of model charged and sterically stabilised polymer colloids by SSIMS and XPS.

Polymer **33**, 1112-1115.

Burt, H.M., Jackson, J.K., Bains, S.K., Liggins, R.T., Oktaba, A.M.C., Arsenault, A.L. and Hunter, W.L. (1995)

Controlled delivery of taxol from microspheres composed of a blend of ethylene-vinyl acetate copolymer and poly(*d,l*-lactic acid).

Cancer Letters **88**, 73-79.

Buscall, R. and Ottewill, R.H. (1986)

The stability of polymer latices, 141-217.

In Polymer Colloids. Eds. Buscall, R., Corner, T. and Stageman, J.F. Elsevier Applied Science Publishers, London.

Carpenter, C.P., Woodside, M.D., Kinkead, E.R., King, J.M., and Sullivan, L.J. (1971)

Response of dogs to repeated intravenous injection of polyethylene glycol 4000 with notes on excretion and sensitization.

Toxicology and Applied Pharmacology **18**, 35-40.

Chen, G.Q., Lin, W., Coombes, A.G.A., Davis, S.S., and Illum, L. (1994)

Preparation of human serum-albumin microspheres by a novel acetone-heat denaturation method.

Journal Of Microencapsulation **11**, 395-407.

Chu, B., Wu, G. and Schneider, D.K. (1994)

A scattering study on intermicellar interactions and structures of polymeric micelles.

J. Polym. Sci.: Part B: Polymer Physics **32**, 2605-2614.

Churchill, J.R. and Hutchinson, F.G. (1986)

Biodegradable amphipathic copolymers.

Eur. Pat. Appl. 85304489.9.

Çiftçi, K., Hincal, A.A., Kaş, H.S., Ercan, M.T. and Ruacan, Ş. (1994)

Microspheres of 5-fluorouracil using poly(dl-lactic acid): *in vitro* release properties and distribution in mice after i.v. administration.

Eur. J. Pharm. Sci. **1**, 249-258.

Çiftçi, K., Hincal, A.A., Kaş, H.S., Ercan, M.T., and Ruacan, Ş. (1994)

Microspheres of 5-fluorouracil using poly(dl-lactic acid): *in vitro* release properties and distribution in mice after i.v. administration.

Eur. J. Pharm. Sci. **1**, 249-258.

Cohen Stuart, M.A., Cosgrove, T., and Vincent, B. (1986)

Experimental aspects of polymer adsorption at solid/solution interfaces.

Adv. Colloid Interface Sci. **24**, 143-239.

Cohn, D. and Younes, H. (1988a)

Biodegradable PEO/PLA block copolymers.

J. Biomed. Mater. Res. **22**, 993-1009.

Cohn, D. and Younes, H. (1988b)

Compositional and structural analysis of PELA biodegradable block copolymers degrading under in vitro conditions.

Biomaterials **10**, 466-474.

Coll, H. (1971)

Behavior of micellar solutions in gel permeation chromatography. A theory based on a simple model, 329-337.

In Gel Permeation Chromatography. Edited by K. H. Altgelt and L. Segal. Marcel Dekker, Inc., New York.

Conti, B., Puglisi, G., Ventura, C.A., Giunchedi, P., Conte, U., Caruso, A. and Cutuli, V. (1994)

Tolmetin poly-D,L-lactide microspheres: *in vitro/in vivo* evaluation.

S.T.P. Pharma Sciences **4**, 269-274.

Conti, B., Genta, I., Modena, T. and Pavanetto, F. (1995)

Investigation on process parameters involved in polylactide-co-glycolide microspheres preparation.

Drug Dev. Ind. Pharm. **21**, 615-622.

Coombes, A.G.A., Lavelle, E.C., Jenkins, P.G., and Davis, S.S. (1995)

Pulsed and sustained immune responses following a single dose of a model antigen associated with resorbable microparticles.

Proceed. Intern. Symp. Control. Rel. Bioact. Mater. **22**, 560-561.

Cornet, C.F and van Ballegooijen, H. (1966)

Rapid turbidimetric determination of theta-conditions.

Polymer, **7**, 293-301.

Couvreur, P. and Puisieux, F. (1993)

Nano- and microparticles for the delivery of polypeptides and proteins.

Advanced Drug Delivery Reviews **10**, 141-162.

Cowley, John M. (1988)

Imaging, 3-37.

In High-Resolution Transmission Electron Microscopy and Associated Techniques.

Eds. Buseck, P.R., Cowley, J.M., Eyring, L. Oxford University Press, New York.

Craig, P. (1990)

Drug Compendium, 890.

In Comprehensive Medicinal Chemistry: the Rational Design, Mechanistic Study and Therapeutic Application of Chemical Compounds. Eds. Hansch, C., Sammes, P.G. and Taylor, J.B. Volume 6.

Creeth, J.M. and Harding, S.E. (1982)

Some observations on a new type of point average molecular weight.

J. Biochem. Biophys. Meth. **7**, 25-34.

Davies, M.C., Brown, A., Eccles, A.J., Humphrey, P. and Vickerman, J.C. (1987)

ToF-SIMS, SSIMS and SIMS imaging of polymeric biomaterials and drug delivery systems.

Proceed. Intern. Symp. Control. Rel. Bioact. Mater. **14**, 234-235.

Davies, M.C. and Short, R.D. (1988)

The surface characterization PLA-PGA and LH-RH loaded PLA-PGA copolymer systems by XPS and SIMS.

Proceed. Intern. Symp. Control. Rel. Bioact. Mater. **15**, 318-319.

Davies, M.C., Short, R.D., Khan, M.A., Watts, J.F., Brown, A., Eccles, A.J., Humphrey, P., Vickerman, J.C. and Vert, M. (1989)

An XPS and SIMS analysis of biodegradable biomedical polyesters.

Surf. Int. Anal. **14**, 115-120.

Davies, M.C. and Lynn, R.A.P. (1990a)

Static secondary ion mass spectrometry of polymeric biomaterials.

Crit. Rev. Biocompat. **5**, 297-341.

Davies, M.C. and Lynn, R.A.P. (1990b)

A review: Secondary ion mass spectrometry (SIMS) of polymeric biomaterials.

Clinical Materials **5**, 97-114.

Davis, S.S. and Illum, L. (1986)

Colloidal delivery systems - opportunities and challenges, 93-110.

In Site-Specific Drug Delivery.

Eds. Tomlinson, E. and Davis, S.S. John Wiley & Sons Ltd., London.

Davis, S.S., Illum, L., and Stolnik, S. (1996)

Polymers in drug-delivery.

Current Opinion in Colloid & Interface Science **1**, 660-666.

Deng, X.M., Xiong, C.D., Cheng, L.M., and Xu, R.P. (1990)

Synthesis and characterization of block copolymers from D,L-lactide and poly(ethylene glycol) with stannous chloride.

J. Polym. Sci., Part C, Polym. Lett. **28**, 411-416.

- Deng, X.M., Xiong, C.D., Cheng, L.M., Huang, H.H. and Xu, R.P. (1995)
Studies on the block copolymerization of D,L-lactide and poly(ethylene glycol) with aluminium complex catalyst.
J. Appl. Polymer Sci. **55**, 1193-1196.
- Denkbaş, E.B., Kaitian, X., Tuncel, A. and Pişkin, E. (1994)
Rifampicin-carrying poly(D,L-lactide) microspheres: Loading and release.
J. Biomater. Sci. Polymer Edn. **6**, 815-825.
- Determann, H. and Michel, W. (1966)
The correlation between molecular weight and elution behaviour in the gel chromatography of proteins.
J. Chromatog. **25**, 303-313.
- Douglas, S.J., Davis, S.S., and Illum, L. (1987)
Nanoparticles in drug delivery.
CRC Critical Reviews in Therapeutic Drug Carrier Systems **3**, 233-261.
- Douglas, S.J. and Davis, S.S. (1986)
Particle size analysis of colloidal systems by photon correlation spectroscopy, 265-276.
In *Targeting of drugs with synthetic systems*.
Eds. G. Gregoriadis, J. Senior and G. Poste. Plenum Press. New York.
- Drake, B., Prater, C.B., Weisenhorn, A.L., Gould, S.A.C., Albrecht, T.R., Quate, C.F., Cannell, D.S., Hansma, H.G., Hansma, P.K. (1989)
Imaging crystals, polymers, and processes in water with the atomic force microscope.
Science **243**, 1586-1589.
- Dunn, S.E., Brindley, A., Davis, S.S., Davies, M.C. and Illum, L. (1994)
Polystyrene-poly(ethylene glycol) (PS-PEG2000) particles as model systems for site specific

delivery. Part 2. The effect of PEG surface density on the *in vitro* and *in vivo* biodistribution. Pharm. Res. **11**, 1016-1022.

Dunn, S.E. (1995)

Biodegradable nanosphere systems for drug targeting.

PhD Thesis, University of Nottingham.

Dunn, S.E., Coombes, A.G.A, Garnett, M.C., Davis, S.S., Davies, M.C., and Illum, L. (1997)

In vitro cell interaction and in vivo biodistribution of poly(lactide-co-glycolide) nanospheres surface modified by poloxamer and poloxamine copolymers.

J. Contr. Rel. **44**, 65-76.

Ehrlich, P. (1906)

Collected Studies in Immunity, 442-447.

Volume 2, John Wiley & Sons, New York.

El Eini, D.I.D., Barry, B.W. and Rhodes, C.T. (1976)

Micellar size, shape, and hydration of long-chain polyoxyethylene nonionic surfactants.

J. Coll. Interface Sci. **54**, 348-351.

Elworthy, P.H. and Lipscomb, F.J. (1968)

Solubilization of griseofulvin by nonionic surfactants.

J. Pharm. Pharmac. **20**, 817-824.

Faers, M.A. and Luckham, P.F. (1994)

Rheology of polyethylene oxide-polypropylene oxide block copolymer stabilized latices and emulsions.

Colloids and Surfaces A: Physicochem. Eng. Aspects **86**, 317-327.

Fessi, H., Puisieux, F. and Devissaguet, J.P. (1988)

Procede de preparation de systemes colloidaux dispersibles d'une substance sous forme de

nanocapsules.

Eur. Pat. Appl. 0274961A1.

Fessi, H., Puisieux, F., Devissaguet, J.Ph., Ammoury, N. and Benita, S. (1989)

Nanocapsule formation by interfacial polymer deposition following solvent displacement.

Int. J. Pharm. **55**, R1-R4.

Firman, P., Haase, D., Jen, J., Kahlweit, M. and Strey, R. (1985)

On the effect of electrolytes on the mutual solubility between H₂O and nonionic amphiphiles.

Langmuir **1**, 718-724.

Furton, K.G. and Norelus, A. (1993)

Determining the critical micelle concentration of aqueous surfactant solutions - using a novel colorimetric method.

J. Chem. Education **70**, 254-257.

Ganong, B.R. and Delmore, J.P. (1991)

Phase separation temperatures of mixtures of Triton X-114 and Triton X-45: Application to phase separation.

Anal. Biochem. **193**, 35-37.

Gao, Z. and Eisenberg, A. (1993)

A model of micellization for block copolymers in solutions.

Macromolecules **26**, 7353-7360.

Goldenberg, M.S., Bruno, L.A., and Rennwanz, E.L. (1993)

Determination of solubilization sites and efficiency of water-insoluble agents in ethylene oxide-containing nonionic micelles.

J. Coll. Interface Sci. **158**, 351-363.

Goodhart, F.W. and Martin, A.N. (1962)

Solubilization of benzoic acid derivatives by polyoxyethylene stearates.

J. Pharm. Sci. **51**, 50-54.

Goodwin, D.A., Goode, R., Brown, L., and Imbornone, C.J. (1971)

¹¹¹In labeled transferrin for the detection of tumors.

Radiology **100**, 175-179.

Gouda, M.W., Ismail, A.A. and Motawi, M.M. (1970)

Micellar solubilization of barbiturates II: Solubilities of certain barbiturates in polyoxyethylene stearates of varying hydrophilic chain length.

J Pharm. Sci. **59**, 1402-1405.

Gref, R., Minamitake, Y., Peracchia, M.T., Trubetskoy, V., Torchilin, V., and Langer, R. (1994)

Biodegradable long-circulating polymeric nanospheres.

Science **263**, 1600-1603.

Gupta, P.K., Johnson, H. and Allexon, C. (1993)

In vitro and in vivo evaluation of clarithromycin/poly(lactic acid) microspheres for intramuscular drug delivery.

J. Contr. Rel. **26**, 229-238.

Güveli, D.G., Davis, S.S. and Kayes, J.B. (1981)

Partial molal volume and light scattering studies on certain polyoxyethylene monohexadecyl ethers, and the effect of added aromatic solutes.

J. Coll. Interface Sci. **86**, 213-225.

Harding, S.E. (1984)

Determination of macromolecular homogeneity, shape, and interactions using sedimentation velocity analytical ultracentrifugation.

Meth. Mol. Biol. **22**, 61-73.

Harding, S.E. (1993)

Chapter 8.

In *Methods in Molecular Biology, Volume 22: Microscopy, Optical Spectroscopy, and Macroscopic Techniques*. Eds. Jones, C., Mulloy, B. and Thomas, A.H.

Humana Press Inc., New Jersey.

Harding, S.E., Huron, J.C. and Morgan, P.J. (1992)

Analytical ultracentrifugation in biochemistry and polymer science, 276-279.

Edited by Harding, S.E., Rowe, A.J. and Huron, J.C. Royal Society of Chemistry, Cambridge, U.K.

Harper, G.R., Davies, M.C., Davis, S.S., Tadros, Th. F., Taylor, D.C., Irving, M.P., and Waters, J.A. (1991)

Steric stabilization of microspheres with grafted polyethylene oxide reduces phagocytosis by rat Kupffer cells *in vitro*.

Biomaterials **12**, 695-700.

Hawley, A.E., Davis, S.S., and Illum, L. (1995)

Targeting of colloids to lymph-nodes - influence of lymphatic physiology and colloidal characteristics.

Advanced Drug Delivery Reviews **17**, 129-148.

Hawley, A.E., Illum, L., and Davis, S.S. (1997)

Lymph node localisation of biodegradable nanospheres surface modified with poloxamer and poloxamine block co-polymers.

FEBS Letters **400**, 319-323.

Hearn, M.J., Briggs, D., Yoon, S.C. and Ratner, B.D. (1987)

SIMS and XPS studies of polyurethane surfaces II. Polyurethanes with fluorinated chain extenders.

Surf. Int. Anal. **10**, 384-391.

Hecht, E. and Hoffmann, H. (1994)

Interaction of ABA block copolymers with ionic surfactants in aqueous solution.

Langmuir **10**, 86-91.

Heya, T., Okada, H., Ogawa, Y., and Toguchi, H. (1994)

In vitro and *in vivo* evaluation of thyrotrophin releasing hormone release from copoly(*dl*-lactic/glycolic acid) microspheres.

J. Pharm. Sci. **83**, 636-640.

Hinze, W.L. and Pramauro, E. (1993)

A critical review of surfactant-mediated phase separations (cloud-point extractions): theory and applications.

Crit. Rev. Anal. Chem. **24**, 133-177.

Horobin, R.W. (1981)

Structure-staining relationships in histochemistry and biological staining. Part 3. Some comments on the intentional and artifactual staining of lipids.

Acta histochemica, Suppl.-Band **XXIV**, S. 237-246.

Hu, D.S.-G. and Liu, H.-J. (1993)

Effect of soft segment on degradation kinetics in polyethylene glycol/poly(L-lactide) block copolymers.

Polym. Bull. **30**, 669-676.

Hu, D.S.-G. and Liu, H.-J. (1994a)

Effect of soft segments and hydrolysis on the crystallization behavior of degradable polyoxyethylene/poly(L-lactide) block copolymers.

Macromol. Chem. Phys. **195**, 1213-1223.

Hu, D.S.-G. and Liu, H.-J. (1994b)

- Structural analysis and degradation behavior in polyethylene glycol/poly(L-lactide) copolymers.
J. Appl. Polym. Sci. **51**, 473-482.
- Huh, Y., Donaldson, G.W., and Johnson, F.J. (1974)
A radiation induced binding of iodine at the surface of uniform polystyrene particles.
Radiat. Res. **60**, 42-53.
- Hurter, P.N. and Hatton, T.A. (1992)
Solubilization of polycyclic aromatic hydrocarbons by poly(ethylene oxide-propylene oxide)
block copolymer micelles: Effects of polymer structure.
Langmuir **8**, 1291-1299.
- Hurter, P.N., Scheutjens, J.M.H.M., and Hatton, T.A. (1993)
Molecular modeling of micelle formation and solubilization in block copolymer micelles. 1. A
self-consistent mean-field lattice theory.
Macromolecules **26**, 5592-5601.
- Huve, P., Verrecchia, T., Bazile, D., Vauthier, C., Couvreur, P. (1994)
Simultaneous use of size-exclusion chromatography and photon correlation spectroscopy for the
characterization of poly(lactic acid) nanoparticles.
J. Chromatog. A **675**, 129-139.
- Illum, L. (1987)
Microspheres and Site Specific Delivery. DSc Thesis, 4-36.
Carson Offset Ltd., Nottingham.
- Illum, L., Davis, S.S., Wilson, C.G., Frier, M., Hardy, J.G., and Thomas, N.W. (1982)
Blood clearance and organ deposition of intravenously administered colloidal particles: the
effect of particle size, nature and shape.
Int. J. Pharm. **12**, 135-146.

Illum, L. and Davis, S.S. (1983)

Effect of the nonionic surfactant Poloxamer 338 on the fate and deposition of polystyrene microspheres following intravenous administration.

J. Pharm. Sci. **72**, 1086-1088.

Illum, L. and Davis, S.S. (1984)

The organ uptake of intravenously administered colloidal particles can be altered using a non-ionic surfactant (Poloxamer 338).

FEBS Letters **167**, 79-82.

Illum, L., Jones, P.D.E., and S. S. Davis, S.S. (1984)

Drug targeting using monoclonal antibody-coated nanoparticles, 353-364.

In *Microspheres and Drug Therapy. Pharmaceutical, Immunological and Medical Aspects.*

Eds. Davis, S.S., Illum, L., McVie, J.G., and Tomlinson, E. Elsevier Biomedical Press, Amsterdam.

Illum, L., Thomas, N.W., and Davis, S.S. (1986a)

Effect of a selected suppression of the reticuloendothelial system on the distribution of model carrier particles.

J. Pharm. Sci. **75**, 16-22.

Illum, L., Hunneyball, I.M., and Davis, S.S. (1986b)

The effect of hydrophilic coatings on the uptake of colloidal particles by the liver and by peritoneal macrophages.

Int. J. Pharm. **29**, 53-65.

Illum, L. and Davis, S.S. (1987)

Targeting of colloidal particles to the bone marrow.

Life Sci. **40**, 1553-1560.

Illum, L., Jacobsen, L.O., Müller, R.H., Mak, E., and Davis, S.S. (1987a)

Surface characteristics and the interaction of colloidal particles with mouse peritoneal macrophages.

Biomaterials **8**, 113-117.

Illum, L., Davis, S.S., Müller, R.H., Mak, E., and West, P. (1987b)

The organ distribution and circulation time of intravenously injected colloidal carriers sterically stabilized with a blockcopolymer - Poloxamine 908.

Life Sci. **40**, 367-374.

Jacobs, P.T., Geer, R.D. and Anacker, E.W. (1972)

A comparison of micellar aggregation numbers as determined by dye solubilization and light scattering.

J. Coll. Interface Sci. **39**, 611-620.

Jalil, R. and Nixon, J.R. (1989)

Microencapsulation using poly(L-lactic acid) I: Microcapsule properties affected by the preparative technique.

J. Microencapsulation **6**, 473-484.

Jeon, S.I., Lee, J.H., Andrade, J.D., and de Gennes, P.G. (1991)

Protein-surface interactions in the presence of polyethylene oxide. I. Simplified theory.

J. Colloid Interface Sci. **142**, 149-158.

Jonsson, B-A., Strand, S-E. and Larsson, B.S. (1992)

A quantitative autoradiographic study of the heterogeneous activity distribution of different In-111-labelled radiopharmaceuticals in rat tissues.

J. Nucl. Med. **33**, 1825-1833.

Juarranz, A., Horobin, R.W. and Proctor, G.B. (1986)

Prediction of in situ fluorescence of histochemical reagents using a structure-staining correlation procedure.

Histochemistry **84**, 426-431.

Juliano, R.L. (1988)

Factors affecting the clearance kinetics and tissue distribution of liposomes, microspheres and emulsions.

Adv. Drug Del. Rev. **2**, 31-54.

Juliano, R.L. and Stamp, D. (1975)

The effect of particle size and charge on the clearance rate of liposomes and liposome encapsulated drugs.

Biochem. Biophys. Res. Commun. **63**, 651-658.

Julienne, M.C., Foussard, F. and Benoit, J.P. (1989)

Characterization of antibiotic-loaded poly(d-l lactide-co-glycolide) nanoparticles produced by evaporation process.

Proceed. Intern. Symp. Control. Rel. Bioact. Mater. **16**, 77-78.

Kabanov, A.V., Chekhonin, V.P., Alakhov, V.Y., Batrakova, E.V., Lebedev, A.S., Melik-Nubarov, N.S., Arzhakov, S.A., Levashov, A.V., Morozov, G.V., Severin, E.S. and Kabanov, V.A. (1989)

The neuroleptic activity of haloperidol increases after its solubilization in surfactant micelles: Micelles as microcontainers for drug targeting.

Febs Letters **258**, 343-345.

Kabanov, A.V., Batrakova, E.V., Melik-Nubarov, N.S., Fedoseev, N.A., Dorodnich, T.Y., Alakhov, V.Y., Chekhonin, V.P., Nazarova, I.R., and Kabanov, V.A. (1992)

A new class of drug carriers: micelles of poly(oxyethylene)-poly(oxypropylene)-poly(oxyethylene) block copolymers as microcontainers for drug targeting from blood in brain.

J. Contr. Rel. **22**, 141-158.

Kabanov, A.V., Nazarova, I.R., Astafieva, I.V., Batrakova, E.V., Alakhov, V.Y., Yaroslavov,

A.A. and Kabanov, V.A. (1995)

Micelle formation and solubilization of fluorescent probes in poly(oxyethylene-*b*-oxypropylene-*b*-oxyethylene) solutions.

Macromolecules **28**, 2303-2314.

Karlström, G. (1985)

A new model for upper and lower critical solution temperatures in poly(ethylene oxide) solutions.

J. Phys. Chem. **89**, 4962-4964.

Katayama, N., Tanaka, R., Ohno, Y., Ueda, C., Houjou, T. and Takada, K. (1995)

Implantable slow release cyclosporin A (CYA) delivery system to thoracic lymph duct.

Int. J. Pharm. **115**, 87-93.

Katime, I., Villacampa, M. and Quintana, J.R. (1994)

Structure and thermodynamics of polystyrene-block-poly(ethylene/propene) micelles in selective solvents.

Macromol. Symp. **84**, 255-265.

Killmann, E., Sapuntzjis, P. and Maier, H. (1992)

Dynamic light scattering for characterization of latices.

Makromol. Chem., Macromol. Symp. **61**, 42-58.

Kim, I.T. and Luckham, P.F. (1992)

The viscoelastic properties of polystyrene particles bearing poly(ethylene oxide)-poly(propylene oxide) ABA block copolymers.

Colloids and Surfaces **68**, 243-259.

Klein, J. and Luckman, P.F. (1982)

Forces between 2 adsorbed polyethylene oxide layers immersed in a good aqueous solvent.

Nature **300**, 429-431

- Klibanov, A.L., Maruyama, K., Beckerleg, A.M., Torchilin, V.P., and Huang, L. (1991)
Activity of amphipathic poly(ethylene glycol) 5000 to prolong the circulation time of liposomes depends on liposome size and is unfavorable for immunoliposome binding to target.
Biochim. Biophys. Acta **1062**, 142-148.
- Krause, H.-J., Schwarz, A. and Rohdewald, P. (1985)
Polylactic acid nanoparticles, a colloidal drug delivery system for lipophilic drugs.
Int. J. Pharm. **27**, 145-155.
- Kricheldorf, H.R. and Meier-Haack, J. (1993)
Polylactones: 22a) ABA triblock copolymers of L-lactide and poly(ethylene glycol).
Makromol. Chem. **194**, 715-725.
- Kulkarni, R.K., Moore, E.G., Hegyeli, A.F., and Leonard, F. (1971)
Biodegradable poly(lactic acid) polymers.
J. Biomed. Mater. Res. **5**, 169-181.
- Kumar, S. and Singh, H.N. (1992)
Competitive solubilisation of sudan-IV and anthracene in micellar systems.
Colloids and Surfaces **69**, 1-4.
- Kwon, G.S., Yokoyama, M., Okano, T., Sakurai, Y., and Kataoka, K. (1993a)
Biodistribution of micelle-forming polymer-drug conjugates.
Pharm. Res. **10**, 970-974.
- Kwon, G.S., Naito, M., Yokoyama, M., Okano, T., Sakurai, Y., and Kataoka, K. (1993b)
Micelles based on AB block copolymers of poly(ethylene oxide) and poly(β -benzyl L-aspartate).
Langmuir **9**, 945-949.
- Kwon, G.S., Yokoyama, M., Okano, T., Sakurai, Y., and Kataoka, K. (1994a)

Enhanced tumor accumulation and prolonged circulation times of micelle-forming poly(ethylene oxide-aspartate) block copolymer-adriamycin conjugates.

J. Contr. Rel. **28**, 334-335.

Kwon, G.S., Suwa, S., Yokoyama, M., Okano, T., Sakurai, Y., and Kataoka, K. (1994b)

Enhanced tumor accumulation and prolonged circulation times of micelle-forming poly(ethylene oxide-aspartate) block copolymer adriamycin conjugates.

J. Contr. Rel. **29**, 17-23.

Kwon, G.S., Naito, M., Yokoyama, M., Okano, T., Sakurai, Y. and Kataoka, K. (1995)

Physical entrapment of adriamycin in AB block copolymer micelles.

Pharm. Res. **12**, 192-195.

Langer, R. (1993)

Polymer-controlled drug delivery systems.

Acc. Chem. Res. **26**, 537-542.

Lasic, D.D. (1992)

Mixed micelles in drug delivery.

Nature **355**, 279-280.

Laurent, T.C. and Killander, J. (1964)

A theory of gel filtration and its experimental verification.

J. Chromatog. **14**, 317-330.

Lavrenko, P.N., Linow, K.J. and Görnitz, E. (1992)

The concentration dependence of the sedimentation coefficient of some polysaccharides in very dilute solution, 517.

In Analytical Ultracentrifugation in Biochemistry and Polymer Science. Eds. Harding, S.E., Rowe, A.J. and Horton, J.C., Royal Society of Chemistry, Cambridge.

- Le Corre, P., Le Guevello, P., Gajan, V., Chevanne, F. and Le Verge, R. (1994)
Preparation and characterization of bupivacaine-loaded polylactide and polylactide-co-glycolide microspheres.
Int. J. Pharm. **107**, 41-49.
- Lee, J.H. and Andrade, J.D. (1988)
Surface properties of aqueous PEO/PPO block copolymer surfactants, 119-136.
In *Polymer Surface Dynamics*, Ed. Andrade, J.D., Plenum Press, New York.
- Leibler, L., Orland, H., and Wheeler, J.C. (1983)
Theory of critical micelle concentration for solutions of block copolymers.
J. Chem. Phys. **79**, 3550-3557.
- Leroux, J.-C., Gravel, P., Balant, L., Volet, B., Anner, B.M., Allémann, E., Doelker, E., and Gurny, R. (1994)
Internalization of poly(D,L-lactic acid) nanoparticles by isolated human leukocytes and analysis of plasma proteins adsorbed onto the particles.
J. Biomed. Mater. Res. **28**, 471-481.
- Lesieur, S., Grabielle-Madelmont, C., Paternostre, M. and Ollivon, M. (1993)
Study of size distribution and stability of liposomes by high performance gel exclusion chromatography.
Chem. Phys. Lipids **64**, 57-82.
- Leyland-Jones, B. (1993)
Targeted drug delivery.
Seminars in Oncology **20**, 12-17.
- Li, S.M., Rashkov, I., Espartero, J.L., Manolova, N., and Vert, M. (1996)
Synthesis, characterization, and hydrolytic degradation of PLA/PEO/PLA triblock copolymers with long poly(L-lactic acid) blocks.

Macromolecules **29**, 50-56.

Liang, W., Tadros, Th.F. and Luckman, P.F. (1992)

Rheological studies on concentrated polystyrene latex sterically stabilized by poly(ethylene oxide) chains.

J. Colloid Inter. Sci. **153**, 131-139.

Lin, W., Coombes, A.G.A., Garnett, M.C., Davies, M.C., Schacht, E., Davis, S.S., and Illum, L. (1994)

Preparation of sterically stabilized human serum albumin nanospheres using a novel Dextranox-MPEG crosslinking agent.

Pharm. Res. **11**, 1588-1592.

Linse, P. (1994)

Micellization of poly(ethylene oxide)-poly(propylene oxide) block copolymer in aqueous solution: effect of polymer impurities.

Macromolecules **27**, 2685-2693.

Linse, P. and Malmsten, M. (1992)

Temperature-dependent micellization in aqueous block copolymer solutions.

Macromolecules **25**, 5434-5439.

Litzinger, D.C., Buiting, A.M.J., van Rooijen, N., and Huang, L. (1994)

Effect of liposome size on the circulation time and intraorgan distribution of amphipathic poly(ethylene glycol)-containing liposomes.

Biochim. Biophys. Acta **1190**, 99-107.

Liu, D., Mori, A., and Huang, L. (1992)

Role of liposome size and RES blockade in controlling biodistribution and tumor uptake of GM₁-containing liposomes.

Biochim. Biophys. Acta **1104**, 95-101.

- Liu, H.-J., Hsieh, C.-T., and Hu, D.S.-G. (1994)
Solute diffusion through degradable semicrystalline polyethylene glycol/poly(L-lactic acid) copolymers.
Polymer Bull. **32**, 463-470.
- Llanos, G.R. and Sefton, M.V. (1993)
Review: Does polyethylene oxide possess a low thrombogenicity?
J. Biomater. Sci. Polymer Edn. **4**, 381-400.
- Lobaskin, V.A. and Pershin, V.K. (1993)
Micellar interactions in solutions of nonionic surfactants: model of hard spheres.
Russian Journal of Physical Chemistry **67**, 280-282.
- Lodge, T. (1994)
Fundamental review: Characterization of polymer materials by scattering techniques, with applications to block copolymers.
Mikrochim. Acta **116**, 1-31.
- Lu, W. and Park, T.G. (1995)
In vitro release profiles of eristostatin from biodegradable polymeric microspheres: Protein aggregation problem.
Biotechnol. Prog. **11**, 224-227.
- Lukowski, G., Müller, R.H., Müller, B.W., and Dittgen, M. (1992)
Acrylic acid copolymer nanoparticles for drug delivery: I. Characterization of the surface properties relevant for in vivo distribution.
Int. J. Pharm. **84**, 23-31.
- Luo, Y.-Z., Stubbersfield, R.B. and Booth, C. (1983)
Oxyethylene-oxypropylene-oxyethylene triblock copolymers crystallised from dilute solution.

Eur. Polym. J. **19**, 107-114.

Luo, Y.-Z., Nicholas, C.V., Attwood, D., Collett, J.H., Price, C., Booth, C., Chu, B. and Zhou, Z.K. (1993)

Block copoly(oxyethylene/oxybutylene/oxyethylene), $E_{40}B_{15}E_{40}$, in aqueous solution: Micellisation, gelation and drug release.

J. Chem. Soc. Faraday Trans. **89**, 539-546.

Malcolmson, C. and Lawrence, M.J. (1993)

A comparison of the incorporation of model steroids into non-ionic micellar and microemulsion systems.

J. Pharm. Pharmacol. **45**, 141-143.

Malmsten, M. and Lindman, B. (1992)

Self-assembly in aqueous block copolymer solutions.

Macromolecules **25**, 5440-5445.

Maste, M.C.L., van Velthoven, A.P.C.M., Norde, W. and Lyklema, J. (1994)

Synthesis and characterization of a short-haired poly(ethylene oxide)-grafted polystyrene latex.

Colloids Surfaces A: Physicochem. Eng. Aspects **83**, 255-260.

Matsushima, Y., and Maeda, H. (1986)

A new concept for macromolecular therapeutics in cancer chemotherapy: mechanism of tumortropic accumulation of proteins and the antitumor agent smancs.

Cancer Res. **46**, 6387-6392.

McLafferty, F.W. (1980)

Interpretation of mass spectra.

3rd edition, University science books, Mill Valley, California.

Menei, P., Daniel, V., Montero-Menei, C., Brouillard, M., Pouplard-Barthelaix, A., and Benoit,

J.P. (1993)

Biodegradation and brain tissue reaction to poly(D,L-lactide-co-glycolide) microspheres.
Biomaterials **14**, 470-478.

Miano, F., Bailey, A., Luckham, P.F. and Tadros, Th.F. (1992)

Adsorption of poly(ethylene oxide)-poly(propylene oxide) ABA block copolymers on carbon black and the rheology of the resulting dispersions.

Colloids and Surfaces **68**, 9-16.

Miyamoto, S., Takaoka, K., Okada, T., Yoshikawa, H., Hashimoto, J., Suzuki, S., and Ono, K. (1993)

Poly(lactic acid)-poly(ethylene glycol) block copolymer. A new biodegradable synthetic carrier for bone morphogenetic protein.

Clinical Orthopaedics and Related Research **294**, 333-343.

Moghimi, S.M. and Patel, H.S. (1989)

Serum opsonins and phagocytosis of saturated and unsaturated phospholipid liposomes.

Biochim. Biophys. Acta **984**, 384-387.

Moghimi, S.M., Porter, C.J.H., Illum, L., and Davis, S.S. (1991a)

The effect of poloxamer-407 on liposome stability and targeting to bone-marrow - comparison with polystyrene microspheres.

Int. J. Pharm. **68**, 121-126.

Moghimi, S.M., Porter, C.J.H., Muir, I.S., Illum, L., and Davis, S.S. (1991b)

Non-phagocytic uptake of intravenously injected microspheres in rat spleen - influence of particle size and hydrophilic coating.

Biochem. Biophys. Res. Commun. **177**, 861-866.

Moghimi, S.M., Hedeman, H., Muir, I.S., Illum, L., and Davis, S.S. (1993a)

An investigation of the filtration capacity and the fate of large filtered sterically-stabilized

microspheres in rat spleen.

Biochim. Biophys. Acta **1157**, 233-240.

Moghimi, S.M., Muir, I.S., Illum, L., Davis, S.S., and Kolbachofen, V. (1993b)

Coating particles with a block-copolymer (poloxamine-908) suppresses opsonization but permits the activity of dysopsonins in the serum.

Biochim. Biophys. Acta **1179**, 157-165.

Moghimi, S.M., Hawley, A.E., Christy, N.M., Gray, T., Illum, L., and Davis, S.S. (1994)

Surface engineered nanospheres with enhanced drainage into lymphatics and uptake by macrophages of the regional lymph-nodes.

FEBS Letters **344**, 25-30

Morgan, P.J., Harding, S.E., Petrak, K. (1990)

Hydrodynamic properties of a polyisoprene/poly(oxyethylene) block copolymer.

Macromolecules, **23**, 4461-4464.

Mortensen, K. and Pedersen, J.S. (1993)

Structural study on the micelle formation of poly(ethylene oxide)-poly(propylene oxide)-poly(ethylene oxide) triblock copolymer in aqueous solution.

Macromolecules **26**, 805-812.

Mukerjee, P. (1971)

Solubilization of benzoic acid derivatives by nonionic surfactants: Location of solubilizates in hydrocarbon core of micelles and polyoxyethylene mantle.

J. Pharm. Sci. **60**, 1528-1531.

Mukerjee, P. (1980)

Solubilization in micellar systems.

Pure & Appl. Chem. **52**, 1317-1321.

Müller, R.H., Koosha, F., Davis, S.S., and Illum, L. (1988)

In vitro and *in vivo* release of In-111 from PHB and PLA nanoparticles.

Proceed. Intern. Symp. Control. Rel. Bioact. Mater. **15**, 378-379.

Nagarajan, R., Barry, M., Ruckenstein, E. (1986)

Unusual selectivity in solubilisation by block copolymer micelles.

Langmuir **2**, 210-215.

Napper, D.H. (1968)

Flocculation studies of non-aqueous sterically stabilized dispersions of polymer.

Trans. Faraday Soc. **64**, 1701-1711.

Napper, D.H. (1970a)

Flocculation studies of sterically stabilized dispersions.

J. Coll. Interface Sci. **32**, 106-114.

Napper, D.H. (1970b)

Steric stabilization and the Hofmeister series.

J. Coll. Interface Sci. **33**, 384-392.

Napper, D.H. (1989)

In Polymeric Stabilisation of Colloidal Dispersions, 8-14.

Academic Press, London.

Ng, C.L., Lee, H.K., and Li, S.F.Y. (1994)

Prevention of protein adsorption on surfaces by polyethylene oxide-polypropylene oxide-polyethylene oxide triblock copolymers in capillary electrophoresis.

J. Chromatography A **659**, 427-434.

Nicholas, C.V., Luo, Y., Deng, N., Attwood, D., Collett, J.H., Price, C., and Booth, C. (1993)

Effect of chain length on the micellization and gelation of block copoly(oxyethylene/

oxybutylene oxyethylene) $E_mB_nE_m$.

Polymer **34**, 138-144.

Niwa, T., Takeuchi, H., Hino, T., Kunou, N., and Kawashima, Y. (1994)

In vitro drug release behavior of D,L-lactide/glycolide copolymer (PLGA) nanospheres with nafarelin acetate prepared by a novel spontaneous emulsification solvent diffusion method.

J. Pharm. Sci. **83**, 727-732.

Noguchi, T., Charman, W.N.A. and Stella, V.J. (1985)

The effect of drug lipophilicity and lipid vehicles on the lymphatic absorption of various testosterone esters.

Int. J. Pharm. **24**, 173-184.

Norman, M.E., Williams, P., and Illum, L. (1993)

Influence of block copolymers on the adsorption of plasma proteins to microspheres.

Biomaterials **14**, 193-202.

O'Dwyer, P.J., King, S.A., Fortner, C.L., and Leyland-Jones, B. (1986)

Hypersensitivity reactions to Teniposide (VM-26): An analysis.

J. Clin. Oncol. **4**, 1262-1269.

Okada, H., Yamamoto, M., Heya, T., Inoue, Y., Kamei, S., Ogawa, Y., and Toguchi, H. (1994)

Drug delivery using biodegradable microspheres.

J. Contr. Rel. **28**, 121-129.

Oranli, L., Bahadur, P. and Riess, G. (1985)

Hydrodynamic studies on micellar solutions of styrene-butadiene block copolymers in selective solvents.

Can. J. Chem. **63**, 2691-2696.

Pandya, K., Bahadur, P., Nagar, T.N. and Bahadur, A. (1993)

Micellar and solubilizing behaviour of Pluronic L-64 in water.

Colloids and Surfaces A: Physicochem. Eng. Aspects **70**, 219-227.

Pavanetto, F., Conti, B., Giunchedi, P., Genta, I. and Conte, U. (1994)

Poly lactide microspheres for the controlled release of diazepam.

Eur. J. Pharm. Biopharm. **40**, 27-31.

Peracchia, M.T., Gref, R., Minamitake, Y., Domb, A., Lotan, N., and Langer, R. (1997)

PEG-coated nanospheres from amphiphilic diblock and multiblock copolymers: Investigation of their drug encapsulation and release characteristics.

J. Contr. Rel. **46**, 223-231.

Pfüller, U., Franz, H. and Preiß, A. (1977)

Sudan black B: Chemical structure and histochemistry of the blue main components.

Histochemistry **54**, 237-250.

Pharmacia (1982)

Pharmacia Fine Chemicals, Gel Filtration: Theory and Practice, 16-22.

Pharmacia, Sweden.

Pingret, F.J.V., Sohm, R.H. and Tadros, Th.F. (1992)

Influence of surfactant adsorption on the rheology of concentrated latex dispersions.

Colloids and Surfaces **65**, 85-93.

Pişkin, E., Tuncel, A., Denizli, A., Denkbaş, E.B., Ayhan, H., Çiçek, H., and Xu, K.T. (1994)

Nondegradable and biodegradable polymeric particles. Preparation and some selected biomedical applications.

ACS Symposium Series **556**, 222-237.

Polverari, M. and van de Ven, T.G.M. (1994)

Dynamic light scattering of suspensions of PEO-coated latex particles.

Coll. Surf. A: Physicochem. Eng. Aspects **86**, 209-228.

Porter, C.J.H., Moghimi, S.M., Davies, M.C., Davis, S.S., and Illum, L. (1992)

Differences in the molecular-weight profile of poloxamer-407 affect its ability to redirect intravenously administered colloids to the bone-marrow.

Int. J. Pharm. **83**, 273-276.

Porter, C.J.H., Moghimi, S.M., Illum, L., and Davis, S.S. (1992)

The polyoxyethylene polyoxypropylene block copolymer poloxamer-407 selectively redirects intravenously injected microspheres to sinusoidal endothelial-cells of rabbit bone-marrow.

FEBS Letters **305**, 62-66.

Prasad, K.N., Luong, T.T., Florence, A.T., Paris, J., Vaution, C., Seiller, M. and Puisieux, F. (1979)

Surface activity and association of ABA polyoxyethylene-polyoxypropylene block copolymers in aqueous solution.

J. Colloid Interface Sci. **69**, 225-232.

Prestidge, C. and Tadros, Th.F. (1988)

Viscoelastic properties of aqueous concentrated polystyrene latex dispersions containing grafted poly(ethylene oxide) chains.

J. Coll. Interface Sci. **124**, 660-665.

Price, N.C. and Dwek, R.A. (1986)

Solutions of macromolecules, 63-92.

In Principles and Problems in Physical Chemistry for Biochemists.

Second edition, Oxford University Press, New York.

Quintana, J.R., Salazar, R.A. and Katime, I. (1995)

Solubilization of homopolymers by block copolymer micelles in dilute solutions: Laser light scattering and viscosity studies on micellar solutions.

J. Phys. Chem. **99**, 3723-3731.

Rashkov, I., Manolova, N., Li, S.M., Espartero, J.L., and Vert, M. (1996)
Synthesis, characterization, and hydrolytic degradation of PLA/PEO/PLA triblock copolymers with short poly(L-lactic acid) chains.
Macromolecules **29**, 50-56.

Ratner, B.D. (1988)
Graft copolymer and block copolymer surfaces, 373-392.
In The Surface Characterisation of Biomaterials.
Ed. Ratner, B.D. Elsevier Science Publishers, Amsterdam.

Reddy, N.K., Fordham, P.J., Attwood, D. and Booth, C. (1990)
Association and surface properties of block-copoly-(oxyethylene/oxypropylene/oxyethylene)
L64.
J. Chem. Soc. Faraday Trans. **86**, 1569-1572.

Redhead, H. (1997)
Drug loading of biodegradable nanoparticles for site specific drug delivery.
PhD Thesis, University of Nottingham.

Richardson, V.J., Jeyasingh, K., Jewkes, R.F., Ryman, B.E., and Tattersall, M.H.N. (1978)
Possible tumor localization of Tc-99m-labelled liposomes: effect of lipid composition, charge and liposome size.
J. Nucl. Med. **19**, 1049-1054.

Roberts, C.J., Wilkins, M.J., Beamson, G., Davies, M.C., Jackson, D.E., Scholes, P.D., Tendler, S.J.B. and Williams, P.M. (1992)
Demonstration of controlled surface modification achievable with a scanning tunnel microscope on graphite, metallic films, organic molecules and polymeric biomolecules.
Nanotechnology **3**, 98-110.

- Roerdink, F., Wassef, N.M., Richardson, E.C., and Alving, C.R. (1983)
Effects of negatively charged lipids on phagocytosis of liposomes opsonized by complement.
Biochim. Biophys. Acta. **734**, 33-39.
- Roerdink, F., Regts, J., van Leeuwen, B., and Scherphof, G. (1984)
Intrahepatic uptake and processing of intravenously injected small unilamellar phospholipid vesicles in rats.
Biochim. Biophys. Acta **770**, 195-202.
- Rolland, A., O'Mullane, J., Goddard, P., Brookman, L., Petrak, K. (1992)
New macromolecular carriers for drugs. 1. Preparation and characterisation of poly(oxyethylene-b-isoprene-b-oxyethylene) block copolymer aggregates.
J. Applied Polymer Science **44**, 1195-1203.
- Rosch, H. (1967)
In *Nonionic Surfactants*, Ed. Shick, M.J., Dekker, New York.
- Rowe, A.J. (1992)
The concentration dependence of sedimentation, 394-396.
In *Analytical Ultracentrifugation in Biochemistry and Polymer Science*. Eds. Harding, S.E., Rowe, A.J. and Horton, J.C., Royal Society of Chemistry, Cambridge.
- Rupert, L.A.M. (1992)
A thermodynamic model of clouding in water/alcohol ethoxylate mixtures.
J. Coll. Interface Sci. **153**, 92-105.
- Rutter, P.R. and Vincent, B. (1980)
In *Microbial Adhesion to Surfaces*, 79-92.
Eds. Berkeley, R.C.W., Lynch, J.M., Melling, J., Rutter, P.R., and Vincent, B. Ellis Horwood, Chichester.

Saito, Y. and Sato, T. (1985)

Effects of polyoxyethylene chain length on micellar structure.

J. Phys. Chem. **89**, 2110-2113.

Saito, Y., Kondo, Y., Abe, M. and Sato, T. (1994)

Solubilization behavior of estriol in an aqueous solution of Pluronic L-64 as a function of concentration and temperature.

Chem. Pharm. Bull. **42**, 1348-1350.

Sánchez, A., Vila-Jato, J.L. and Alonso, M.J. (1993)

Development of biodegradable microspheres and nanospheres for the controlled release of cyclosporin A.

Int. J. Pharm. **99**, 263-273.

Sanders, A.H. and Connell, D.S. (1980)

In Light Scattering in Liquids and Macromolecular Solutions, 173-182.

Edited by Degiorgio, V., Corti, M. and Giglio, M. Plenum, New York.

Sansdrap, P. and Moës, A.J. (1993)

Influence of manufacturing parameters on the size characteristics and the release profiles of nifedipine from poly(DL-lactide-co-glycolide) microspheres.

Int. J. Pharm. **98**, 157-164.

Saunders, Martin (1993)

Personal communication, SmithKline Beecham, Herts., UK.

Schick, M.J., Atlas, S.M. and Eirich, F.R. (1962)

Micellar structure of non-ionic detergents.

J. Phys. Chem. **66**, 1326-1333.

Schmolka, I.R. and Raymond, A.J. (1965)

Micelle formation of polyoxyethylene-polyoxypropylene surfactants.

J. Am. Oil Chem. Soc. **42**, 1088-1091.

Scholes, P.D. (1994)

The Preparation and Characterisation of Biodegradable Microspheres for Site Specific Drug Delivery.

PhD Thesis, University of Nottingham.

Scholes, P.D., Davies, M.C., Illum, L., and Davis, S.S. (1992)

Radiolabelling of biodegradable microspheres for site specific drug delivery.

Proceed. Intern. Symp. Control. Rel. Bioact. Mater. **19**, 154-155.

Scholes, P.D., Coombes, A.G.A, Illum, L., Davis, S.S., Vert, M., and Davies, M.C. (1993)

The preparation of sub-200 nm poly(lactide-co-glycolide) microspheres for site-specific drug delivery.

J. Cont. Rel. **25**, 145-153.

Schott, H. (1973)

Salting in of nonionic surfactants by complexation with inorganic salts.

J. Coll. Interface Sci. **43**, 150-155.

Schott, H. and Han, S.K. (1976)

Effect of inorganic additives on solutions of nonionic surfactants III: CMC's and surface properties.

J. Pharm. Sci. **65**, 975-978.

Senior, J., Delgado, C., Fisher, D., Tilcock, C., and Gregoriadis, G. (1991)

Influence of surface hydrophilicity of liposomes on their interaction with plasma protein and clearance from the circulation: studies with poly(ethylene glycol)-coated vesicles.

Biochim. Biophys. Acta **1062**, 77-82.

Shah, S.S., Zhu, K.J., and Pitt, C.G. (1994)

Poly-DL-lactic acid: Polyethylene glycol block copolymers. The influence of polyethylene glycol on the degradation of poly-DL-lactic acid.

J. Biomater. Sci. Polymer Edn. **5**, 421-431.

Shakesheff, K.M., Davies, M.C., Jackson, D.E., Roberts, C.J., Tendler, S.J.B., Brown, V.A., Watson, R.C., Barrett, D.A., Shaw, P.N. (1994)

Imaging the surface of silica microparticles with the atomic force microscope: a novel sample preparation method.

Surface Science Letters **304**, L393-L399.

Shute, R. (1995)

Personal communication, Zeneca Pharmaceuticals, Mereside, Macclesfield, UK.

Smith, Graham C. (1994)

In Surface Analysis by Electron Spectroscopy - Measurement and Interpretation, 1-14.

Plenum Press, New York.

Spenlehauer, G. Veillard, M. and Benoît, J.-P. (1986)

Formation and characterization of cisplatin loaded poly(*d,l*-lactide) microspheres for chemoembolization.

J. Pharm. Sci. **75**, 750-755.

Squire, P.G. (1964)

A relationship between the molecular weights of macromolecules and their elution volumes based on a model for sephadex gel filtration.

Arch. Biochem. Biophys. **107**, 471-478.

Stolnik, S., Davies, M.C., Illum, L., Davis, S.S., Boustta, M., and Vert, M. (1994a)

The preparation of sub-200nm biodegradable colloidal particles from poly(beta-malic

acid-co-benzyl malate) copolymers and their surface modification with poloxamer and poloxamine surfactants.

J. Contr. Rel. **30**, 57-67.

Stolnik, S., Dunn, S.E., Garnett, M.C., Davies, M.C., Coombes, A.G.A., Taylor, D.C., Irving, M., Purkis, S.C., Tadros, Th., Illum, L., and Davis, S.S. (1994b)

Surface modification of poly(lactide-co-glycolide) nanospheres by biodegradable poly(lactide)-poly(ethylene glycol) copolymers.

Pharm. Res. **11**, 1800-1808.

Stolnik, S., Garnett, M.C., Davies, M.C., Illum, L., Bousta, M., Vert, M., and Davis, S.S. (1995a)

The colloidal properties of surfactant-free biodegradable nanospheres from poly(beta-malic acid-co-benzyl malate)s and poly(lactic acid-co-glycolide).

Coll. Surf. A- Physicochem. Eng. Aspects **97**, 235-245.

Stolnik, S., Illum, L., and Davis, S.S. (1995b)

Long circulating microparticulate drug carriers.

Advanced Drug Delivery Reviews **16**, 195-214.

Streletzky, K. and Phillies, G.D.J. (1995)

Temperature dependence of Triton X-100 micelle size and hydration.

Langmuir **11**, 42-47.

Stubičar, N. and Petres, J.J. (1981)

Micelle formation by Tritons in aqueous solution.

Croatica Chemica Acta **54**, 255-266.

Sturesson, C., Carlfors, J., Edsman, K. and Andersson, M. (1993)

Preparation of biodegradable poly(lactic-co-glycolic) acid microspheres and their in vitro release of timolol maleate.

Int. J. Pharm. **89**, 235-244.

Sun, W.-B., Ding, J.-F., Mobbs, R.H., Heatley, F., Attwood, D. and Booth, C. (1991)
Preparation of a diblock copoly(oxybutylene/oxyethylene) and study of its micellisation and surface properties in dilute aqueous solution.

Coll. Surf. **54**, 103-111.

Szoka, F. and Papahadjopoulos, D. (1980)

Comparative properties and methods of preparation of lipid vesicles (liposomes).

Annu. Rev. Biophys. Bioeng. **9**, 467-508.

Tadros, Th.F. (1992)

The viscoelastic properties of concentrated suspensions.

Chemistry and Industry, 907-913.

Tadros, Th.F. and Vincent, B. (1980)

Influence of temperature and electrolytes on the adsorption of poly(ethylene oxide)-poly(propylene oxide) block copolymer on polystyrene latex and on the stability of the polymer-coated particles.

J. Phys. Chem. **84**, 1575-1580.

Takeoka, Y., Aoki, T., Sanui, K., Ogata, N., Yokoyama, M., Okano, T., Sakurai, Y., and Watanabe, M. (1995)

Electrochemical control of drug release from redox-active micelles.

J. Contr. Rel. **33**, 79-87.

Tan, J.S., Butterfield, D.E., Voycheck, C.L., Caldwell, K.D., and Li, J.T. (1993)

Surface modification of nanoparticles by PEO/PPO block copolymers to minimize interactions with blood components and prolong blood circulation in rats.

Biomaterials **14**, 823-833.

Tas, J., Frederiks, W.M. and Frank, J.J. (1980)

A new approach to the staining of lipids with sudan black B: A study by means of polyacrylamide model films containing liposomes.

Acta Histochemica., Suppl. -Band **XXI**, S., 123-129.

Thakkar, A.L. and Hall, N.A. (1967)

Micellar solubilization of testosterone I: in aqueous solutions of polysorbates.

J. Pharm. Sci. **56**, 1121-1125.

Thakur, M.L. and McKenney, S. (1985)

Techniques of cell labeling: an overview

In Radiolabeled cellular blood elements, pathophysiology, techniques and scintigraphic applications, 67-88.

Ed. M.L. Thakur. Plenum press, New York.

Thomas, G., and Goringe, M.J. (1979)

Transmission Electron Microscopy of Materials, 1-24.

John Wiley & Sons, New York.

Tokiwa, F. and Matsumoto, T. (1975)

Effect of inorganic electrolytes on the cloud point of polyoxyethylene dodecyl ether.

Bull. Chem. Soc. Japan **48**, 1645-1646.

Tomlinson, E. (1983)

Microsphere delivery systems for drug targeting and controlled release.

Int. J. Pharm. Tech. & Prod. Mfr. **4**, 49-57.

Torchilin, V.P., Trubetskoy, V.S., Milshcheyn, A.M., Canillo, J., Wolf, G.L., Papisov, M.I.,

Bogdanov, A.A., Narula, J., Khaw, B.A., and Omelyanenko, V.G. (1994)

Targeted delivery of diagnostic agents by surface-modified liposomes.

J. Contr. Rel. **28**, 45-58.

Uchida, T., Yoshida, K. and Goto, S. (1996)

Preparation and characterization of polylactic acid microspheres containing water-soluble dyes using a novel w/o/w solvent evaporation method.

J. Microencapsulation **13**, 219-228.

van Holde, K.E. (1985)

Sedimentation, 110-136.

In Physical Biochemistry.

Second edition, Prentice-Hall, Inc., Englewood Cliffs, New Jersey.

van Oss, C.J. (1987)

Phagocytosis as a surface phenomenon.

Ann. Rev. Microbiol. **32**, 19-39.

Vandorpe, J., Schacht, E., Stolnik, S., Garnett, M.C., Davies, M.C., Illum, L., and Davis, S.S. (1996)

Poly(organo phosphazene) nanoparticles surface modified with poly(ethylene oxide).

Biotech. Bioeng. **52**, 89-95.

Vert, M., Schwarch, G., and Coudane, J. (1995)

Present and future of PLA polymers.

J.M.S. - Pure Appl. Chem. **A32**, 787-796.

Vickerman, J.C. (1988)

Static secondary ion mass spectrometry for surface analysis, 155-215.

In Spectroscopy of surfaces.

Eds. R.J.H. Clark and R.E. Hester. John Wiley and Sons, Chichester, U.K.

Vickerman, J.C. (1989)

Introducing Secondary Ion Mass Spectrometry, 1-8.

In Secondary Ion Mass Spectrometry. Principles and Applications.

Eds. Vickerman, John C., Brown, Alan, and Reed, Nicola M. Oxford University Press, New York.

Wagenaar, B.W. and Müller, B.W. (1994)

Piroxicam release from spray-dried biodegradable microspheres.

Biomaterials **15**, 49-54.

Wan, L.S. and Lee, P.F.S. (1974)

CMC of polysorbates.

J. Pharm. Sci. **63**, 136-137.

Wang, Q., Yu, G.-E., Deng, Y., Price, C. and Booth, C. (1993)

Eluent gel permeation chromatography: application to the association of block copolymer F127 in aqueous solution.

Eur. Polym. J. **29**, 665-669.

Wanka, G., Hoffmann, H. and Ulbricht, W. (1990)

The aggregation behavior of poly-(oxyethylene)-poly-(oxypropylene)-poly-(oxyethylene)-block-copolymers.

Coll. Polym. Sci. **268**, 101-117.

Washington, C. (1992)

Photon correlation spectroscopy, 135-167.

In Particle size analysis in pharmaceuticals and other industries: theory and practice.

Ellis Horwood, Chichester, W. Sussex, UK.

Watts, J.F. (1990a)

Electron spectroscopy: some basic concepts, 1-9.

In An introduction to surface analysis by electron spectroscopy.

Oxford University Press, New York.

Watts, J.F. (1990b)

The electron spectrum: qualitative and quantitative interpretation, 26-34.

In An introduction to surface analysis by electron spectroscopy.

Oxford University Press, New York.

Wichert, B. and Rohdewald, P. (1993)

Low molecular weight PLA: a suitable polymer for pulmonary administered microparticles?

Microencapsulation **10**, 195-207.

Woodle, M.C. (1993)

Surface-modified liposomes: assessment and characterisation for increased stability and prolonged blood circulation.

Chemistry and Physics of Lipids **64**, 249-262.

Woodle, M.C., Engbers, C.M., and Zalipsky, S. (1994)

New amphipathic polymer-lipid conjugates forming long-circulating reticuloendothelial system-evading liposomes.

Bioconjugate Chem. **5**, 493-496.

Xiong, C.D., Cheng, L.M., Xu, R.P. and Deng, X.M. (1995)

Synthesis and characterization of block copolymers from D,L-lactide and Poly(tetramethylene ether glycol).

J. Appl. Polym. Sci. **55**, 865-869.

Yan, C., Rill, W., Hewetson, J., Tammariello, R., Malli, R., and Kende, M. (1995)

Intranasal immunization with ricin toxoid (RT) vaccine encapsulated in polymeric microspheres against aerosol challenge.

Proceed. Intern. Symp. Control. Rel. Bioact. Mater. **22**, 39-40.

Yang, Y.-W., Deng, N.-J., Yu, G.-E., Zhou, Z.-K., Attwood, D. and Booth, C. (1995)

Micellization of diblock and triblock copolymers in aqueous solution. New results for oxyethylene/oxybutylene, oxyethylene/oxypropylene, and oxyethylene/alkyl systems.

Langmuir **11**, 4703-4711.

Yokoyama, M. (1992)

Block copolymers as drug carriers.

Crit. Rev. in Therapeutic Drug Carrier Systems **9**, 213-248.

Yokoyama, M., Miyauchi, M., Yamada, N., Okano, T., Sakoura, Y., Kataoka, K., Inoue, S. (1990)

Polymer micelles as novel drug carrier, adriamycin-conjugated poly(ethylene glycol)-poly(aspartic acid) AB block copolymer.

J. Contr. Rel. **11**, 269-278.

Yokoyama, M., Okano, T., Sakurai, Y., Ekimoto, H., Shibazaki, C., and Kataoka, K. (1991)

Toxicity and antitumor activity against solid tumors of micelle-forming polymeric anticancer drug and its extremely long circulation in blood.

Cancer Res. **51**, 3229-3236.

Yokoyama, M., Sugiyama, T., Okano, T., Sakurai, Y., Naito, M., and Kataoka, K. (1993)

Analysis of micelle formation of an adriamycin-conjugated poly(ethylene glycol)-poly(aspartic acid) block copolymer by gel permeation chromatography.

Pharm. Res. **10**, 895-899.

Yokoyama, M., Kwon, G.S., Okano, T., Sakurai, Y., and Kataoka, K. (1994a)

Development of micelle-forming polymeric drug with superior anticancer activity.

ACS Symposium Series **545**, 126-134.

Yokoyama, M., Kwon, G.S., Okano, T., Sakurai, Y., Ekimoto, H., and Kataoka, K. (1994b)

In vivo antitumor activity of polymeric micelle anticancer drug against murine C 26 tumor.

J. Contr. Rel. **28**, 336-337.

Yokoyama, M., Okano, T., Sakurai, Y., and Kataoka, K. (1994c)

Improved synthesis of adriamycin-conjugated poly(ethylene oxide)-poly(aspartic acid) block copolymer and formation of unimodal micellar structure with controlled amount of physically entrapped adriamycin.

J. Contr. Rel. **32**, 269-277.

Yokoyama, M., Kwon, G.S., Okano, T., Sakurai, Y., Naito, M., and Kataoka, K. (1994d)

Influencing factors on in vitro micelle stability of adriamycin-block copolymer conjugates.

J. Contr. Rel. **28**, 59-65.

Youxin, L. and Kissel, T. (1993)

Synthesis and properties of biodegradable ABA triblock copolymers consisting of poly(L-lactic acid) or poly(L-lactic-co-glycolic acid) A-blocks attached to central poly(oxyethylene) B-blocks.

J. Contr. Rel. **27**, 247-257.

Youxin, L., Volland, C. and Kissel, T. (1994)

In-vitro degradation and bovine serum albumin release of the ABA triblock copolymers consisting of poly(L (+) lactic acid), or poly(L (+) lactic acid-co-glycolic acid) A-blocks attached to central polyoxyethylene B-blocks.

J. Contr. Rel. **32**, 121-128.

Yu, G-E, Deng, Y., Dalton, S., Wang, Q.G., Attwood, D., Price, C. and Booth, C. (1992)

Micellisation and gelation of triblock copoly(oxyethylene/ oxypropylene/ oxyethylene), F127.

J. Chem. Soc. Faraday Trans. **88**, 2537-2544.

Zareie, H.M., Kaitian, X., and Pi_kin, E. (1996)

STM images of PDLLA-PEG copolymer micelles.

Colloids Surfaces A: Physicochem. Eng. Asp. **112**, 19-24.

Zee-Cheng, R.K.-Y. and Cheng, C.C. (1989)

Delivery of anticancer drugs.

Meth. Find. Exp. Clin. Pharmacol. **11**, 439-529.

Zhang, L., Xiong, C.D., and Deng, X.M. (1995)

Biodegradable polyester blends for biomedical application.

J. Appl. Polymer Sci. **56**, 103-112.

Zhang, X., Jackson, J.K., and Burt, H.M. (1996)

Development of amphiphilic diblock copolymers as micellar carriers of taxol.

Int. J. Pharm. **132**, 195-206.

Zhou, Z. and Chu, B. (1988a)

Light-scattering study on the association behavior of triblock polymers of ethylene oxide and propylene oxide in aqueous solution.

J. Colloid Interface Sci. **126**, 171-180.

Zhou, Z. and Chu, B. (1988b)

Anomalous micellization behavior and composition heterogeneity of a triblock ABA copolymer of (A) ethylene oxide and (B) propylene oxide in aqueous solution.

Macromolecules **21**, 2548-2554.

Zhu, K.J., Xiangzhou, L. and Shilin, Y. (1986)

Preparation and properties of D,L-lactide and ethylene oxide copolymer: a modifying biodegradable polymeric material.

J. Polym. Sci. Part C Polym. Lett. **24**, 331-337.

Zhu, K.J., Bihai, S. and Shilin, Y. (1989)

“Super microcapsules” (SMC). I. Preparation and characterization of star polyethylene oxide (PEO)-polylactide (PLA) copolymers.

J. Polym. Sci. Part A Polym. Chem. **27**, 2151-2159.

Zhu, K.J., Xiangzhou, L. and Shilin, Y. (1990)

Preparation, characterization, and properties of polylactide (PLA)-poly(ethylene glycol) (PEG) copolymers: a potential drug carrier.

J. Appl. Polym. Sci. **39**, 1-9.